

New Correlations Between the Watson Characterization Factor (K_w)
and Properties of Coal-Derived Materials

M.B. Perry and C.M. White

Division of Coal Science
Pittsburgh Energy Technology Center
P.O. Box 10940
Pittsburgh, PA 15236

Introduction

Coal liquefaction products, like petroleum, are largely composed of hydrocarbons that are highly variable in properties depending on the feedstocks used and the processing conditions. In 1933, Watson and Nelson [1] emphasized that the value of physical property data on petroleum fractions is "... limited by the difficulty of correlating them into relationships of general applicability." Petroleum scientists and engineers have defined a set of mathematical and graphical expressions, or correlations, that permit the estimation of properties of these complex mixtures. Among these is a parameter termed the characterization factor (K_w), introduced by Watson and Nelson in 1933 [1] to denote the "paraffinicity" of petroleum hydrocarbon fractions. The Watson characterization factor is defined as follows:

$$K_w = \frac{(T_b)^{1/3}}{S}$$

1)

where T_b is the mid-boiling point in degrees Rankine ($^{\circ}R$) and
 S is the specific gravity at 60 degrees Fahrenheit ($^{\circ}F$).

In addition to characterizing the "paraffinicity," K_w has been used to estimate other properties. Watson and Nelson [1] demonstrated that K_w was useful for estimating the molecular weight and specific heat of petroleum fractions. Watson et al. [2] related K_w to percent hydrogen, kinematic viscosity, and critical temperature of petroleum-derived products. Smith and Watson [3] found K_w to obey mixing rules. More recently, Wilson et al. [4] demonstrated that K_w was useful for estimating the critical pressure of coal liquids.

Initially, coal scientists and engineers used the bank of correlations developed for petroleum to estimate the properties of coal liquefaction products; however, it is now accepted that estimation of properties of coal liquids from existing petroleum data can introduce large errors [5]. The deviations of properties from estimated values are believed to be caused by the higher concentration of polar compounds and by the more aromatic nature of coal liquids relative to petroleum. Since the Watson characterization factor was originally introduced to denote "paraffinicity," a high correlation with percent hydrogen and the atomic-hydrogen-to-carbon ratio is expected. That is, the contribution of aromatic constituents to the properties of the mixture should be contained in this characterization factor. Attempts to account for the contribution of polar constituents to the properties of complex mixtures are more difficult.

An assessment of the role of polar constituents in a coal liquid should ideally begin with a physical separation of the sample into functionally similar fractions. Methods used for the physical separation of coal-derived materials into chemical class fractions are numerous and varied, making the comparisons of data from the literature difficult. Because of the relatively high content of polar materials, sample components from coal-derived products may be adsorbed irreversibly onto liquid chromatographic stationary phase materials. Although specific detectors are necessary for making the fraction cuts, no suitable non-

destructive method is available for obtaining quantitative results for chemical class fractions using existing chromatographic detectors. Therefore, the fractions that are to be subjected to further characterization must be collected, the solvents removed, and the resulting fractions weighed to obtain quantitative results for the recovery of chemical class fractions. This is manpower-intensive and expensive, and can lead to imprecise results. High performance liquid chromatography (HPLC) eliminates some of the problems cited above. The speed and ease with which samples can be analyzed make HPLC appear as an attractive alternative to the more classical methods. Some major problems, however, still exist. To escape the need to pack the chromatographic column with new adsorbent after each separation, many HPLC methods require that only hexane-soluble materials are subjected to the chemical class separation; hexane insolubles are grouped into a broad, varied, and chemically undefined fraction called "asphaltenes." Asphaltenes from coal-derived materials may contain a high percentage of polar constituents that are not accounted for in polar class fractions. As mentioned previously, quantitation of the class fractions in these materials is difficult with most existing HPLC detectors. If correlations are found to be a function of the polar content of coal-derived materials, then it is necessary to characterize these constituents as carefully as possible if existing correlations are to be improved or new ones are to be developed.

This manuscript introduces a correlation between the Watson characterization factor and weight percent of polar constituents of narrow-boiling (50°F) distillate cuts of a coal-derived material from the H-Coal process. Similar correlations have been found for data previously reported by Gray et al. [5] for coal-derived distillate fractions from an SRC-II process. Finally, multiple linear least-squares treatment of the combined data from the H-Coal and SRC-II distillates correlates K_w with weight percent polars, atomic H/C, and mid-boiling point of the distillates. These new correlations relating the polar content of coal-derived liquids to the Watson characterization factor may be particularly significant because, as noted by Gray et al. [5], deviations of the observed properties of coal liquids from values predicted by correlations based on petroleum data are, in part, due to the higher concentration of polar materials in coal liquids. Therefore, any insight into the relationship between the polar content of coal liquids and other properties is valuable.

Experimental

The H-Coal liquid was produced at the Catlettsburg H-Coal Pilot Plant on September 25, 1981, while processing Illinois No. 6 coal in the synfuel mode of operation. A blend of "light oil" and "heavy oil" products (1:1.5) was distilled by Chevron into narrow-range distillates (50°F), or pseudocomponents. Specifically, 50°F boiling-range fractions were obtained over the boiling range from 400°F to 850°F; the start to 400°F fraction and the 850°F vacuum bottoms were also obtained. The preparative liquid chromatographic separation procedure applied to the H-Coal samples was a modification of methods that have been reported previously [6,7,8,9]. Briefly, bases were first removed by a nonaqueous ion-exchange procedure [7], and the remaining acid-neutral fraction was separated by column chromatography with alumina [8]. This separation scheme produced fractions corresponding to saturates, neutral aromatics, neutral nitrogen compounds, nitrogen bases, and acids. In addition to the functional class separations, several chemical and physical measurements were made on these distillates.

Determination of Bulk Properties

The mid-boiling point was determined by ASTM Method D-2887 [10]. Water was determined by the Karl Fischer method [11] using sodium tartrate dihydrate for standardization. Elemental analyses for carbon and hydrogen were performed as described by Houde et al. [12]. Specific gravity at 60°F was determined using a

pycnometer standardized with boiled deionized water. The atomic hydrogen/atomic carbon numbers were corrected to a dry basis using the Karl Fischer water results.

The multiple linear least-squares regressions, associated statistical parameters, and graphics were obtained on a PRO-350 (Digital Equipment Corporation) computer using a statistical software package, RS/1 (a trademark of BBN Research Systems in Cambridge, Mass.).

Results and Discussion

A correlation does not necessarily imply a cause/effect relationship; rather, it only confirms an observed mathematical relationship for a given data set. If a correlation is found to be in agreement with measured values for a large population, it can be viewed as useful for general predictions of a given property. In the case of coal-derived materials, properties may vary as a function of the sampling point, the unit sampled, the process, and the feed coal used. The present investigation compares correlations with the Watson characterization factor from coal liquids derived from the SRC-II and H-Coal processes, both of which used bituminous feed coals. For reasons cited earlier, data from those samples significantly soluble in hexane are presented for comparison. Results from property measurements relevant to this manuscript are presented with the associated data for the correlations (Tables 1, 2, 3, and 4).

A correlation obtained using a multiple linear least-squares regression is evaluated for "goodness-of-fit" using several criteria. The software employed in this work (RS/1) prompts the operator to select the best fit that can be obtained from the input data. The best fit is characterized by having a coefficient of linear multiple determination (R^2) close to one, a large F-Value (Regression Mean Square/Residual Mean Square), a low standard deviation, and a low significance level. Variables are selected or deleted from the multiple determination based on the partial correlation and significance level of that variable. This evaluation of property correlations with the Watson characterization factor employed comparable data from H-Coal distillates and SRC-II distillates. With noted exceptions, only the best fit, as described above, is reported.

Part I. Correlations of K_w with H-Coal Data

A plot of K_w versus mid-boiling point (K) is given in Figure 1a, and a plot of weight percent polars (bases, acids, and neutral nitrogen compounds from Table 1) versus mid-boiling point is given in Figure 1b. The range of K_w values exhibited by these H-Coal distillates is small, 9.84 to 10.37. A comparison of these plots (Figure 1) reveals a negative correlation between total polars and K_w . A linear least-squares regression of weight percent polars versus K_w reveals a correlation coefficient (R) of -0.941, significant at the 99% confidence level for $N = 7$. The equation resulting from the regression is the following:

$$K_w = -0.0239 (\text{wt\% polars}) + 10.63 \quad 2)$$

A correlation based on a multiple linear regression including the H/C data with the weight percent polars versus K_w did not yield a good fit for predicting K_w ; the result of the regression is the following:

$$K_w = -0.0239 (\text{wt\% polars}) - 0.0109 (\text{H/C}) + 10.642 \quad 3)$$

The coefficient of linear multiple determination (R^2) = 0.885 for the regression represented by Equation (3). If, however, the mid-boiling point (K) is introduced, a multiple linear least-squares fit to the same data correlates percent polars, mid-boiling point (K), and atomic H/C versus K_w with $R^2 = 0.980$. The multiple regression equation is the following:

$$K_w = -0.0199 (\text{wt\% polars}) + 0.00265 (\text{mid-boiling point, K}) + 1.52 (\text{H/C}) + 7.12 \quad 4)$$

These data, including the observed, predicted, residual values, percent difference (%Δ), and associated statistical parameters, are given in Table 2.

Part II. Correlations with K_w for Data from Distillates of SRC-II

In 1983, Gray and coworkers published a paper [5] and an extended report [13] that included the results of analyses of a series of 19 narrow-boiling distillate fractions of a product generated from SRC-II processing of Powhatan No. 5 Mine coal on Process Development Unit P-99 (located at Gulf's Research Center, Harmorville, Pa.). Chemical class fractions were obtained for each distillate fraction. Fluorescence Indicator Analysis (FIA) was applied to distillate fractions boiling below 589 K, yielding saturate, olefin, and total aromatic class fractions. "The polar fraction from FIA was calculated from three components: the phenolics content of the aromatics from a mass spectrometer analysis, nitrogen content, and sulfur content [5]." Preparative HPLC was used to separate the hexane-soluble portion of cuts boiling above 493 K into saturates and olefins, neutral aromatics, and polar aromatics. Hexane insolubles were grouped together as "asphaltenes." Results from property measurements relevant to this manuscript are presented with the associated data for the correlations (Tables 3 and 4).

A plot of K_w versus mid-boiling point (K) of the 14 distillate fractions considered is given in Figure 1a, and a plot of weight percent polars is given in Figure 1b. The range of values for K_w is larger than that for the H-Coal distillates, 9.76 to 11.74. The shape of the K_w plot appears to be slightly bimodal. As in the case of the H-Coal results (also Figure 1), comparison of the plots appears to reveal a negative correlation of total polars versus K_w . Note that the SRC-II case includes data from a much wider boiling range than was included in the H-Coal case. A linear least-squares treatment of the data derived from the SRC-II samples 1-7 in Table 3 (N=7, as in the H-Coal case) yields a correlation coefficient of -0.969, significant at the 99.9% confidence level, for weight percent polars versus K_w . However, if all 14 SRC-II distillates are included in a least-squares treatment of K_w with percent polars, the correlation coefficient is reduced to -0.5773, statistically significant at the 95% confidence level but useless for accurate property prediction. However, as shown below, K_w is not simply a function of polars present, and the dependence of K_w on other properties is more important as the boiling range covered by the pseudocomponents is increased. The resulting linear least-squares correlation for the 14 SRC-II distillates is given in Equation (5).

$$K_w = -0.0262 (\text{wt\% polars}) + 10.87 \quad 5)$$

Equation (5), resulting from a linear least-squares treatment of the SRC-II data, is strikingly similar to Equation (2) resulting from the same treatment of the H-Coal data. A multiple linear least-squares regression of the data for the 14 SRC-II distillates correlates weight percent polars and atomic H/C versus K_w with $R^2 = 0.9943$. The multiple regression equation that fits the K_w data is the following:

$$K_w = -0.0118 (\text{wt\% polars}) + 1.84 (\text{H/C}) + 8.03 \quad 6)$$

These data, including the observed, predicted, residual values, percent deviation, and associated statistical parameters, are given in Table 3. The resulting Equation (6), which represents a best fit of the SRC-II data, should be compared with Equation (3), which was a poor fit for the H-Coal data. Both data sets yield a negative correlation with total polars, but the dependence on H/C in this regression of the data is different.

Although Equation (6) represents the best fit of the SRC-II data, a good fit for the correlation of K_w with percent polars, H/C, and mid-boiling point (K) is given in Equation (7).

$$K_w = -0.0106 (\text{wt\% polars}) + 0.000651 (\text{mid-boiling-point, K}) + 2.05 (\text{H/C}) + 7.38 \quad 7)$$

The value of R^2 was 0.995, and the F-Value was 605.8. A comparison of Equation (7) for SRC-II distillates and Equation (4) for the H-Coal distillates reveals the relative significance of each variable to the correlation with K_w .

Part III. Correlations with K_w for Combined H-Coal and SRC-II Data

The plots of K_w (Figure 1a) and weight percent polars (Figure 1b) versus mid-boiling point of the distillates reveal several similarities in these data sets. The K_w values are similar. In the range of mid-boiling points between 490 K and 550 K, the trends for weight percent polars are similar. The divergence of the trends for weight percent polars in the two data sets is suspect based on the similarity of K_w in the data sets. One plausible explanation can be found in the differences in the procedures used to isolate the polar fractions. Gray [13] reported 17.4% asphaltenes in the distillate cut at mid-boiling point 671.3 K. In the SRC-II case, these asphaltenes (hexane insolubles) were removed from the sample before the polars were isolated by preparative HPLC. Surely, the asphaltenes included polars as constituents that were not recovered. On the other hand, asphaltenes were not removed from the H-Coal distillates; instead, the entire sample was subjected to the complete separation scheme. The highest-boiling H-Coal distillate (mid-boiling point = 650.8 K) included in the combined data sets contained 6.9% hexane insolubles that would not have been analyzed for polars in the procedure used by Gray.

A multiple linear least-squares treatment of the combined data (combining 7 H-Coal distillates and 14 SRC-II distillates) correlates weight percent polars, mid-boiling point (K), and H/C versus K_w with $R^2 = 0.987$. The multiple regression equation that best fits the combined data is the following:

$$K_w = -0.00685 (\text{wt\% polars}) + 0.00278 (\text{mid-boiling point, K}) + 2.73 (\text{H/C}) + 5.28 \quad 8)$$

These data, including the observed and predicted values, are given in Table 4; the observed versus the predicted K_w are plotted in Figure 2.

Conclusions

A negative correlation exists for the weight percent polar constituents versus K_w for distillates derived from these coal liquids. Undoubtedly, K_w is also a function of the aromatics present; but the contributions of the aromatic functionality should be contained in the H/C measurement. At least for these data sets, the weight percent of neutral aromatics does not change significantly in adjacent distillates, whereas significant concentrations of polars are confined to two distinct regions within the boiling range of the distillates (see Table 1).

The relative contributions of acids and bases to this correlation are difficult to assess. Gray and coworkers [5,13] did not separate these polar sub-fractions. However, a high correlation with polars, although not the same correlation, was found for the SRC-II data and for the H-Coal data. There is no reason to assume that the same correlation exists for acidic or basic components of the polar fraction. There is also no reason to assume that their relative contributions to K_w would not change from sample to sample. Changes in K_w attributed to the weight percent polars present may also reflect the degree of association

between the acidic and basic components. The role of both functional groups should be assessed.

It is unlikely that correlations that would be generally applicable to coal liquids can be extracted from only two data sets. However, the data sets presented were obtained on coal liquids produced from two different bituminous feed coals from different processes. Yet, an excellent correlation is found that fits the data for the characterization factor, K_w . Subbituminous feed coals may yield different fits for the Watson characterization factor.

Acknowledgments

We would like to acknowledge several coworkers for their contributions to this work, including Frank McCown who performed the separation of bases by non-aqueous ion exchange, Mike Ferrer who assisted in performing the alumina separations, and Joseph Hackett for performing the mid-boiling point determinations on the H-Coal distillates. We would also like to acknowledge Dennis Finseth and James Gray for illuminating discussions and advice.

A portion of the research on the H-Coal was performed while Mildred Perry was under appointment to the U.S. Department of Energy Post-Graduate Research Training Program administered by Oak Ridge Associated Universities.

Disclaimer

Reference in this report to any specific product, process, or service is to facilitate understanding and does not necessarily imply its endorsement or favoring by the United States Department of Energy.

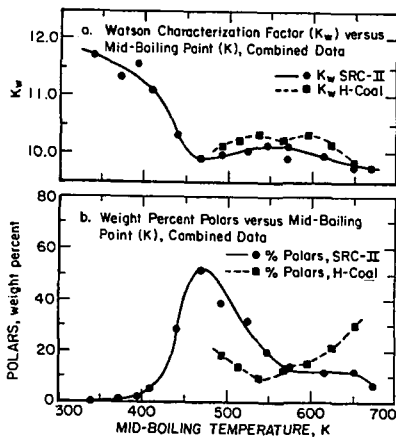


Figure 1 - Profile of K_w and Weight % Polars as a Function of Mid-Boiling Temperature (K) for Combined H-Coal and SRC-II Data.

References

1. Watson, K.M., and Nelson, E.F. Ind. Eng. Chem., 1933, 25, 880.
2. Watson, K.M., Nelson, E.F., and Murphy, G.B. Ind. Eng. Chem., 1935, 27, 1460.
3. Smith, R.L., and Watson, K.M. Ind. Eng. Chem., 1937, 29, 1408.
4. Wilson, G.M., Johnston, R.H., Hwang, S.-C., and Tsonopoulos, C. Ind. Eng. Chem., Process Des. Dev., 1981, 20, 94.
5. Gray, J.A., Brady, C.J., Cunningham, J.R., Freeman, J.R., and Wilson, G.M. Ind. Eng. Chem., Process Des. Dev., 1983, 22, 410.
6. Perry, M.B., White, C.M., Finseth, D.H., Sprecher, R.F., and Retcofsky, H.L. Proc. NATO ASI Application of New Spectroscopic Techniques to Coal Science. B.M. Lynch, ed., Martinus Nijhoff Publishers, BV, Dordrecht, The Netherlands, to be published in 1985.
7. Green, J.B., Hoff, R.J., Woodward, P.W., and Stevens, L.L. Fuel, 1984, 63, 1290.
8. Later, D.W., Lee, M.L., Bartle, K.D., Kong, R.C., and Vassilaros, D.L. Anal. Chem., 1981, 53, 1612.
9. Schiller, J.E., and Mathiason, D.R. Anal. Chem., 1977, 49, 1225.
10. Annual Book of ASTM Standards, 1980, Part 24, 788-796.
11. Mitchell, J., Jr., and Smith, D.M. Aquamestry, 2nd Ed., Part III, 1980, 5, 107-136.
12. Houde, M., Champy, J., and Furminieux, R. J. Micro Chem., 1979, 24, 300-309.
13. Gray, J.A. DOE Report DOE/ET/10104-7 (DE81025929), 1981.

Table 1.

Weight Percent of Various Compound Classes in H-Coal Distillates,
Normalized to 100 Percent Recovery

Mid-Boiling Point, K	Saturates	Neutral Aromatics	Bases	Acids	Neutral Nitrogen
493.6	30.0	51.0	8.76	10.0	0.24
513.6	31.0	55.0	5.50	6.5	2.00
538.0	29.5	60.5	3.15	6.5	0.35
566.9	25.5	61.0	7.90	4.5	1.10
595.8	22.5	61.5	7.29	8.5	0.21
623.0	13.9	63.9	11.50	6.3	4.40
650.8	13.0	56.0	22.06	8.0	0.94

Table 2.

Results of Multiple Linear Least-Squares Regression of K_w Using Weight Percent Polars, Mid-Boiling Point, and Atomic H/C for H-Coal Distillates

$$K_w = -0.019876(\text{wt\% polars}) + 0.00265(\text{mid-boiling point, K}) \\ + 1.521086(\text{H/C}) + 7.118681^a$$

Mid-Boiling Point, K	Weight Percent Polars	H/C (dry)	K_w (observed)	K_w (predicted)	Residual ^b	% Δ^b
493.6	19.0	1.375	10.15	10.140	0.009	0.092
513.6	14.0	1.351	10.26	10.256	0.003	0.033
538.0	10.0	1.360	10.37	10.414	-0.044	0.429
566.9	13.5	1.235	10.25	10.231	0.018	0.182
595.8	16.0	1.277	10.34	10.322	0.017	0.173
623.0	22.2	1.198	10.17	10.150	0.019	0.189
650.8	31.0	1.076	9.84	9.864	-0.024	0.244

Variable Name	Coefficient Value	Standard Deviation	Sig. Level
Weight Percent Polars	-0.019876	0.003605	0.011745
Mid-Boiling Point, K	0.002650	0.000696	0.031869
H/C (dry)	1.521086	0.459905	0.045481

Analysis of Variance Table

	Sum of Squares	DF	Mean Square	F Value	Sig. Level	Multi R ²	Std Deviation of Regression
Regression	0.183857	3	0.061286	49.88	0.0016	0.9803	0.0351
Residual	0.003686	3	0.001229				

$$\% \Delta = (|\text{Residual}| / K_w \text{ observed}) \times 100$$

^aCoefficients and constant term generated by RS/1 before adjusting to appropriate significant figures.

^bCalculated before rounding off K_w (predicted).

Table 3.

Results of Multiple Linear Least-Squares Regression of K_w Using
Percent Polars and Atomic H/C for SRC-II Distillates

$$K_w = -0.011807(\text{wt\% polars}) + 1.840546(\text{H/C}) + 8.028509^a$$

Mid-Boiling Point, K	Weight Percent Polars	H/C (dry)	K_w (observed)	K_w (predicted)	Residual ^b	% Δ^b
339.7	0.00	2.040	11.74	11.783	-0.045	0.387
372.4	1.60	1.846	11.36	11.408	-0.046	0.406
393.6	2.50	1.898	11.59	11.493	0.095	0.824
410.2	5.70	1.699	11.12	11.088	0.035	0.319
439.7	29.50	1.487	10.33	10.417	-0.085	0.824
468.6	52.00	1.353	9.92	9.905	0.012	0.129
493.0	39.55	1.316	9.99	9.985	0.002	0.028
524.7	32.40	1.279	10.05	10.001	0.053	0.527
547.4	20.95	1.315	10.16	10.201	-0.044	0.442
571.9	13.80	1.131	9.92	9.948	-0.032	0.328
573.0	14.45	1.208	10.13	10.082	0.050	0.497
615.2	12.10	1.090	9.96	9.892	0.062	0.630
650.2	12.85	1.027	9.76	9.767	-0.003	0.038
671.3	7.30	1.015	9.76	9.810	-0.055	0.564

Variable Name	Coefficient Value	Standard Deviation	Sig. Level
Weight Percent Polars	-0.011807	0.001115	0.0001
H/C (dry)	1.840546	0.051536	0.0001

Analysis of Variance Table

	Sum of Squares	DF	Mean Square	F Value	Sig. Level	Multi R ²	Std Deviation of Regression
Regression	6.521707	2	3.260854	959.38	0.0001	0.9943	0.0583
Residual	0.037388	11	0.003399				

$$\% \Delta = (|\text{Residual}| / K_w \text{ observed}) \times 100$$

^aCoefficients and constant term generated by RS/1 before adjusting to appropriate significant figures.

^bCalculated before rounding off K_w (predicted).

Table 4.

Results of Multiple Linear Least-Squares Regression of K_w for Combined Data:
SRC-II (Rows 1 to 14) and H-Coal (Rows 15 to 21)

$$K_w = -0.006847(\text{wt\% polars}) + 0.002776(\text{mid-boiling point, K}) \\ + 2.734032(\text{H/C}) + 5.279782^a$$

Sample No.	Weight Percent polars	H/C (dry)	Mid-Boiling Point, K	K_w (observed)	K_w (predicted)	Residual ^b	% Δ^b
1	0.00	2.040	339.7	11.74	11.800	-0.062	0.533
2	1.60	1.846	372.4	11.36	11.351	0.010	0.096
3	2.50	1.898	393.6	11.59	11.546	0.042	0.369
4	5.70	1.699	410.2	11.12	11.024	0.099	0.891
5	29.50	1.480	439.7	10.33	10.363	-0.031	0.310
6	52.00	1.353	468.6	9.92	9.924	-0.006	0.066
7	39.55	1.318	493.0	9.99	9.977	0.010	0.102
8	32.40	1.279	524.7	10.05	10.013	0.040	0.407
9	20.95	1.315	547.4	10.16	10.251	-0.094	0.932
10	13.80	1.131	571.9	9.92	9.867	0.048	0.492
11	14.45	1.208	573.0	10.13	10.076	0.056	0.559
12	12.10	1.090	615.2	9.96	9.886	-0.069	0.701
13	12.85	1.027	650.2	9.76	9.805	-0.041	0.427
14	7.30	1.015	671.3	9.76	9.869	-0.113	1.161
15	19.00	1.375	493.6	10.15	10.279	-0.129	1.274
16	14.00	1.351	513.6	10.26	10.303	-0.043	0.423
17	10.00	1.360	538.0	10.37	10.423	-0.053	0.513
18	13.50	1.235	566.9	10.25	10.137	0.112	1.096
19	16.00	1.277	595.8	10.34	10.315	0.024	0.236
20	22.20	1.198	623.0	10.17	10.132	0.037	0.367
21	31.00	1.076	650.8	9.84	9.816	0.023	0.243

Variable Name	Coefficient Value	Standard Deviation	Sig. Level
Weight Percent Polars	-0.006847	0.001725	0.0010
H/C (dry)	2.734032	0.237914	0.0001
Mid-Boiling Point, K	0.002776	0.000667	0.0010

$$\% \Delta = (|\text{Residual}| / K_w \text{ observed}) \times 100$$

^aCoefficients and constant term generated by RS/1 before adjusting to appropriate significant figures.

^bCalculated before rounding off K_w (predicted).

Table 4. (Continued)

Analysis of Variance Table							
	Sum of Squares	DF	Mean Square	F Value	Sig. Level	Multi R ²	Std Deviation of Regression
Regression	6.875659	3	2.291886	437.59	0.0001	0.9872	0.0724
Residual	0.089038	17	0.005238				

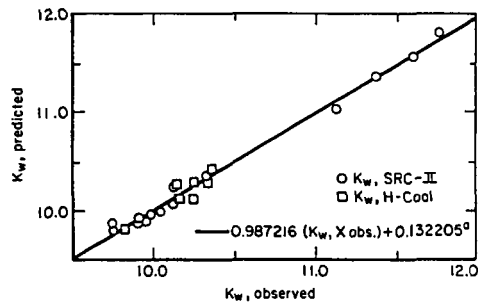


Figure 2 - Plot of K_w (observed) for Combined SRC-II and H-Coal Data versus K_w (predicted) by Multiple Regression).

^aEquation for linear least-squares line of best fit.

PRODUCT DISTRIBUTION FROM THE HYDROGEN DONOR
CONVERSION OF EASTERN U.S. SHALE

Donald C. Cronauer
David A. Danner
Laurine G. Galya
Jeffrey Solash
A. Bruce King
Roger F. Vogel

Gulf Research & Development Company
P. O. Drawer 2038
Pittsburgh, PA 15230

INTRODUCTION

Extensive deposits of oil shale have been found⁽¹⁾ in the Eastern U.S. While these deposits are reasonably rich in organic carbon content, the shales yield only about 10 gal/ton of rock by simple retorting, Fischer Assay (FA). This represents only about one-third of the available carbon, so techniques, such as hydrogen donor solvation, are being applied to increase carbon recovery. The objective of this paper is to summarize yield data from the conversion of two Eastern U.S. shales and to provide a characterization of products from two representative runs.

EXPERIMENTAL

Two samples of Eastern U.S. shales were used. The first was taken from the Hilpat site (Fleming Co., KY), and it is classified as a Cleveland member, Ohio shale. The second shale was mined at the Black Shale No. 1 site, Marysville (Clark Co., IN). It is a Clegg Creek member, New Albany (Devonian) shale. The shales had Fischer Assays of 10.1 and 11.8 gal/ton and carbon contents of 12.2 and 12.0, respectively. The solvents were obtained from Fisher Scientific, and they were used as received.

The experiments were made in a "cascade unit" consisting of a series of three reactors arranged such that a feed slurry of shale with solvent, tetralin, was injected from a feed tank into a preheated reactor. After the reaction period of 1 hr, the products were quickly transferred into a cold receiver, from which they were recovered for analysis. The amount of slurry retained in the feed tank was determined by toluene flushing and Soxhlet extraction. The gases were analyzed using a Carle 111A unit. The liquid portion of the raw slurry product was analyzed by GC/MS (Finnigan 9600). The raw slurry was filtered; the filtrate was stripped (N_2 @ 90°C) to recover "reactor residue", and the cake was Soxhlet extracted to recover toluene insolubles and asphaltenes. The reactor and receiver were also flushed with toluene and the slurry was analyzed as shown in the material balances of Figures 1 and 2. In summary, the products consisted of gases, distillate (the

liquids identified by GC/MS boiling between C_4 and about C_{20} , but excluding donor solvent, namely tetralin, naphthalene, 1-methylindan, and butylbenzene), reactor residue (bottoms from filtrate stripping), asphaltenes (toluene solubles from Soxhlet extraction), and toluene insolubles.

A material balance of the Indiana shale run (445°C, 60 min) is given in Figure 1. Of the 148 g of moisture free (MF) shale placed in the feed tank, 104 g was transferred to the reactor. This shale was recovered as 93 g toluene insolubles, 1.3 g asphaltenes (toluene solubles), 3.4 g reactor residue, 2.4 g distillates, and 2.8 g of gases (including H_2S , CO_2 , etc. but not including N_2 transfer gas). On a mineral matter basis, recovery was 98%, and on a carbon basis, namely shale carbon fed vs product carbons (excluding solvent) the balance was 96.6%.

A comparable run was made with Hilpat shale (see Figure 2). Of the 146 g MF shale charged, 141 was transferred to the reactor. The shale was recovered as 121 g toluene insolubles, 3.9 g asphaltenes, 2.6 g reactor residue, 4.4 g distillate, and 2.2 g gases (but H_2S was not determined). The material balance of mineral matter was about 98%, and the carbon balance was 99.6%.

Using as a basis 100 units of organic carbon in the feed shale, the overall distribution of product fractions from both the FA and donor solvent runs is given in Table 1. The product fractions are categorized as shale-derived or solvent-derived. All hydrocarbon gases are assumed to be shale related. With the exception of solvent dimers (i.e. ditetralin, etc.), all distillates are assumed to be shale-derived. Adducted tetralin and naphthalene derivatives, as estimated from 1H and ^{13}C NMR, are reported as such. Toluene insolubles are considered to be unconverted shale. (All of these assumptions will be discussed below.)

Gases

The yields of gases from the FA pyrolyses were essentially the same as those of the donor solvent runs, namely about 12% for Indiana shale and 6% for Hilpat shale. On a carbon basis, the distribution of gases was $C_1 > C_2 > C_3 > C_4 > CO_2 + CO$.

Distillates

The recoveries of distillate, designated oil, from the FA pyrolysis of Indiana and Hilpat shales were 11.8 and 10.0 gal/ton or 32 and 29% carbon recoveries. The oils had similar levels of hydrogen (10.1 wt%), nitrogen (1.2 wt%), and sulfur (1.6 and 1.8 wt%). The Hilpat-derived oil contained more oxygen, though (3.1 vs 1.7 wt%).

As shown in Figures 3 and 4, the boiling point distributions of the two oils were greatly different. The Hilpat oil was of much higher boiling point, and it also contained a regular pattern of alkyl components above the broad envelope of compounds. The MS signals of about 105 primary components

of both fractions were characterized. The distributions of the compound classes are shown in Table 2. While both oils contained the same level of alkanes (25%), Hilpat oil contained more alkanes (17 vs 10%). The Indiana derived oils had much higher levels of cycloalkanes and cycloalkenes (15 and 11% vs 4 and 0.5%, respectively). While both oils had comparable levels of alkylbenzenes (27-30%), the Hilpat-derived oil contained much higher levels of alkyl naphthalenes and indanes (13 and 10% vs 1 and 2%, respectively). In summary, the Indiana shale oil contained more cycloparaffins while the Hilpat shale oil contained more alkyl naphthalenes and indanes.

The compilation of GC/MS results of the donor solvent runs are also given in Table 2. While the distillate product of the pyrolysis of Indiana shale is about evenly divided between paraffins, cycloparaffins and substituted benzenes (C_1 through C_6), the donor solvent product has these components in addition to naphthalenes and hydronaphthalenes. In the case of Hilpat shale, pyrolysis distillate primarily consists of paraffins, benzenes and naphthalenes, and the donor process results in an increase in the level of naphthalenes and hydronaphthalenes.

Several aspects should be considered in discussing the above yields. First, Eastern shale is somewhat coal-like and aromatic systems would be expected in the product. Second, pyrolysis results in the rupture of bonds, and the abstraction of available hydrogen from sources such as hydronaphthalenes. Third, there is a high level of basic catalytic surface available which would promote alkylation, isomerization, and dimerization. Therefore, tetralin and naphthalene available from the solvent system are likely to become alkylated if free alkyl groups are available from the cracking of shale kerogen.

It appears that all of these aspects are present with major differences between the two shales. In the case of Indiana shale, much less solvent dimerization is observed than with Hilpat shale, namely 0.1 out of 15.7% distillate yield versus 2.3 out of 23.6%. It would appear that the rock matrix of the Indiana shale would have a relatively low activity for alkylation, and therefore, much of the high yield of naphthalenes and hydronaphthalenes may be shale-derived. Fortuitously, an Indiana run (430°, 30 min) was made in which some flush toluene was left in the reactor from a previous clean-up. The ratio of toluene to tetralin (or shale) was about 3:1. A high yield of alkylbenzenes was observed (28% vs 11%). In particular, 15% of the total distillate product was xylene, while the normal yield is 1-2%. The yield of ethylbenzene was 8.8%, while the normal yield is about 3%. Due to an apparent high level basicity of Hilpat shale and because a high yield of dimers is observed in the distillate product (i.e. 10% of the distillate; 2% of the total product), it would appear that even more transalkylation occurred in the processing of Hilpat shale.

As a test of transalkylation, two micro-autoclave experiments were made at 450°C and an hr reaction period using equal charges of Hilpat shale and tetralin. The first run was made with commercial tetralin, and the second with tetralin having a ^{13}C label at the α -position. Experimental techniques

are summarized in reference 2. The distillate liquids from both runs were characterized by GC/MS. Specific chromatographic peaks that appeared to be solvent-derived were studied by examining the most intense ion and the corresponding ^{13}C ion to calculate the amount of that component due to ^{13}C -labeled solvent.

In the case of 1-methylnaphthalene, 78% of this product in the distillate was derived from the donor solvent (^{13}C -tetralin) and 22% from the shale. The following specific components were also identified as being donor solvent-derived: 2-methylnaphthalene-86%, 1-ethylnaphthalene-82%, 2-ethylnaphthalene-88%, 1-methyltetralin-86%, ethyltetralin-88%, and propyltetralin-86%. In summary, about 70% of the naphthalene and tetralin sub-fractions of the distillate of the Hilpat run was solvent-derived after the alkylcarbons are subtracted off. Therefore, of the 21.3% "shale-derived" distillates listed in Table 1 for Hilpat shale, about 6.0% may actually be solvent-derived with the remaining 15.3% being shale-derived. (While the catalytic activity of the Indiana shale appears to be low, a detailed experiment would be necessary to confirm that less transalkylation would occur than that observed with Hilpat shale.)

Heavy Liquids

The heavy liquid products of the donor solvent runs consisted of asphaltenes and reactor residue; no appreciable toluene extractables were found in the FA solids. The following table summarizes the analyses of the combined heavy fractions from the Hilpat and Indiana runs:

<u>Element</u>	<u>Carbon</u>	<u>Hydrogen</u>	<u>H/C</u>	<u>Nitrogen</u>	<u>Oxygen</u>	<u>Sulfur</u>
<u>Shale</u>						
Indiana	82.4	7.1	1.03	2.4	2.3	5.8
Hilpat	86.3	7.1	0.99	1.9	1.5	3.2

In summary, the H/C ratios of these heavy products were essentially the same and the Indiana shale-derived product was higher in heteroatom content. As a note: the reactor residues were higher in hydrogen, nitrogen and oxygen than the asphaltenes, but lower in sulfur.

The characteristics of the residue and asphaltene fractions were examined by ^1H and ^{13}C NMR using experimental techniques outlined in another paper presented at this meeting.⁽³⁾ Spectra contain a large number of sharp signals in the aromatic region. These sharp signals are due to the presence of trimers and adducted species produced from the solvents. The broad underlying resonance in the aromatic region is due to aromatic material from the shale. The aromaticities of these oils are high, in the range of 75-80% of the total carbon. The aromatic region can be divided into three basic regions; substituted alkyl/aryl/heteroatom (133.5 ppm - end of aromatic); bridge carbon (133.5-129.5 ppm); and non-substituted aromatic carbon. In addition, an estimate of the aromatic carbon from tetralin/naphthalene is made

and given in Table 3. Another structural parameter available from ^{13}C NMR is the chain ratio. The higher the chain ratio the longer the chain. However, an average chain length cannot be computed in this case because the sample is a mixture of aromatic and aliphatic structures. The aliphatic structural parameters given in Table 3 are from ^1H NMR which gives a better analysis of this region than ^{13}C NMR.

An examination of the NMR data given in Table 3 shows that the asphaltenes derived from the two shale samples are similar. A comparison of the asphaltenes of the two shales shows slight differences in the aliphatic carbon, α to aromatic carbon content, hydroaromatic content and long chain content. The higher α to aromatic carbon content in the Indiana shale liquid is in agreement with the larger amount of alkyl substituted aromatic carbon. The slightly higher level of hydroaromatic carbon in the Hilpat shale is due to both tetralin and to hydroaromatic structures in the shale. The higher level of long chain material in the Hilpat shale corresponds with the higher chain ratio in this sample.

The Indiana spectra have more sharp lines than the Hilpat spectra in the aromatic region indicating the presence of more adducted tetralin and naphthalene. This is also reflected in the naphthalene content of the Indiana shale heavy product. The Indiana shale heavy product also has more heteroatom/aryl substituted aromatic carbon than does the Hilpat. This is partially due to both adducted naphthalene and to the higher heteroatom content of the Indiana asphaltenes.

Rock Matrix, Minerals

Due to apparent different catalytic properties of the two shales, an x-ray mineral analysis was done using a Philips APD-3100 diffractometer. The results were analyzed using a technique, "X-Ray Powder Diffraction Search System," of G. G. Johnson of Penn State University. While both the Indiana and Hilpat shales have quartz (50-60%) and montmorillonite (6-10%) as major components, the Hilpat shale contains more alkali metal (Na, K) components than does the Indiana shale. As pointed out by K. Tanabe⁽⁴⁾, the more basic a catalyst (or clay), the more likely that it is to promote polymerization, isomerization and alkylation. This observation is consistent with the results discussed herein.

CONCLUSIONS

Extensive conversion of two samples of Eastern U.S. Shale has been accomplished using a hydrogen donor solvent system in a DOE sponsored project. In a series of previously reported autoclave runs, the extent of conversion of the organic carbon varied from 20 to 75% depending upon temperature, reaction time, and solvent type. As a comparison, the Fischer Assay (FA) conversions of these shales were about 40%. Selected products from the FA runs and two "cascade unit" (slurry injection) runs made at 450°C and 1 hr using a donor-solvent process were analyzed by elemental, GC/MS, and NMR techniques. The yields of gases from the donor-solvent and FA processes were

about equivalent. More distillates were recovered from the FA runs but heavy fractions were recovered from the donor-solvent process while not present from the FA runs. Compositional trends observed in the FA liquids, such as high levels of alkanes and cycloalkanes, appeared to carry over into the liquids from the donor-solvent systems. Two experiments were made using either unlabeled or ^{13}C -labeled donor solvent, tetralin, to isolate solvent derived products from those generated from the kerogen. It was shown that a high level of transalkylation occurred between the shale-derived species and the solvent; therefore, a portion of the donor solvent can appear in the higher boiling distillate fractions. Similarly, a sizable level of solvent adduction with the shale-derived heavy fractions occurs. These reactions appear to be related to shale basicity.

ACKNOWLEDGMENT

Funding of this project was provided in part by the U.S. Department of Energy under Contract DE-AC01-82FE60194. We also acknowledge R. Watts of DOE and D. L. Fuller, W. B. Payne, and L. J. Chertik for experimental assistance. T. L. Youngless and J. T. Swansiger provided the characterization of the samples for the transalkylation experiments.

REFERENCES

1. Duncan, D. C. and Swanson, V. E., "Organic-Rich Shales of the United States," U. S. Geol. Survey, Circ. No. 523, 1965.
2. Cronauer, D. C., Danner, D., Solash, J., Seshadri, K. S., "Conversion of Eastern Shale with Hydrogen Donor Solvents," Symp. Papers: Synthetic Fuels From Oil Shale and Tar Sands, IGT, Louisville, KY meeting, May 1983, p. 407-424.
3. Galya, L. G., Cronauer, D. C., and Solash, J., "Adduction in Donor Solvent Conversion of Eastern Oil Shale," ACS Chicago Meeting, 1985.
4. Tanabe, K., Solid Acids and Bases: Their Catalytic Properties, Academic Press, Tokyo, 1970, 136.

Table 1
Distribution of Products on a Carbon Basis

<u>Shale</u> <u>Run Conditions</u> (°C/MIN)	<u>Indiana</u>		<u>Hilpat</u>	
	<u>F.A.</u> 500/40	<u>Tetralin</u> 445/60	<u>F.A.</u> 500/40	<u>Tetralin</u> 441/60
<u>Yield (on Carbon)</u>				
<u>Gases</u>	12.7	11.1	5.8	6.6
<u>Distillates</u>				
Shale-derived	32.5	15.6	29.3	21.3
Solvent-derived(1)	--	0.1	--	2.3
<u>Total</u>	<u>32.5</u>	<u>15.7</u>	<u>29.3</u>	<u>23.6</u>
<u>Reactor Residue</u>				
Shale-derived	--	18.7	--	12.2
Solvent-derived(2)	--	3.0	--	1.2
<u>Total</u>	<u>0.0</u>	<u>21.7</u>	<u>0.0</u>	<u>13.4</u>
<u>Asphaltenes</u>				
Shale-derived	--	7.0	--	18.0
Solvent-derived(2)	--	1.1	--	1.7
<u>Total</u>	<u>0.0</u>	<u>8.1</u>	<u>0.0</u>	<u>19.7</u>
<u>Toluene Insolubles</u>	60.3	40.0	60.3	36.3
<u>Total Shale-derived</u>	105.5	92.4	95.4	94.4
<u>Total Solvent-derived</u>	0.0	4.2	--	5.2
<u>Total</u>	<u>105.5</u>	<u>96.6</u>	<u>95.4</u>	<u>99.6</u>

Notes: (1) Dimers, only; a part of the shale-derived distillate may be alkylated solvent, though - see text.

(2) Tetramers plus adducted solvent.

Table 2
Compound Classification of Distillates

Run No.	Indiana Shale		Hilpat Shale	
	Fischer Assay	Donor Run	Fischer Assay	Donor Run
Distribution (RIC area %)				
Alkanes	26.2	25.7	24.9	18.7
Alkenes	10.0	0.2	16.5	0.0
Cycloalkanes	15.5	13.7	4.2	6.6
Cycloalkenes	10.7	2.0	0.5	1.2
Alkylbenzenes	30.0	11.9	26.6	13.7
Alkyl naphthalenes	1.2	21.9	12.8	22.2
Indanes	2.3	4.5	12.0	16.2
Alkyl tetralins and				
H _x naphthalenes	--	13.4	--	21.4
Heterocompounds	4.1	6.7	2.5	--
	100.0	100.0	100.0	100.0

Table 3
Structural Parameters From ¹H and ¹³C NMR of Asphaltenes
Derived From the Donor Solvent Conversion of Indiana and Hilpat Shales

Shale	Indiana	Hilpat
<u>% Aromatic Carbon</u>		
% alkyl substituted	8.9	7.0
% heteroatom/aryl substituted	20.9	15.4
total alkyl or heteroatom/aryl substituted	29.8	22.4
% bridge carbon	10.1	10.9
% non-substituted carbon	37.6	43.8
Total Aromatic Carbon	77.5	77.1
<u>% Aliphatic Carbon</u>		
% α methyls	4.3	3.7
% α CH ₂	4.6	3.3
% hydroaromatic	3.2	4.4
% long chain material	10.4	11.5
Total Aliphatic Carbon	22.5	22.9
Chain Ratio	2.6	3.9
<u>Adducted Solvent</u>		
% tetralin*	0.0	0.7
% naphthalene*	13.1	8.0

* Present as adducted species or trimers or tetrimers; no monomers or dimers were observed by GC techniques.

FIGURE 1 MATERIAL BALANCE OF THE INDIANA SHALE CASCADE UNIT RUN

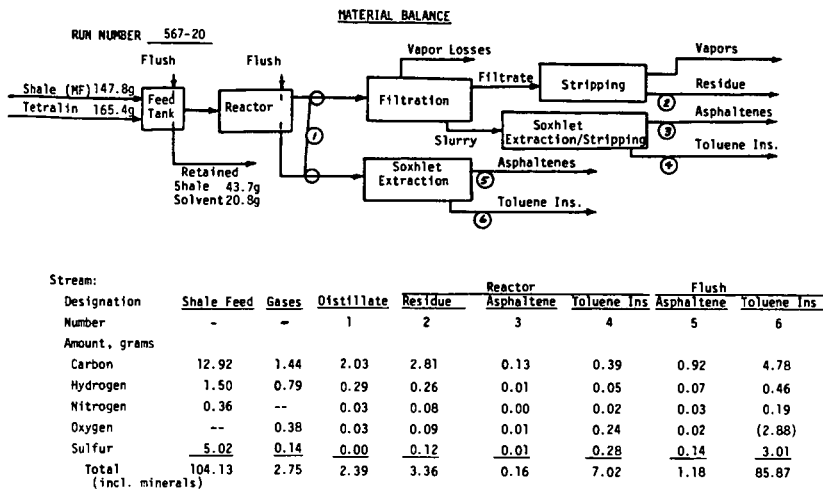
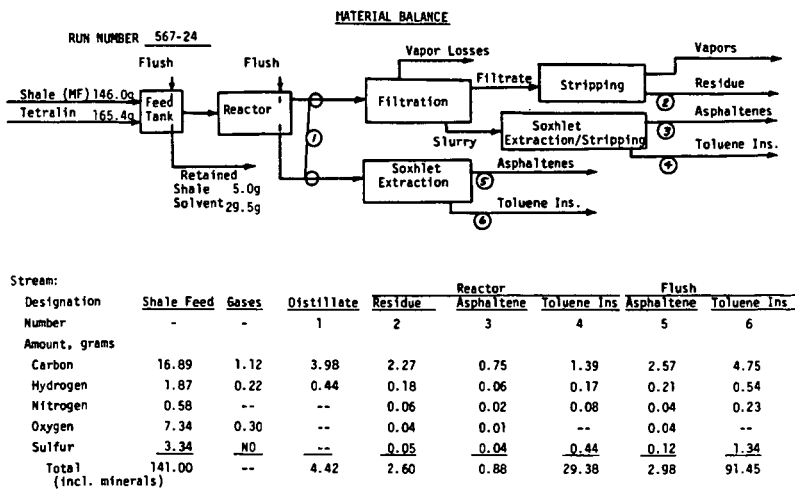


FIGURE 2 MATERIAL BALANCE OF THE HILPAT SHALE CASCADE UNIT RUN



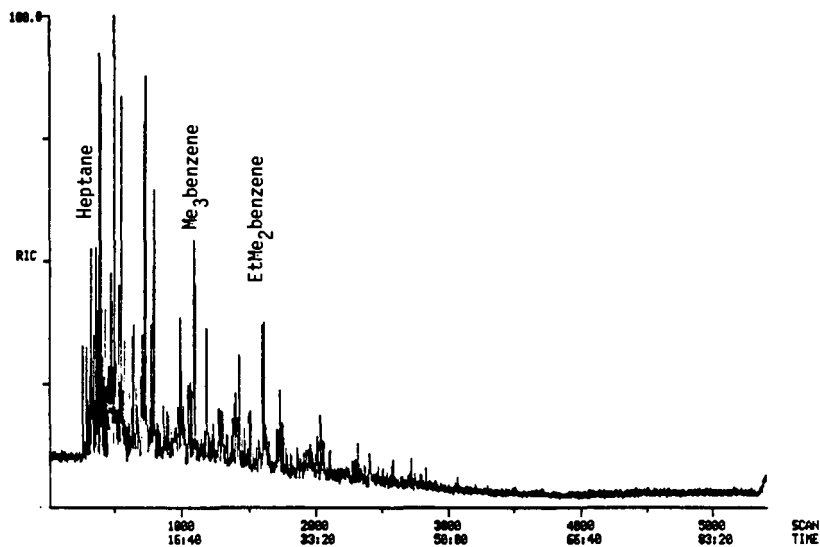


FIGURE 3 GC/MS (RIC) SCAN OF INDIANA SHALE FA OILS

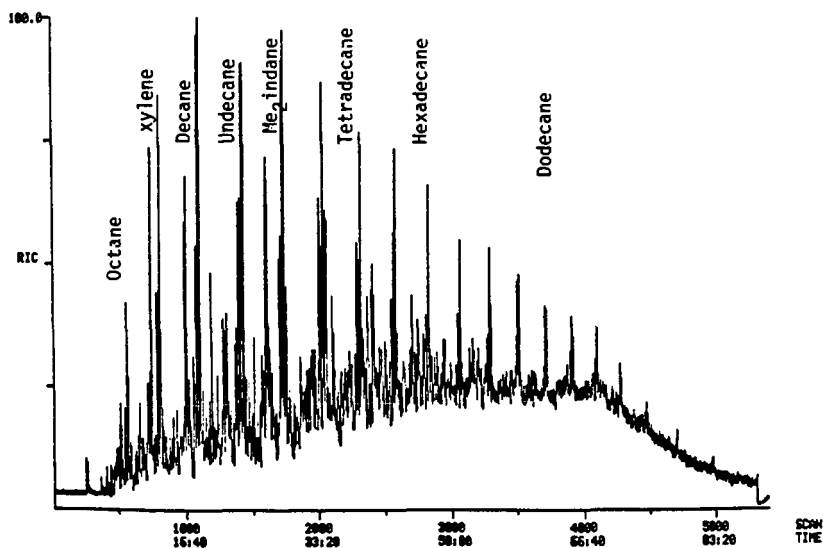


FIGURE 4 GC/MS (RIC) SCAN OF HILPAT SHALE FA OILS

HPLC-FTIR ANALYSIS OF POLAR COAL-DERIVED MATERIAL

P. G. Amateis, J. W. Hellgeth and L. T. Taylor
Department of Chemistry

Virginia Polytechnic Institute and State University
Blacksburg, VA 24061

INTRODUCTION

The detailed analysis of coal-derived products (CDP) is hampered by several factors. Their composition is not only extremely complex but also extremely heterogeneous as to component classes. Unlike petroleum products, most of the CDP is of relatively high molecular weight and exhibits a relatively large heteroatom (N,O,S) content. In addition, a major portion of the CDP is non-distillable which does not permit the use of many of the procedures previously developed for the analysis of crude oils. In this regard, different methods of analysis are required. For the nonvolatile CDP fractions, these analytical techniques are still in the exploratory stage. A combined condensed phase separation-spectrometric means of analysis seems especially suited for these materials. On-line analysis also appears highly attractive in view of the heterogeneous nature of the precursor feed coals and the desirability of rapid, discriminatory analytical procedures by the coal conversion industry. Depending on the functionalities of interest, a variety of combination techniques (separation-spectrometric) can be envisioned for nonvolatile CDP's.

Various spectroscopic techniques applied to isolated fractions have provided detailed structural information but each suffers from not being able to distinguish individual components. The coupling of HPLC separations directly with highly information-specific spectrometric detectors "on-line" may provide the potential for the identification of many of the components of these complex mixtures. Infrared spectrometry yields characteristic and often specific absorbances for many organic functionalities and particularly for many of the heteroatom containing compounds which need to be analyzed. IR also seems a very logical choice as a detector for the HPLC separation of CDP's since it is easily adapted to a flowing stream. We wish to describe the application of a HPLC-FTIR system to a coal-derived residuum.

RESULTS AND DISCUSSION

The coal-derived samples employed in this study were received from the Kerr McGee Corporation. Liquefaction conditions were as follows:

Wyodak #3 feed coal
100% THQ; S:C, 2:1
1100 psi H₂, 30 minutes, 785°F

After the reaction was terminated, gases were vented from the reactor and the reaction vessel was emptied of its contents. Some residuum and process solvent remained in the vessel. This material was removed by washing the vessel with tetrahydrofuran (THF). Material which was solubilized in this way was designated THF solubles. A preliminary preparative separation on the THF solubles was performed in order to remove the relatively large amount of 1,2,3,4-tetrahydroquinoline (THQ) known to be present in the THF-solubles sample. Fraction 1, eluted with hexane, was indeed found to contain almost exclusively THQ. Fraction 2 whose analysis is described below contained only a small amount of THQ.

A microbore scale chromatographic separation of fraction 2 with UV and FTIR detection is shown in Figure 1. Upon examination of the UV trace, it is seen that most peaks elute in the same region as previously found for simple basic nitrogen model compounds. The numbers over the peaks in Figure 1B correspond to individual

spectra obtained throughout the HPLC-FTIR run. There is a large amount of saturation reflected in each file spectrum as evidenced by the relatively intense CH stretching modes between 2800 and 3000 cm^{-1} . This is perhaps an indication of alkyl side chains on an aromatic ring. Two major components in this fraction are THQ (file 203) and quinoline (file 225). File 201 indicates the presence of N-methylaniline as shown by its comparison with the spectrum of the model compound. Obviously, another component(s) is also represented in file 201 since the two spectra do not perfectly agree. Some of the other files have not been identified although these contain bands consistent with nitrogen heterocyclic compounds. A match with model compound spectra has not been made. The spectrum corresponding to file 235 is interesting. The component represented in this file elutes after quinoline, but it is not resolved from quinoline. This spectrum contains a weak NH stretch, and rather intense C=C and C=N bands at 1598 cm^{-1} and 1500 cm^{-1} in addition to two bands at 1324 cm^{-1} and 1296 cm^{-1} . The material giving rise to this spectrum is suspected to be due to a THQ dimer. This component will be examined in further detail when the fraction's mass spectrum is discussed.

A survey of all files indicated the presence of several different carbonyl species. Figure 2 shows the carbonyl stretching region (1800-1600 cm^{-1}) for selected spectra taken throughout the entire run. The band at 1600 cm^{-1} which is present in every file is due to an aromatic C=C ring stretch. Early in the run (file 190), before elution of THQ, bands at 1677 and 1690 cm^{-1} are observed. These bands are seen in all files up to 201. After THQ elutes (file 203) an unique band at 1660 cm^{-1} is seen in file 217 prior to elution of quinoline (file 225). Finally, compounds elute between files 244-250 with a characteristic FTIR absorbance at 1774 cm^{-1} .

A tertiary amide exhibits a band near 1650 cm^{-1} . This could correspond to the band in file 217 but not file 190. A type of ketone is also possible. Our preferred assignment is that hydroxypyridine or a similar compound could be responsible for the IR absorbance in this region. Many of these types of compounds exist exclusively in the keto form. Enamines such as tetrahydropyridine are known to be susceptible to reaction with oxygen to yield similar type compounds. A similar kind of reaction could well be occurring with THQ during liquefaction. Single injections of 2-hydroxypyridine and 4-hydroxypyridine support this assignment in that these compounds elute with retention times similar to those of compounds found in files 190-217. Figure 3 shows the IR spectrum of 2-hydroxypyridine and 4-hydroxypyridine for comparison with file spectra 190 and 217.

The 1774 cm^{-1} band in files 244-250 is higher in frequency than is seen in many types of carbonyl compounds and is therefore more easily assigned. A five-membered γ -lactone has a band at 1770 cm^{-1} . The presence of such a species is likely since THF was used to isolate the original sample. It is known that in the presence of coal-derived material THF adducts readily to the coal material and can be converted to γ -butyrolactone under rather mild conditions.

To confirm assignments made on the basis of HPLC-FTIR as well as to gain additional information, THF solubles fraction 2 was subjected to field ionization mass spectrometry (FIMS). The sample was 100% volatile in the spectrometer in the temperature range employed (48-451°C). Spectra were collected over eight temperature ranges and these were then summed into one over-all spectrum. This composite spectrum is shown in Figure 4. The number average molecular weight is 328 for this fraction and the weight average molecular weight is 396. An overall ratio of odd to even mass peaks equal to 0.84 was calculated for this sample. It appears from this O/E ratio that almost half the material in fraction 2 contains an odd number of nitrogen atoms.

Examining the individual temperature ranges affords more information than an examination of the summed spectrum alone. Each temperature gives rise to a spectrum that is simpler than the composite spectrum since all the compounds are not present

in each range. The first temperature range examined (48-83°C) has an O/E ratio of 4.36. Obviously, compounds having an odd number of nitrogen atoms dominate. The most intense peaks are THQ ($m/e = 133$) and quinoline ($m/e = 129$). These compound assignments can be confidently made (as opposed to the isomers 1,2,3,4-tetrahydro-isoquinoline and isoquinoline) because of the information obtained from HPLC-FTIR. Also, from the FTIR analysis, N-methylaniline can be said to be at least in part responsible for the peak at 107. The other possible isomers of $m/e = 107$ were not observed by FTIR.

FIMS suggests the presence of compounds not indicated by FTIR. These include indole or propylpiperidine ($m/e=117$) and their homologues ($m/e = 131$), ethylaniline or a C_1 homologue of mass 107 ($m/e = 121$) and indanol ($m/e = 134$). Some compounds indicated by FIMS may also have been suggested by the FTIR analysis but a lack of model compounds and/or spectral library prevented exact assignment. For example, these might include homologues of THQ and quinoline ($m/e = 143, 147, 157, 161$). A hydroxyquinoline is suggested at mass 145 which supports an earlier assignment made via HPLC-FTIR.

In the second temperature range (87-110°C), in addition to compounds seen in the first temperature range, compounds of higher molecular weight are detected. The O/E ratio changes dramatically due to the nature of the compounds being volatilized during this temperature range. The O/E ratio is now 0.96. In the third temperature range (110-122°C) the O/E ratio decreases even further to 0.49. The mass peaks increasing most in intensity during the second and third temperature ranges are $m/e = 260-266$. With the exception of THQ, these peaks are the most intense ones in the FIMS summed spectrum. The suggested compounds for $m/e = 260-266$ are dimers of THQ and related "phenylquinoline-type" compounds.

The presence of such compounds in coal liquefaction products has been previously speculated. It has been noted that nitrogen-containing liquefaction solvents, while enhancing the liquefaction process by increasing the amount of soluble product, also produced non-distillable products and resulted in severe solvent loss. The suggestion was made that the liquefaction solvent was being incorporated into the coal structure or otherwise reacting to produce higher molecular weight materials. Unidentified IR spectra obtained by HPLC-FTIR can be associated with compounds of m/e 260-266 found in the FIMS spectra. Model compounds are unfortunately unavailable for exact assignment by either method.

In the higher temperature ranges, the O/E ratio approaches 1.00. This suggests that each high molecular weight specie has been "tagged" with THQ. As seen from the summed spectrum in Figure 4, these high mass peaks ($> m/e = 320$) are not very intense. Such high mass peaks could be due to trimers of THQ and related compounds.

ACKNOWLEDGMENTS

Acknowledgments to the Electric Power Research Institute and the Department of Energy (DE-FG22-81PC40799) for funding this project and to Kerr McGee Corp. for sample preparation are gratefully extended.

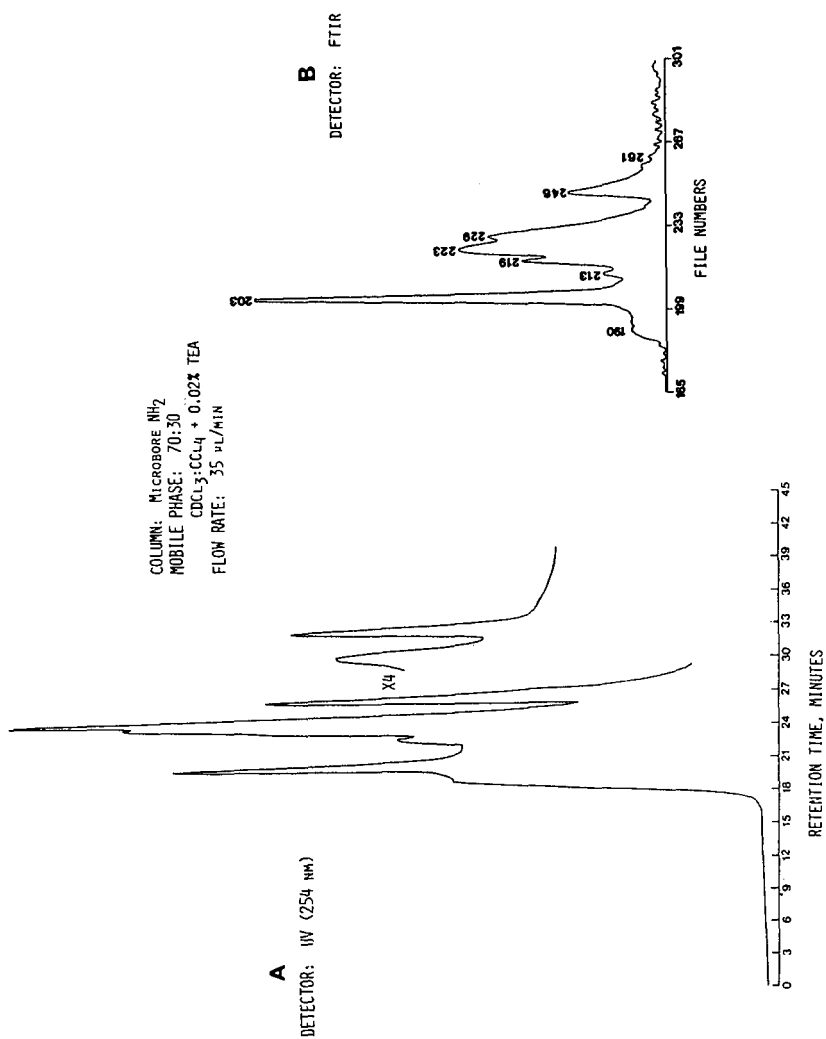


Figure 1

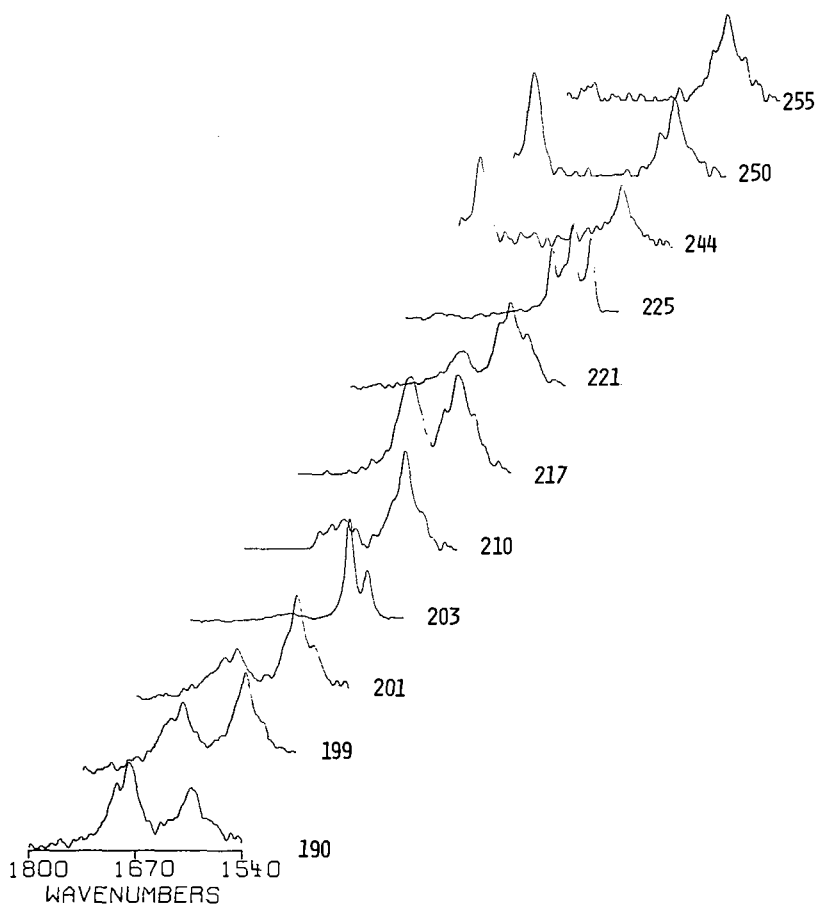


Figure 2. Carbonyl stretching region for selected spectra obtained during the separation of THF Solubles fraction 2.

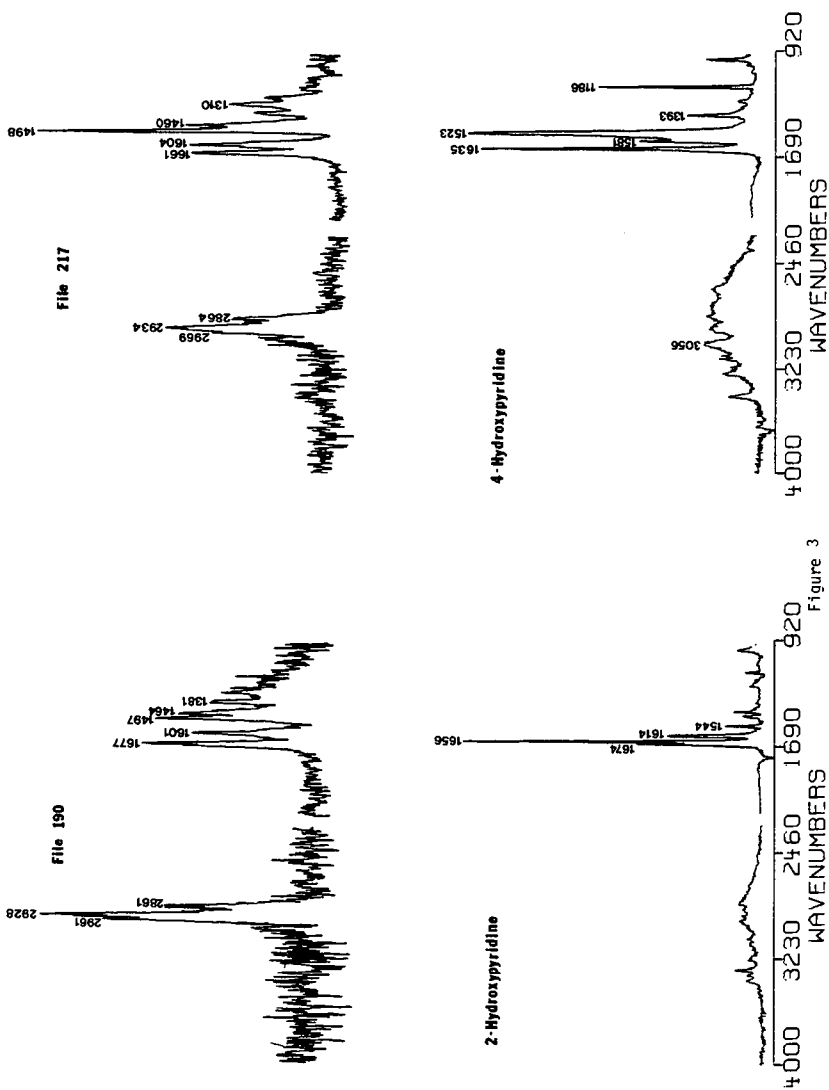


Figure 3

A31104. SUM I = 48 TO 451 DEG C' N AV MW=328 WT AV MW=396

VPI-AMATEIS, THF SOLUBLE, FRACTION #2 1-8

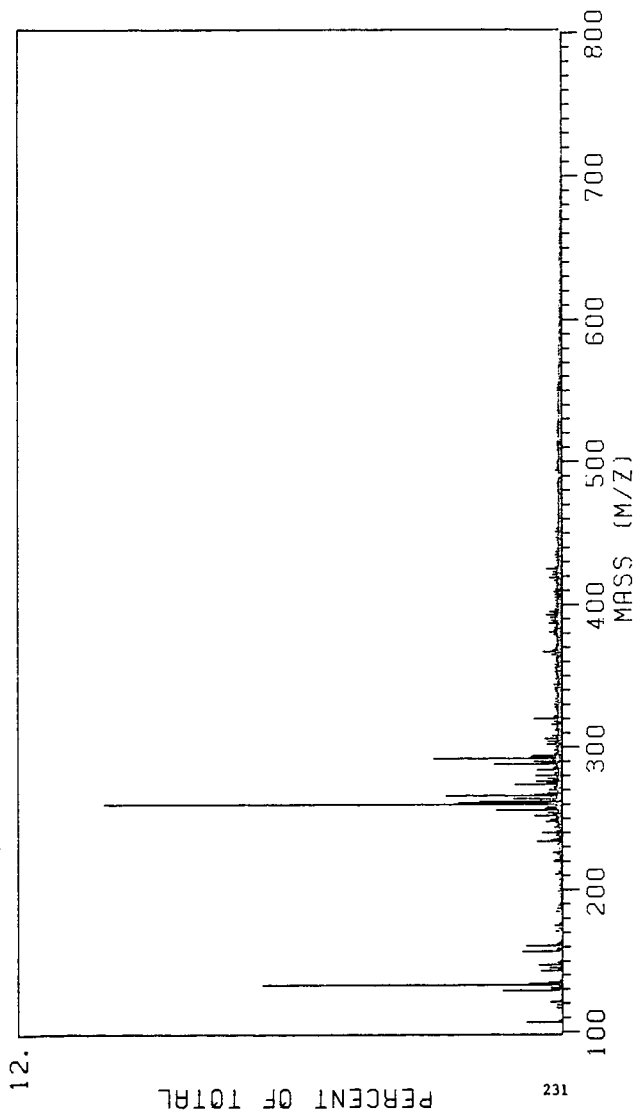


Figure 4

ELEMENTAL AND NMR CHARACTERIZATION OF TARS FROM
ENTRAINED-FLOW FLASH PYROLYSIS OF COAL

Muthu S. Sundaram* and Meyer Steinberg
Process Sciences Division
Department of Applied Science
Brookhaven National Laboratory
Upton, NY 11973

and

Konda R. Ramalingam
Department of Medicinal Chemistry
College of Pharmacy
University of Michigan
Ann Arbor, Michigan 48109

ABSTRACT

A New Mexico sub-bituminous coal was flash pyrolyzed in an He atmosphere in an entrained downflow tubular reactor at temperatures from 700°C to 1000°C and at 50 psi. In addition to C₁-C₂ gases, CO and BTX, as high as 9.8% of the dry, ash-free coal was converted to tar at 700°C. The tars were characterized via elemental analysis and ¹H NMR spectroscopy. ¹H NMR data show that the structural characteristics of the tars with respect to hydrogen type distribution depend on the severity of the reaction conditions. The non-aromatic hydrogen content of the tars decreased with increase in the pyrolysis temperature whereas the aromatic hydrogen content of the tars followed an opposite trend.

INTRODUCTION

The devolatilization of coal by rapid or flash heating produces primary tar as a result of thermal decomposition and depolymerization of the starting material. The extent of alteration of the physico-chemical properties of the primary devolatilization products via subsequent decomposition reactions depends on the process conditions in the pyrolyzer. For some types of coal, the primary devolatilization may be complete in a very short residence time, i.e., within the first few feet of a reactor. The primary products, if allowed to pass through additional length of a fully heated reactor, undergo extensive secondary reactions and the quality and quantity of the resulting end products depend on the severity of the reaction conditions.

(1.4)

The effects of various process parameters on the yield and the kinetics of formation of gaseous products and light organic chemicals such as BTX have been studied extensively.⁽¹⁻³⁾ In most instances, analysis of the above high volatile products were made with the use of on-line GC instrumentation. However, low volatile, high molecular weight and multi-functional tar fraction is complex in nature and requires special handling. It is also noted that the yield of tar fraction is generally low when compared to that of other high volatile products. In consequence, characterization studies on tar from coal pyrolysis experiments are limited.

In an effort to obtain a better picture of the progressive changes that accompany coal devolatilization, we applied several modern analytical techniques to gas, liquid, tar and char products from the pyrolysis of a sub-bituminous coal. In a previous paper, the effects of temperature, residence time and the pyrolysis atmosphere on the yields of gaseous products and BTX were reported.⁽⁴⁾ In this paper, we present the results of elemental and ¹H NMR characterization of tars from the same set of pyrolysis experiments. The results of capillary-GC/MS and pyrolysis-GC/MS characterization of oil and asphaltene fractions of the tars as well as SEM and FTIR analyses of the chars will be reported elsewhere.

EXPERIMENTAL

Pyrolysis Experiments:

A New Mexico sub-bituminous coal with analysis shown in Table 1 was flash pyrolyzed in a highly instrumented 1-in. I.D. by 8-ft long entrained downflow tubular reactor. The reactor system has been described in detail previously.⁽⁵⁾ Multiple analyses of CO_x, C₁-C₂ gases and BTX are made via an on-line GC and the products heavier than BTX are collected in a Freon cooled (~40°C) condenser. At the end of each experiment, the reactor is washed with vythane and the washings are combined with the contents of the condensers. From the liquid mixture, vythane is distilled off in a rotary evaporator to obtain the tar product.

Analytical Characterization:

A Perkin-Elmer elemental analyzer was used to determine the elemental composition of tars. The C, H and N content of the tars were determined directly and (O + S) was obtained by difference.

Proton-NMR spectra at 60 MHz were obtained with a Varian Model EM-360 Spectrometer. The samples were dissolved in CDCl₃ and the spectra were recorded at an ambient temperature of ~25°C with tetramethylsilane (TMS) as internal standard reference.

RESULTS AND DISCUSSION

Figure 1 shows the percent carbon conversion to CH_4 , C_2H_4 , CO_x and BTX as a function of temperature and residence time. At all residence times, the yield of ethylene maximized at 900°C , whereas that of CO_x continued to increase with temperature. By taking gas and BTX samples from different sample taps located at every 2-ft length of the reactor, the yield data for these products corresponding to at least four different residence times of the coal particles can be obtained from one single run.

The tar is collected at the end of the run and the yield corresponding to the longest coal particle residence time only is available from a particular run. In the set of experiments reported here, the longest coal particle residence time was 1.5 - 1.6 sec. The tar yield decreased with pyrolysis temperature as shown in Figure 2. Roughly half of the tar was made up of hexane soluble oil, the remaining being hexane-insoluble but benzene-soluble asphaltenes.

The effect of pyrolysis temperature on the absolute elemental composition of unfractionated tars is shown in Figure 3. There is a marked difference in the elemental composition of the tars obtained at 700° and 800°C . Particularly noticeable is the difference in oxygen content of these tars. At temperatures higher than 800°C , there is no significant variation in the elemental composition of tars.

Weighted distribution of C, H, N and O in tar can be more useful than the elemental composition alone. This is obtained by taking the elemental analysis data together with the tar yields. From a knowledge of coal feed rate and the weighted elemental distribution in tar, one can determine the actual amount of a particular element that remains in the tar as percent of original feed. The overall expression can be written as follows:

$$\% \text{Conv.}_X \text{tar} = \frac{\%X_{\text{tar}} \times W_{\text{tar}} (\text{gm})}{r_{\text{coal}} (\text{gm/min}) \times t_r (\text{min}) \times [\%X_{\text{coal}} (1-a)]}$$

where,

$\%X_{\text{tar}}$	= Percent composition of element X in tar
W_{tar}	= Amount of tar collected
r_{coal}	= Coal feed rate
t_r	= Duration of coal feed
$\%X_{\text{coal}}$	= Percent composition of element X in coal
a	= Fraction of ash in coal
$\% \text{Conv.}_X \text{tar}$	= Percent of element X in original feed that remains in tar

Figure 4 shows the effect of temperature on the calculated amounts of total C, H, N and (O+S) remaining in tar. Most of the decline in the retention of elements in tar occurs between 700° and

800°C. The quality and quantity of tar is almost unaffected on increasing the pyrolysis temperature from 900° to 1000°C. The ease of removal of elements from tar follows the order: O>H>C>N.

In Figure 1, it was noticed earlier that the carbon conversion to gases and BTX increased with temperature. This increase in gases and BTX yields is found to be attributed to the secondary decomposition reactions of the tar rather than to additional coal devolatilization. This is shown in Figure 5, in which total carbon conversion to all products (hydrocarbon gases + CO_x + BTX + tar) is plotted against temperature. There is no significant change in carbon conversion as the temperature is increased from 700° to 1000°C. Thus, in the case of pyrolysis of coal in the presence of an inert gas, such as helium, devolatilization is almost complete by 700°C, the lowest temperature used in the BNL reactor. The tar yield has been reported to maximize at 600°C in the case of pyrolysis of a Texas lignite in a continuous bench-scale reactor⁽⁶⁾.

¹H and ¹³C NMR spectroscopy has been widely used to characterize coal-derived liquids⁽⁷⁻¹⁰⁾. The ¹H NMR spectra (60 MHz) of the tars derived from the BNL reactor are shown in Figure 6. The assignment of a given chemical shift range to a particular type of hydrogen is based on the suggestions by Stoppel and Bartle⁽¹¹⁾. The percentage distribution of hydrogen under a given category is obtained by dividing the area integrated within the chemical shift range corresponding to that category by total area integrated.

The calculated ¹H-NMR hydrogen distribution in tars is listed in Table 2. The effect of temperature on hydrogen distribution is graphically shown in Figure 7. The aromatic hydrogen distribution in the tars increases with pyrolysis temperature, whereas there is a decrease in all other forms of hydrogen. The main difference between different curves is in their slopes. The only exception is hydrogen in β -position to an aromatic ring, the distribution of which is not affected by temperature.

The actual amount of aromatic hydrogen and non-aromatic hydrogen (phenolic hydrogen + aliphatic hydrogen) in tar can be calculated from the ¹H NMR hydrogen distribution data, % hydrogen content of the tar and the tar yield. The actual amounts of aromatic and non-aromatic hydrogen in tar are plotted against temperature in Figure 8. The actual amounts of both types of hydrogen decrease with increase in temperature, the trend being similar to the one noted in Figure 4.

CONCLUSION

A series of flash pyrolysis conclusion experiments with a New Mexico sub-bituminous coal in a downflow entrained tubular reactor shows that the devolatilization process is complete by 700°C in a helium atmosphere. Further increase in temperature causes the secondary cracking of tar leading to the formation of lighter products without enhancing devolatilization itself. The ease of removal of elements

from pyrolysis tar as a function of temperature follows the order: O>H>C>N. On a compositional basis, the distribution of aromatic hydrogen in tars increased with temperature, whereas that of all other forms of hydrogen followed an opposite trend. However, the actual amounts of all forms of hydrogen present in total tar decreased with increase in pyrolysis temperature.

ACKNOWLEDGMENT

This work was done under U.S. Department of Energy Contract No. AC02-76CH00016 and administered by Morgantown Energy Technology Center, Morgantown, W. VA.

REFERENCES

1. Howard, J.B., Peters, W.A., and Serio, M.A., "Coal Devolatilization Information for Reactor Modeling: Assessment of Data and Apparatus Availability with Recommendations for Research", EPRI Report No. AP-1803, Res. Proj. No. 986-5, Palo Alto, CA. (1981).
2. Gavalas, G.R., Coal Pyrolysis. Elsevier, New York, pp 39-69 (1982).
3. Talwalker, A.T., A Topical Report in Coal Pyrolysis. Report No. DOE/MC/19136-1408, 1983.
4. Sundaram, M.S., Steinberg, M., and Fallon, P.T., ACS Fuel Div. Prepr., 30 (1985).
5. Sundaram, M.S., Steinberg, M., and Fallon, P.T., "Flash Hydropyrolysis of Coals for Conversion to Liquid and Gaseous Fuels: Summary Report", DOE/METC/82-48 (1982). BNL Report No. 51537.
6. Calkins, W.H., ACS Fuel Div. Prepr., 28(5), 85 (1983).
7. Retwfsky, H.L. and Link, T.L., High Resolution ^1H -, ^2H -, and ^{13}C -NMR in Coal Research, 22, Analytical Methods for Coal and Coal Products, Vol. II.
8. Petrakis, L., Young, D.C., Ruberto, R.G., and Gates, B.C., Ind. Eng. Chem. Proc. Des. Dev., 22, 298 (1983).
9. Young, D.C. and Galya, L.G. Presented at the 189th ACS National Meeting, Div. Pet. Chem., Paper No. 51, Miami, FL, April 28 - May 3, 1985.
10. Allen, D.T., Presented at the 189th ACS National Meeting, Div. Pet. Chem., Paper No. 52, Miami, FL, April 28-May 3, 1985.
11. Stompel, Z.J., and Bartle, D., Fuel, 62, 900 (1983).

TABLE 1. ANALYTICAL DATA FOR NEW MEXICO SUB-BITUMINOUS COAL

Ultimate Analysis	(wt % dry)	Ultimate Analysis	(dry)
Carbon	: 55.9	Volatile Matter	: 34.9
Hydrogen	: 4.3	Fixed Carbon	: 42.4
Nitrogen	: 1.1	Ash	: 22.8
Sulfur	: 1.0		
Oxygen (by diff.)	: 14.9		

TABLE 2. FLASH PYROLYSIS OF NEW MEXICO SUB-BITUMINOUS COAL
50 psi HELIUM, 1.5 sec RESIDENCE TIMEHYDROGEN DISTRIBUTION IN TAR FRACTIONS (^1H NMR)

Hydrogen Type	^1H Chemical Shift Range (ppm from TMS)	Temperature, $^{\circ}\text{C}$			
		700	800	900	1000
Aromatic	6.5-9.0	27.4	43.9	57.5	64.7
Phenolic	5.5-6.5	5.7	3.9	2.3	1.5
Olefinic	4.5-5.5	9.4	6.1	2.3	1.5
Benzylic	3.3-4.5	11.3	8.8	4.6	4.4
CH_3, CH_2 , and $\text{CH}-\alpha$ to an aromatic ring	2.0-3.3	24.5	19.9	17.1	11.8
CH_2 and $\text{CH } \beta$ to an aromatic ring (naphthenic)	1.6-2.0	4.7	2.7	2.6	2.9
$\beta\text{-CH}_3, \text{CH}_2$ and $\text{CH}-\gamma$ to an aromatic ring	1.0-1.6	12.3	12.0	11.9	11.8
CH_3 γ or further from an aromatic ring	0.5-1.0	4.7	2.7	1.8	1.5

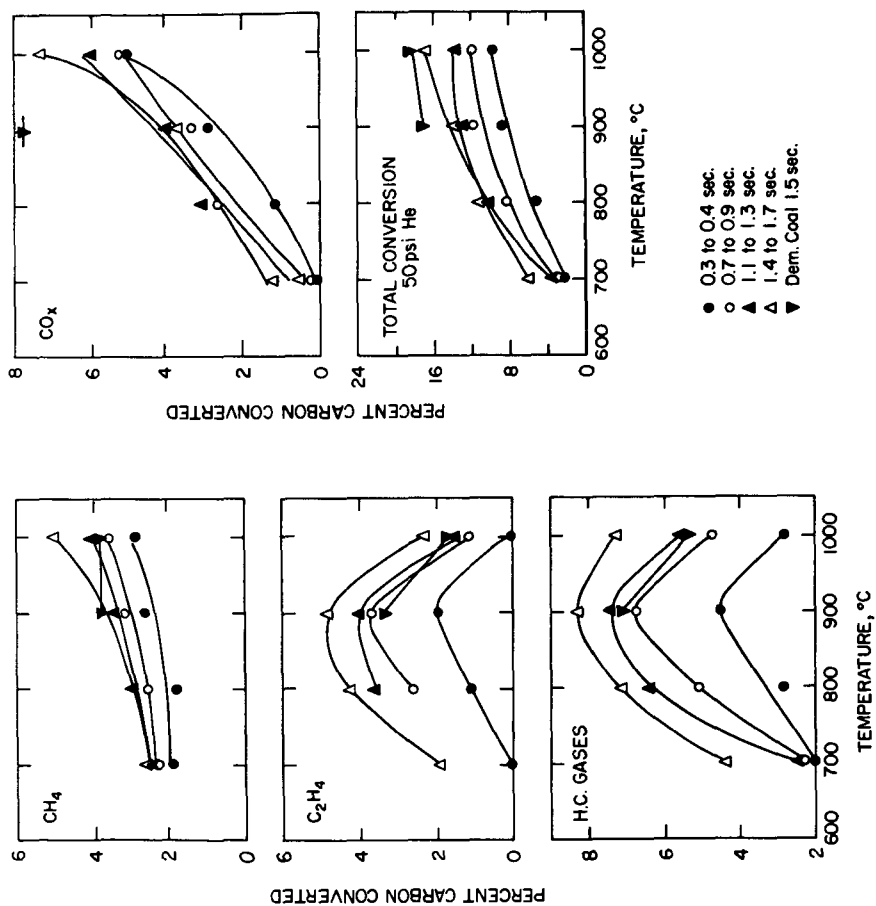


Figure 1. Effect of Temperature on Carbon Conversion to Gases and BTX.

Figure 2. Effect of Temperature on Tar Yield.

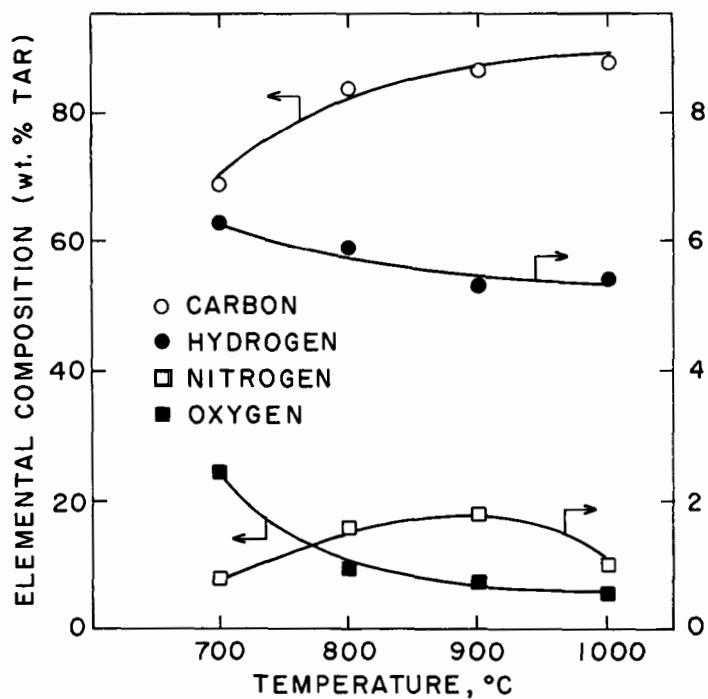
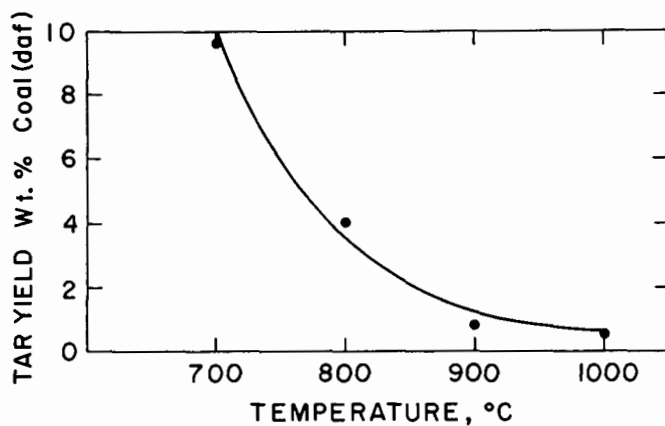


Figure 3. Effect of Temperature on Elemental Composition of Tar.

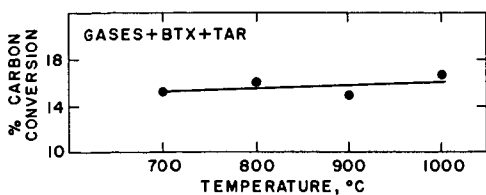


Figure 5. Effect of Temperature on Total Carbon Conversion to Gases, BTX, and Tar.

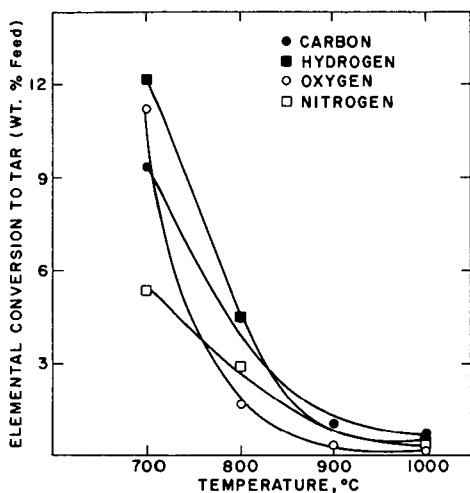


Figure 4. Effect of Temperature on Elemental Conversion to Tar.

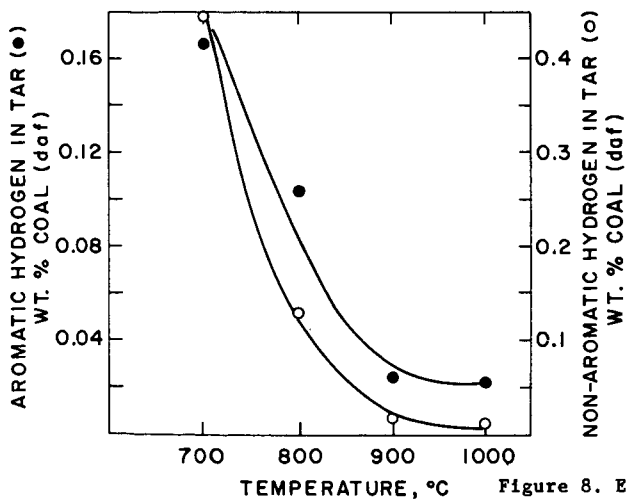


Figure 8. Effect of Temperature on Total Aromatic and Total Non-Aromatic Hydrogen in Tar.

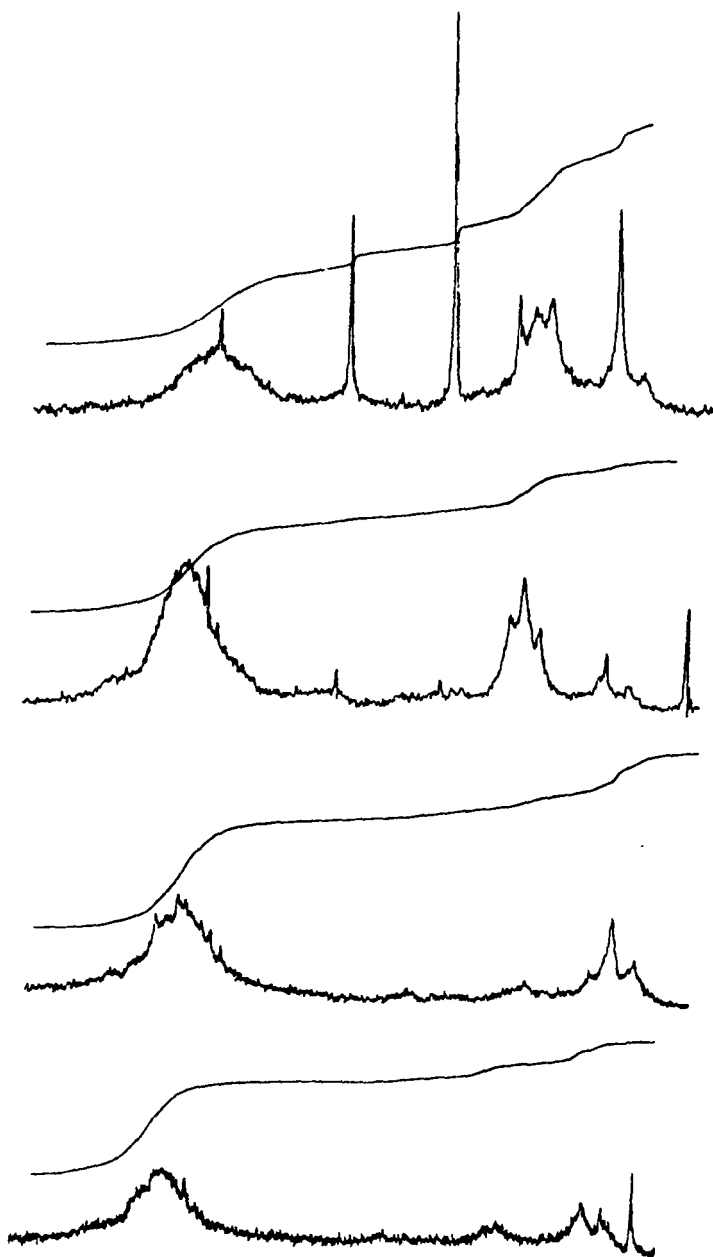


Figure 6. 60 MHz ^1H NMR Spectra of Pyrolysis Tars.

¹H NMR HYDROGEN DISTRIBUTION IN TAR

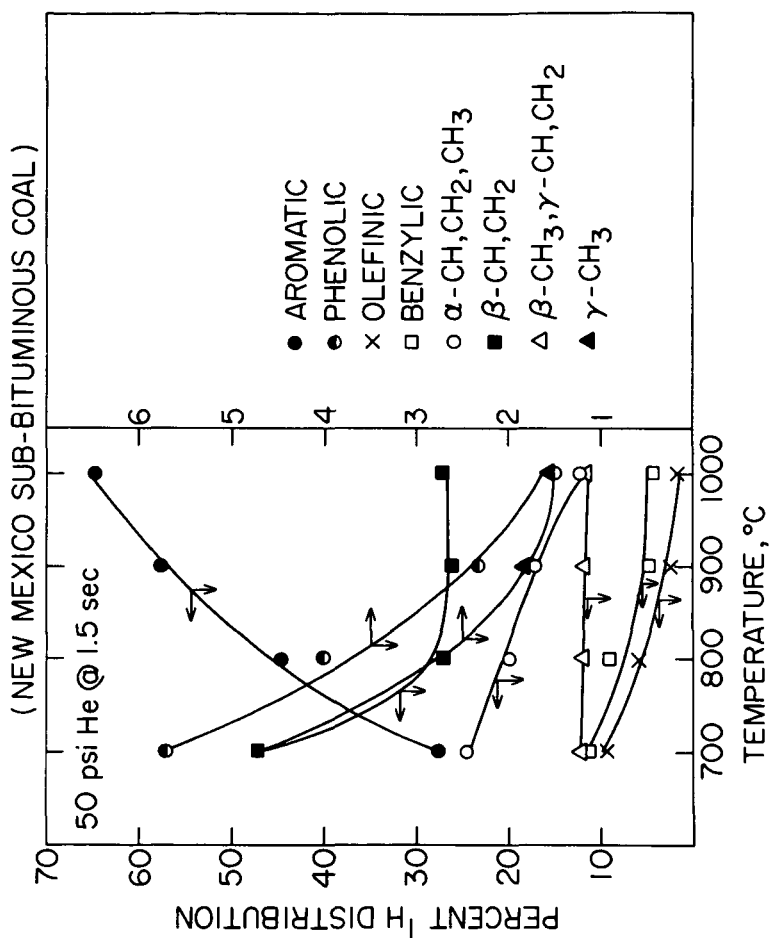


Figure 7. Effect of Temperature on Hydrogen Distribution in Tar.

CHARACTERIZATION OF RESIDUUM FRACTIONS
PREPARED BY FRACTIONAL DESTRUCTION

R.P. Warzinski, A.R. Strycker, and R.G. Lett

U.S. Department of Energy
Pittsburgh Energy Technology Center
Pittsburgh, Pennsylvania 15236

ABSTRACT

Fractionation with supercritical fluids, termed fractional destruction, is being developed at the Pittsburgh Energy Technology Center (PETC) for use on liquefaction residua. In this process, the density of a supercritical fluid is used to promote reflux in a manner analogous to temperature in a conventional distillation. This paper presents elemental, spectroscopic, and chromatographic analyses of residuum fractions prepared by this method. Emphasis is on the use of liquid chromatography as a relatively rapid method for obtaining important characterization data, such as molecular weight and chemical functionality. Such data are necessary for monitoring the daily operation of the Fractional Destruction Unit at PETC.

INTRODUCTION

Characterization of fossil fuels by distillation is limited in application to the extent that nonvolatile components occur in the fluid. For complex fluids such as those derived from heavy crude oils, tar sands, shale oil, or coal, more than half of the fluid may be nonvolatile residuum (1). To overcome this limitation, PETC is currently developing a supercritical-fluid-based fractionation process. The process is termed either fractional destruction (2) or supercritical distillation (3). Using this procedure, a residuum may be fractionated according to the solubility of its constituent components in the supercritical fluid. The novel aspect of this approach is the incorporation of a system to promote a reflux of the less-soluble components onto a packed bed. The liquid reflux is caused by increasing the temperature of the fluid phase at constant pressure, thereby decreasing the density of the supercritical fluid and its carrying capacity for residuum. The use of reflux results in rectification of the residuum in a manner analogous to conventional distillation (2, 4). At PETC an experimental unit has been constructed to operate in this manner and has been used to fractionate coal-derived distillate and residuum (4, 5). This unit is called the Fractional Destruction Unit (FDU). The purpose of this report is to present chemical, chromatographic, and spectroscopic characterization data for a set of coal-derived residuum fractions prepared by this process.

Operation of the FDU required the development of appropriate analytical methods to monitor the fractionation of residuum. Procedures common to conventional distillation, such as GC-simulated distillation, are limited to distillates; and more sophisticated analytical techniques, such as field ionization mass spectrometry, are too time-consuming and expensive to use on a daily basis. To overcome these difficulties, liquid chromatographic procedures previously developed for distillable coal-derived materials were adapted for use with residuum. The object of this report is to present the chromatographic characterization data and the corresponding chemical and spectroscopic results for a set of coal-derived residuum fractions prepared by the fractional destruction process.

EXPERIMENTAL

Residuum Fractionation

The FDU basically consists of two major components: (a) the fractional destruction vessel (FDV) where the supercritical fluid and residuum come in contact; and (b) a separator that subsequently disengages the residuum from the solvent in the overhead stream from the FDV (5). The novel feature of the FDV is an integral column in which reflux is generated by means of a hot finger onto a packed bed. In the work reported here, 1000 g of residuum from the Wilsonville Advanced Coal Liquefaction Test Facility was fractionated using cyclohexane ($T_c = 553.4$ K, $P_c = 4.074$ MPa) as the supercritical fluid. This residuum was collected from the T102 vacuum distillation tower during Run 242. The run was made in a Short-Contact-Time Integrated Two-Stage Liquefaction mode using Illinois No. 6 coal from the Burning Star mine (6). During the time this sample was collected, the T102 vacuum tower was operated at 594 K and 3.4 KPa. The cyclohexane was obtained in drum quantities at greater than 99 percent purity and used as received.

Figure 1 summarizes the fractionation in terms of the residuum concentration in the overhead as a function of the extent of destruction. The residuum concentration value was calculated from the amount of residuum brought overhead and the amount of cyclohexane pumped through the FDV during that collection period. Most of the points in this figure represent 30-minute collection periods. The total time on stream was 19.06 hours, which spanned three working days. The gaps in the line in Figure 1 indicate the points at which the fractionation was terminated by shutting the FDU down at the end of each working day.

In the FDU, the residuum charge was contacted with cyclohexane at a T_r , or T/T_c , of 1.02 and a P_r , or P/P_c , of 1.3. An initial temperature difference of 60 K between the extraction section and the reflux section of the apparatus was established to promote reflux. As shown in Figure 1, this resulted in an initial overhead concentration of approximately 2.4 gram residuum per g-mole of cyclohexane. By contrast, the overhead concentration of residuum in the absence of reflux, i.e., isothermal operation, is approximately five times greater. Six fractions were collected as indicated in Figure 1. As the overhead concentration of residuum decreased, the temperature difference across the FDV was reduced to increase the density in the reflux section and thus permit more residuum in the overhead stream. During collection of the final fraction, the temperature in the reflux section was the same as that in the extraction zone.

Owing to inefficiency in the separator, some of the residuum brought overhead is collected with the spent solvent. This material is recovered by distilling the solvent in a rotary evaporator. The overall efficiency of the separator during the fractionation reported here was 67 percent. In this study, the residuum recovered from the solvent was not combined with that recovered from the separator because independent analysis of this material will provide valuable information concerning operation of the separator. Current work is aimed at improving the separator efficiency through optimization of operational parameters and design.

Characterization

The elemental analyses were performed at PETC using ASTM techniques that were modified for use with coal-derived materials. The vapor pressure osmometry (VPO) molecular weights were single-point determinations in pyridine at 353 K and were performed at Huffman Laboratories, Inc., Wheatridge, Colo.

The gel permeation chromatography (GPC) was performed using PLgel 100A⁰ columns manufactured by Polymer Laboratories, Ltd., Shropshire, U.K., with THF as the eluent. An evaporative analyzer from Applied Chromatography Systems (USA), Inc.,

State College, Pa., was used in conjunction with a conventional refractive index detector to monitor the separation. The molecular weights reported here were calculated using the data obtained from the evaporative analyzer. In this detector, the eluent from a liquid chromatographic column is nebulized with a gas, the solvent is vaporized from the resulting droplets, and the remaining nonvolatile sample particles pass through a light-scattering photometer. This detector is more sensitive than the refractive index detector and is especially suited for GPC of high molecular weight coal derivatives (7). The calibration curve was constructed using polystyrene standards for molecular weights greater than 1000, and a series of pure aromatic compounds for the lower molecular weights. A correction for polystyrene molecular weights that was developed by Reerink and Lijzenga (8) with petroleum bitumens and asphaltenes was used in constructing the GPC calibration curve.

Chemical class fractionation was performed using a high performance liquid chromatography (HPLC) method similar to that proposed by Matsunaga (9). In this procedure, the residuum sample is dissolved in tetrahydrofuran, filtered to remove particulates, and separated on a u-Bondapack NH₂ column from Waters Associates, Milford, Mass., using a hexane/THF gradient. Using this procedure, the sample is separated on the basis of the number of double bonds and functionality. One unresolved problem with this method is the extent to which the separation is affected by the solubility of the sample in hexane. This aspect is still under investigation.

Spectroscopic analyses included near-infrared, ¹H-NMR, and field ionization mass spectrometry (FIMS). The near-infrared measurements were made on dilute methylene chloride solutions of the fractions. The ¹H-NMR spectra were acquired in d₅-pyridine. The FIMS data were obtained from SRI International, Menlo Park, Calif.

DISCUSSION OF RESULTS

The elemental analysis and VPO data are summarized in Table 1 for the six fractions collected. Important trends to note in the elemental composition of the fractions as the destruction proceeds are the increase in heteroatom concentration and the decrease in the hydrogen-to-carbon ratio. The molecular weight data also exhibit a regular increase in going from the first to the last fractions. These observations indicate that the separation in the cyclohexane fractional destruction proceeds according to the relative volatility of the sample components. This may not be the case when associating solvents are used as supercritical fluids (10).

The number average molecular weights (\bar{M}_n) of the six overhead fractions calculated from FIMS and GPC are compared to the VPO determinations in Figure 2. The data are in good agreement except for the FIMS results for the higher molecular weight fractions. Except for the third fraction, sample volatilization exceeded 90 percent. The low results for the last two fractions are primarily due to termination of the spectra at 800 amu. Future FIMS data will be collected out to 2000 amu. The advantage of using GPC is that it is much faster and more easily automated than the other methods. This capability has been invaluable in making decisions concerning daily operation of the FDU.

The GPC profiles of the six fractions are compared in Figure 3. The weight average molecular weights are also shown. Similar data on fractions collected during a non-reflux, isothermal experiment show much broader distributions and little difference between the first and last fractions. Operation in the reflux mode, as shown in Figure 3, produces narrower fractions, with an obvious trend to larger molecules as the fractionation proceeds. The transition between Fractions 4 and 5 is noteworthy. Referring back to Figure 1, the overhead concentration also increases dramatically at this same time.

Figure 4 contains results for the chemical class fractionation performed using HPLC. Even though the development of this procedure is still in its early stages, the results yield important information concerning the molecular properties of the fractions obtained by supercritical fluid fractionation. The qualitative chemical class distinctions indicated in Figure 4 were estimated from the retention of neutral, acidic, and basic fractions obtained from an SRC II distillation cut (588 K to 755 K) by column chromatography. The neutral species are more concentrated in the first fractions (see Figure 4). The later fractions are depleted of neutral species and show increasingly higher concentrations of more polar compounds. These observations are tentative until the extent to which the separation is affected by the hexane solubility of the samples is determined.

The near-infrared spectra reveal only small differences in the amounts of free -OH and relative -NH functionality in the soluble fractions. The absolute weight percent of oxygen as free -OH only increased from 0.6 to 0.7 between the first and last fractions. The increase in pyrrolic N-H functionality paralleled the increase in nitrogen content of the fractions.

More interesting results were obtained from mean molecular parameters calculated using the $^1\text{H-NMR}$ data. A summary of some of the trends is shown in Figure 5. Going from left to right, the data points in this figure represent Fractions 1 to 6, respectively. Position on the abscissa indicates the mid-point of the fraction. The most notable change is in the calculated total number of rings (aromatic, heterocyclic, hydroaromatic, naphthenic) per average molecule, which shows the most marked change after Fraction 4. This is consistent with the molecular weight and GPC data. The trend in the number of aromatic rings per molecule parallels this observation. There is an increase of about one heterocyclic ring per average molecule between Fractions 1 and 6. The calculated number of ring (aromatic plus heterocyclic) clusters per average molecule is about 1.5 for the first four fractions but then increases to about 2 in the last two fractions.

CONCLUSION

The development of the fractional destruction concept was motivated by the need to extend distillation technology to coal-derived systems containing intractable residuum. In order to provide daily information on the operation of the FDU, GPC procedures were developed to rapidly characterize the residuum fractions. In the long term, alternate procedures such as GPC will be necessary to monitor the performance of demonstration and commercial plants that utilize or generate residuum-containing streams. The complexity of fossil fuels also demands similar procedures for monitoring the more polar, associating species. This provides impetus for the development of HPLC separations such as the one reported here.

In summary, the trends in the characterization data of a set of residuum fractions prepared by fractional destruction show that as the fractionation proceeds, the average composition of the fractions shifts to higher molecular weight, lower hydrogen-to-carbon ratio, and increased heteroatom content. The data also show an increase in both the average size and average number of aromatic ring clusters in the components, along with larger ring clusters, and more ring clusters per molecule. The transitions are generally smooth; however, an abrupt change occurs in some of these trends during the latter part of the fractionation.

DISCLAIMER

Reference in this report to any specific product, process, or service is to facilitate understanding and does not necessarily imply its endorsement or favoring by the United States Department of Energy.

REFERENCES

- (1) Brule, M.R., Kumar, K.H., and Watanasiri, S. Oil & Gas Journal, February 11, 1985, 87.
- (2) Zosel, K. Angew. Chem., Int. Ed., 1978, 17(10), 702.
- (3) Brule, M.R., Rhodes, D.E., and Starling, K.E. Fuel, 1981, 60, 638.
- (4) Warzinski, R.P., and Ruether, J.A. Fuel, 1984, 63, 1619.
- (5) Warzinski, R.P. Paper presented at the ACS meeting, Fuel Division Symposium entitled Chemistry and Processing in Supercritical Fluids, Chicago, 1985.
- (6) Technical Progress Report by Catalytic, Inc., DOE Report No. DOE/PC/50041-19, July, 1983.
- (7) Bartle, K.D., and Zander, M. Erdoel Kohle, Erdgas, Petrochem. Brennst. Chem., January, 1983, 36, 15.
- (8) Reerink, H., and Lijzenga, J. Analytical Chemistry, 1975, 47(13), 2160.
- (9) Matsunaga, A. Analytical Chemistry, 1983, 55(8), 1375.
- (10) Vasilakos, N.P., Dobbs, J.M., and Parisi, A.S. Ind. Eng. Chem., Process Des. Dev., 1985, 24(1), 121.

TABLE 1. Analyses of the T102 Residuum and the Products of Fractional Distraction with Cyclohexane

	RUN 242 ^a T102 RESIDUUM	FRACTION NUMBER						RESIDUE
		1	2	3	4	5	6	
C	79.1	88.1	87.7	87.3	87.8	87.6	87.3	73.0
H	5.9	8.0	7.7	7.5	7.4	7.4	6.7	4.7
O ^b	4.0	2.6	3.2	3.7	3.2	3.3	4.0	4.6
N	1.3	0.8	0.9	0.9	1.0	1.0	1.2	1.5
S	1.0	0.5	0.5	0.6	0.6	0.7	0.8	1.9
ASH	8.7	---	---	---	---	---	---	14.3
H/C	0.89	1.08	1.05	1.02	1.00	1.01	0.91	0.77
M _N (VPO, 353 K, PYRIDINE)		389	413	433	481	588	638	c

^aApproximately 8 percent unconverted coal content. ^bDetermined by difference. ^cNot completely soluble.

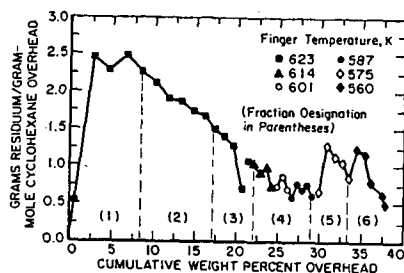


Figure 1. Summary of Fractional Distraction of Wilsonville T102 Residuum.

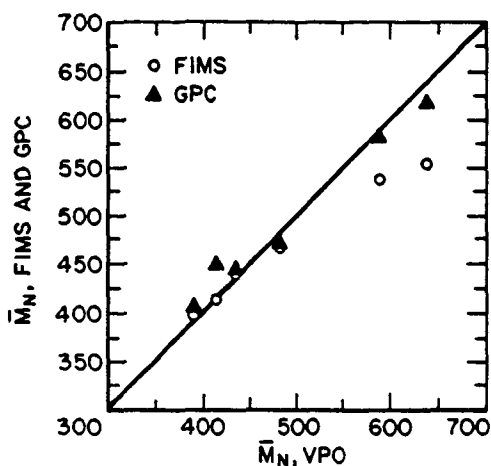


Figure 2. Comparison of Number Average Molecular Weight Determinations for Wilsonville Residuum Fractions Prepared by Fractional Destruction.

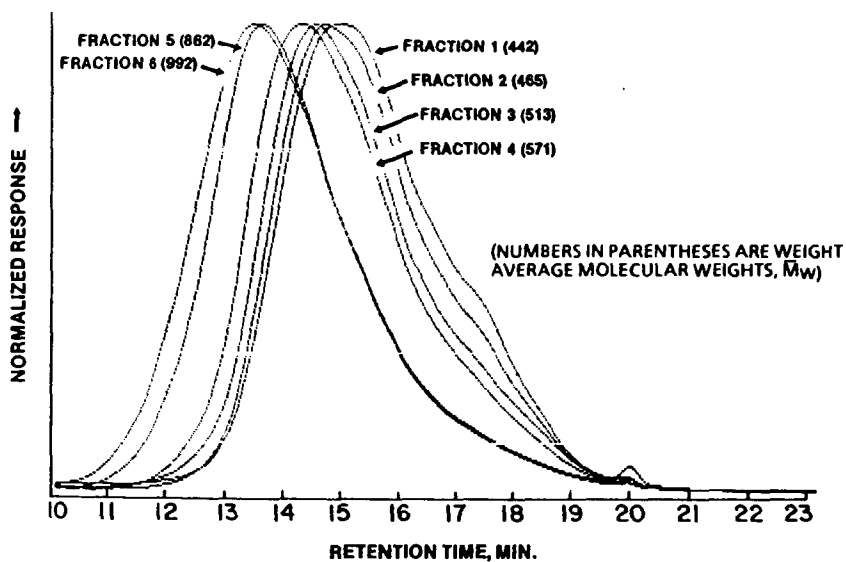


Figure 3. GPC of Wilsonville Residuum Fractions Prepared by Fractional Destruction.

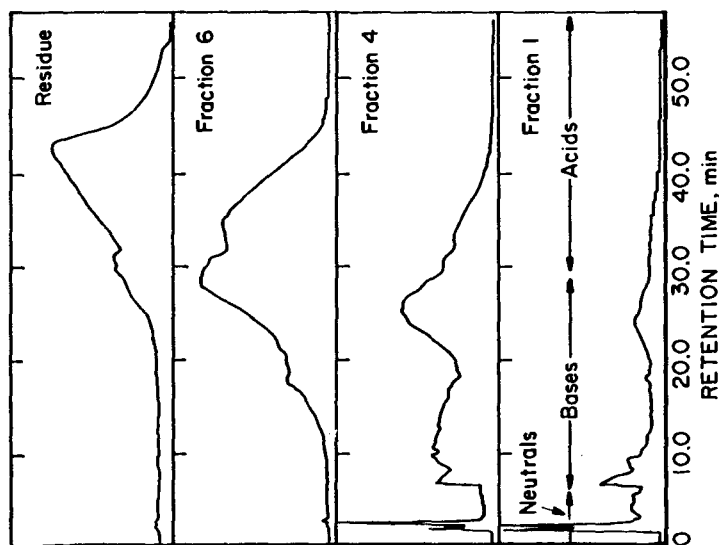


Figure 4. HPLC Separation of Wilsonville Residueum Fractions Prepared by Fractional Destruction.

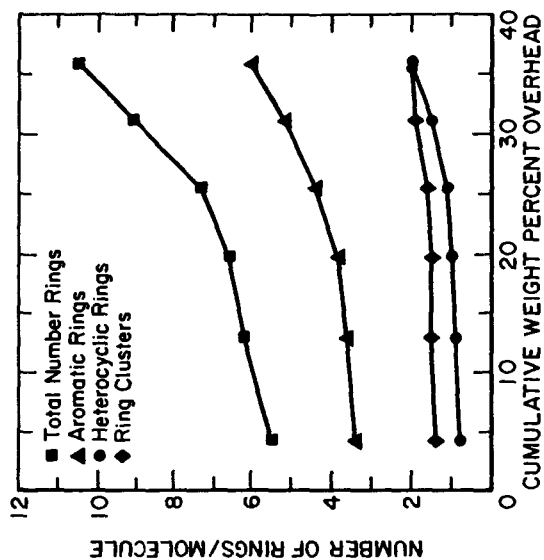


Figure 5. Summary of Average Molecular Ring Parameters for Wilsonville Residueum Fractions Prepared by Fractional Destruction.

Solubility and Viscosity Studies of Coal-Derived Preasphaltenes

Martin B. Jones and J. Karol Argasinski

University of North Dakota, Department of Chemistry
Grand Forks, North Dakota 58202, USA

INTRODUCTION

The high viscosity and poor solubility of coal-derived preasphaltenes (PA) are detrimental to the utility of those materials as fuel sources. These physical properties have been widely studied and may be ascribed to non-covalent interactions such as hydrogen bonding and charge transfer (1). For that reason, several researchers have examined dissolvability of coal-derived liquids or extraction and swelling of coal as a function of solvent parameters (2-11) and viscosity as a function of polarity and molecular weight (12-19).

Roy and coworkers (2) have studied extractability of coal at 35°C as a function of the dielectric constant of dipolar aprotic solvents. The results, however, were ambiguous: dimethylsulfoxide (DMSO, $\epsilon = 46.6$) was comparable to pyridine ($\epsilon = 12.3$) and better than ethylenediamine ($\epsilon = 14.2$). Hombach (3) determined solubility parameters for coals of differing ranks by measuring the spectrophotometric absorbance of extracts obtained by treating the coals with binary solvent mixtures. The parameters ranged from ca. 20.4 to 23.0 $\text{J}^{1/2} \text{cm}^{-3/2}$ and, as expected, showed little dependence on the chemical nature of the solvents in the mixture. Likewise, Weinberg and Yen (4) determined solubility parameters for a high volatile bituminous (hvb) coal by swelling measurements and for hvb coal liquefaction products by dissolvability in various solvents and solvent mixtures. Two maxima were observed in the swelling spectrum of the coal at 22.5 and 28.6 $\text{J}^{1/2} \text{cm}^{-3/2}$. Benzene-soluble liquefaction products (asphaltenes) exhibited maximum dissolvability in solvents (pure or mixtures) with δ values of ca. 19-26 $\text{J}^{1/2} \text{cm}^{-3/2}$. Benzene-insoluble liquefaction products (preasphaltenes) were dissolved to the greatest extent in solvents with δ values of ca. 23.5 $\text{J}^{1/2} \text{cm}^{-3/2}$. Marzec, et al. investigated possible correlations of solvent acceptor and donor numbers (AN and DN, respectively) with extractability (5-7) and swelling (7,8) of hvb coal at ambient temperatures. Both the extract yield and the swelling ratio increased with increases in the DN or DN-AN values of solvents.

Bockrath and coworkers have reported that aggregation of asphaltenes and preasphaltenes significantly contributes to the viscosity of coal-derived liquids (14). Further studies demonstrated that phenolic content, representative of intermolecular hydrogen bonding, was relatively more important than molecular weight to the viscosity of coal-derived asphaltenes (15). Likewise, Tewari, et al., from studies of coal liquids (16, 17) and model compounds (17), have shown that hydrogen bonding, primarily involving phenolic OH and nitrogen bases, is largely responsible for the viscosity of the coal liquids. Additional evidence for the importance of hydrogen bonding was provided by derivatization experiments. Gould, et al., found that silylation of coal liquefaction bottoms resulted in a four- to seven-fold reduction in viscosity (13). Patel, et al. reported a substantial increase in the dissolvability of solvent-refined lignite in nonpolar solvents after silylation or acetylation (20), attributable to disruption of intermolecular hydrogen bonding.

In connection with a study of intermolecular attractive forces in coal-derived liquids, we have measured the quantitative dissolvability of coal preasphaltenes in various solvents. Described herein are the results of those measurements and correlation of the data to five solvent parameters: δ , net hydrogen bonding index (ϕ), DN, DN-AN, and DN/AN. In addition, we have determined relative viscosities (η_{rel}) of native and acetylated PA samples of narrow molecular weight ranges and various model compounds. These measurements were carried out in an effort to determine the relative importance of molecular weight, hydrogen bonding and charge transfer to overall viscosity.

EXPERIMENTAL

The solvents employed in this study were reagent grade, obtained from commercial suppliers, and were used without further purification. A modified version of the solvent extraction procedure of Steffgen, et al. (21) was used to separate the preasphaltenes (THF soluble, toluene insoluble) from total liquefaction samples obtained from the University of North Dakota Energy Research Center. Room temperature acetylation of a sample of PA from run 80 was accomplished following the method of Baltisberger, et al. (22). Both acetylated and native PA-80 samples were separated into narrow molecular size fractions by preparative gel permeation chromatography on Bio beads S-X3 or S-X8.

The quantitative dissolvability of the preasphaltene samples was determined by mixing 30 mg of PA with 3 ml of solvent in a stoppered test tube in an ultrasonic bath for 1 minute. Vacuum filtration of the solution through either ordinary filter paper or 5.0 μ m type LS Millipore filters yielded the insoluble residue. Increasing the mixing time to 5 minutes did not increase the amount of preasphaltene dissolved.

Relative viscosities (η_{rel}) of the PA samples and model compounds were measured at 20°C in Canon-Fenske flow-type viscosimeters.

RESULTS AND DISCUSSION

Typical solubility parameter curves are obtained when the dissolvabilities of representative preasphaltenes are plotted as a function of Hildebrand solubility parameters (δ). The preasphaltenes exhibit maximum dissolvability in solvents with δ ca. 22-23 $\text{J}^{1/2} \text{cm}^{-3/2}$, in good agreement with the data of Hombach (3) and Weinberg and Yen (4). However, individual solvents with a range of solubility parameters from 18.4 to 24.5 $\text{J}^{1/2} \text{cm}^{-3/2}$ are good solvents (i.e., > 80% dissolvability) for the preasphaltenes. Two solvents, THF and DMF, are consistently well above the smooth curve that may be drawn through the solubility parameter data, reflecting the inability of the predominantly nonpolar Hildebrand solubility parameter to adequately account for their behavior as solvents for preasphaltenes. These results are not unexpected. Larsen, et al. (9) have observed that the swelling of pyridine extracted Illinois No. 6 coal by solvents capable of hydrogen bonding interactions cannot be accounted for solely by the nonpolar δ value. Excellent correlation was obtained between excess swelling (i.e., swelling beyond that expected on the basis of δ) and the heat of hydrogen bonding of the solvents with *p*-fluorophenol (9).

The net hydrogen bonding index (θ) (23) takes into account both the formation of new solvent-solute hydrogen bonds and the cleavage of existent solvent-solvent hydrogen bonds. Thus, methanol, a strongly hydrogen-bonded solvent, has a negative value of θ , indicating its tendency to maintain solvent-solvent hydrogen bonds rather than form new solvent-solute hydrogen bonds. The aprotic solvent DMF behaves in just the opposite fashion, since it cannot hydrogen bond to itself. Plots of PA dissolvability versus θ reveal a general trend of increasing dissolvability with increasing θ . However, this parameter may not be used as a reliable predictor of individual solvent effectiveness due to the excessive scatter of the data. For example, on the basis of θ values, acetone would be forecast to be comparable in dissolving power to THF, a prediction that is not borne out experimentally.

Other researchers have noted that dissolvability of coal-derived liquids is a function of more than one structural feature of the materials. For example, Snape and Bartle (24) have found that an empirically derived solubility parameter which incorporates terms for OH concentration (representing hydrogen bonding and acid-base complexation), ratio of bridgehead aromatic to total carbons (representing π - π complexation), and molecular weight clearly distinguishes solubility categories of oils, asphaltenes, and preasphaltenes. Baltisberger, et al. (25) have obtained good distinction between asphaltenes and preasphaltenes employing a two term parameter based on OH concentration (representing hydrogen bonding) and molar density of hydrogen (moles H/100 g sample) (representing π - π and dispersive interactions). Since

coal-deriv. liquids exhibit more than one type of solute-solute interaction (vide supra), solvents which completely dissolve these materials must be capable of more than one type of solute-solvent interaction. Undoubtedly, this is the reason for the failure of solubility parameters such as δ or θ , which are based primarily on one type of interaction, to adequately predict solvent effectiveness for dissolution of preasphaltenes.

Gutmann's donor-acceptor theory of solvent-solute interactions is nonspecific in nature (26). All types of interactions - hydrogen bonding, π - π charge transfer, n - π charge transfer, acid-base complexation, and others are included in the donor number (DN)-acceptor number (AN) concept. Thus, this theory is potentially more useful for predicting the extent of preasphaltene dissolvability in various solvents.

The dissolvability of the PA samples tends to increase with increasing DN values of the solvents, consistent with the results of Marzec and coworkers (5-8). However, considerable data scatter exists in plots of DN versus dissolvability. For example, even though DMSO has a substantially larger DN value than does THF (29.8 vs. 20.0, respectively), it is a poorer solvent than THF for the preasphaltenes. Thus, DN values may not be employed as the sole predictor of utility of a given solvent for preasphaltene dissolvability.

The results of Marzec, et al. (5-8) were interpreted in terms of the importance of solvent donor interactions with coal acceptor species (which are either part of the macromolecular network or molecules within the pore structures). Although no correlation between extractability and solvent AN values was found, these values were important in determining solvent efficiency. Solvents with large values for both DN and AN, e.g. water and methanol, were incapable of extracting the coal, presumably because solvent donor-acceptor interactions were greater than solvent donor-coal acceptor interactions. To incorporate the acceptor properties of the solvents, Marzec, et al. plotted extractability of coal vs. donor number minus acceptor number (DN-AN) values (5). The spread of data in the resulting graphs was substantial, particularly at larger DN-AN values. Our results for analogous plots, i.e., PA dissolvability vs. solvent DN-AN values, also disclosed an unsatisfactory amount of scatter. These values are, therefore, no more reliable for use in predicting solvent effectiveness for PA dissolution than are DN values.

A second parameter for assessing the relative importance of solvent donor numbers and acceptor numbers is the ratio of DN to AN. Qualitatively, at least, this ratio measures the strength of the solvent-solute interaction for the solvent acting as donor vs. acting as acceptor. For dissolution to occur, the solvent donor and acceptor sites must replace the solute donor and acceptor sites. Thus, this ratio may also be interpreted as giving information regarding the relative contributions of the donor sites and the acceptor sites in the solute to the overall intermolecular interactions. Plots of DN/AN vs. preasphaltene dissolvability are presented in Figure 1. They are similar in appearance to the Hildebrand solubility parameter plots, but with less scatter of data than the latter graphs. Furthermore, the range of values exhibited by good solvents (> 80% dissolvability) is smaller for the DN/AN plots (1.7-2.5) than for the solubility parameter plots (18.4-24.5 $\text{J}^{1/2} \text{ cm}^{-3/2}$). Figure 2 illustrates that DN/AN values may also be correlated to extractability or swelling of coal. As anticipated, the maximum extractability or swelling of coal and the maximum dissolvability of PA samples were exhibited by solvents with similar DN/AN values (ca. 2). This similar trend in preasphaltene dissolvability and coal extractability or swelling lends further credence to the suggestion of Weinberg and Yen (4) that molecules similar to those found in liquefaction products exist in virgin coal, probably within a macromolecular pore structure. The maximum of 2 observed in the DN/AN plot suggests that the contribution to the total intermolecular attractions of the preasphaltenes by electron donor sites (e.g. oxygen functionalities, electron-rich aromatic systems) outweighs the contributions by electron acceptor sites (e.g. electron deficient aromatic systems, phenolic protons). Whether this is the result of the relative number of donor vs. acceptor sites or the strength of the sites as electron donors or acceptors is unclear.

The value of DN/AN for solvents seems to be more reliable as a predictor of solvent effectiveness for preasphaltenes, coal extractability or coal swelling than are DN, DN-AN, θ , or δ . These results, then, are in agreement with the observations of Snape and Bartle (24) and Baltisberger, et al. (25), since the DN/AN parameter encompasses more than one type of intermolecular interaction.

Because of the nonspecificity of the DN/AN parameter, little information concerning the relative contributions of hydrogen bonding and charge transfer to the total intermolecular interactions of the PA samples may be gleaned from the dissolvability study. Previous researchers have demonstrated that viscosity measurements can provide useful data concerning intermolecular interactions, particularly hydrogen bonding (12-19). Therefore, a preliminary investigation focusing on viscosity measurements of a preasphaltene sample and model compounds was undertaken. Actual viscosities of the materials were not determined, since the preasphaltenes and most of the model compounds were solids at room temperature. Rather, viscosities of solutions of the samples in THF were measured relative to that of the pure solvent (η_{rel}).

To assess the importance of molecular weight to relative viscosity, a preasphaltene from run 80 (PA80) was separated into narrow molecular weight fractions by preparative GPC on Biobeads S-X3 and S-X8. The relative viscosities of the fractions vs. concentration are illustrated in figure 3. The expected trend, i.e., an increase in relative viscosity with an increase in molecular weight, was observed (cf. curves a, f, h, i), with one exception. The fraction with the lowest molecular weight (6-N) exhibited the second largest increase in relative viscosity (curve e). This result was suggestive of a strong interaction between THF and fraction 6-N. To test the nature of the interaction, PA80 was subjected to acetylation at room temperature, according to the procedure of Baltisberger, et al. (22). Following separation by preparative GPC, the relative viscosities in THF were again measured. Fractions 1 (highest molecular weight) and 6 (lowest molecular weight) exhibited the largest changes upon acetylation (cf. curves a and b, curves e and g). The intermediate molecular weight fractions evinced slight or no changes in relative viscosity. Derivatization of coal-derived liquids by acetylation has previously been demonstrated to disrupt intermolecular hydrogen bonding (20). Thus, the substantial decreases in relative viscosities for fractions 1 and 6 may be attributed to a diminution in the number of hydrogen bond donating moieties in the acetylated samples. These results argue for hydrogen bonding to be of greater importance than molecular weight for viscosity of preasphaltenes, in agreement with previous reports (15). Further evidence for this interpretation is the observation that the relative viscosity of a sample of polystyrene (which cannot hydrogen bond to THF) with $M_w = 2500$ is less than that of fraction 1-N ($M_w = 1950$).

From the preasphaltene samples, we were not able to assess the influence of charge transfer on viscosity. Thus, relative viscosities of a carefully selected set of model compounds in THF were measured (figure 4). In the ensuing discussion, all comparisons will be made at a constant concentration of 0.25 M. Charge transfer between the nonbonding electrons of the THF oxygen and the π electron system of the model compounds does seem to play at least a minor role in determining relative viscosities. The greater relative viscosity of naphthalene (curve h) compared to tetralin (curve i) may be ascribed to the enhanced π system of naphthalene. One might be tempted to apply the same reasoning to the observed increase in relative viscosity upon going from naphthalene (curve h) to phenanthrene (curve d) to pyrene (curve b). A plot of relative viscosity vs. reduction potentials (a measure of the ability of the aromatic molecule to act as an electron acceptor in a charge transfer complex) for naphthalene, phenanthrene and pyrene reveals a general trend of increasing relative viscosity as the reduction potential becomes more positive (i.e., as the molecule becomes easier to reduce). However, the data are scattered on either side of a least-squares line. In a homologous series, an increase in molecular weight is accompanied by an increase in viscosity, due to increased London (dispersion) forces. Thus, molecular weight should also be considered. A plot of relative viscosity vs. molecular weight for naphthalene, phenanthrene and pyrene is linear and

contains less scatter of data than does the reduction potential plot. Thus, molecular weight is probably more important in determining relative viscosity than is charge transfer.

The effect of hydrogen bonding on relative viscosity can also be seen in figure 4. 2-Naphthol (curve c) has a much greater relative viscosity than does 2-methoxynaphthalene (curve e). The difference between the two arises from the ability of 2-naphthol to donate hydrogen bonds to THF. Furthermore, hydrogen bonding must play a more important role in determining the relative viscosity of the model compounds than does charge transfer. This can be seen by comparing the relative viscosity of quinoline (curve g) to 1,2,3,4-tetrahydroquinoline (THQ, curve f). Quinoline may be considered analogous to naphthalene, since both possess two fused aromatic rings, and THQ to tetralin, since both possess a reduced ring fused to an aromatic ring. However, unlike the naphthalene-tetralin pair, quinoline possesses a lesser relative viscosity than THQ. This result must arise from the hydrogen bond donating capability of THQ.

In summary, the greatest influence on relative viscosity of model compounds and preasphaltenes in THF appears to be hydrogen bonding. Second in influence is molecular weight, a measure of the extent of London forces. Finally, charge transfer seems to be only a minor contributor to overall relative viscosity of the samples.

ACKNOWLEDGEMENTS

The authors gratefully acknowledge the financial support of the U.S. Department of Energy (Grant No. DE-FG22-83PC60808), helpful discussions with Professors R. J. Baltisberger, V. I. Stenberg, and N. F. Woolsey, and the University of North Dakota Energy Research Center for providing total liquefaction samples and analytical data.

REFERENCES

1. For a recent review, see Stenberg, V.I., Baltisberger, R.J., Patel, K.M., Raman, K. and Woolsey, N.F. in "Coal Science"; Gorbaty, M.L., Larsen, J.W. and Wender, I., Eds.; Academic Press: New York, 1983; Vol. 2, Chapter 3.
2. Roy, J., Banerjee, P. and Singh, P.N. Indian J. Technol. 1976, 14, 298.
3. Hombach, H.-P. Fuel 1980, 59, 465.
4. Weinberg, V.L. and Yen, T.F. Fuel 1980, 59, 287.
5. Marzec, A., Juzwa, M., Betlej, K. and Sobkowiak, M. Fuel Process. Technol. 1979, 2, 35.
6. Pajak, J., Marzec, A. and Severin, D. Fuel 1985, 64, 64.
7. Marzec, A. and Kisielow, W. Fuel 1983, 62, 977.
8. Szeliga, J. and Marzec, A. Fuel 1983, 62, 1229.
9. Larsen, J.W., Green, T.K. and Chiri, I. Proc. Int. Conf. Coal Science (Pittsburgh, PA) 1983, 277.
10. Liotta, R., Brown, G. and Isaacs, J. Fuel 1983, 62, 781.
11. Green, T.K., Kovac, J. and Larsen, J.W. Fuel 1984, 63, 935.
12. Sternberg, H.W., Raymond, R. and Schweighardt, F.K. Science 1975, 188, 49.
13. Gould, K.A., Gorbaty, M.L. and Miller, J.D. Fuel 1978, 57, 510.
14. Bockrath, B.C., LaCount, R.B. and Noceti, R.P. Fuel Process. Technol. 1977/1978, 1, 217.
15. Bockrath, B.C., LaCount, R.B. and Noceti, R.P. Fuel 1980, 59, 621.
16. Tewari, K.C., Hara, T., Young, L.-J.S. and Li, N.C. Fuel Process. Technol. 1979, 2, 303.
17. Tewari, K.C., Kan, N.-s., Susco, D.M. and Li, N.C. Anal. Chem. 1979, 51, 182.
18. Young, L.-J.S., Hara, T. and Li, N.C. Fuel 1984, 63, 816.
19. Young, L.-J.S., Yaggi, N.F. and Li, N.C. Fuel 1984, 63, 593.
20. Patel, K.M., Stenberg, V.I., Baltisberger, R.J., Woolsey, N.F. and Klabunde, K.J. Fuel 1980, 59, 449.
21. Steffgen, F.W., Schroeder, K.T. and Bockrath, B.C. Anal. Chem. 1979, 51, 1164.
22. Baltisberger, R.J., Patel, K.M., Woolsey, N.F. and Stenberg, V.I. Fuel 1982, 61, 848.

23. Nelson, R.C., Figurelli, V.F., Walsham, J.G. and Edwards, G.D. J. Paint Technol. 1970, 42, 644.
24. Snape, C.E. and Bartle, K.D. Fuel 1984, 63, 883.
25. Baltisberger, R.J., Woolsey, N.F., Schwan, J.F., Bolton, G and Knudson, C.L. Am. Chem. Soc. Div. Fuel Chem. Prepr. 1984, 29(5), 43.
26. Gutmann, V. "The Donor-Acceptor Approach to Molecular Interactions", Plenum Press, New York, 1978.

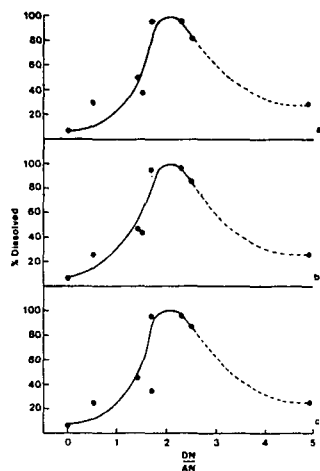


Figure 1. Dissolvability of preasphaltenes as a function of donor number divided by acceptor number (DN/AN) values of solvents. (a) Run 93; (b) Run 98; (c) Run 99.

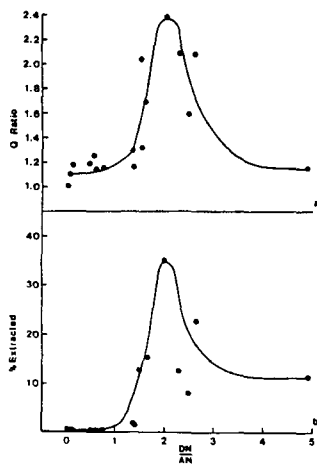


Figure 2. (a) Swelling of coal as a function of DN/AN values of solvents. Data from Reference 8. (b) Extractability of coal as a function of DN/AN values of solvents. Data from Reference 5.

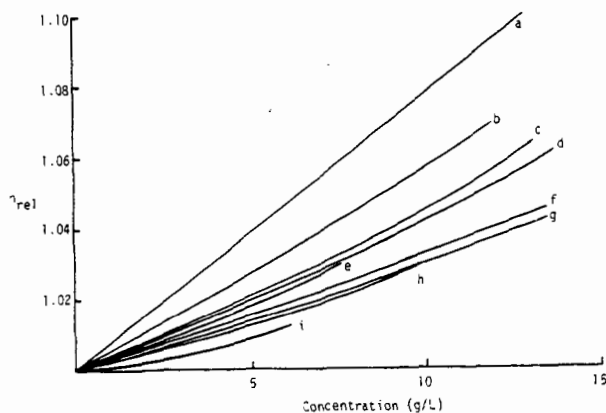


Figure 3. Relative viscosity of fractionated PABO (native, N, and acetylated, A) as a function of concentration. Molecular weights were determined by GPC. (a) fraction 1-N, $\bar{M}_w = 1950$; (b) fraction 1-A, $\bar{M}_w = 1800$; (c) unfractionated PABO-N; (d) unfractionated PABO-A; (e) Fraction 6-N, $\bar{M}_w = 135$; (f) fractions 2-N, $\bar{M}_w = 1050$ and 2-A, $\bar{M}_w = 950$; (g) fractions 3-A, $\bar{M}_w = 670$ and 6-A, $\bar{M}_w = 120$; (h) fraction 3-N, $\bar{M}_w = 720$; (i) fractions 5-N, $\bar{M}_w = 250$ and 5-A, $\bar{M}_w = 240$.

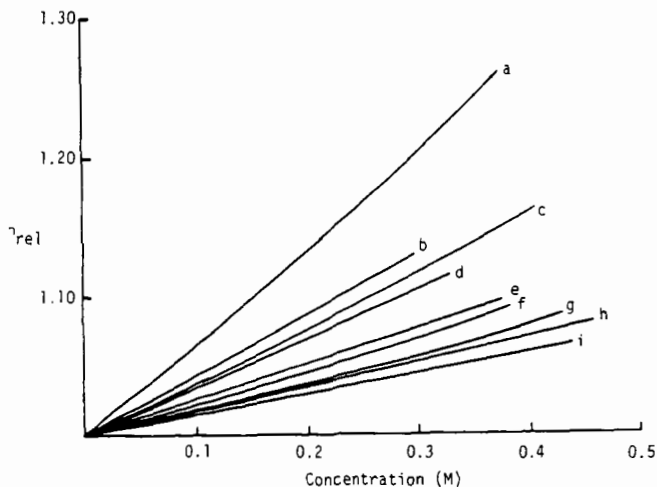


Figure 4. Relative viscosity of model compounds as a function of concentration. (a) 2,7-dihydroxynaphthalene; (b) pyrene; (c) 2-naphthol; (d) phenanthrene; (e) 2-methoxynaphthalene; (f) 1,2,3,4-tetrahydroquinoline; (g) quinoline; (h) naphthalene; (i) tetralin.

POLYSTYRENE AND POLY(VINYL NAPHTHALENE) OLIGOMERS
FOR MOLECULAR WEIGHT ANALYSIS OF COAL LIQUIDS

R.J. Baltisberger, M.B. Jones and J.F. Schwan

Department of Chemistry, University of North Dakota,
Grand Forks, ND 58202

INTRODUCTION

Knowledge of the structure of coal derived asphaltenes and preasphaltenes is of significant value because of the current interest in conversion of coals to liquid fuels and/or chemical feedstocks. Considerable effort has been devoted to analyses of the chemical composition and to the postulation of possible structures of these complex aromatic materials (1-3). Physical properties of coal derived liquids (CDL) such as viscosity, solubility, and melting points are to a large extent determined by chemical composition. Molecular size and the distribution of sizes of CDL are also of critical importance to the aforementioned properties. Snape and Bartle (4) have published a paper describing an empirical solubility parameter which relates the average molecular weight, the wt % acidic OH (a measure of polarity) and ratio of junction aromatic carbons to total carbon (a measure of π - π and dispersive interactions) to solubilities of CDL in pentane, benzene and pyridine.

The techniques most commonly used to measure average molecular weights are vapor pressure osmometry (VPO) and gel permeation chromatography (GPC). VPO yields only a number average molecular weight value (M_n) while GPC techniques can give both M_n and a weighted average molecular weight (M_w). Measurement of M_n and M_w by GPC techniques requires knowledge of the detector response on a per weight basis over the range of masses studied. A constant absorbance per gram of material would be most desirable if, for example, a UV detector is used. A second requirement, which is the focus of this report, is that suitable standards be available for the calibration of the GPC column. Mulligan et al. (5) showed that narrow polystyrene fractions ($M_w/M_n < 1.10$) and a series of polynuclear standards without highly condensed structures can be used to calibrate an analytical GPC column for use with the analysis of super-critical gas extracts of coal. It was concluded that the above standards gave reliable molecular weight values for coal derived mixtures containing cata condensed aromatics with alkyl or aryl-aryl linkages between aromatic systems.

Our study was initiated to determine what types of standards would be suitable for the GPC analysis of highly condensed peri aromatics that would result during coal liquefaction under SRL or donor solvent conditions. Analysis of highly condensed aromatic oligomers synthesized in this study indicates that these molecules are subject to retardation and considerable scatter on GPC columns relative to polystyrene standards. The retardation does not appear to be a function of absorption, but rather a length reduction of the oligomer due to aromatic condensation. The GPC response can be made linear by multiplication of the molecular weight by H_{aru}/C_{ar} (a measure of aromatic condensation). These size corrected molecular weights are linear with retention volume, but are not colinear with the retention volume of polystyrene or poly(vinyl naphthalene) (PVN) oligomers of narrow molecular ranges ($M_w/M_n < 1.1$). Coal derived liquids from SRC-I or SRC-II type processes have H_{aru}/C_{ar} values more like the highly condensed aromatics synthesized in our study. Narrow molecular weight fractions of these SRC materials are retarded relative to polystyrene and poly(vinyl naphthalene) standard responses. The response of SRC materials are colinear with the response of highly condensed aromatic standards when the "corrected molecular weight" is plotted versus retention volume.

EXPERIMENTAL

Materials

Polystyrene standard oligomers were obtained from Polysciences, Inc. Other standard compounds and poly(vinylnaphthalene) oligomers were synthesized from various starting materials. The details of these syntheses are described in previous reports (6). Poly(vinyl naphthalene) and polystyrene oligomers were synthesized by anionic polymerizations in diethyl ether initiated by *n*-butyllithium at a proper ratio of initiator to substrate to establish the polymer size. Solvent refined lignite (SRL) asphaltene and preasphaltene samples were obtained from the University of North Dakota Energy Research Center. The samples were produced using synthesis gas or hydrogen at 27.6 MPa and 460°C with or without recycle of the vacuum bottoms of the product. The lignite used was a North Dakota seam, Beulah three.

Preparative Scale GPC

Prior to GPC separation all the SRL samples were acetylated in order to convert the hydroxyl sites to their acetate forms. The SRL asphaltenes and preasphaltenes were further separated into narrow molecular weight fractions using a 50 mm id x 120 cm glass column packed with Bio-Beads S-X3 (200-400 mesh) styrene-divinyl benzene. Freshly distilled toluene or pyridine was used as the solvent. The polydispersity indices for the SRL fractions, M_w/M_n , were measured to be in the range 1.05 to 1.15 using the analytical chromatographic analyses described below. Polystyrene and poly(vinyl naphthalene) oligomers were also isolated into narrow molecular weight ranges using benzene as the solvent with S-X8 or S-X3 columns. Elemental analyses of the fractions were performed by Spang Microanalytical Laboratory and number average molecular weights were determined in our laboratory using a Wescan Model 117 Vapor Pressure Osmometer. In normal runs, 2-3 concentrations over the range 1 to 50 g/kg of pyridine were employed for extrapolation to infinite dilution.

Analytical Scale GPC

Analytical scale GPC analyses (HPLC) were carried out using three 10 nm and one 50 nm μ -styragel columns in series, with THF (UV grade, Burdick and Jackson) as the mobile phase. A Laboratory Data Control Model 1205 UV Monitor was used as the detector (254 nm) and a Waters Model UK6 injector was used to inject samples of about 10 μ l at 10 mg/ml. Samples were filtered across a 0.5 μ m millipore filter prior to injection. The flow rate was usually maintained at 1.0 mL/min to prevent pressures in excess of 1000 psig.

RESULTS AND DISCUSSION

The influence of aromatic ring condensation is illustrated in Figure 1a for plots of logarithm MW versus length of model compounds and polystyrene. The model compounds consist of aromatics from benzene to pyrene with methylene, ether or aryl-aryl linkages. The length was estimated using Dreiding stereomodels assuming the oligomers are fully extended in the THF solvent used in the GPC experiments. The corrective nature of the H_{ar}/C_{ar} (fraction of edge aromatic carbons) is shown in Figure 1b. The slope changes from 0.024 ± 0.003 in Figure 1a to 0.026 ± 0.0015 in Figure 1b. Polystyrene, which is a different shaped polymer with benzene pendant groups follows its own linear plot (slope = 0.015 ± 0.0035). Figure 2a illustrates the log MW versus retention volume for both polystyrene and the model compounds. Note the highly condensed model compounds lie above the polystyrene line, which is consistent with a reduced volume or length per molecule. The inclusion of the H_{ar}/C_{ar} term with MW greatly reduces the scatter of the models. The slope changes from -0.049 ± 0.008 in Figure 2a to -0.058 ± 0.004 in Figure 2b. The uncertainties reported are at the 90% confidence levels. The uncertainty of the models are reduced by 50% by use of the factor H_{ar}/C_{ar} .

That SRL narrow molecular weight fractions tend to elute at longer times relative to polystyrene is illustrated in Figure 3a. This retardation would be consistent with these SRL samples being so condensed that the length of the molecules has been shortened relative to the polystyrene standards. The application of H_{aru}/C_{ar} to the MW term drops the SRL compounds below the polystyrene line as shown in Figure 3. However, the scatter is improved with SRL slopes of -0.067 ± 0.005 in Figure 3a to -0.061 ± 0.003 in Figure 3b. The uncertainty is reduced because the highest and lowest MW fractions are the most condensed for these SRL samples. Mulligan et al. (5) reported that polystyrene and not highly condensed aromatic model compounds could be used to calibrate GPC columns for super-critical gas (SCG) extracts of coal. The aromatic portions of SCG extracts would not be nearly as condensed as the recycle SRL samples used in our work.

Two additional types of oligomers are being synthesized and studied. First, poly(vinyl naphthalene) and poly(vinyl phenanthrene) oligomers from 300 to 3000 g/mole are being prepared to test the significance of the length factor. The length of these oligomers is predominantly determined by the alkyl chain, as with polystyrene. A second set of oligomers of polynuclear aromatic moieties connected by aryl-aryl, methylene and ether linkages in the range 600 to 3000 g/mmol are being synthesized to extend the range of the highly condensed oligomers.

Four poly(vinyl naphthalene) oligomers from 300 to 2000 g/mol when plotted on Figure 2a fall on the same line as polystyrene. Poly(vinyl naphthalene) oligomers are shorter molecules with less molar volume than a polystyrene oligomer of similar molecular weight. Thus, one would predict that poly(vinyl naphthalene) should elute at longer retention times relative to polystyrene, contrary to the observed results. The data suggest that the PVN oligomers are associated with more THF molecules than are the polystyrene oligomers, giving a larger volume (or length) to the PVN materials or that neither oligomer is fully extended in the THF solvent. Further studies will be carried out to test these hypotheses.

ACKNOWLEDGEMENT

The research was supported by DOE through contract number DE-FG22-81PC40810. We thank Sandra Wagner and Dr. S. P. Rao for synthesis of some of the model compounds.

REFERENCES

1. Uden, P.C.; Siggia, S.; Jensen, H.B. "Analytical Chemistry of Liquid Fuel Sources", ACS, Adv. in Chem. Series, 170; Washington, D.C., 1978.
2. Bunger, J.W.; Li, N.C. "Chemistry of Asphaltenes", ACS, Adv. in Chem. Series, 195; Washington, D.C., 1981.
3. Davidson, R.M. "Coal Science", Vol. I; Gorbaty, M.L.; Larsen, J.W.; Wender, I., Eds.; Academic Press: New York, 1982; Chapter 4.
4. Snape, C.E.; Bartle, K.D. Fuel, 1984, 63, 883.
5. Mulligan, M.; Bartle, K.D.; Gibson, C.; Taylor, N.; Mills, D. "Abstract of Papers", Int. Conf. on Coal Science, Duesseldorf, FRG, Sept. 1981; pp 882, Paper E-15.
6. Baltisberger, R.J.; Jones, M.B. DOE Report, PC/40810-5, April, 1983; *ibid*, PC/40810-3, Sept., 1982.

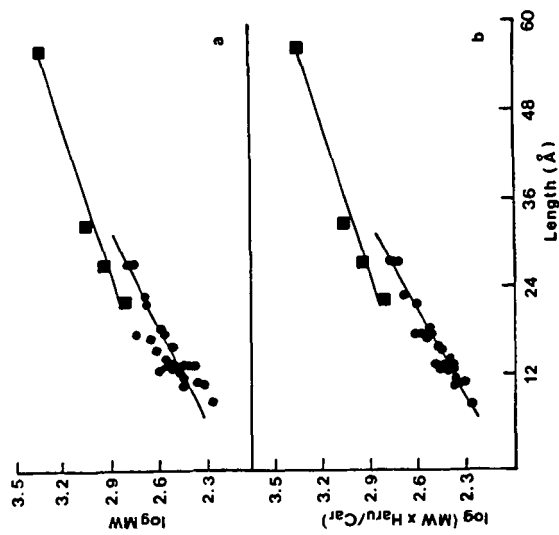


Figure 1. Molecular Weight versus Length.
Polystyrene (■) Model Compounds (○)

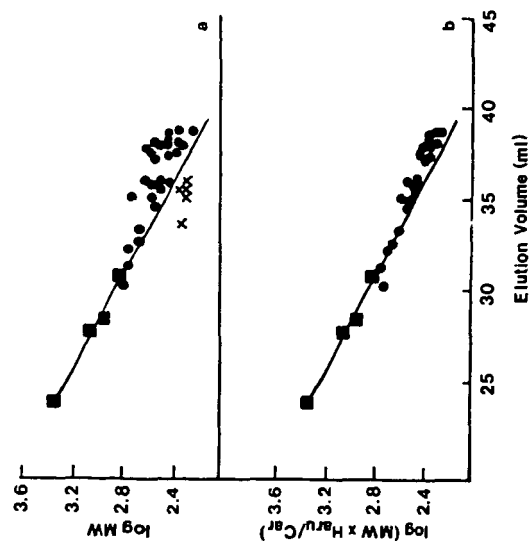


Figure 2. Molecular Weight and Elution Volume Response.
Polystyrene (■) Model Compounds (○)

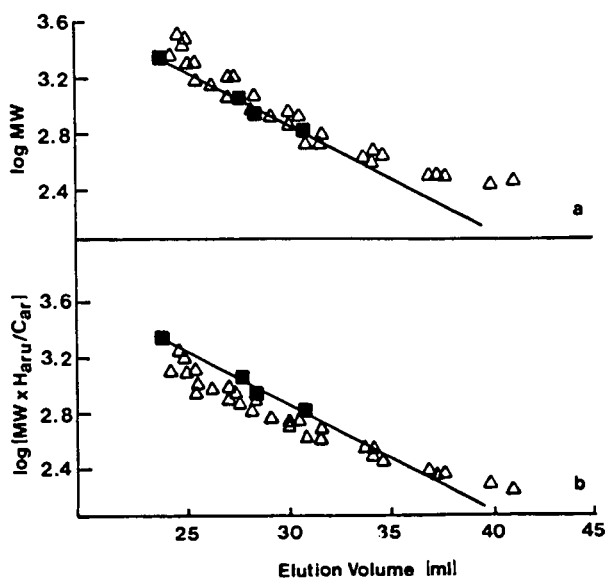


Figure 3. SRL Response.
Polystyrene (■) SRL (Δ)

COAL EXTRACTION BY COMPRESSED FLUIDS: A NEW PARAMETER

Mohamed A. Serageldin and Abdullatef I. Hamza

Michigan Technological University
Chemistry and Chemical Engineering
Houghton, Michigan 49931

INTRODUCTION

Extraction of coal and similar materials with dense gases may become an important way of obtaining organic chemicals. The resulting hydrocarbon residue is also a better fuel. Many studies [1-17] were undertaken to understand the effect of a solvent on hydrocarbon yield and nature of the extract; the yield was found to depend on pressure (or density), temperature and extraction time.

To evaluate the potential of a solvent under near liquid densities, a number of parameters were adopted:

1. The first, a gas solubility parameter, which has the following form [15].

$$\delta_g = 1.25 P_c^{\frac{1}{2}} \cdot \rho_g / \rho_l \quad (1)$$

$$= \delta_l \cdot \rho_g / \rho_l \quad (2)$$

where P is the critical pressure, ρ_g gas density, ρ_l liquid density of δ_l liquid density and δ_l the liquid solubility parameter which is constant for a given material [18,19]. Equation (1) was used by several researchers to express the effectiveness of a number of solvents under dense gas [11, 15, 20, 21] and dilute gas [14, 22] conditions. Vasilakos et al. [11] showed that for pure paraffins tested at one temperature there is a linear relationship between yield and increase in solvent molecular weight. However, such a correlation is reduced when different groups of solvents are lumped together [20]. On the otherhand, for a pure solvent, a parabolic expression is necessary to represent the change in yield with solubility parameter i.e. the yield decreased after a point with increase in the solubility parameters. The occurrence of a maximum in the yield curve was also observed when extraction was performed with dilute gases [14,22]. The maximum can be accounted for using equation (3) which was originally derived by Hilderbrand and Scott [18,19] and adapted for gases [16].

$$\phi_1^2 v_2 (\delta_2 - \delta_1)^2 = -RT \ln \frac{Y_2}{Y_1} \quad (3)$$

where ϕ , V and Y refer respectively to volume fraction, molar volume and mole fraction in the gas phase. The subscripts 1 and 2 refer to solvent and solute, respectively. Accordingly, a maximum solubility would occur when $\delta_1 = \delta_2$. This did not occur, however in the case of mixed solvents [14,22].

2. The second parameter is derived using the virial equation of state after making a number of approximations [23,24]:

$$\ln \frac{C_2}{C_2^0} = (V_2 - 2B_{12})/V \quad (4)$$

where C_2 is the concentration of the solute in the vapor solvent mixture and C_2^0 that in the absence of the solvent gas both recorded at the same temperature. V and V_2 refer respectively to the molar volume of the mixture and solute. B_{12} is the interaction second virial coefficient.

$$1/2 B_{12} = (B_{11} + B_{22})/2$$

$$\text{then } \ln \frac{C_2}{C_2^0} = \frac{(V_2 - B_{22}) - B_{11}}{V} \quad (5) \text{ [ref.1]}$$

B_{11} and B_{22} are the second virial coefficients for solvent and solute respectively. They represent interactions of pairs of like molecules. They are a function of temperature only. A plot of $-B_{11}$ against extraction yield for a group of solvents, including alcohols, aromatics and paraffins, resulted in a maximum in the yield curve which seems to shift to lower values of $-B_{11}$ with temperature. Fong et al. [1] attributed the lower yield at the higher values of $-B_{11}$ to the size and shape of the solvent molecules.

3) Other parameters have also been suggested:

For example, the critical temperature was reported [10,12,24] to follow closely extraction yield. Kershaw [10] suggested the use of the product of the boiling temperature T_b (K) and the density of solvent at 20°C.

A NEW PARAMETER

A theoretical description of the factors that control the solubility of a hydrocarbon material in a dense gas is rather involved and will invariably contain functions that will be either difficult to measure experimentally or to calculate. Therefore, an intuitive approach was preferred for the sake of simplicity.

There are numerous illustrations in the literature that point to the dependence of the amount of a solute, Y_2 , dissolved in a solvent on both the density, ρ , and temperature, T , of a dense gas i.e.:

$$Y_2 = \psi(\rho, T) \quad (6)$$

If a generalized relationship is to be found between temperature and density the above physical properties should be written in their reduced form according to the principle of corresponding states [25].

$$\text{Hence } Y_2 = \psi(\rho_r, T_r, \omega) \quad (7)$$

The acentric factor, ω , by Pitzer et al. [25] was included in equation (7) to account for the deviation of a complex fluid from simple fluid behavior due to intermolecular interactions.

Since an increase in pressure will increase the density while an increase in temperature produces the opposite effect, the following dependence of Y_2 on the reduced density and temperature is proposed [$\rho_r = 1/V_r$]:

$$Y_2 = A \exp(-E/RT) \cdot \left(\frac{\omega}{V_r T_r} \right)^n \quad (8)$$

where A and n are dimensionless constants; E is the activation energy; R , is the gas constant; T is the absolute temperature; ω is the acentric factor; V the reduced molar volume of the gas mixture and T_r is the reduced temperature. The exponential term was introduced to account for the effect of temperature on the distribution of the solvent molecules.

DISCUSSION

To test the model the experimental results for three combination of solvent-solute system [7,17] were compared: (i) Naphthalene-fluoroform, (ii) Naphthalene-carbon dioxide and (iii) Phenanthrene-carbon dioxide. This choice enabled us to evaluate the effect of the solvent tested on the values of E/R and the constant A on the one hand and on the suitability of the proposed form of equation (8) on the other hand. However, the predicted values of Y_2 will also depend on the success of the Soave-Redlich Kwong [26] equation which was used to evaluate the molar volume V and to a lesser extent on the values of the critical properties, (Tables 1 to 4). A sample of the results for the model compounds is shown in Tables 5 and 6. The values of A and E/R in equation (8) were obtained by regression analysis and are given in Table 7.

Several points are worthy of note:

- 1- A and E/R for fluoroform are lower than those for carbon dioxide.
- 2- The values of Y_2 in a phenanthrene-carbon dioxide system were better correlated by equation (8) than in the Naphthalene carbon dioxide system.
- 3- In the Naphthalene-fluoroform system the first set of data at each temperature (e.g. $P = 60.5 \times 10^5 \text{ N/m}^2$ in Table 5) were omitted because of the large deviation. This did not significantly alter the values of A, E/R or r.

Tables 8-11 shows the results for coal. Because extraction was performed at only one temperature, equation (8) was rewritten as follows:

$$\% \text{ Ext.} = a + b. \omega/V T_r \quad (9)$$

The predicted values for the paraffins and aromatics (Tables 8 and 10) are far better than those for the alcohols (Table 9). This is also indicated by the higher values of r in Table 11.

At this stage it is appropriate to compare the predictions with equation (9) to those involving other parameters mentioned before. Table 12 shows the results when the solubility parameter in equation (1) was compared to extraction for the same solvent groups studied in Table 11. The results show that both $\omega/V T_r$ and δ represent well the paraffins and alcohols but that the first parameter provides a better indicator for the aromatics. The same can be said about T_b and of a number of other parameters (see Table 13). The suggestion by Kershaw [10] that the product of T_b and the density at 20°C is a useful parameter to estimate conversion is interesting considering that T_b is proportional to the enthalpy of vaporization, ΔH_v , at 298 K [19]. For a large number of non polar hydrocarbons boiling between 285 and 408 K, the relationship with extraction was as follows:

$$\% \text{ Ext.} = \frac{T_b}{V} = \frac{140 + 0.0269\Delta H_v}{V}; r = 1.0 \quad (10)$$

which explains the high correlation coefficient recorded in Table 13. The constants in equation (10) will depend on the solvent group regressed. Considering that ΔH_v at the critical point is zero, the use of an equation containing room temperature parameters to correlate together data of several groups of supercritical solvents would at first seem questionable unless a significant part of solute was extracted during the heating up stage i.e. below supercritical

conditions. However, most of the parameters discussed in this report can in one case or another be linearly related to extraction yield:

$$\% \text{ Ext.} = a + b \theta \quad (11)$$

where θ can be visualized to have the form of the cohesive energy density or internal pressure as defined in Hilderbrand and Scott [18,19].

$$\theta = \frac{c}{V} \quad (12)$$

Therefore, for a function to be successful the value of c should closely represent molecular interaction which explains the success of room temperature parameters and of simple physical parameters for predicting dense extraction in the case of one group of solvents and its failure when different mixed groups are analyzed together.

CONCLUSIONS

1. A new parameter was presented which predicts well the effect of varying the temperature and pressure of a pure solvent on yield, using model compounds.
2. In the case of coal the parameter $\omega/V T_c$ was consistently highly correlated with percent extraction, whereas the linear correlation with δ was lower in the case of the aromatics. It was also lower in the case of the alcohols with $-B_{11}$.
3. Parameters based on one or two physical properties (e.g. T_b , T_c) may be useful in predicting the trend produced by one group of solvents. However it is not wise to generalize their usefulness for groups of solvents.

REFERENCES

1. Fong, W. S., Chan, P. C. F., Pichaichanarong, Corcoran, W. H. and Lawson, D., Chapter 17, pp. 377-394, "Chemical Engineering at Supercritical Fluid Conditions" (Eds. Paulaitis et al.), Ann Arbor Science Publishers, (1983).
2. Scarrah W. P., Chapter 18, pp. 395-407 "Chemical Engineering at Supercritical Fluid Conditions" (eds. Paulaitis et al.) Ann Arbor Science Publishers, (1983).
3. Monge, A. and Prausnitz, J. M., Chapter 7, pp. 159-171 "Chemical Engineering at Supercritical Fluid Conditions" (Eds. Paulaitis et al.) Ann Arbor Science Publishers, (1983).
4. Paulaitis, M. E., Mc Hugh, M. A., and Chai, C. P., Chapter 6, pp. 139-158 "Chemical Engineering at Supercritical Fluid Conditions" (Eds., Paulaitis et al.) Ann Arbor Science Publishers, (1983).
5. Olcay, A., Tugrul, T., and Calimli, A., Chapter 19, pp. 409-417 "Chemical Engineering at Supercritical Fluid Conditions" (Eds. Paulaitis et al.) Ann Arbor Science Publishers, (1983).
6. Pullen J. R. "Solvent Extraction of Coal", Report number ICTIS/TRIS November 1981, IEA Coal Research, London.
7. Reid, R. C., and Schmitt, W. J., "The Influence of the Solvent Gas on Solubility and Selectivity in Supercritical Extraction". Paper presented at the Annual meeting of AIChE, San Francisco, Nov. 25-30, 1984.
8. Kim, S. and Johnston, K. P., "Theory of the pressure Effect in Dense Gas Extraction". Paper presented at the Annual meeting of AIChE, San Francisco, Nov. 25-30, 1984.
9. Sunol, A. K. and Beyer, G. H. "Mechanism of Supercritical Extraction of Coal". Paper presented at the Annual Meeting of AIChE, San Francisco, Nov. 25-30, 1984.
10. Kershaw, J. R., Fuel Processing Technology, 5, pp. 241-246 (1982).
11. Vasilakos, P. N., Dobbs, J. M., and Parisi, A. S., preprint Am. Chem. Soc., Div. Fuel Chem. Vol. 28 (4) pp. 212-227, (1983).

12. Whitehead, J. C. and Williams D. F., J. Inst. Fuel 48, pp. 182-184 (1975).
13. Mortimer, J. Fuel 59, pp. 782-786 (1982).
14. Anglovich, J. M., M. S. Thesis, University of Wyoming, 1968.
15. Giddings, J. C., Science 162, pp. 167-73 (1968).
16. Bowman, Jr. L. M., Ph.D. Thesis, University of Utah, 1976.
17. Kurnick, R. T., Holla, S. J. and Reid, R. C., J. Chem. Eng. Data 26, pp. 47-51 (1981).
18. Hilderbrand, J. H., Prausnitz, J. M., and Scott, R. L., "Regular and Related solutions". Van Nostrand Reinhold Co., 1970.
19. Hilderbrand, J. H., and Scott, R. L. "Solubility of Nonelectrolytes". (Third Edition) ACS Monograph Ser. 17. Reinhold Publishing Corporation, 1950.
20. Jezko, J., Gray, D. and Kershaw, J. R., Fuel Processing Technology 5, pp. 229-239 (1982).
21. Blessing, J. E. and Ross, D. S., Amer. Chem. Soc. Symp. S.Er., No. 71. pp. 171-185 (1978).
22. Angelovich, J. M., Pastor, G. R. and Silver, H. F., Ind. Eng. Chem. Process Des. Develop. 9, pp. 106-109 (1970).
23. Rowlinson, J. S. and Richardson, J. S., Advances in Chemical Physics, Vol. II, pp. 85-118 (Ed. Prigogine). Interscience Publishers, Inc., New York (1959).
24. Paul, P. F. M. and Wise, W. S., "The Principles of Gas Extraction", Mills and Boon Ltd., (1971).
25. Reid, R. C. J., Prausnitz, J. M., and Sherwood, T. K., "The Properties of Gases and Liquids". (Third Edition) McGraw Hill Book Co., 1977.
26. Soave, G. Chemical Engineering Science, 27, pp. 1197-1203, (1972).
27. Timmermans, J. Physico Chemical Constants of Pure Organic Compounds, Vol. II, Elsevier Publishing Co., 1965.

Table 1. Physical Properties of Paraffin Solvents [Ref. 25].

Solvent	T_c, K	P_c, atm	$V_c, m^3/kgmol$	ω
Pentane	469.6	33.3	0.304	0.251
Hexane	507.4	29.3	0.370	0.260
Heptane	540.2	27.0	0.432	0.351
Octane	568.8	24.5	0.492	0.394
Nonane	594.6	22.8	0.548	0.444
Decane	617.7	20.8	0.603	0.490
Undecane	638.8	19.4	0.660	0.535
Dodecane	658.3	18.0	0.713	0.562

Table 2. Physical Properties of Alcohol Solvents [Ref. 25].

Solvent	T_c, K	P_c, atm	$V_c, m^3/kgmol$	ω
Methanol	512.6	79.9	0.118	0.559
Ethanol	516.2	63.0	0.167	0.635
Isopropanal	508.3	47.0	0.220	0.424
Isobutanol	547.7	42.4	0.273	0.588
Cyclohexanol	625.0	37.0	0.327	0.550
m-cresol	705.8	45.0	0.310	0.464

Table 3. Physical Properties of Aromatic Solvents [Ref. 25].

Solvent	T_c, K	P_c, atm	$V_c, m^3/kgmol$	ω
Benzene	562.1	48.3	0.259	0.212
Toluene	591.7	40.6	0.316	0.257
O-xylene	630.2	36.8	0.369	0.314

Table 4. Physical Properties of Solvents Used with Naphthalene and Phenanthrene.

Solvent	T_c, K	P_c, atm	$V_c, m^3/kgmol$	ω
Fluoroform ^a	299.0	48.8	0.133	0.275
Carbon Dioxide ^b	304.2	72.8	0.094	0.225

(a) Reid and Schmitt [Ref. 7]

(b) Reid et al [Ref. 25]

Table 5. Experimental and Predicted Vapor Mole Fraction, Y_2 , of Naphthalene in Naphthalene - Fluoroform System² at $T = 318^\circ\text{K}$.

$P \times 10^{-5}$ N/m ²	v^a m ³ /kgmol	$\omega/V_r T_r$	$Y_2 \cdot 10^3$		%Diff.
			Exp. ^b	Pred. ^c	
60.5	0.238	0.145	0.857	1.187	-38.51
73.3	0.159	0.217	3.300	2.846	13.76
96.1	0.116	0.298	7.040	5.654	19.89
141.3	0.094	0.367	10.090	8.855	12.24
221.0	0.081	0.427	12.300	12.246	0.44
351.3	0.072	0.481	13.400	15.847	-18.26

- (a) Soave Redlich-Kwong [Ref. 26]
(b) From Reid and Schmitt [Ref. 17]
(c) Using Equation (9)

Table 6. Experimental and Predicted Vapor Mole Fraction, Y_2 , of Phenanthrene in Phenanthrene - Carbon Dioxide System at $T = 328^\circ\text{k}$.

$P \times 10^{-5}$ N/m ²	v^a m ³ /kgmol	$\omega/V_r T_r$	$Y_2 \cdot 10^3$		%Diff.
			Exp. ^b	Pred. ^c	
120.0	0.102	0.191	0.465	0.509	-9.46
160.0	0.077	0.255	1.510	1.370	9.27
200.0	0.068	0.290	2.140	2.114	1.21
240.0	0.063	0.313	2.790	2.769	0.75
280.0	0.059	0.331	3.190	3.356	-5.20

- (a) Soave Redlich-Kwong Equation [Ref.26]
(b) From Kurnick, Holla and Reid [Ref. 17]
(c) Using Equation (8)

Table 7. Regression Analysis Data for Model Compounds.

Solvent class	A	E/R	n	Data Points	r
Naphthalene Fluoroform ^a	26.90×10^3	-4058. \pm 567	2.16	18	0.97
Naphthalene Fluoroform ^a	29.73×10^3	-4215. \pm 342	1.76	15	0.98
Naphthalene Carbon Dioxide ^a	29.58×10^5	-4822. \pm 504	2.98	36	0.96
Phenanthrene Carbon Dioxide ^b	14.69×10^5	-5289. \pm 366	3.44	15	0.99

(a) Reid and Schmitt [Ref. 7]

(b) Kurnick, Holla and Reid [Ref. 17]

Table 8. Experimental and Predicted Values of Material
Extracted from Coal Using Paraffin Solvents

Solvent	$\omega/V_r T_r^a$	% Extraction		% Difference
		Exp. ^b	Pred. ^c	
Pentane	0.146	18.43	18.73	-1.47
Hexane	0.227	19.26	19.18	0.42
Heptane	0.335	19.70	19.79	0.40
Octane	0.451	20.70	20.44	1.26
Nonane	0.625	21.17	21.42	-1.18
Decane	0.745	22.75	22.10	2.36
Undecane	0.921	23.16	23.10	0.26
Dodecane	1.079	23.56	23.98	-1.78

(a) V from Reference 11.

(b) Vasilakos et al [Ref. 11] at T=673K and V=0.364 m³/Kgmol

(c) from Equation (9)

Table 9. Experimental and Predicted Values of Material
Extracted from Coal Using Alcohol Solvents.

Solvent	$/V_r T_r^a$	% Extraction		% Difference
		Exp. ^b	Pred. ^c	
Methanol	0.191	18.90	18.15	3.97
Ethanol	0.313	25.50	28.71	-12.59
Isopropanol	0.261	28.80	24.28	1.57
Isobutanol	0.544	45.30	48.73	-7.57
Cyclohexanol	0.741	61.80	65.80	-6.47
m-Cresol	0.839	79.70	74.34	6.73

(a) V from reference 20.

(b) Jezko et al [Ref. 20] at T=723 K and P=20MPa

(c) from Equation (9)

Table 10. Experimental and Predicted Values of Material
Extracted from Coal Using Aromatic Solvents.

Solvent	$\omega/V_r T_r^a$	% Extraction		- % Difference
		Exp. ^b	Pred. ^c	
Benzene	0.209	37.90	37.01	2.35
Toluene	0.319	39.20	40.70	-3.83
O-xylene	0.480	46.70	46.09	1.31

(a) V from reference 20.

(b) Jezko et al [Ref. 20] at T=723K and P=20MPa

(c) from Equation (9)

Table 11. Regression Analysis Data for Coal.

Solvent Group	%Ext = $a + b(\omega/V_r T_r)$		Data Points	r
	a	b		
Paraffins ^a	17.90±0.27	5.63±0.42	8	0.98
Alcohols ^b	1.63±4.22	86.65±7.81	6	0.98
Aromatics ^b	30.0±3.38	33.5±9.56	3	0.92

(a) Vasilakos et al. [Ref. 11] (b) Jezko et al. [Ref. 20]

Table 12. Regression Analysis Data for Coal using Solubility Parameter δ from equation (1).

Solvent Group	%Ext = $a + b\delta$		Data Points	r
	a	b		
Paraffins ^a	11.21±0.68	3.05±10.21	8	0.98
Alcohols ^b	-12.37±1.95	15.40±0.50	6	1.00
Aromatics ^b	-16.53±37.63	13.04±8.47	3	0.64

(a) Vasilakos et al. [Ref. 11] (b) Jezko et al. [Ref. 20]

Table 13. Regression Analysis Data for Selected Physical Properties with % Extraction

Solvent Group	Linear Regression Coefficient, r						
	T_b^a	ρ_{25}^b	ρ_{exp}^c	$T_b \rho_{25}^c$	$T_b \rho_{exp}^c$	T_c^a	$-B_{11}^d$
	K	kg/m ³	kg/m ³	K.kg/m ³	K.kg/m ³	K	m ³ /kgmol
Paraffins	0.98	0.86	0.99	0.97	0.99	0.98	0.98
Alcohols	0.99	0.93	0.99	0.96	0.99	0.96	0.96
Aromatics	0.55	0.00	0.73	0.49	1.00	0.90	0.93

- (a) T_b and T_c from Reid et al [Ref. 25];
 (b) ρ at 25 °C, from Timmermans [Ref. 27];
 (c) ρ_{exp} , from experimental data in references [11,20]
 (d) B_{11} calculated according to ref. 25.

THE DYNAMICS OF THE THERMAL SOLUBILIZATION OF ILLINOIS NO. 6 COAL.

Tetsuo Aida, Bogdan Slomka, Julianna C. Shei,
Yu-Ying Chen, and Thomas G. Squires

Ames Laboratory,
Iowa State University
Ames, Iowa 50011

INTRODUCTION

The role of retrogressive reactions in limiting the rate and extent of coal liquefaction has long been recognized (1). While the negative impact of these phenomena on the overall conversion is clear, their chemical nature and the extent of their impact have yet to be elucidated. This is due, in part, to the complexity of the problem and, more importantly, to technical difficulties in resolving and investigating consecutive dynamic processes at high temperatures and pressures.

Almost forty years ago, Neuworth (2) and Glenn and his co-workers (3) addressed this problem by equipping an autoclave with a cold head receiver. In this way, they hoped to suppress retrogressive reactions by removing distillable products from the hot reaction zone as soon as they were formed. More recently, two other approaches have been utilized. Short contact time (SCT) experiments have been employed as a means of controlling secondary reactions in hopes that primary processes will dominate the conversion (4). In this approach, tubing bombs containing the coal liquefaction mixture are rapidly heated to an appropriate temperature, maintained at these conditions for a short time, and quickly cooled to room temperature. Other investigators (5,6,7) have placed liquefaction products (e.g. SRC) in an autoclave under liquefaction conditions in order to explore secondary retrogressive phenomena.

However, it should be quite obvious that experimental approaches which **confine starting materials, intermediates, and products to the same reaction space** throughout the course of the conversion are simply incapable of resolving productive and counter-productive processes. From this perspective, autoclaves and tubing bombs promote (rather than inhibit) secondary interactions between unreacted coal and primary products, thus obscuring primary pathways in the conversion process. Consequently, dynamic analysis of conversion rates and products is not only difficult in batch systems, but interpretations of the results from these experiments in terms of fundamental processes are tenuous.

In contrast, fixed bed flow mode reactors are capable of rapid removal and quenching of conversion products and, when appropriately designed, also provide temperature and pressure programing flexibility. As a means of isolating and investigating the fundamental phenomena which comprise coal conversion, we have developed a unique, rapid heating, flow mode microreactor system and have used it to investigate the dynamics of the thermal solubilization of coal. Important features of our apparatus include:

- *programable solvent residence times (1 to 30 seconds)
- *programable heating rates (up to 150°C/minute)
- *temperature and pressure programability
- *rapid quenching of reactor effluent
- *continuous, "on-line" optical density monitoring of same
- *data acquisition and manipulation capability
- *time resolved product collection (up to 2 samples/minute).

The soundness of this approach to resolving fundamental processes which comprise coal liquefaction was examined in a series of experiments. In the first set of experiments, this apparatus was used in a temperature programming mode to generate benzene solubilization rate profiles for five coals of varying rank. Another set of experiments focused on our continuing investigation of supercritical water as a medium for coal solubilization (8). Here, conversion rate profiles and liquid chromatographic product analysis were used to compare water and benzene as solvents for the thermal solubilization of Illinois No. 6 coal.

EXPERIMENTAL

General

Coals from the Ames Laboratory Coal Library were used for these studies; analytical data for the coals is given in Table 1. Prior to use, coals were ground, sized to 200 x 400 mesh, riffled to insure uniformity, and dried at 110°C overnight under vacuum. All solvents were HPLC grade or better; samples and solvents were stored under nitrogen.

Solubilization Procedure

Flow mode solubilization experiments using benzene and water were carried out in an improved version of our flow mode reactor (9). New features include continuous, "on-line" optical density monitoring of the reactor effluent; real time data acquisition of optical density, temperature, and pressure; and an improved time resolved product collection system. In a typical experiment, a preweighed amount (25-200 mg) of 200-400 mesh coal was placed in the tubular reactor and fixed in place by 2 stainless steel frits. After connecting the reactor and purging the apparatus with nitrogen, the entire system was

Table 1 Analysis of Ames Laboratory Coals

COAL	C	Ultimate analysis, % ^a				Volatile Matter ^a
		H	N	S _{org}	O(diff)	
Dietz No.1 & 2	74.35	5.26	1.09	0.44	18.86	38.6
Illinois No.6	80.60	5.63	1.56	2.35	9.81	40.4
Kentucky No.9	82.48	5.89	1.91	2.36	7.34	44.2
Pittsburg No.8	85.08	6.53	1.54	2.72	4.09	44.8
Lower Kittanning	90.04	4.82	1.66	0.68	2.69	18.4

a. Dmmf basis; wt % mineral matter = 1.13(wt % Ash) + 0.47(wt % S_{pyr}) + 0.5(wt % Cl).

filled with solvent and pressurized at room temperature before adjusting the solvent flow to 1.0 ml/minute. The reactor was then inserted into the preheated furnace at the same time that the reactor booster heater was turned on. The targeted initial temperature was always attained and stabilized within the first 3 to 5 minutes; and temperature and pressure were controlled during the conversion according to a predetermined program. Temperature and pressure profiles in the coal bed, as well as the optical density profile of the product stream, were recorded throughout the conversion. At the end of the experiment, the reactor was quickly cooled to ambient temperature while purging with nitrogen; and the residue was removed from the reactor and (in some cases) weighed. Solubilization yields in Table 2 are reported on a dry, mineral matter free basis.

Liquid Chromatographic Analysis of Products

Products of coal solubilization were analyzed by reverse phase high-performance liquid chromatography on a 4.1 mm x 300 mm - Bondapak (phenyl/corasil) column supplied by Alltech Associates, Inc. Samples were prepared for analysis by first stripping the solvent from the solubilization product: benzene was removed under a slow stream of nitrogen at room temperature while samples containing water were heated in a water bath (60°C) under reduced pressure.

The dry samples were then dissolved in 1 ml of tetrahydrofuran and 10 μ l was injected onto the column. Excellent (and reproducible) separation was achieved at a flow rate of 1 ml/minute using gradient elution techniques. The initial solvent composition was 38.1% methanol, 27.6% water, 23.9% acetonitrile, and 10.4% tetrahydrofuran. Chromatograms were recorded using a variable wavelength uv detector set at 254 nm.

RESULTS & DISCUSSION

Conversion Rate Profiles for Representative Coals

For an Illinois No.6 coal, we have previously found a linear correlation between gravimetrically determined conversions and effluent absorbance integrated with respect to time (integrated absorbance, IntA) (10); and this provides a basis for interpreting the integrated absorbance curve as the conversion rate profile. We have also shown that, at 260°C, benzene solubilization has no detectable thermal chemical component while, above 350°C, the conversion is dominated by pyrolytic processes (9).

In the first series of experiments with "on-line" optical density monitoring, five coals of varying rank were extracted with benzene in constant pressure, staged temperature experiments. The physical extraction stage, conducted for 20 minutes at 260°C, was followed by a pyrolysis stage at 390°C for the final 25 minutes. Figures 1 and 2 show the relative absorbance traces recorded at 500 nm for 26 μ lmg samples of these coals. In view of the relationship between conversion and absorbance, these curves actually represent conversion rate profiles in which extraction and thermal chemical solubilization have been resolved through temperature programming. Furthermore, the peak areas offer a measure of the extent of conversion at each stage of the experiment.

Figure 1 illustrates the distinct dynamic behavior of three coals (Dietz No. 1&2, %C = 74.4; Illinois No. 6, %C = 80.6; L. Kittanning, %C = 90.0) of different rank under identical conversion conditions. As expected, widely different amounts of material were extracted from these coals at 260°C; but the time required for complete physical extraction was approximately the same. We interpret this to mean that extraction sites within the coal particles were accessed at approximately the same rate for all three coals. From this perspective, extraction rate data generated with this apparatus can be used to estimate reaction site accessibility under various conditions.

The pyrolysis portions of the curves ($t > 20$ minutes) are even more characteristic. Again, the extents of conversion differ widely but are roughly the same as those determined using batch methods. However, in contrast to the 260°C results, the rates of solubilization, especially for Lower Kittanning coal, also vary widely. The thermal chemical solubilization of this higher rank coal is practically complete within 1 to 2 minutes while most of the Illinois No.6 coal is converted a 5 to 10 minute period. From these conversion rate profiles, it is apparent that there is a small but critical "time window" for effectively redirecting chemical pathways under these pyrolysis conditions. The former profile also demonstrates that the reactor system can resolve events with a time constant of less than a minute. The lower limit of this resolution has not yet been experimentally established.

Figure 2 shows similar temperature programmed solubilization rate profiles for three more nearly equivalent coals: Illinois No. 6, %C = 80.6; W. Kentucky No. 9, %C = 82.5; Pittsburgh No. 8, %C = 85.1. As expected, the two lower rank coals exhibit nearly equivalent behavior in both the extraction and pyrolysis stages. At this point, it is not clear whether the small difference in the second stage patterns is significant. The most striking comparison is between the dynamic behavior of Pittsburgh No.8 and that of the two lower rank coals. While a substantially higher conversion was expected for the 85% carbon coal, it is quite interesting that the entire difference reported to the extraction stage. We are continuing to investigate this phenomenon.

Aqueous vs. Benzene Solubilization of Illinois No. 6 Coal

Total weight loss determinations, "on-line" optical density monitoring, and staged pressure programming were used to compare benzene and water as solvents for the thermal solubilization of Illinois No.6 coal; the results are summarized in Table 2. On the basis of both weight loss and, more clearly, integrated absorbance, conversion in benzene at 360°C is greater for single stage solubilization (Exp. No.1) than for staged pressure conversion (Exp.No.2). These results are consistent with the general observation that, in the supercritical phase, the solubility of a substance increases with fluid density. During the low pressure (low density) stage, extraction of liquefaction products is inefficient; and, consequently, a portion of the unextracted products undergoes secondary "fixing" (retrogressive) reactions to form a more refractory material. This "fixed" material is no longer recoverable and cannot be extracted when the fluid phase density is increased to that of the one stage experiment (3180 psi).

In contrast, such retrogressive behavior is not observed when

Table 2. Thermal Solubilization of Illinois No. 6 Coal

Exp No	Solvent	--- First stage ---				--- Second stage ---				Total	Weight
		Temp (°C)	Press (psi)	Time (min)	Int Abs ^a	Temp (°C)	Press (psi)	Time (min)	Int Abs ^a	Int Abs ^a	Loss ^b (%)
8	C ₆ H ₆	360	3180	60	709	-	-	-	-	709	35.6
6	C ₆ H ₆	360	1280	20	153	360	3180	40	314	467	33.2
17	H ₂ O	370	2950	60	-	-	-	-	-	-	36.1
68	H ₂ O	370	1925	60	-	370	2950	60	-	-	35.9
2	C ₆ H ₆	390	3180	60	644	-	-	-	-	644	38.5
4	C ₆ H ₆	390	1500	20	210	390	3180	40	175	385	35.0
3	H ₂ O	390	3700	60	135	-	-	-	-	135	-
7	H ₂ O	390	1950	20	19	390	3700	40	114	133	45.0

a. Integrated Absorbance: area under the 500 nm absorbance trace; normalized to 25.0 mg of starting coal.

b. Dmmf basis.

water is used as the solvent for thermal solubilization of Illinois No. 6 coal. At 370°C, the total conversion of Illinois No. 6 coal in a two stage experiment (Exp. No. 68) is comparable to the conversion obtained in a single stage experiment (Exp. No. 17). Either water is acting to inhibit retrogressive reactions or the products of these "fixing" reactions are reactive in (with?) water but not in benzene.

The last four experiments, conducted at 390°C, were designed to further explore solvent induced differences in solubilization behavior. We reasoned that, at higher temperatures, retrogressive pathways should be more important and, thus, differences attributable to these phenomena might be more clearly discernable. The relative absorbance traces for benzene and water solubilization of Illinois No. 6 coal are presented in Figures 3 and 4, respectively; and integrated absorbance values for the various stages of these experiments are included in Table 2. Distinct differences in the dynamic solubilization behavior in benzene (Figure 3) and water (Figure 4) suggests that the conversion is proceeding via different chemical pathways in the two solvents. A comparison of the single stage and two stage integrated absorbance values for benzene (Exp. Nos. 2 & 4) and water (Exp. Nos. 3 & 7) further supports this notion.

This hypothesis, that the thermal solubilization of Illinois No. 6 coal proceeds differently in benzene than it does in water, was tested by analyzing the solubilization products with high performance liquid chromatography. Using a reverse phase method, the first and second stage products from the pressure programmed benzene solubilization (Exp. No. 4) were compared to their water derived counterparts (Exp. No. 7). The resulting chromatograms for the low pressure products are overlaid in Figure 5 and the high pressure overlay is shown in Figure 6. Unquestionably, the products produced in both stages of the benzene conversion are different from those obtained in the corresponding stages of aqueous solubilization. The nature of these differences will be the focus of further investigation.

These experiments illustrate rather clearly the usefulness of the flow mode approach as a means of isolating particular conversion phenomena and investigating dynamic behavior during coal liquefaction.

ACKNOWLEDGEMENT

Portions of this research were supported by U.S. Department of Energy Grant No. DE-FG22-82PC50786 for which we are grateful. However, any opinions, findings, conclusions, or recommendations expressed herein are those of the authors and do not necessarily reflect the views of DOE.

REFERENCES

1. van Krevelen, D.W. in "Coal"; Elsevier: New York, 1961; pp. 201-216.
2. Neuworth, M.B. J. Am. Chem. Soc. **1947**, 69, 1653.
3. Glenn, R.A.; De Walt, C.W. Fuel **1953**, 32, 157.
- 4a. Neavel, R.C. Fuel **1976**, 55, 273.
- 4b. Mitchell, T.O.; Whitehurst, D.D. Prepr. Pap.-Am. Chem. Soc., Div. Fuel Chem. **1976**, 21(2), 127.
5. Burke, F.P.; Winschel, R.A.; Jones, D.C. Fuel **1985**, 64, 15.
6. Painter, P.C., et. al. Fuel **1979**, 58, 233.
7. Ouchi, k.; Makabe, M.; Yoshimoto, I.; Itoh, H. Fuel **1984**, 63, 449.
8. Slomka, B.; Aida, T.; Squires, T.G. Prepr. Pap.-Am. Chem. Soc., Div. Fuel Chem. **1985**, 30(2), 368.
9. Squires, T.G.; Aida, T.; Chen, Y.Y.; Smith, B.F. Prepr. Pap.-Am. Chem. Soc., Div. Fuel Chem. **1983**, 28(4), 228.
10. Unpublished results from this laboratory.

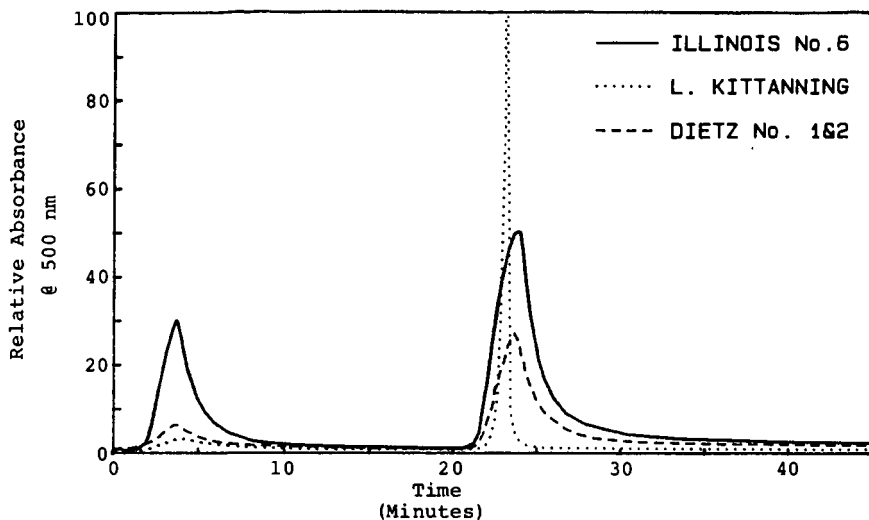


Figure 1. Staged Temperature Benzene Solubilization of Different Rank Coals. First Stage: 260°C/3180 psi; Second Stage: 390°C/3180 psi.

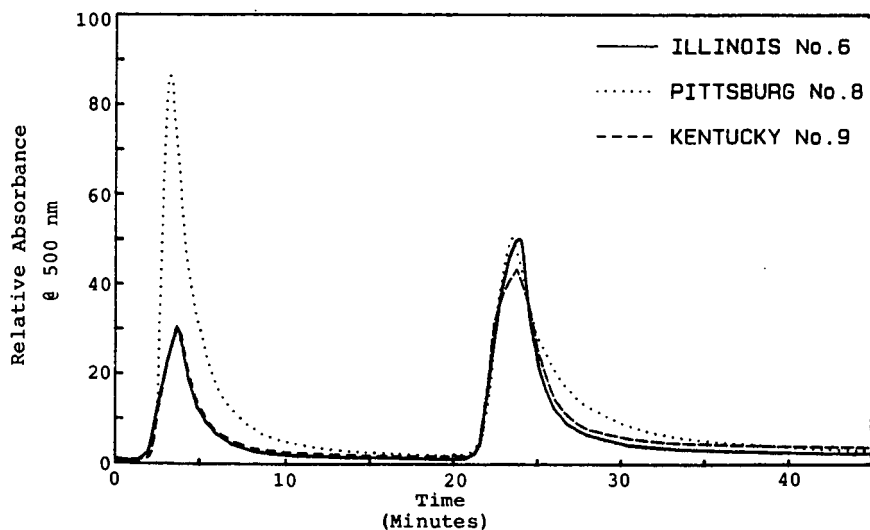


Figure 2. Staged Temperature Benzene Solubilization of Similar Rank Coals. First Stage: 260°C/3180 psi; Second Stage: 390°C/3180 psi.

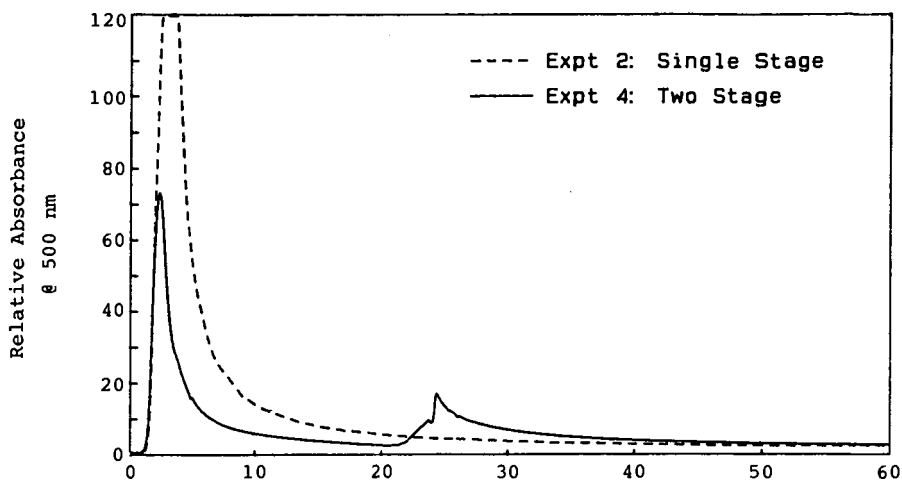


Figure 3. Effect of Pressure on Benzene Solubilization of Illinois No6 Coal at 390°C. Single Stage:3180 psi;Two Stage:1500/3180 psi.

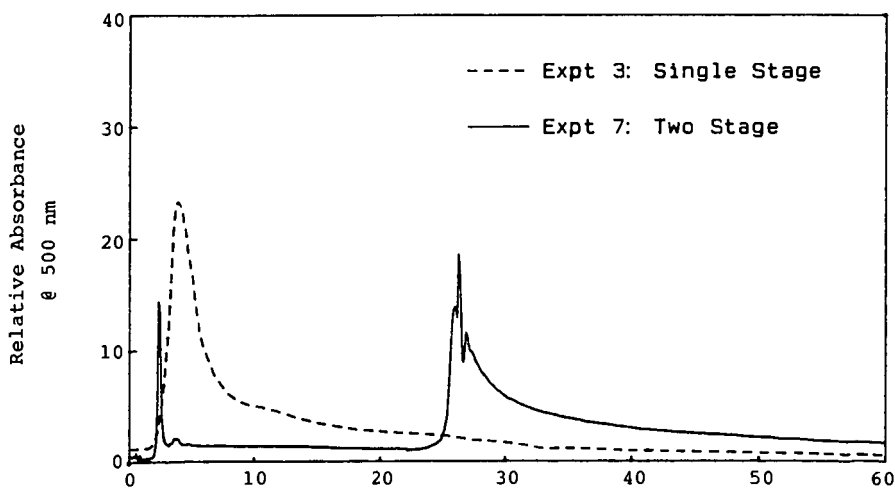


Figure 4. Effect of Pressure on Aqueous Solubilization of Illinois No6 Coal at 390°C. Single Stage:3700 psi;Two Stage:1950/3700 psi.

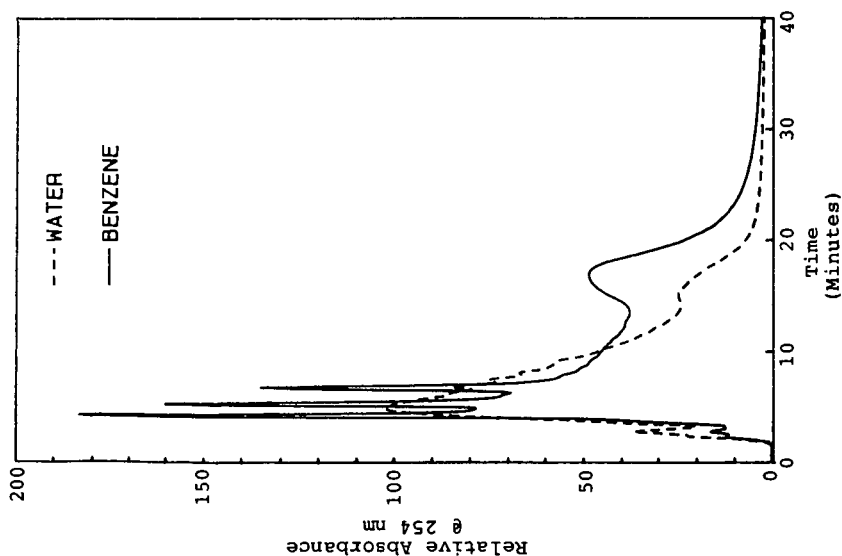


Figure 5. Chromatograms of Low Pressure Products from Staged Pressure Solubilization of Illinois No.6 Coal.

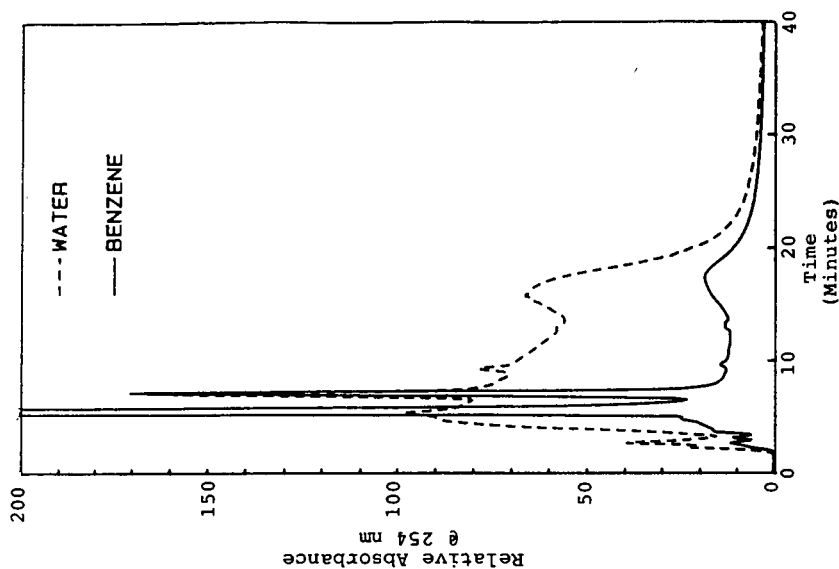


Figure 6. Chromatograms of High Pressure Products from Staged Pressure Solubilization of Illinois No.6 Coal.

Hydrogen Transfer Between 9,10-Positions in Anthracene and Phenanthrene

R. L. Billmers, L. L. Griffith, S. E. Stein

Chemical Kinetics Division
National Bureau of Standards
Gaithersburg, MD 20899

Introduction

The transfer of hydrogen between polyaromatic structures is an essential part of any realistic model of coal conversion chemistry. Not only do these processes affect the distribution of available hydrogen, but they are also intimately involved in certain C-C and C-O bond-breaking and bond-forming processes and may even control free-radical concentrations [1].

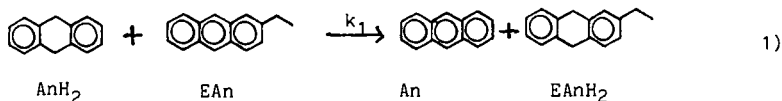
Chemical mechanisms responsible for these processes are not known. Currently, not only is there debate over the relative significance of individual reaction steps, but there are questions concerning the fundamental nature of these reactions, specifically, do they proceed by concerted, by free radical, or even by ionic steps.

Largely because of their intermediacy in reactions of tetralin, H-transfer reactions involving 1,2- and 1,4-dihydronaphthalene have been widely studied [2-5]. However, competitive addition and isomerization paths are open to these species, resulting in rather complex reaction mechanisms.

As a possibly simpler model system, we have chosen to study the transfer of hydrogen to the 9,10-positions of anthracene from 9,10-dihydrophenanthrene and from other 9,10-dihydroanthracene molecules. The particular stability of 9,10-dihydro structures as well as the absence of alternative pathways results in simpler mechanisms. Moreover, these three-ring structures themselves are of direct interest in coal chemistry. Experiments were done in sealed, evacuated pyrex tubes using conventional techniques [6].

9,10-Dihydroanthracene/2-Ethylanthracene Studies


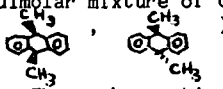
The kinetics of H-transfer from one anthracene structure to another was examined using the 2-ethyl group as a label,



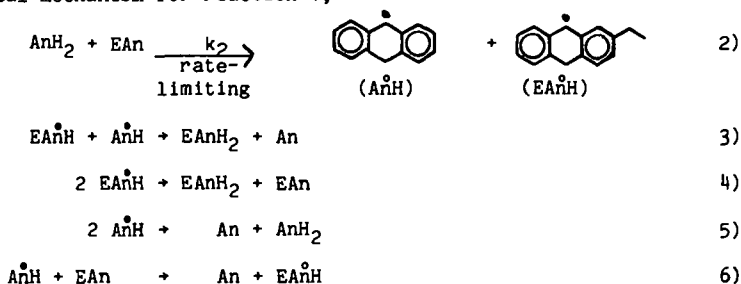
Rates followed the simple second-order expression (Figure 1),

$$\frac{d[\text{EAnH}_2]}{dt} = 10^{9.64 \pm 0.12} \exp\{-36,800 \pm 400 \text{ cal/RT}\} [\text{AnH}_2][\text{EAn}]$$

over the range $0.1 \lesssim [\text{AnH}_2]/[\text{EAn}] \lesssim 10$, and from undiluted AnH_2/EAn mixtures to mixtures diluted up to a factor of 100 in biphenyl. Rates were unaffected by heavy doses of radical initiators (1,1',2,2'-tetraphenylethane and 9,9'-bifluorene).

Addition of sufficiently large amounts of An to AnH_2/EAn mixtures caused a lowering of the rate of EAnH_2 formation (Figure 2). Using 9,10-dimethylantracene (, DMAn) in place of EAn led to a nearly equimolar mixture of cis- and trans- 9,10-dimethyl-9,10-dihydroanthracene ()

These observations are consistent with the following non-chain, free radical mechanism for reaction 1,



where step 6 is effective only when $[\text{AnH}_2]/[\text{EAn}] \lesssim 0.1$. Under most conditions, the observed rate is one-half the rate of reaction 2.

We rule out the importance of concerted reactions for the following reasons. (1) Concerted H_2 -transfer to DMAn would have formed only the cis isomer, but the product was 40-50% trans; (2) H-transfer to DMAn by $\text{HMn}(\text{CO})_5$ [7], which could not have occurred by conventional concerted processes, also led to nearly equimolar quantities of the cis- and trans-isomers; (3) equilibrium studies [8] have shown the cis-isomer to be slightly more stable from the trans-isomer; (4) separate studies showed that the cis-isomer did not isomerize to the trans-isomer under our conditions; (5) the slowing of the rate for EAnH_2 formation with added An cannot be explained by a concerted process.

In further support of our mechanism, the measured activation energy, along with the literature heat of the reaction $\text{AnH}_2 + \text{An} + \text{H}_2$ [9], yields a bond strength of $78.4 \pm 1.4 \text{ kcal mol}^{-1}$ for the AnH-H bond, in good agreement with a recently published value [10].

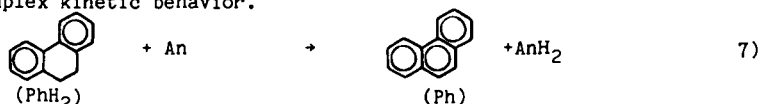
From the decline in rate with added An, we derive an approximate rate constant for k_6 of $110 \text{ M}^{-1}\text{s}^{-1}$ at 250°C . Assuming an A-Factor of $10^{8.5} \text{ M}^{-1}\text{s}^{-1}$, this reaction has an activation energy of $18.4 \text{ kcal mol}^{-1}$, in

agreement with the general conclusion of McMillen and co-workers [11] that such reactions (β -H-atom transfer) occur at rates comparable to those of conventional H-atom metathesis ($A\cdot + BH \rightarrow AH + B\cdot$).

The key result of our experiments is that molecular disproportionation, a step often proposed as a radical initiation step, is the critical step in H-transfer between 9,10-anthracene positions. Our results also provide indirect evidence for the occurrence of a β -H-transfer step, a potentially very significant step in hydrogen transfer mechanisms, but one which has only rarely been supported by kinetic evidence. More direct information on this reaction type was obtained in the following studies.

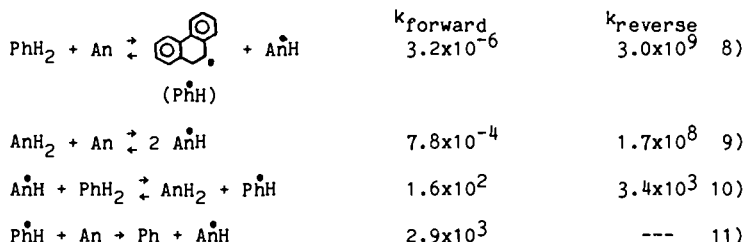
9,10-Dihydrophenanthrene/Anthracene Studies

Reaction 7 was studied at 350°C and was found to exhibit highly complex kinetic behavior.



The primary source of this complexity was the involvement of the product AnH_2 in the reaction (Figure 3). AnH_2 sharply catalyzed the reaction at low concentrations and moderately inhibited it at high concentrations.

A detailed computer model of this reaction was developed based on available and estimated rate and thermodynamic data. This model, given below, fits our results quite well (Figures 3-5).



This model contains two initiation steps (reactions 8 and 9). The predominant one depends on relative concentrations of PhH_2 and AnH_2 (they are equally effective at $[\text{AnH}_2] \sim 0.004 [\text{PhH}_2]$). The free radical chain described by reactions 10 and 11 was essential for modeling results. A sensitivity analysis of this model is in progress, and these rate constant values are therefore preliminary.

The question of whether H-transfer from PhH to An , step 11, proceeded through a direct, single step (β -H-transfer) or through a free H-atom intermediate ($\text{PhH} \rightarrow \text{Ph} + \text{H}$; $\text{H} + \text{An} \rightarrow \text{AnH}$), was answered in favor of the direct process on the basis of results of biphenyl dilution studies of $\text{PhH}_2/\text{An}/\text{AnH}_2$ mixtures (Figure 5).

A number of interesting features emerge from this mechanism.

(1) The catalytic effect of AnH_2 is a result of its facility for forming radicals through molecular disproportionation (reaction 9). This step is virtually the same as the rate limiting step in the AnH_2/EAn mechanism (reaction 2). (2) In the absence of sufficient AnH_2 , PhH_2 donation to An served as the major radical initiation step. Since the PhH-H bond is considerably greater than the AnH-H bond [1], this initiation step is far slower than the AnH_2/An initiation step. (3) In this reaction, the $\beta\text{-H}$ -transfer step (reaction 11) is considerably more rapid than the corresponding step in the EAn/AnH_2 mechanism (reaction 6). Using an A -factor of $10^{8.5} \text{ M}^{-1}\text{s}^{-1}$, the activation energy for reaction 11 is $14.4 \text{ kcal mol}^{-1}$, 4 kcal mol^{-1} lower than for reaction 6. This difference is probably due to the exothermicity of reaction 11 ($14 \pm 4 \text{ kcal mol}^{-1}$ [1,12]) compared to the thermoneutral nature of reaction 6. (4) The primary "reason" for the complex, chain reaction in the PhH_2/An mechanism appears to be to the high PhH-H bond strength compared to the AnH-H bond. This effectively shifts the former reaction to higher temperatures where chain reactions can occur. The above-mentioned facility of reaction 11 compared to reaction 6 also enhances chain reaction rates.

Conclusions

These studies indicate that H -transfer reactions among polyaromatic species proceed by free radical processes. Molecular disproportionation is the primary source of free radicals, and $\beta\text{-H}$ -transfer is a critical propagation step in chain reactions. Rates derived in these studies for both of these elementary processes provide a basis for estimating rates for related reactions. Mechanisms in the EAn/AnH_2 and An/PhH_2 reactions contain similar reaction steps, but follow entirely different kinetic laws.

In coal-related systems, An/AnH_2 structures can provide an efficient, steady supply of free radicals. The low bond strength of AnH-H is responsible for its special effectiveness as an H -donor in both radical-forming and radical-transfer steps [13]. The relatively high strength of the An-H bond allows the AnH radical to serve as an effective radical sink.

In a sense the Ph/PhH_2 system is opposite that of the An/AnH_2 system. The first bond (PhH-H) is significantly stronger and the second bond (Ph-H) weaker than corresponding bonds in AnH_2 . Therefore, PhH_2 is not nearly as effective as a free radical trap or initiator as is AnH_2 . On the other hand, PhH_2 can effectively hydrogenate molecules by $\beta\text{-H}$ -atom transfer to them through the labile PhH radical.

From a thermodynamic standpoint, PhH_2 is a more powerful hydrogenation agent than AnH_2 , and can irreversibly hydrogenate a wider range of structures [14]. However, AnH_2 is less prone to irreversible loss than PhH_2 and is therefore more likely to play a continuing role in hydrogen transfer mechanisms after PhH_2 structures have been destroyed.

Acknowledgement

This work was supported by a grant from the Gas Research Institute, Chicago, Illinois.

REFERENCES

1. Stein, S. E. in "New Approaches in Coal Chemistry", ACS Symp. Ser. 1981, **169**, Amer. Chem. Soc: Washington, D.C., p. 97.
2. Virk, P.S.; Bass, D. S.; Eppig, C. P.; Ekpanyong, D. J. Am. Chem. Soc. Div. Fuel Preprints 1979, **24**, (2), 144.
3. King, H. H.; Stock, L. M. Fuel 1981, **60**, 748.
4. Allen, D. T.; Gavalas, G. R. Int. J. Chem. Kinetics 1983, **15**, 219
5. Franz, J. A.; Camaioni, D. M.; Beishline, R. R.; Dalling, D. K. J. Org. Chem. 1984, **49**, 3563.
6. Stein, S. E.; Robaugh, D. A.; Alfieri, A. D.; Miller, R. E. J. Am. Chem. Soc. 1982, **104**, 6567.
7. Sweanyu, R; Butler, S. C.; Halpern, J. J. Organometallic Chem. 1981, **213**, 487.
8. Harvey, R. B; Arzadon, L.; Grant, J.; Urberg, K. J. Amer. Chem. Soc. 1969, **91**, 4535.
- 9a. Cox, J. D.; Pilcher, G. "Thermochemistry of Organic and Organometallic Compounds" 1970, Academic Press: New York
- 9b. Shaw, R.; Golden, D. M.; Benson, S. W. J. Phys. Chem. 1977, **81**, 1716.
10. McMillen, D. F.; Golden, D. M. Ann. Rev. Phys. Chem. 1982, **33**, 493.
11. McMillen, D. F.; Ogier, W. C.; Chang, S. J.; Fleming, R. H.; Malhotra, R. Proceedings Int. Conf. Coal Sci. 1983, Pittsburgh, PA, p. 199
12. Stein, S. E. in "Coal Conversion Chemistry", R. Schollosberg, ed., Pergamon Press, in press.
13. Poutsma, M. L. in "Free Radicals", Vol. II., Kochi, J. ed.; Wiley: New York, 1973, p. 113.
14. Kline, E. A.; Harrison, M. E.; Farnum, B. W. Am. Chem. Soc. Fuel Chem. Div. Preprints 1982, **27**(3), 18; 1983, **28**(5), 155.

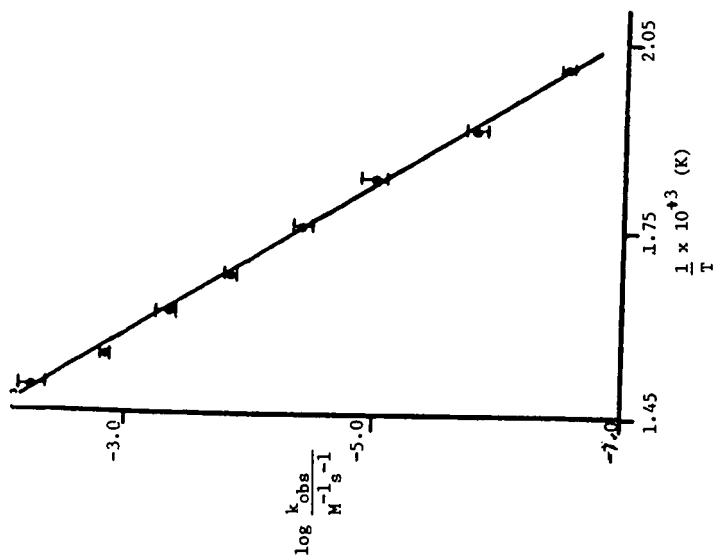


FIGURE 1. Arrhenius Plot for the Reaction
 $\text{EAn} + \text{AnH}_2 + \text{EAnH}_2 + \text{An}$ (Reaction
 2) Based on values obtained for
 $0.1 \leq [\text{AnH}_2]/[\text{EAn}] \leq 5.0$

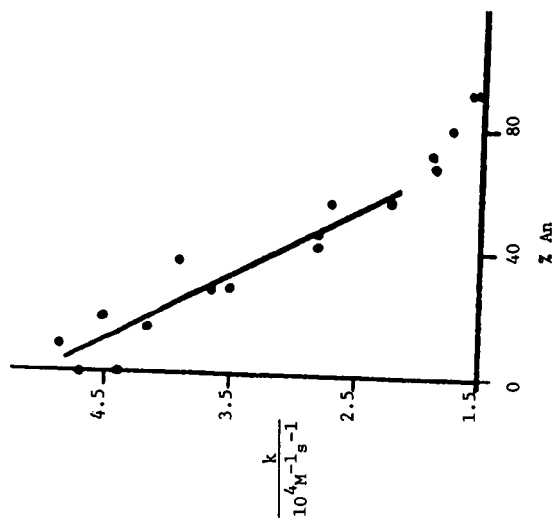
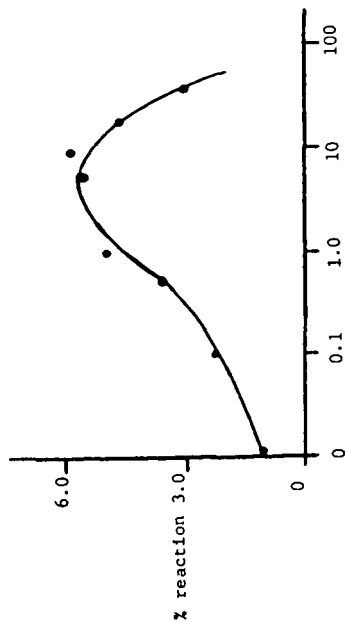


FIGURE 2. Effect of Added Anthracene
 on Reaction 2: $[\text{AnH}_2]/[\text{EAn}]$
 $\sim 0.2\text{M}$; biphenyl was used as
 diluent; 350 C, 15 min.



% AnH₂ added

FIGURE 3. Effect of added AnH₂ on the Rate of the Reaction PhH₂ + An + Ph + AnH₂. T = 350 C, times ~ 5 min, [PhH₂]/[An] ~ 0.05. Results of our kinetic model are shown by the solid line.

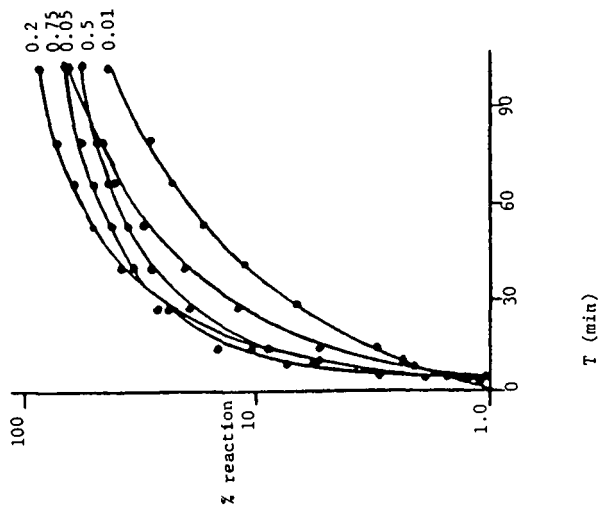
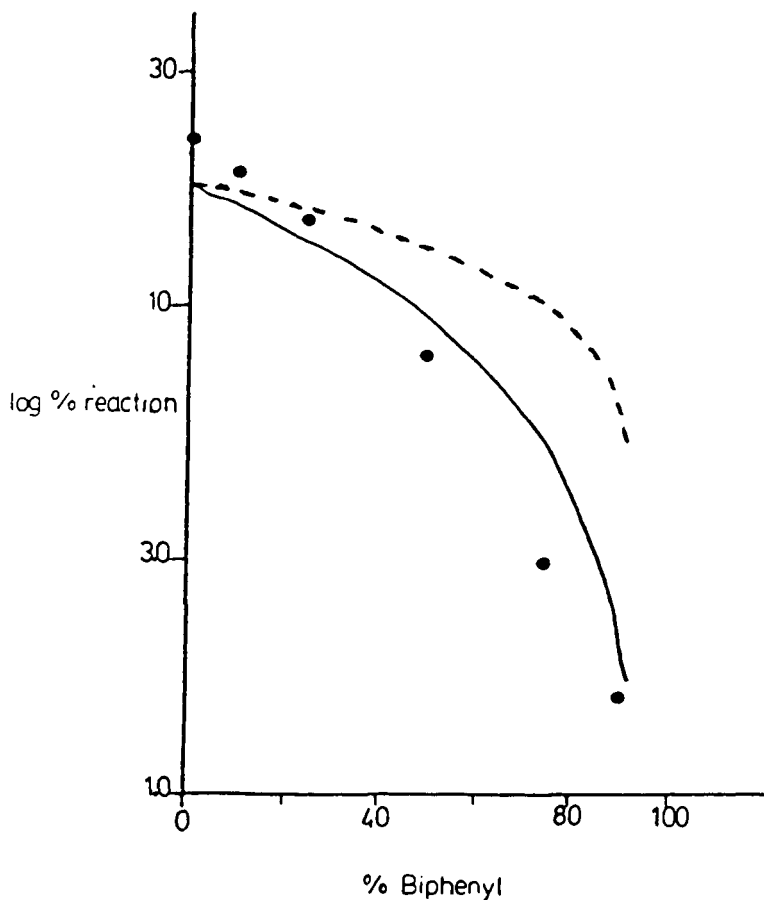


FIGURE 4. Percent Reaction for PhH₂ + An + Ph + AnH₂ at 350 C. Numbers at end of curves are initial [PhH₂]/[An] ratios. Points are experimental data - the line is from the kinetic model (see text).

FIGURE 5. Effect of Dilution by Biphenyl on the Rate of
 $\text{PhH}_2 + \text{An} \rightarrow \text{Ph} + \text{AnH}_2$. $T = 350^\circ\text{C}$, 30 min.
 $[\text{PhH}_2], [\text{AnH}_2]$.. Computer model is the solid line,
 broken line is for model containing the sequence
 $\text{PhH} \rightarrow \text{Ph} + \text{H}$, $\text{H} + \text{An} \rightarrow \text{HAn}$ in place of the direct
 reaction ($\text{PhH} + \text{An} \rightarrow \text{Ph} + \text{AnH}$)



THE RELATION BETWEEN TAR AND EXTRACTABLES FORMATION AND CROSSLINKING DURING COAL PYROLYSIS

E. M. Suuberg, Division of Engineering, Brown University, Providence, RI 02912

P. E. Unger*, Department of Chemical Engineering, Carnegie-Mellon University, Pittsburgh, PA 15213. *Present Address: Shell Development Co., Houston, Tx.

J. W. Larsen, Department of Chemistry, Lehigh University, Bethlehem, PA 18015

ABSTRACT

This paper presents a combined study of tar and extractables formation and crosslinking processes during rapid pyrolysis of coal. Tar and extractables were characterized by gel permeation chromatography, and crosslinking by a solvent swelling technique. The behaviors of coals ranging in rank from low volatile bituminous to a lignite were examined. It was noted that the low rank coal crosslinks at a much lower temperature than the high volatile bituminous coals, and that the low volatile bituminous coal is already highly crosslinked to begin with. These observations may help explain the widely differing yields and nature of tars and extractables produced by pyrolysis of these different ranks of coal.

INTRODUCTION

It has recently been shown that the technique of solvent swelling, as has been applied to the analysis of the macromolecular structure of coals¹, can also be applied to the analysis of chars produced by pyrolysis². This technique is utilized in this paper to help shed further light on the complex processes of "depolymerization" and charification that occur during pyrolysis of coals. In particular, the differences manifested by coals of different ranks are considered.

EXPERIMENTAL

The analyses of the four coals examined in this study are provided in Table 1. All samples used in this study had particles in the size range 53-88 μ m. Pyrolysis was performed in an electrically heated wire mesh, which assures uniform and rapid heating of all particles. All experiments were performed with a heating rate of roughly 1000 K/s, up to the indicated peak temperature, followed by cooling at a rate between 200 and 400 K/s. All pyrolyses were performed either in vacuum or in atmospheric pressure helium.

Table 1
Ultimate Analyses of Coals Examined*

	<u>C</u>	<u>H</u>	<u>O</u>	<u>N</u>	<u>S</u>	<u>Ash</u>	<u>Mois- ture</u>
Bruceton Pitts, No. 8 bituminous	80.4	5.3	6.7	1.6	1.0	4.6	1.7
Hillsboro Ill. No. 6 bituminous	67.2	4.6	12.3	1.2	3.4	11.7	8.6
W. Va. Pocahontas low volatile bit.	84.4	4.2	3.7	0.3	0.5	6.8	0.2
Beulah, No. Dakota Lignite	66.7	3.7	19.5	0.9	0.8	9.3	32.4

*All results on a dry basis except moisture, which is reported on an as-received basis. All analyses by Huffman Laboratories, Inc.

As used in this paper, the term "tars" refers to room temperature condensable products which have been expelled from the particles during pyrolysis. These materials generally have a molecular weight greater than 100, and are more than 97% soluble in tetrahydrofuran (THF). Extractables are materials left behind in the char, which are THF soluble. The extraction procedure is very mild,

involving a 1-hour ultrasonicated soak in THF (during which time the THF reached reflux temperatures). The sum of tar plus extractables is referred to as metaplast--the softened, transportable fraction of the coal. It is important to bear in mind that the estimate of metaplast obtained by summing tar plus extractables is a minimum value for that present in the coal during actual pyrolysis, since some recombination reactions may occur between extractables and unextractable char during cooling.

The analysis of the molecular weight distributions of the tars and extractables is performed by gel permeation chromatography (GPC), as has been described elsewhere³. It should be noted that calibration of the GPC columns was performed by vapor phase osmometric measurement of the molecular weights of actual fractionated samples of Bruceton coal tars.

The solvent swelling technique has also been described elsewhere^{1,2}. It involves measurement of the height of columns of coals and chars immersed in pyridine, in order to determine volumetric swelling ratios in the presence of the solvent. With a knowledge of the nature of solvent-coal interaction, this information can be used to estimate molecular weight between crosslinks in the coals and chars.

RESULTS AND DISCUSSION

In an earlier communication, it was shown that the Bruceton bituminous coal apparently crosslinks at a somewhat higher temperature than does the North Dakota lignite². This is consistent with the viewpoint that early crosslinking prevents softening of low rank coals during pyrolysis. This observation is also consistent with the low tar formation tendency of low rank coals, in the sense that tar precursors are quickly crosslinked into the char of low rank coals, prior to their escape.

The solvent swelling tendency of the coal chars has been used as a qualitative index of the extent of crosslinking; the higher the swelling ratio, the lower the degree of crosslinking. In this manner, comparative solvent swelling data are shown for all four ranks of coal, in Figure 1.

The low volatile bituminous coal swells to an extent of less than 5% in both the unpyrolyzed state and as a char. Consequently, it is difficult to say much about changes in the network structure of this coal during pyrolysis, based on solvent swelling information.

The Illinois #6 high volatile bituminous coal has swelling behavior very similar to that observed for the Bruceton high volatile bituminous coals. Both these coals soften markedly and both yield copious amounts of tar during pyrolysis. As noted previously², both these coals show little further tar formation at temperatures above about 900 K, a temperature at which new crosslink formation is quite measurable by this technique. It may be noted that the tars of these coals also show remarkably similar molecular weight distributions¹.

In contrast, little tar formation is seen at temperatures much in excess of 700 K in the case of the North Dakota lignite². On the basis of the high volatile bituminous and lignite data it might be tempting to ascribe significance to a swelling ratio of about 2 as the lowest value at which tar formation is possible. This of course is inappropriate, since the low volatile Pocahontas coal yields significantly more tar than the lignite, despite its highly crosslinked nature. Table 2 shows the yields of tar from the Pocahontas sample.

Table 2
Pocahontas Tar Yields

<u>Temperature (K)</u>	<u>Yield (wt. %, as received)</u>	<u>MW_N</u>
737	3.0	244
1083	9.1	199

The number average molecular weight of the Pocahontas tar is seen to significantly decline with increasing temperature. The actual molecular weight distributions are seen in Figure 2. The molecular weight distributions shown in Figure 2 (and later in Figure 3) are partially integrated molecular weight distributions. The ordinate represents the weight percent of tar at any molecular weight ± 100 mass units of the abscissa value.

The sharp peak of the Pocahontas tar molecular weight distribution in the range 300-500 is quite different than that of the tars of lower rank bituminous coals; as shown previously, these coals have a peak in the range from 600 to 700³. The implication appears to be that the Pocahontas coal is as highly crosslinked to start, that it is unlikely that enough bonds can break so as to yield large tar fragments. Or, viewed another way, the larger the fragment of coal to be released by bond breakage processes, and the higher the crosslink density, the lower the probability that enough bonds can be broken during pyrolysis in order to release the fragment.

Figure 3 shows the variation of molecular weight distribution with temperature for the North Dakota lignite. The number average molecular weight at 737 K is 323, whereas at 1133 K it is 279. The decrease in number average molecular weight of the tar species with increasing temperature in the case of the lignite (and the low volatile bituminous coal) is contrary to what might be expected based on vapor pressure arguments (higher temperatures should promote vaporization of even larger fragments of the coal). This trend towards lower number average molecular weight of fragments with increasing severity of thermal treatment is, however, consistent with the data that imply a higher degree of crosslinking with a more severe thermal treatment. It has been shown that in a polycondensation process, the molecular weight of extractables decreases with extent of polycondensation⁴. This behavior is not observed in the case of the high volatile bituminous coals, which show little variation of either number average molecular weight or molecular weight distributions with increasing temperature³. Presumably this reflects the fact that little crosslinking occurs during the active tar formation period².

The molecular weight distributions of the extracts of the Bruceton high volatile bituminous coal have been shown previously³. These data are summarized in Table 3, along with data on the metaplast (sum of tar plus extractables) molecular weight distribution for this same coal.

Table 3
Molecular Weight Distributions of Extractables and Metaplast
from Bruceton Bituminous Coal*

<u>Molecular Weight Range</u>	<u>Extractables</u>	<u>Metaplast</u>
100-1100	17% wt.	46% wt.
1100-2100	31%	31%
2100-3100	24%	13%
3100-4100	13%	5%
>4100	15%	5%
NO. AVG. MOL. WT.	1002	533

*All results for vacuum pyrolysis to a peak temperature of roughly 740K.

The difference between the extractables and metaplast arises from the fact that the latter contains a substantial contribution of species which were sufficiently light so as to have evaporated and been measured as tar, outside the particle.

A comparison of the number average molecular weight of the extractable pyrolysis fragments and the number average molecular weight between crosslinks is useful in characterizing the manner in which the crosslinked structure breaks down. In order to calculate the molecular weight between crosslinks from solvent swelling data, the Flory-Rehner equation is often employed², but is subject to criticism when applied to highly crosslinked, rigid networks^{6,7}. Nevertheless, the Flory-Rehner equation is often used as an approximation because of the lack of information concerning the repeat unit size, needed for more sophisticated models^{8,9}. The Flory-Rehner equation may be expressed as:

$$\bar{M}_c = - \frac{\rho_c M_s}{\rho_s} \frac{\phi^{1/3}}{\ln(1-\phi) + \phi + X\phi^2}$$

where ρ_c is the density of the original coal, ρ_s is the density of the solvent, M_s is the molecular weight of the solvent, X is the solvent-network interaction parameter, and ϕ is the inverse of the swelling ratio. The evaluation of X is also difficult, particularly since pyridine is a specifically interacting solvent. Table 4 shows a range of X values and their effect on \bar{M}_c for the Bruceton coal (or char up to about 800 K).

Table 4
Typical Values of \bar{M}_c for Bruceton Coal

X	\bar{M}_c
0.3	1105
0.4	1464
0.5	2172
0.6	4204

The range of \bar{M}_c obtained by this method compares well with estimates based on a rigid chain model applied to comparable ranks of coal⁹, in the range $x = 0.3$ to 0.5 . It is seen that the extractable and transportable fragments of the coal have a number average molecular weight which is comparable to or smaller than the number average molecular weight between crosslinks, for any reasonable value of X .

CONCLUSIONS

1. A lignite is seen to crosslink at much lower pyrolysis temperatures than high volatile bituminous coals. A low volatile bituminous coal is already too highly crosslinked to use solvent swelling to track pyrolysis behavior.
2. The downward shift in molecular weight distributions of pyrolysis tars with increasing temperature from a lignite and a low volatile bituminous coal is consistent with occurrence of polycondensation during pyrolysis.
3. Pyrolysis fragments appear to be, on average, comparable in size to or smaller than the number average molecular weight between crosslinks in a Bruceton bituminous coal.

ACKNOWLEDGEMENT

E. M. Suuberg gratefully acknowledges the support of the U. S. D. O. E. (Grants DE-FG22-81PC40803 and DE-AC18084FC1061) and J. W. Larsen thanks the Exxon Educational Foundation and the Gas Research Institute for support of this work.

REFERENCES

1. Green, T. K., Kovac, J. and Larsen, J. W., *Fuel*, **63**, 935 (1984) and references cited therein.
2. Suuberg, E. M., Lee, D. and Larsen, J. W., "Temperature Dependence of Crosslinking Processes in Pyrolyzing Coals", accepted for publication in *Fuel*.
3. Unger, P. E. and Suuberg, E. M. *Fuel*, **63**, 606 (1984).
4. Van Krevelen, D. W., *Fuel*, **44**, 229 (1965).
5. Flory, P. J. and Rehner, J., *J. Chem. Phys.*, **11**, 521 (1943).
6. Larsen, J. W. and Kovac, J., *Am. Chem. Soc. Symp. Series No. 71*, J. Larsen, Ed., 36 (1978).
7. Lucht, L. M. and Peppas, N. A., *Am. Chem. Soc. Symp. Series No. 169*, B. Blaustein, B. Bockrath, and S. Friedman, Eds., 43 (1981).
8. Kovac, J., *Macromolecules*, **11**, 362 (1978).
9. Peppas, N., Lucht, L., Hill-Lievens, M., and Hooker, A., D.O.E. Final Technical Report DE-FG22-80PC30222, U. D. Department of Energy, August 1983.

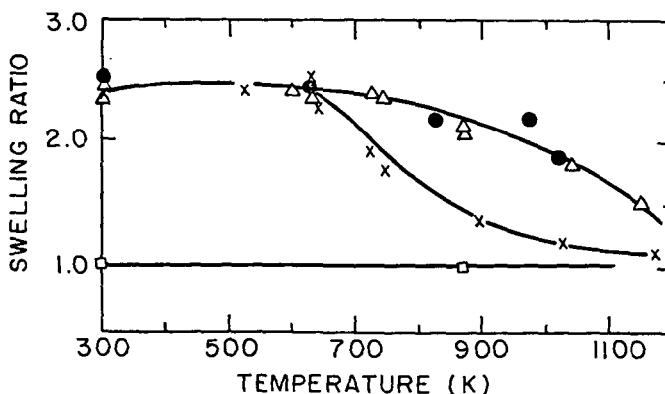


Figure 1. Pyridine swelling ratio as a function of peak pyrolysis temperature for four coals. (●) Illinois No. 6, (Δ) Bruceton, (X) Beulah Lignite, (□) Pocahontas.

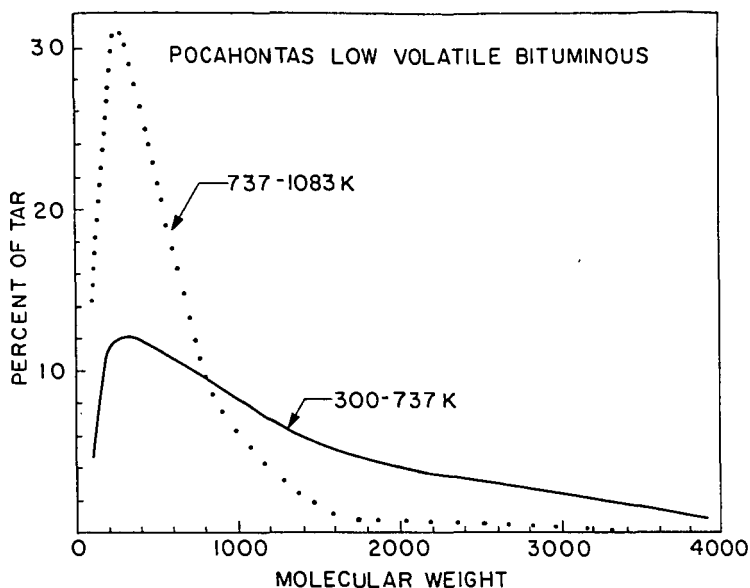
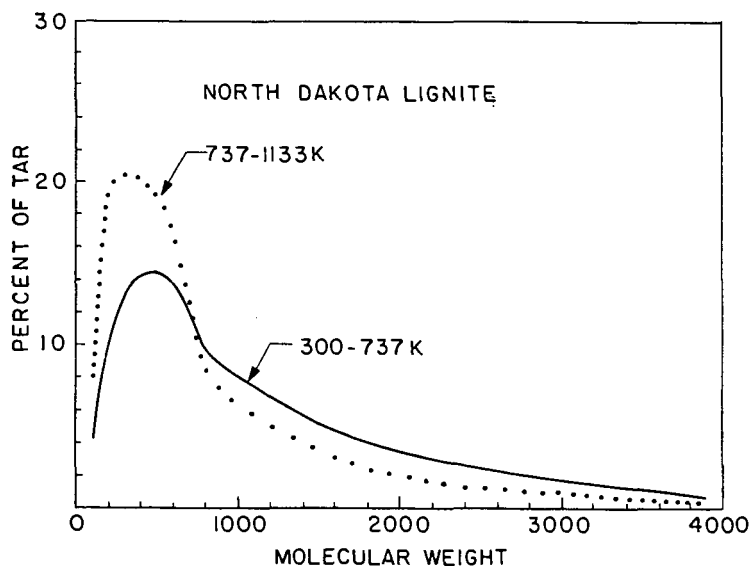


Figure 2 (top). Molecular weight distribution of tars evolved during pyrolysis of Pocahontas low volatile bituminous coal. Curves show range of pyrolysis temperatures over which the tar was evolved. Partially integrated curves, as described in text.

Figure 3 (bottom). Molecular weight distribution of tars evolved during pyrolysis of Beulah lignite. Curves show range of pyrolysis temperatures over which the tar was evolved. Partially integrated curves.



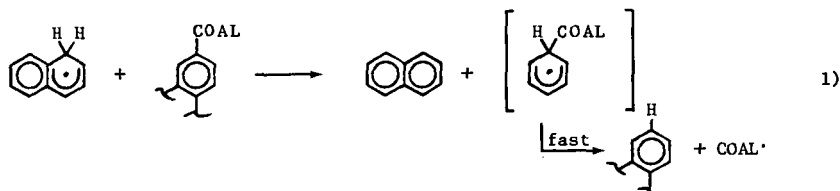
HYDROGENOLYSIS IN COAL LIQUEFACTION AND PYROLYSIS: THE RELATIVE IMPORTANCE OF SOLVENT RADICALS AND FREE HYDROGEN ATOMS

Donald. F. McMillen, Ripudaman Malhotra,
Sou-Jen Chang, and S. Esther Nigenda

Department of Chemical Kinetics, Chemical Physics Laboratory
SRI International, Menlo Park, CA 94025

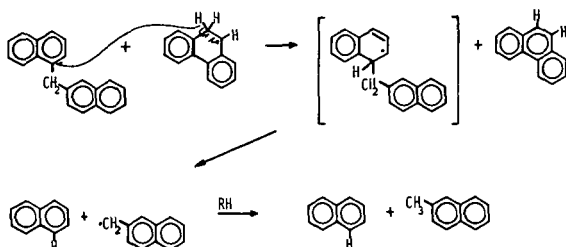
INTRODUCTION

The conventional view of coal structural fragmentation during liquefaction and pyrolysis has for many years been that those bonds in the coal structure that are weak enough, simply undergo scission in a purely thermal mannner. In this view, the relative effectiveness of the various process conditions is necessarily determined by the extent to which these conditions prevent the thermally generated radicals from recombining or undergoing other "retrograde" reactions. Despite recent suggestions by several different groups that the traditional thermal-bond-scission-radical-capping mechanism is inadequate to explain the phenomenology of donor-solvent coal liquefaction (1-6), this model continues to retain its position as the most widely invoked explanation of coal-structure degradation during liquefaction. Furthermore, in those cases where it is recognized that cleavage of coal linkages includes processes that are not spontaneous thermal cleavages, but are actually engendered by the solvent system, this promoted cleavage is usually attributed solely to cracking by free hydrogen atoms (7,8). In this paper we wish to further support our contention (1,2) that a significant part of the structural fragmentation occurring during coal liquefaction is not "spontaneous", but results from a previously undocumented fundamental reaction, "radical-hydrogen-transfer" (RHT), to aromatic positions bearing aliphatic (or ether) linkages in the coal structures (reaction 1).



It is no longer at issue whether alternatives to thermal scission of inherently weak bonds exist under donor solvent coal liquefaction conditions: The observed cleavage (1,5,7) of very strong alkyl-aryl bonds in hydroaromatic media, at 400°C, in the absence of H₂ pressure, on coal liquefaction time scales, (reaction 2) has demonstrated that what are formally defined as hydrogenolyses do take place under conditions where free hydrogen atoms have been thought to be unimportant. The fundamentally intriguing and possibly technologically important question that remains is whether or not this cleavage simply involves the ipso addition of free hydrogen atoms, and if does not, then by what mechanism does it take place.

In order to help answer the above question, we wish to present results that (1) demonstrate the relative importance of free hydrogen atoms and solvent "hydrogen-carrier radicals" for bond scission in the donor solvent system most



Bond cleavage half-life at 400°C \approx 20h

likely (of those systems generally studied) to generate "free" hydrogen atoms, and (2) suggest the relative importance of the two transfer modes for solvent systems that are much less likely to generate free hydrogen atoms (and not coincidentally are better coal liquefaction solvents).

EXPERIMENTAL PROCEDURE

Dihydroanthracene, 9,10-dihydrophenanthrene, tetralin, pyrene and 1- and 2-methylnaphthalene were obtained from Aldrich, and 1,2'-dinaphthylmethane was obtained from Carnegie-Mellon University. All were used without further purification. 4,5-Dihydropyrene was prepared by the procedure of Friedman et al. (8).

Model compounds reactions were conducted in sealed, 4-mm-od, fused silica ampoules that were loaded, together with some solvent (to equalize pressure), into a 3/8-in. od, Swagelok-capped stainless steel jacket. This assembly was heated in a molten salt bath temperature controlled to $\pm 0.5^\circ\text{C}$ for the prescribed reaction time, and then quenched in a water bath. Product mixtures were analyzed by GC, and when necessary, by GC/MS.

RESULTS

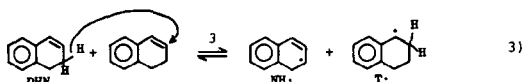
The Use of 1,2-Dihydronaphthalene Disproportionation Stoichiometry to Determine the Mode of Hydrogen Transfer

1,2-Dihydronaphthalene and its rapid disproportionation at 400°C to naphthalene and tetralin provides a unique opportunity to study the mechanism by which hydrogen atoms are transferred among the various hydronaphthalene structures. Since hydrogen transfer by either radical hydrogen transfer or free hydrogen atoms can result in the same products, distinction between the two modes in many other systems must be by inferences drawn from kinetic measurements through numerical modeling. However, in the case of dihydronaphthalene, determination of the naphthalene/tetralin product ratio as a function of dilution with an inert solvent provides an internal measure of the fraction of hydrogen transfers that occurs by radical hydrogen transfer and the fraction that occurs by addition of free hydrogen atoms. The disproportionation of 1,2-dihydronaphthalene is known to occur by a radical chain process initiated by a molecule induced homolysis (or reverse radical-disproportionation (5,9,10)), with the only uncertain reaction

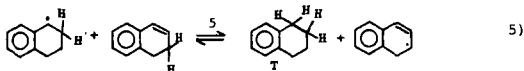
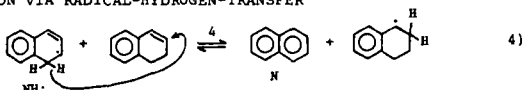
being the hydrogen transfer step that is the subject of this paper. The result of competition between transfer via free hydrogen atoms and direct bimolecular transfer from a radical carrier can be seen by inspection of the alternative reaction sequences.

DISPROPORTIONATION OF 1,2-DIHYDRONAPHTHALENE

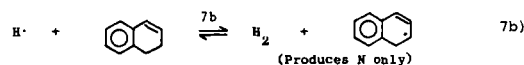
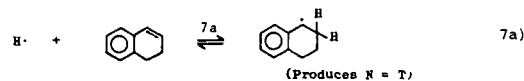
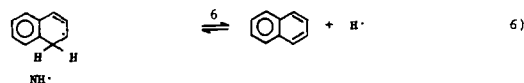
INITIATION/TERMINATION



PROPAGATION VIA RADICAL-HYDROGEN-TRANSFER



PROPAGATION VIA FREE H[•]



To the extent that disproportionation proceeds by way of the propagation steps 4 and 5, the ratio of naphthalene/tetralin will be identically equal to 1.0. However, to the extent that unimolecular hydrogen-atom elimination (reaction 6) from the 1-hydronaphthyl radical (1-NH[•]) competes with bimolecular radical-hydrogen-transfer (reaction 4), the free hydrogen atoms thus produced can either add to or abstract from DHN (reactions 7a and 7b, respectively). H-atom addition results in equal quantities of naphthalene and tetralin, just as does radical-hydrogen-transfer (reaction 4), but abstraction produces H₂ and naphthalene with no production of tetralin. The naphthalene/tetralin product ratio (N/T) is determined both by the ratio of radical-hydrogen-transfer/elimination and by the fraction of those free hydrogen atoms produced that go on to add to DHN rather than abstracting from it. Therefore, measurement of the change in N/T as a function of dilution with an inert solvent (one that hydrogen atoms cannot readily add to or abstract from, such as biphenyl) provides a determination of both of these branching ratios.

The steady-state algebra for this determination is simplest if we restrict consideration to initial reaction rates of a system that is far from equilibrium (i.e. DHN/N, DHN/T > 1). In that case we need to consider only the forward reac-

tions of the various propagation steps, and find the naphthalene/tetralin production ratio given by equation (8).

$$\frac{N}{T} \approx \frac{d[N]}{d[T]} = \frac{\frac{k_4 [\text{DHN}]}{k_6} + 1}{\frac{k_4 [\text{DHN}]}{k_6} + \frac{k_{7a}}{k_{7a} + k_{7b}}} \quad \left. \vphantom{\frac{d[N]}{d[T]}} \right\} F \quad 8)$$

In Figure 1 is plotted a set of curves that correspond to the relationship described by equation 8 between the ratio of naphthalene production rate to tetralin production rate and the extent of DHN dilution. Each curve is for a given value of "F," the fraction of those free hydrogens produced that go on to add to DHN.

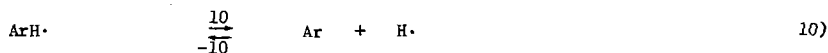
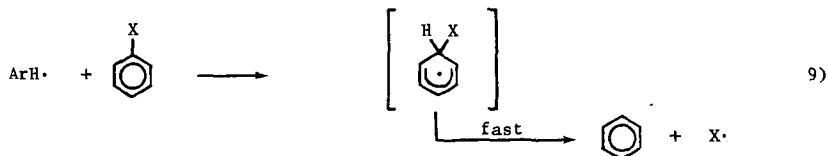
Inspection of the general form of these curves shows it to be intuitively reasonable. Consider first, movement along the abscissa of Figure 1: for a given fraction of free hydrogen atoms that add (F fixed), the more the DHN is diluted, the more NH^\cdot will be diverted from the bimolecular RHT process (reaction 4) to the unimolecular H-elimination process (reaction 6), and the greater will be the excess of naphthalene that results from H abstraction (reaction 7b). The result of movement from one value of F to another is also reasonable: for a given DHN concentration, the lower the fraction of H that add (and therefore, the higher the fraction that abstract), the greater will be the excess of naphthalene. In the limit of no addition (F = 0), as $(\text{DHN}) \rightarrow 0$, $N/T \rightarrow \infty$. On the other hand, in the limit where all free H^\cdot add (and none abstract), the final result will not depend on the branching between RHT and elimination: N/T will be 1.0 at all levels of DHN dilution, as shown for the bottom curve in Figure 1. In the limits where the bimolecular transfer to elimination ratio (k_4/k_6) is very high or very low, either RHT or elimination of hydrogen atoms will dominate at all practical levels of (DHN), and the observed (N/T) will not vary with DHN concentration. In other words, equation 8 is useful only when radical hydrogen transfer and elimination are competitive, and when addition is not the exclusive pathway for free H-atoms.

Also shown in Figure 1 are points corresponding to measured N/T ratios in a series of experiments performed at 385°C for initial concentrations of DHN in biphenyl ranging from 2 to 30 mM. The data clearly can be well fitted to the functional form of equation 8. The best fit corresponds to a value of 1.08 l/m for k_4/k_6 , and 0.68 for F. This means that of every 100 NH^\cdot formed, (1.08/2.08)100, or 52, will transfer their hydrogen bimolecularly (at 1.0 M concentration of the acceptor DHN), and 48 will eliminate a hydrogen atom. Of the 48 free hydrogen atoms, 68%, or a total of 33, will add, and 15 will abstract. This means that 52 out of 85 hydrogen transfers proceed through the direct bimolecular process. Thus these results are consistent with the results of Franz and co-workers (5), who reported that the hydrogenolysis of diphenylmethane in this system was, under similar conditions, always accompanied by at least some H_2 formation, and therefore could not be used as unequivocal qualitative evidence for operation of an RHT mechanism. In the present case, the measured effects of dilution and algebraic separation presented above provide, within the accuracy and precision limits of the data, an unequivocal determination of the relative importance of radical-hydrogen-transfer and free hydrogen atom addition.

Implications of Solvent-Radical-Mediated-Hydrogen-Transfer

One may question how relevant the above branching is for hydrogen transfer in coal liquefaction, where the potential recipients in the coal structure may be present at effective concentrations much less than 1 M. While it is true that in

the present circumstances, the acceptor (DHN) concentrations are fairly high (0.09 to 1.25 M), the pool of carrier molecules (naphthalene) is fairly low. What this means is that if the NH^\cdot cannot transfer its hydrogen directly to the DHN, it will eliminate. In actual coal liquefaction systems, good donor solvents contain a substantial portion of polycyclic aromatic components (PCAH) which increase the chances that when any given ArH^\cdot cannot transfer its H atom directly to a cleavable linkage in the coal structure, and therefore eliminates the H atom instead, the large pool of PCAH will react rapidly with the H to reform the carrier ArH^\cdot :



It is clear that increasing (Ar) increases the rate of Reaction -10, and therefore the fraction of radicals present as ArH^\cdot . By this mechanism, the available hydrogen "atoms" are shuttled around in a form that can only transfer them (and cannot produce H_2) until they are successfully transferred to a cleavable coal structure. Thus, we reiterate our previous suggestion (1,2) that it is by this "shuttling" mechanism that good coal solvents successfully promote the transfer of hydrogen atoms to cleavable positions in the coal structure, while minimizing the free hydrogen-atom production and therefore the formation of H_2 . Such formation of H_2 can be very wasteful, since H_2 that is formed through hydrogen atom abstraction reactions is then unavailable for liquefaction purposes, unless the hydrogen pressure is very high or catalysts are present.

It is interesting to note that the maximum in liquefaction effectiveness as a function of temperature that is often seen between 430° and 460°C could be a reflection of the fact that while an increase in the concentration of carrier radicals ArH^\cdot is desirable, and this can be achieved by going to higher temperatures, one also wants to limit the fraction of ArH^\cdot that eliminate hydrogen and generate H_2 by abstraction reactions. Given that the unimolecular hydrogen atom elimination reactions of ArH^\cdot will have the highest activation energies of all loss processes for ArH^\cdot , it is not surprising that an optimum temperature would be reached, above which the principal hydrogen "transfer" reaction would be the useless one of dehydrogenating the hydroaromatic structures in the coal and donor solvent to make H_2 .

It should also be noted that the results of Vernon (7), showing facile hydrogenolysis of bibenzyl, were obtained at substantial H_2 pressures (> 500 psi), at temperatures $> 430^\circ\text{C}$, and in the absence of substantial amounts of hydroaromatic or polycyclic aromatic solvent components. From the above discussion, it is clear that these conditions will tend to minimize formation of ArH^\cdot in the first place, and to minimize the chances that any H^\cdot produced will be converted to ArH^\cdot by the pool of Ar. Furthermore, the high hydrogen pressure provides a route to H via hydrogen abstraction from H_2 by thermally generated benzyl radicals, as invoked by Vernon. Thus, there is no conflict between the results of Vernon and those presented here: in retrospect it can be stated that the conditions used in his work are those expected to minimize the importance of transfer from solvent radicals ArH^\cdot , and to maximize the importance of free hydrogen atoms. In fact, as noted by Ross (11), the cleavage observed by Vernon is decreased by increasing

hydroaromatic content in the solvent. Since this trend is counter to that observed in actual coal liquefaction, the mode of cleavage observed by Vernon would appear not to be representative of the bulk of the coal structure cleavage obtained in solvents of high donor content.

Accuracy of the RHT/Elimination Determination

Given the limited range of observed N/T ratios in Figure 1, it is appropriate to ask how precise the present determination of the radical-hydrogen-transfer/elimination ratio actually is. The two most important qualifications are that equation 8 is a differential expression, derived for initial conditions where the only important propagation reactions are 4, 5, 7a and 7b, and the reverse of these reactions can be neglected. Furthermore, the assumption is that side reactions are relatively unimportant. The first criterion is met by measuring product ratios in the initial stage of the reaction when the system is far from equilibrium. The latter criterion is marginally satisfied by choosing reaction conditions that are a compromise between excessive free hydrogen atom elimination (favored by high temperatures), and excessive formation of dimeric DHN products (favored by low temperatures and high DHN concentrations(5)). This choice provides a fairly narrow window in which to make measurements, and coupling product formation could not be completely avoided. However, for all but the point at the highest DHN concentration (30 mM), the amount of DHN coupling product formation was less than about 10%. The effect of this minor amount of coupling product on the derived branching ratios is assessed below.

Examination of the DHN coupling products identified in the thorough study by Franz and co-workers (5) indicates that these products are formed primarily, but not exclusively, at the expense of tetralin formation. If we make even the extreme assumption that the coupling products observed in our experiments were formed exclusively at the expense of tetralin, and correct the observed N/T ratios accordingly, the value of F remains essentially unchanged, and the value of RHT/elimination increases by about 30%. Thus, inaccuracies due to formation of coupling products in side reactions cannot invalidate the general conclusion that the hydrogen carrier radical in tetralin/naphthalene systems (the 1-NH[•] radical) transfers hydrogen bimolecularly to dihydronaphthalene at rates competitive with transfer by free hydrogen atoms.

Importance of Radical Hydrogen Transfer in Other Solvent Systems

The results above demonstrate that in the radical chain disproportionation of 1,2-dihydronaphthalene, hydrogen is transferred from a solvent radical to another olefinic or aromatic system, in a bimolecular reaction that was, until this work (1,2), without precedent in the chemical literature. Now one obvious question is, "How important is this reaction under conditions that more closely mimic those in donor solvent coal liquefaction?" In order to help answer this question, we have studied the cleavage of a very strongly bonded model compound in a number of donor solvent systems. At 400°C in common donor solvent systems, 1,2'-dinaphthylmethane (DNM) exhibits cleavage half-lives (forming methylnaphthalenes and naphthalene) of 3 to 200 hours, as shown in reaction 2 above. This is unquestionably a "solvent-promoted" cleavage, since no cleavage (i.e. % reaction < 0.1%) can be seen in 20 hours in pure aromatic solvents ($t_{1/2} > 10,000$ hours). In fact the ca. 85 kcal/mol strength of the central bond (14) is such that the half-life for spontaneous thermal rupture is on the order of 100-million hours (3,12). Dinaphthylmethane is somewhat harder to cleave than analogous phenanthrene derivatives would be, and much harder to cleave than similar anthracene derivatives (2,3,12,13). Of all the single methylene bridges between aromatic groups, the only one more difficult to cleave in a hydrogenolysis process than dinaphthylmethane is that in diphenylmethane. The point is that dinaphthylmethane is in all likelihood

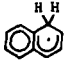
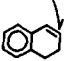

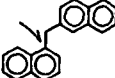
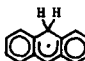
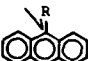
a relatively severe test of the bond-cleaving ability of a coal liquefaction solvent system.

Because of its unsymmetrical coupling, we have with 1,2'-dinaphthylmethane not only an indicator of the hydrogen transfer activity of a solvent system, but also an indicator of the mode of transfer. Since the 1-position of naphthalene is preferred for hydrogen atom addition or transfer (by ~ 4 kcal/mol, compared to the 2-position (3,12,13) the ratio of product resulting from attack at the 1-position to that resulting from attack at the 2-position provides a measure of the selectivity of the transfer agent and therefore an indication of the nature of the transfer process.

Thermochemistry of Hydrogen Transfer in Selected Systems

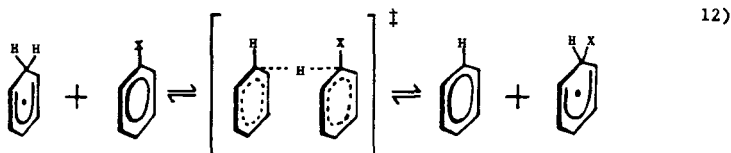
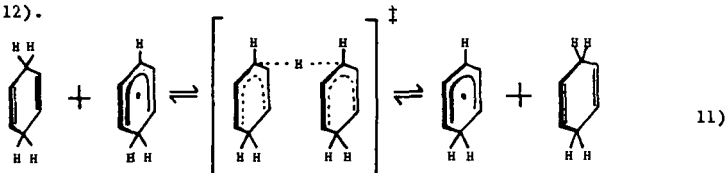
As a basis for anticipating the relative importance of radical-hydrogen-transfer (RHT) in the dihydronaphthalene system discussed above and in other solvent and acceptor systems, we need at least to know the relevant thermodynamic values. In Table 1 are given measured or estimated enthalpy (1,3,12,13) values for RHT and hydrogen atom elimination for dihydronaphthalene disproportionation (1), dinaphthylmethane cleavage in tetralin (2) and in 9,10-dihydroanthracene (3), and for 9-alkylanthracene cleavage in 9,10-dihydroanthracene (4). On the basis of these values rough estimates can be made of the ratio of RHT to H[•] elimination.

Table 1 THERMOCHEMICAL VALUES FOR HYDROGEN TRANSFER^a

System	ArH [•]	Ar-X	$\Delta H^\circ, \text{kcal/mol}$		est. E_a		$k_{\text{RHT}}(\text{ArX})/k_{\text{elim.}}$
			H [•] elim.	RHT	H [•] elim.	RHT	
1			+30	-15	31	13	(1.1)
2			+30	0	31	16	0.1
3		"	+45	+15	46	28	1.1
4	"		+45	0	46	16	10 ⁴

^aValues taken directly from, or estimated on the basis of, data in references 3,12, and 13.

The ratio of the RHT rate to the H[•] elimination rate for the first system is in fact the ratio whose determination is discussed above. The estimation of the H[•] elimination rate constant is subject to relatively little uncertainty, since the intrinsic activation energy for hydrogen-atom elimination is known (14,15) to be no more than about 1 kcal/mol. The "estimated" rate constant for RHT was then adjusted to fit the measured RHT/elimination ratio by assuming that the generic A-factor for RHT (reaction 11) was 10^{8.5} l/m-sec, a well-accepted (3,15) "representative" value for the ubiquitous and geometrically similar metathesis reaction (Reaction 12).



This adjustment resulted in an activation energy of 13 kcal/mol, not unreasonable for a 15 kcal/mol exothermic transfer, in view of measured activation energies (3,5) of about 16 kcal/mol for thermoneutral metathesis reactions involving two resonance-stabilized radicals. This adjustment provides a reasonable base for semi-quantitative speculation about the relative rates of RHT and elimination for the other three systems in Table 1.

When DNM (rather than 1,2-DHN) is the acceptor of the hydrogen, the transfer from the NH[•] radical is now nearly thermoneutral (assuming transfer to the aromatic naphthalene system is otherwise similar to transfer to the isolated double bond of 1,2-DHN) and one would expect a slightly higher intrinsic activation energy. This results in the expectation that RHT in system 2 may now be as much as 10X slower than elimination. In the third system, transfer from the 9-hydroanthryl radical (AnH[•]) to DNM is 15 kcal/mol endothermic, and elimination is about 45 kcal/mol endothermic. Assuming symmetrical behavior of the potential energy surface moving from exothermic to thermoneutral to endothermic RHT, the intrinsic activation energy would again be 13 kcal/mol (making $E_a^{\text{obs}} = 13 + 15 = 28$ kcal/mol). The net result is to make the RHT/elimination ratio the same as case number one, where RHT was 15 kcal/mol exothermic.

The largest change in the series is expected for the fourth system. Here, for thermoneutral transfer from an anthracene carrier to an anthracene acceptor, the anticipated activation energy for RHT drops by more than 10 kcal/mol as compared to System 3, while that for H[•] elimination remains constant, and the RHT is expected to exceed elimination by more than three orders of magnitude. Stein and co-workers have recently completed (16) studies on one example of System No. 4 (9,10-dihydroanthracene/9-ethylanthracene) and have apparently found the kinetics of hydrogen transfer to be wholly inconsistent with hydrogen transfer by way of free hydrogen atoms, but consistent with the radical-mediated bimolecular transfer process invoked in this work. We find this agreement gratifying. However, we also note that the evidence we provide in this paper for the importance of

Radical-Hydrogen-Transfers even in the less "favored" systems, 1 and 3, is a much stronger suggestion of its widespread significance in coal liquefaction.

Implications for Coal Liquefaction

From the above discussion, it seems clear that the "hottest" hydrogen carrier radical is not necessarily the best for coal liquefaction. Clearly, what is desired is maximum reactivity coupled with the maximum attainable selectivity for RHT and against H-atom elimination. In general, this will be best obtained through maximum numbers of ArH^\cdot of reactivity low enough that H-elimination is not a substantial side reaction. This criterion is more successfully met by the tri- and tetracyclic PCAH systems than by the tetralin/naphthalene systems.

In order to determine the relative importance of RHT and free hydrogen atom addition as hydrogenolysis pathways in Systems 2 and 3 and related systems, we are using, as an indicator, the internal or positional selectivity in the cleavage of 1,2'-dinaphthylmethane. In various experiments performed thus far, in which the donor solvents have included tetralin, dihydrophenanthrene, dihydroanthracene, dihydropyrene, tetrahydroquinoline, and indoline, the fully aromatic counterparts of some of these solvents, and mixtures of the pure solvents with coals or coal products, we have observed the ratio of 2-methylnaphthalene/1-methylnaphthalene to range from about 2.2 to 4.8. Some of these data are shown in Figure 2, where the observed ratio is plotted as a function of the endothermicity of hydrogen transfer from the respective solvent radical ArH^\cdot .

The variation in selectivity shown in Figure 2 demonstrates, at a minimum, that the hydrogen transfer which results in the DNM cleavage is not, in all cases, due to free hydrogen atoms. The increase in selectivity as the hydrogen transfer becomes more endothermic indicates either that (1) the transfer is in all cases by an RHT process that naturally becomes more selective as the reactivity of ArH^\cdot decreases, or (2) that in the case of the system of least selectivity (tetralin/naphthalene), the transfer is wholly or partly via free hydrogen atoms, and that the proportion of transfer by RHT increases as the radicals ArH^\cdot become less reactive. In either event, these data provide unequivocal evidence that transfer via free hydrogen atoms could be the sole mode of cleavage, at most, only for the naphthalene/tetralin system.

The data in Figure 2 do not illustrate the additional fact that the 2-Me-N/1-Me-N ratio can vary not only as a function of solvent system, but also as a function of the acceptor concentration in the solvent. For instance, in the case of dihydroanthracene, the ratio varies from about 3 to about 7, depending on whether the solvent is predominantly dihydroanthracene or anthracene, respectively. This is in accord with the observation made above, namely that if a successful encounter with a cleavable coal structure is not made before the hydrogen atom is unimolecularly eliminated from the original ArH^\cdot carrier, a large pool of the aromatic component acts as a temporary acceptor for the hydrogen atom. Thus, for a given ArH^\cdot steady-state concentration, the likelihood that an acceptor will receive a hydrogen atom in an RHT process is a function not only of the acceptor concentration, but also of the Ar concentration in the solvent pool. In experiments currently underway, we are determining the cleavage product ratio as a function of DNM and Ar concentrations. If, by sufficiently disfavoring and favoring the RHT process relative to transfer via free hydrogen atoms, we can reach a single demonstrable minimum for all solvent systems and unique maxima in the 2:1-methylnaphthalene product ratios for each solvent system then we will have determined the product ratios for cleavage purely by free hydrogen atoms on the one hand and purely by RHT on the other hand. Having determined these values, the product ratios observed under other conditions will be a direct and unequivocal measure of the relative contribution of cleavage by the two hydrogen transfer modes. Such results should put us one significant step closer to the goal of understanding the chemistry by which hydrogen can be shuttled from one

position in the solvent or coal structure to engender cleavage at another position, while minimizing the requirement for high hydrogen pressures or heterogeneous catalysts. Finally, an awareness of the importance of hydrogen-transfer-promoted bond cleavage in coal liquefaction suggests that it is also important in coal pyrolysis, and that a better understanding of the process would allow it to be augmented under the conditions of pyrolysis.

ACKNOWLEDGEMENTS

The authors wish to acknowledge the support of the U.S. Department of Energy under contracts DE-FG22--84PC70810 and DE-AC22-81PC40785.

REFERENCES

1. D. F. McMillen, W. C. Ogier, S. J. Chang, R. H. Fleming, and R. Malhotra, Proceedings of the 1983 International Conference on Coal Science, Pittsburgh, Pennsylvania, 15-19 August, 1983, p. 199.
2. D. F. McMillen, W. C. Ogier, R. H. Fleming and R. Malhotra, "Mechanisms of Hydrogen Transfer and Scission of Strongly Bonded Coal Structures in Donor-Solvent Systems", to be submitted to Fuel.
3. S. E. Stein, "A Fundamental Chemical Kinetics Approach to Coal Conversion," in Advances in Chemistry Series 192, American Chemical Society, Washington, DC, 1982, p. 97.
4. a. B. C. Bockrath, E. Bittner, and J. McGrew, J. Am. Chem. Soc., **106**, 135 (1984).
b. D. H. Finseth, B. C. Bockrath, D. L. Cillo, E. G. Illig, R. F. Sprecher, H. L. Retcofsky, and R. G. Lett, Am. Chem. Soc. Fuel Div. Preprints **28**, (5) 17 (1983).
5. a. J. A. Franz, D. M. Camaioni, R. R. Beishline, and D. K. Dalling, "Molecule-Induced Homolysis in Coal Chemistry: Radical Initiations, Reactions, and Hydrogen Atom Production from 1,2-Dihydronaphthalene," presented at the American Chemical Society National Meeting, Seattle, WN, 14-18 March 1983, Paper No. 155.
b. J. A. Franz, R. O. Barrows, and D. M. Camaioni, J. Am. Chem. Soc. **106**, 3964 (1984).
c. J. A. Franz, D. M. Camaioni, R. R. Beishline, and D. K. Dalling, J. Org. Chem. **49**, 3563 (1984).
6. a. K. R. Brower, Fuel **56**, 245 (1977).
b. K. R. Brower, J. Org. Chem. **47**, 1889 (1982).
7. L. W. Vernon, Fuel **59**, 102 (1980).
8. S. Friedman, S. Metlin, A. Sredi, and I. Wender, J. Org. Chem. **24**, 1287 (1959).
9. D. T. Allen and G. R. Cavalas, Int. J. Chem. Kinetics **15**, 219, (1983)

10. a. H.-H. King and L. M. Stock, Fuel **60**, 748 (1981).
- b. H.-H. King and L. M. Stock, Fuel **61**, 257 (1982).
11. D. S. Ross, private communication.
12. D. McMillen and D. M. Golden, "Hydrocarbon Bond Dissociation Energies," Ann. Rev. Phys. Chem. **33**, 497 (1982).
13. W. C. Herndon, J. Org. Chem. **46**, 2119 (1981).
14. S. W. Benson, Thermochemical Kinetics, 2nd ed. John Wiley and Sons, Inc., New York, 1976.
15. J. A. Kerr and S. J. Moss CRC Handbook of Bimolecular and Termolecular Gas Reactions, Vol. 1, CRC Press, Inc. Boca Raton, Florida, 1981.
16. S. E. Stein, private communication.

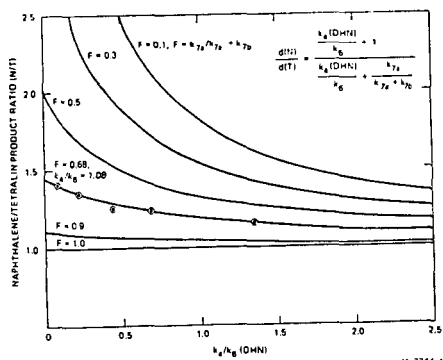


FIGURE 1 EFFECT OF DILUTION WITH BIPHENYL ON THE PRODUCT RATIO IN THE DISPROPORTIONATION OF 1,2-DIHYDRONAPHTHALENE AT 385°C

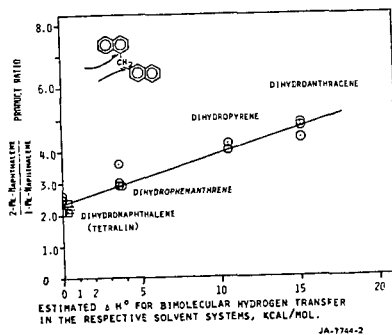


FIGURE 2 SELECTIVITY FOR HYDROGEN TRANSFER FROM SOLVENT RADICALS. RATIO OF ONE-POSITION TO TWO-POSITION TRANSFER TO DINAPHTHYLMETHANE

HYDROGEN UTILIZATION DURING THE EARLY STAGE OF COAL LIQUEFACTION

B.C. Bockrath, D.H. Finseth, and E.G. Illig

U.S. Department of Energy
Pittsburgh Energy Technology Center
P.O. Box 10940
Pittsburgh, Pennsylvania 15236

In the study of the chemistry of direct coal liquefaction, many of the more interesting aspects concern the initial conversion of coal into products extractable by polar solvents such as tetrahydrofuran. Among these are questions about the type and extent of the various chemical reactions necessary to convert the macromolecular matrix of coal to extractable fragments. The breakdown of the matrix is often depicted as a consequence of thermolysis of cross-linking bonds in coal. However, it is not yet clear to what extent the actions of the solvents, reducing gases, or catalysts applied to the coal are confined to events after the initial thermolytic reactions or to what extent they act directly on the macromolecular matrix itself.

Hydrogen transfer reactions are common to all stages of coal liquefaction. In previous work [1,2], a method was developed and used to determine net hydrogen utilization in the course of liquefaction. The total organic feed and the total organic product were considered in this analysis. The use of hydrogen was divided into four categories according to the type of reaction involved. These include (1) the production of light hydrocarbon gases, (2) removal of heteroatoms, (3) hydrogenation/dehydrogenation reactions involving changes in aromaticity, and (4) the sum of matrix cleavage reactions and condensation reactions. This same method has now been used to determine the changes in the amount of reactions in these four categories during the early stages of coal conversion. A wide variety of conversion conditions was surveyed to explore the sensitivity of hydrogen utilization to important process variables. These variables include the temperature, the reducing gas, the catalyst, and the use of water rather than an organic solvent as the liquefaction medium.

Experimental

Coal liquefaction was conducted in a 0.5-L stirred autoclave. In a typical experiment, 30 to 50 g (maf) of coal ground to pass 60 mesh was charged to the autoclave along with water or coal-derived solvent. When used, the solvent was a distillate cut (240°C-450°C) obtained from operations at the SRC-II pilot plant formerly at Ft. Lewis, Wash. The autoclave was pressurized with the appropriate amount of gas to obtain the desired partial pressure at operating temperature. Heat-up times to liquefaction temperatures were about 45 minutes. The autoclave was held at temperature for the specified time and then rapidly cooled by means of internal water-cooling coils. Grab samples of the off-gas were taken for analysis by gas chromatography as the autoclave was depressurized.

Conversion data were obtained by subjecting the entire autoclave contents to exhaustive Soxhlet extraction with tetrahydrofuran (THF). After extraction, the residues were dried in a vacuum oven at 110°C and weighed. Conversion values were based on the weight of dried residue.

The method used to determine hydrogen utilization data has been described [1]. In brief, the elemental analyses were obtained for the feed coal and the liquefaction solvent. The liquid products were separated into methylene chloride extracts and residues by Soxhlet extraction. Elemental analyses and carbon aromaticities were obtained for both fractions. The carbon aromaticities were

determined by ^{13}C NMR using CP/MAS techniques on the insoluble fractions, and high resolution ^{13}C NMR in CD_2Cl_2 for the extracts. An estimate of the amount of hydrocarbon gas produced was also made on the basis of gas chromatographic analysis of the grab sample of off-gas and the estimate of gas volume based on pressure measurements.

The coal was an Illinois No. 6 bituminous coal from the River King mine. The elemental analysis on an maf basis was as follows: C, 73.7%; H, 5.6%; N, 1.5%; O, 14.8%; and S, 4.5%. The ash content was 13.6% on a dry basis.

Results and Discussion

Dispersed catalysts may be effective in coal conversion at relatively low liquefaction temperatures, especially at low solvent-to-coal ratios. Figure 1 contains conversion data as a function of solvent-to-coal ratio obtained after holding the temperature at 350°C for 60 minutes under 2000 psia hydrogen. As reflected by tetrahydrofuran conversion values, the effect of adding ammonium molybdate (1% molybdenum on maf coal weight) becomes pronounced at low solvent/coal ratios. In this sense, use of catalyst under H_2 pressure reduces the demand for the large quantities of recycle solvent normally required for good conversion in the absence of catalyst. High conversions may thus be obtained at low solvent/coal ratios. Regarding the mechanism of liquefaction, these data indicate that catalysts can play a role in the breakdown of the coal matrix that leads to the initial formation of extractable products.

Table 1 compares the effects of liquefaction temperature on hydrogen utilization at the more conventional solvent/coal ratio of 2. The two catalysts used, ammonium molybdate and tin tetrachloride, were thought to act in liquefaction by different means [3]. The former is noted for hydrogenation activity, and the latter is not. However, differences in the hydrogen utilization data between the two were not striking.

As determined earlier [1,2], temperature has a large effect on the pattern of utilization. There is a change from net hydrogenation to net dehydrogenation between 375°C and 425°C. The net change at 400°C was zero. Hydrogen partial pressure at temperature was roughly the same, 2000 psia, in all cases. The direction of the change from net hydrogenation to net dehydrogenation is expected from thermodynamic considerations. At equilibrium, higher temperatures generally favor the formation of aromatic compounds from hydroaromatic compounds by release of hydrogen. These data emphasize the important effect of temperature and the degree of control possible within a short span of temperature centered around 400°C.

The addition of the catalysts at 425°C had a large effect on the amount of hydrogen consumed during the cleavage of matrix bonds. The method measures net hydrogen utilization without regard to the details of the chemical mechanism. Thus, from these data alone it cannot be said whether the increase in hydrogen use is due to promotion of bond cleavage directly or to the prevention of condensation reactions between reactive fragments created by simple thermal bond scission. At 375°C, there was little net change in matrix bonds in the presence of ammonium molybdate and no net change in the absence of catalyst. Of course, since only net changes are measured, this does not necessarily mean that matrix bond cleavage did not occur. It may be that cleavage reactions are nearly balanced by condensation reactions.

The amount of hydrogen consumed to remove heteroatoms is relatively small, as expected under mild liquefaction conditions. Almost all of this hydrogen is used in the removal of oxygen. There is essentially no change in nitrogen content and only a small reduction of organic sulfur.

In a separate series of autoclave experiments, liquefaction with water was compared to that with the organic liquefaction solvent. In some respects, interpretation of the data obtained with water was simplified because now all of the organic liquefaction products originate from the coal. However, coal may behave quite differently in water than in organic solvents. In particular, conversions in water vary greatly depending on the type and partial pressure of the reducing gas and on the type of catalyst used.

Table II contains liquefaction data obtained at 350°C. At this mild temperature, conversions are very low using water as a solvent under hydrogen. By comparison, conversions were much higher even at a shorter contact time using SRC-II distillate. They were also less sensitive to hydrogen partial pressure in the hydrocarbon solvent.

When coal was recovered from the experiments with water and hydrogen at room temperature partial pressures less than 1500 psia, it appeared not to have agglomerated nor to have lost its particulate nature. Sufficient conversion to cause agglomeration did occur under 2000 psia hydrogen partial pressure. In contrast, under only 1000 psia room temperature partial pressure of CO, the coal was generally recovered as an agglomerated mass. Conversions were much higher under CO than under hydrogen at the same pressure and were improved further by use of ammonium molybdate and even more so by basic catalysts, K_2S in particular. Clearly, the mechanisms of liquefaction must be quite different according to whether CO or H_2 is used as the reducing gas. These findings are similar to those of an earlier comparison of hydrogen and carbon monoxide used with water in the presence or absence of base [4].

Hydrogen utilization data were obtained for a variety of reaction conditions with water (Table III). Many of these hydrogen utilization values are larger than those in Table I. If the speculation that coal accounts for the majority of the reactions using hydrogen when organic solvent is present is accepted, then the increase in the absolute magnitude of the utilization values is easily understood. The organic solvent may act as a diluent that reduces the observed amount of hydrogen used or given up per 100 carbons of the total feed. In water, however, all of the carbon is associated with the coal, thus resulting in observation of larger changes. Aside from this dilution factor, there seems to be a general trend for coal to give up hydrogen more readily by dehydrogenation and condensation reactions in water than does the total mixed feed of coal and recycle solvent.

In water, temperature is again a major determinant of the pattern of hydrogen utilization. At 400°C there is an overall net loss of hydrogen by coal. Generally, the loss is split between dehydrogenation reactions and condensation reactions. The latter are reflected as negative values for matrix cleavage. In contrast, at 350°C under CO, there is little change in total hydrogen in the absence of catalyst. In the presence of KOH, there is a sizable uptake of hydrogen.

The type of reducing gas has a large influence at 350°C. With either H_2 or N_2 replacing CO, there is again a large net loss of hydrogen by coal. The loss is accounted for by both dehydrogenation and condensation, as it was at 400°C.

Other general trends are also apparent. Gas make is virtually nil at 350°C. The loss of heteroatoms, which is almost totally due to loss of oxygen in these experiments, is not as great at 350°C as at 400°C. The exception to this observation is the higher value at 350°C for the one experiment run for 120 minutes. Thus, the rate of loss may be slower at the lower temperature.

The role of catalyst is also closely related to liquefaction temperature. Although the data are incomplete, addition of KOH markedly increases the total amount of hydrogen taken up by coal at 350°C. At 400°C, the difference on addition

of KOH is mostly associated with an increased loss of hydrogen by condensation reactions.

The reaction conditions surveyed here indicate that hydrogen utilization varies considerably with liquefaction conditions. Temperature, reducing gas, and catalyst were major influences. These data provide added confidence that the analytical method reveals real changes in liquefaction mechanisms. A full picture of hydrogen utilization requires a much more extensive comparison among the myriad of process parameters. Further studies now under way are aimed at identifying other critical parameters, such as reaction time.

References

1. D.H. Finseth, B.C. Bockrath, D.L. Cillo, E.G. Illig, R.F. Sprecher, H.L. Retcofsky, and R.G. Lett, Am. Chem. Soc. Div. Fuel Chem. Preprints, 28(5), 17 (1983).
2. B.C. Bockrath, E.G. Illig, D.H. Finseth, and R.F. Sprecher, Am. Chem. Soc. Div. Fuel Chem. Preprints, 29(5), 76 (1984).
3. P.-L. Chien, G.M. Sellers, and S.W. Weller, Fuel Processing Technology, 7, 1 (1983).
4. D.S. Ross, and Q. Nguyen, Fluid Phase Equilibria, 10, 319 (1983).

Acknowledgements

We are indebted to R.F. Sprecher for the NMR analyses essential to this work, to W.L. Lipinski for assistance with the autoclave liquefactions, and to B.M. Thames for assistance with the analysis of the liquefaction products.

Table I. Coal Conversion and Hydrogen Utilization for Catalyzed and Non-Catalyzed Liquefaction¹

<u>Catalyst</u>	<u>Temperature</u>	<u>Heteroatom Removal</u>	<u>Hydrogenation</u>	<u>Matrix Cleavage</u>	<u>Gas Make</u>	<u>Total²</u>
Ammonium Molybdate	375°C	1	2	2	0	5
SnCl ₄	375°C	0	4	0	0	4
Ammonium Molybdate	400°C	2	0	2	0	4
None	425°C	2	-5	5	1	3
Ammonium Molybdate	425°C	2	-4	11	2	11
SnCl ₄	425°C	1	-4	10	2	9

¹All liquefactions under approximately 2000 psia hydrogen partial pressure at operating temperature, using 2 parts solvent and 1 part maf coal.

²All utilization numbers in hydrogens per 100 carbons in feed slurry.

TABLE II. Coal Conversion at 350°C

<u>Solvent</u> ¹	<u>Gas, psia</u> ²	<u>Time, min.</u>	<u>Catalyst</u> ³	<u>Conversion</u> ⁴
SRC-II	H ₂ , 200	15		66
SRC-II	H ₂ , 1000	15		68
SRC-II	H ₂ , 2000	15		75
SRC-II	H ₂ , 3000	15		80
Water	H ₂ , 1100	60		16
Water	N ₂ , 1010	60		12
Water	H ₂ , 1100	60	AmMo (0.2%)	19
Water	H ₂ , 1500	60		33
Water	H ₂ , 2000	60		57
Water	CO, 1000	60		63
Water	CO, 1010	60	K ₂ S (2%)	93
Water	CO, 1010	60	AmMo (0.2%)	71
Water	CO, 1020	60	AmMo (0.4%)	82
Water	CO, 1000	60	KOH (1%), AmMo (0.4%)	86

¹Two parts solvent used to one part coal, by weight.

²With SRC-II, pressure is measured at operating temperature. With water, pressure is measured at room temperature.

³Catalyst loading is weight percent on maf coal. For ammonium molybdate, AmMo, based on weight of molybdenum.

⁴Based on residue weights after exhaustive Soxhlet extraction with tetrahydrofuran.

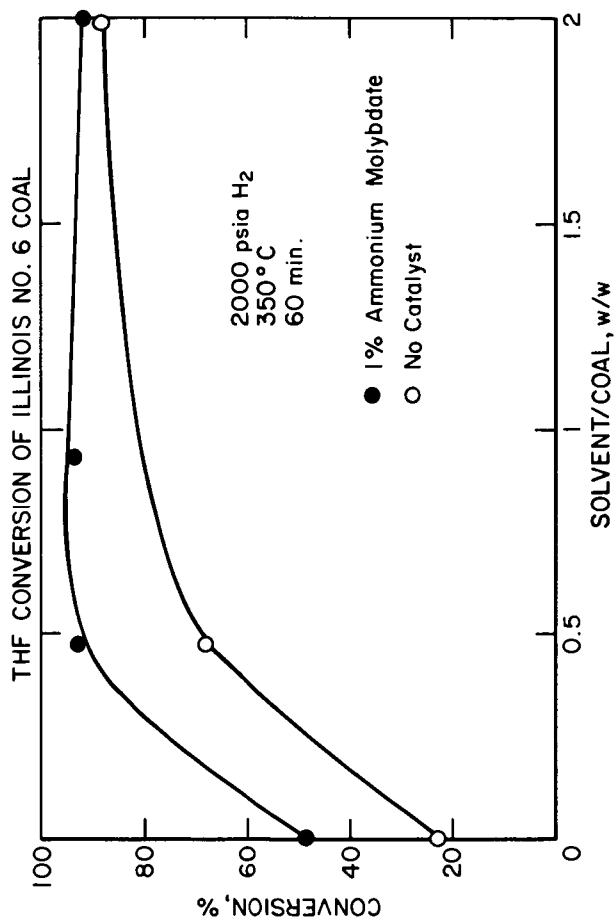
Table III. Hydrogen Utilization for Liquefaction in Water

Temperature	Catalyst ¹	Pressure ² , psia	Time, min.	Heteroatom Removal	Hydrogenation	Matrix Cleavage	Gas Make	Total ³
400°C		750	15	4	-9	-2	2	-5
400°C		800 (H ₂)	20	3	-11	-5	1	-12
400°C	KOH	800	20	6	-7	-7	2	-6
400°C	KOH	800	60	7	-6	-5	2	-2
400°C	Na ⁺ HCOO ⁻	730	20	6	-12	-5	2	-9
350°C		1000	120	5	-1	-1	0	2
350°C		1000	60	3	-2	0	0	1
350°C	KOH	1000	60	3	NA	NA	0	9
350°C	AmMo	1000	60	3	-1	-1	0	1
350°C		1000 (H ₂)	60	2	-5	-8	0	-11
350°C		1000 (N ₂)	60	4	-7	-7	0	-10

¹Catalyst loadings were 1% by weight of KOH or sodium formate, or 0.4% of ammonium molybdate, AmMo.

²Pressure measured at room temperature. Reducing gas used is CO unless otherwise indicated.

³Hydrogen utilization in hydrogens per 100 carbons in coal.



THE NATURE OF VITRINITE SECONDARY FLUORESCENCE

Rui Lin, Alan Davis, D.F. Bensley and F.J. Derbyshire

Coal Research Section
College of Earth and Mineral Sciences
The Pennsylvania State University
University Park, PA 16802

INTRODUCTION

In recent years, the phenomenon of vitrinite fluorescence has been noted and related to thermoplastic behavior (1-5). Huminite/vitrinite fluorescence can be divided into primary and secondary stages of fluorescence. Primary vitrinite fluorescence is inherited from biopolymers; it decreases markedly in intensity from the peat stage to the subbituminous C/B rank and, within the same range, the wavelength of its maximum spectral intensity shifts from 520 to 660 nm. Following the loss of most of the primary fluorescence, a secondary vitrinite fluorescence begins to develop, and this in turn becomes extinct at low volatile bituminous rank (ca. 1.8% Rm) (4). It is the secondary vitrinite fluorescence, within the bituminous rank range, which is well correlated with thermoplastic properties.

Although the fluorescence of all coal macerals has been the subject of intensive study during recent years, the chemical basis of the phenomenon is little understood. Teichmüller(3-4) has attributed the secondary fluorescence of vitrinite to the presence of absorbed "bitumen" which has been generated during coalification from liptinite and lipid substances incorporated in the vitrinite. Ottenjann et al.(2) noted the parallelism between vitrinite fluorescence and solvent extraction yields, and also suggested that the fluorescence is due to the presence of "bitumen". Of course, this idea was speculative and required further chemical confirmation.

Recent studies(6-10) of the structure of vitrinite suggest that this maceral can be regarded as occurring in two distinct phases. One is considered to be a relatively more condensed three-dimensional aromatic network system. The other, called "mobile phase", is thought of an assembly of relatively small molecules located, even partly trapped, within the network.

In the present work, coal extracts have been obtained by a series of Soxhlet extractions of coals with solvents of decreasing strength. HPLC has been used to further separate the "oil" (hexane-soluble) into aliphatic, aromatic and polar fractions. Each component and fraction was examined by reflected blue-light microscopy to determine which are actively fluorescent.

In order to study the development of the mobile phase as a result of coalification, and the associated changes in secondary fluorescence and thermoplastic behavior, a suite of 14 coals was tested. The spectral fluorescence characteristics of the vitrinite, yield of chloroform-soluble material, and the Gieseler fluidity of all these coals have been measured.

EXPERIMENTAL

Coal Samples

The fourteen coals used in these experiments were obtained from the Penn State Coal Sample Bank; they had been stored in a nitrogen atmosphere at minus 20 mesh size. Table I lists some compositional data for these coals.

Table 1

Sample number (PSOC)	Romax (%)	Petrographic composition (dmmf)			Sample number (PSOC)	Romax (%)	Petrographic composition (dmmf)		
		V	I	E			V	I	E
773	0.54	91.0	5.7	3.3	1198	1.45	89.4	10.4	0.2
780	0.70	89.8	9.5	0.7	1136	1.53	89.7	10.3	0.0
779	0.73	90.4	8.1	1.5	1330	1.75	92.1	7.9	0.0
1296	0.87	91.6	3.8	4.6	1281	0.63	84.1	7.2	8.7
1299	0.93	91.9	6.2	1.9	1142	0.88	87.0	8.7	4.3
815	0.97	91.5	3.9	4.6	1336	0.92	85.1	10.1	4.8
1196	1.30	89.6	10.4	0.0	1340	1.01	80.4	9.1	10.5

Solvent Extraction and Fractionation

Coal samples were ground to minus 60 mesh in a glove box in which a flow of nitrogen was maintained. Moisture was removed at 60° C overnight in a vacuum oven. Approximately 5 g of dried coal samples were extracted for 48 h in a Soxhlet apparatus fed with a stream of nitrogen. The resulting extracts and residues were vacuum dried for 12 h to remove any solvent. Fig. 1 is a flow chart of the progressive solvent extraction and fractionation scheme employed. Pyridine and chloroform extractions were performed at the solvent boiling points; the chloroform soluble fraction was then separated into the oil and asphaltene fractions with hexane at room temperature.

The HPLC fractionation of the "oil" was performed with a Waters Associates' instrument equipped with a semi-preparative Whatman column (Partisil Magnum 9/50 PAC). The oil was dissolved in hexane and injected into the sample loop. Separation of three fractions is based on the absorbance response detected (Fig. 2). The aliphatic and aromatic fractions were the first two fractions to be eluted, in that order. Finally, by using the back flush valve and eluting a small amount of methylene chloride, the polar fraction was collected from the column.

Fluorescence Microscopy

The fluorescence examinations and measurements were performed with a Leitz MPV-II microscope system equipped with the following accessories:

- i) HBO 100-watt ultra-high pressure mercury lamp;
- ii) Ploempak 2.1 vertical illuminator with a BD 390-490/RKP510 LP515 filter for qualitative examination and a BP340-380/RKP400 LP430 filter for quantitative measurement;
- iii) Double grating monochromator;
- iv) Water-cooled, broad spectral response photomultiplier; and
- v) Calibration tungsten lamp, 12v, 100 watt, color temperature 3200K.

Data were processed with a PDP 11/02 computer. All measured spectra were corrected prior to analysis for both system variation and background interference. System variation was determined by measuring the deviation from the known spectrum of the calibration lamp. This correction permits compensation for any optical

distortion within the system. Background measurements taken from a non-fluorescing object, in this case fusinite, are employed to reduce the influence of the immersion oils' self-fluorescence and fluorescence interference from the epoxy resin binder. Corrected spectra were all adjusted to values of relative intensity. Identical electrical and optical configurations were employed for each sample series to provide comparable results. For final comparisons of spectral fluorescence, the spectra were normalized to 100% maximum fluorescence intensity.

To prepare the coal extracts and fractions for microscopic study, they were redissolved at low concentration in their corresponding solvents and a drop placed on a glass slide. The solvents were removed by drying in a flow of nitrogen. Glass cover slips were placed over the dried specimens for reflected blue-light study under oil immersion. Raw coals and the pyridine-insoluble fractions were molded into pellets with epoxy resin prior to polishing according to the ASTM procedure(11).

Gieseler Fluidity

The fluid behavior of the coal samples was tested with an automated Gieseler plastometer(12). For each run, 5 g of minus 40 mesh coal was packed into the cylinder. The cylinder assembly was heated in a solder bath and heated from 330°C at 3°C/min. Because of the very high fluidity displayed by some Lower Kittanning samples a torque of 20 g-in. was used rather than the standard 40 g-in. (9.96 mN/m).

THE ORGANIC CHEMISTRY OF FLUORESCENCE

Aliphatic Compounds

Very few aliphatic and saturated cyclic organic compounds fluoresce. Saturated hydrocarbons like ethane, hexane and cyclohexane and simple unsaturated hydrocarbons like ethylene display no visible or ultraviolet fluorescence(13). All electrons in aliphatic compounds are either very tightly bound or are involved in sigma bonding. The absorption of ultraviolet energy by a saturated molecule usually results in bond dissociation. Important exceptions are the aliphatic aldehydes and ketones; in these, the non-bonding electrons on the carbonyl oxygen can be excited to antibonding C=O π orbitals without severe disruption of molecular bonding(14). Some polyenes also give a visible fluorescence(13,15).

Aromatic Compounds

The majority of fluorescing organic compounds are those possessing large conjugated systems, in which there are electrons less strongly bound within the molecule than sigma electrons, and heteroatoms (N, O, S, etc.), in which n electrons, can be promoted to antibonding orbitals by absorption of excitation energy. Hence, the aromatics and polars should be our main concerns.

Most aromatic compounds are fluorescent. The condensed aromatics, of which vitrinite is largely composed, can be subdivided into linearly and nonlinearly condensed aromatics. Linearly condensed aromatics are those in which benzene rings are fused in a straight chain; their fluorescence displays an increasing wavelength with increase in the number of rings and of conjugated double bonds(15). This is brought about by a decrease in the energy difference between the lowest excited state and the ground state. The fluorescence generated decreases markedly for aromatic hydrocarbons containing more than three phenyl rings in a straight chain. Nonlinearly condensed aromatics generally do not follow this trend. Their fluorescence is very dependent on molecular configuration. But it is generally true that the fluorescence is at longer wavelengths in compounds containing larger ring systems, although there are some exceptions(16).

Polar Compounds

Polar compounds which are derived from aromatic hydrocarbons by substitution are fluorescent mostly because of the existence of n electrons in heteroatoms or polar functional groups ($-SH$, $-OH$, $-NH_2$). The fluorescence of aromatic hydrocarbons is usually altered by ring substitution. The substitution of these polar functional groups or heteroatoms onto the aromatic molecule usually causes a shift into longer wavelengths(13-15). Consequently, these compounds generally fluoresce in a longer wavelength regime than the corresponding aromatic molecules.

FLUORESCENCE OF THE VITRINITE EXTRACTS AND FRACTIONS

HPLC Fractions

Aliphatics: As observed under the microscope, this fraction is mostly non-fluorescent. Aliphatic compounds usually have a fluorescence quantum yield (defined according to Becker(16) as the quanta emitted per exciting quantum absorbed) of zero, because of the types of electron bonding described above. However, a small portion of this fraction displays a fluorescence which has a spectral peak at 450 nm or below and decreases progressively at longer wavelengths (Fig. 3). The spectral distribution is very similar to that of the aromatics, although the intensities are quite different. Several possibilities may account for the fluorescence of this small portion of the aliphatic fraction:

- i) aliphatic aldehydes or ketones;
- ii) aliphatic polyenes;
- iii) aromatic impurities resulting from imperfect fractionation.

Aromatics: This fraction is very highly and actively fluorescent. The fluorescence spectrum has a peak at 450 nm or just below and decreases in intensity with increasing wavelength (Fig. 3).

Compounds which have been used as standards for HPLC fractionation of aromatics include: fluorene; naphthalene; phenanthrene; 3,4-benzo-(a)-pyrene; 9, 10-benzo-phenanthrene; 9, 10-dihydroanthracene; 2, 3-dimethylnaphthalene and 1-phenylheptane(17). The spectral fluorescence of some of these compounds (fluorene, anthracene and naphthalene) as well as that of chrysene have been reported by Hagemann and Hollerbach(18). These spectra also peak at short wavelengths, from 430 to 450 nm, and have a similar distribution to those of coal-derived aromatics. It is suggested that the aromatic fractions obtained in the present study are composed of similar molecules; the actual spectra represent the overlapping fluorescence responses of such compounds.

Polars: Like the aromatics, this fraction is also very highly and actively fluorescing. Although the spectrum in this particular case (Fig. 3) is doubly peaked, other coals have yielded dissimilar spectra. The first peak here occurs at 490 nm, and the second, which is the maximum, at 660 nm. A close similarity exists between the spectral distribution of this fraction and that of the oil from which the polars are derived (Fig. 4). The peaks for the polar fraction occur at 30 nm higher, and the maximum is at the longer wavelength.

Oil (hexane soluble)

The fluorescence spectrum of this component also is doubly peaked; the maximum occurs at 460 nm, and a second peak at 627 nm (Fig. 4). The shift of the peak positions to a longer wavelength in the case of the polar fraction may be due to the substantial absence of aromatic substances which have fluorescence peaks at very short wavelengths. As mentioned earlier, substitution of polar functional groups onto the aromatic structure can result in a red shift of the spectrum.

Asphaltene (hexane insoluble)

The spectrum for this fraction peaks at 690 nm (Fig. 4). The aromatics in this fraction are relatively more condensed than those in the oil fraction; hence, their fluorescence spectra peak at longer wavelengths.

γ -Fraction (chloroform soluble)

This component has a heterogeneous fluorescence even at very small concentrations. At least three different fluorescence entities can be recognized (Fig. 5). The wavelengths of the maximum fluorescence intensities of these three entities are 562, 627 and 698 nm. Entities 1 and 2 appear to correspond to the "oil", and entity 3, whose spectrum peaks at a longer wavelength, appears to be composed of asphaltene-like material according to their fluorescence characteristics.

β -Fraction (chloroform insoluble fraction of pyridine solubles)

The fluorescence of this fraction has a very similar spectral distribution to those of the untreated vitrinite and the pyridine extracts and residues, but has a lower intensity (Fig. 6). The lower intensity probably can be attributed to the removal of chloroform-soluble materials, which are actively fluorescent. The β -fraction is primarily composed of relatively more condensed aromatics, which may have been derived from the network disintegration.

α -Fraction (pyridine insoluble) and Pyridine-Soluble Fraction

These two fractions and the Vitrinite in the unextracted coal have very similar spectral distributions (Fig. 6). This is consistent with the results that pyridine extracts are chemically similar or identical to the pyridine-insoluble residue; the nature of these two fractions closely resemble that of the parent coal(19).

Vitrinite

The spectrum of this maceral is very similar to that of the pyridine extract and residue as discussed above (Fig. 6). There are, however, differences in fluorescence intensity between the untreated vitrinite and the pyridine extract and residue which are not fully understood. Further studies are being conducted.

The Aromatic Network

The fluorescence of this phase cannot be directly investigated because of our inability to completely separate the mobile phase from the aromatic network system without modifying the structure of the latter. The following indirect lines of evidence suggest that the network system is too condensed to show visible fluorescence in coals beyond the subbituminous B stage:

- i) Huminite/vitrinite primary fluorescence is lost when the coal rank reaches subbituminous C/B stage. This indicates that any inherited chemical structure, for example that derived from lignin, would be too condensed to have a visible fluorescence,
- ii) More condensed aromatics generally have a relatively low fluorescence intensity and a longer wavelength of maximum fluorescence intensity,
- iii) Highly aromatized systems such as fusinite, anthracitic macerals and coals carbonized at temperatures greater than 500-600°C do not visibly fluoresce,
- iv) The fluorescence of coked anthracene shifts into the longer wavelength region and decreases in intensity with increased coking temperature.

FLUORESCENCE CHARACTERISTICS AND FLUID BEHAVIOR OF A COAL RANK SUITE

Vitrinite primary fluorescence is lost as the rank increases beyond subbituminous C/B stage. At this stage, the secondary fluorescence begins to develop, the intensity of which increases up to the high volatile A bituminous stage (ca. 0.9% Ro max). Beyond this rank, fluorescence intensity decreases markedly(4). This trend for vitrinite fluorescence corresponds to changes in the yield of chloroform extracts and the maximum Gieseler fluidity displayed by the coals (Fig. 7).

Within the sub C/B-hvAb range just discussed the proportion of mobile phase has been built up. Possible contributions to the development of this mobile phase have resulted from:

- i) oligomerization associated with the network polymerization,
- ii) migration of petroleum-like substances derived from liptinites and lipoid substances(3-4).

At high volatile A bituminous rank, where secondary fluorescence, chloroform yield and fluidity all reach a maximum level, the wavelength of maximum fluorescence has been shifted into the infrared region(4). At higher ranks, the maximum intensity in the visible region decreases (Fig. 7). This, and the associated decreases in chloroform yields and fluid behavior is related to the gradual cracking of the mobile phase into gaseous products that accompanies aromatic condensation. These conclusions are consistent with the observation that the fluorescence of chloroform extracts undergoes a red shift with increasing rank(18).

The visible fluorescence of vitrinite is finally lost at low volatile bituminous rank (above 1.8% Ro max)(4). This corresponds to a loss of fluid behavior and a very low chloroform extraction yield.

SUMMARY AND CONCLUSIONS

Vitrinite can be considered to be composed of two phases: a mobile phase and a network phase (Fig. 8). The mobile phase contains actively and highly fluorescent aromatics, polar groups and a small proportion of aliphatic groups. These fractions absorb excitation energy and emit a part of this energy as fluorescence. The fluorescence spectra of these separate fractions are very different from those where they are combined in a complex system like vitrinite. This is because of both intramolecular and intermolecular interaction between the fluorescing molecules and the molecules in the network environment. This interaction can cause a certain degree of fluorescence quenching. As a result the fluorescence of vitrinite has a much lower intensity and a longer wavelength than those of the mobile phase fractions which it contains. So, the aromatic network system, which acts as the host for the fluorescing molecules in the mobile phase, though not actively fluorescent in the visible region, influences the overall vitrinite fluorescence character.

The build-up of the mobile phase in the bituminous rank range results in the maximum development of vitrinite secondary fluorescence, and is also manifested in optimum chloroform extraction yields and fluid behavior.

LITERATURE CITED

1. Ottenjann, K., Wolf, M. and Wolff-Fischer, E., Proc. Int. Conf. Coal Sci., Int. Energy Agency, 86-91(1981).
2. Ottenjann, K., Wolf, M. and Wolff-Fischer, E., Glückauf-Forschungshefte 43, H.4, 2(1982).

3. Teichmüller, M., "Fluoreszenzmicroscopische Änderungen von Liptiniten und Vitriten mit zunehmendem Inkohlungsgrad und ihre Beziehungen zu Bitumenbildung und Verkokungsverhalten", Geol. Landesamt Nordrhein-Westfalen, Krefeld (1982).
4. Teichmüller, M. and Durand, B., *Int. J. Coal Geol.* 2, 197(1983).
5. Wolf, M., Wolff-Fischer, E., Ottenjann, K. and Hagemann, H.-W., *Prepr. Meet. 36th Int. Comm. Coal Petrology, Commission 3, Oviedo*, 14pp. (1983).
6. Given, P.H. and Derbyshire, F.J., *The Mobile Phase in Coals: Its Nature and Modes of Release*, Tech. Rep. No. DOE-PC-60811-1,2 from the Penn State Univ. to U.S. Dep. Energy under Contract No. DE-FE22-83PC60811, (1984).
7. Green, T., Kovac, J., Brenner, D. and Larsen, J.W., in *"Coal Structure"* (Ed. R.A. Meyers), Academic Press, New York, 199-282 (1982).
8. Larsen, J.W., in *"Chemistry and Physics of Coal Utilization"* (Eds. B.R. Cooper and L. Petrakis), *Am. Inst. Phys.*, New York, 1-27 (1980).
9. Lucht, L.M. & Peppas, N.A., in *"Chemistry and Physics of Coal Utilization"* (Eds. B.R. Cooper and L. Petrakis), *Am. Inst. Phys.*, New York, 28-48 (1980).
10. Lucht, L.M. & Peppas, N.A., *Am. Chem. Soc. Symp. Ser.* 169, 43 (1981).
11. American Society for Testing and Materials (ASTM), *Annu. Book ASTM Stand.* 5.05, 378 (1984).
12. American Society for Testing and Materials (ASTM), *Annu. Book ASTM Stand.* 5.05, 355 (1984).
13. Förster, T., *"Fluoreszenz Organischer Verbindungen"*, Vandenhoeck & Ruprecht, Göttingen (1951).
14. Wehry, E.L., in *"Fluorescence: Theory, Instrumentation and Practice"* (Ed. G.G. Guilbault), M. Dekker, New York, 37-132 (1967).
15. Pringsheim, P., *"Fluorescence and Phosphorescence"*, Interscience, New York (1949).
16. Becker, R.S., *"Theory and Interpretation of Fluorescence and Phosphorescence"*, John Wiley & Sons, New York (1969).
17. Neill, P.H. and Given, P.H., *The Dependence of Liquefaction Behavior on Coal Characteristics Part VI: Relationship of Liquefaction Behavior of a set of High Sulfur Coals to Chemical Structural Characteristics*, Tech. Rep. No. DOE/PC/40784-T4 from the Penn State Univ. to U.S. Dep. Energy under Contract No. DE-AC22-81-PC-40784 (1984).
18. Hagemann, H. & Hollerbach, A., in *"Geology of Coal, Oil Shales and Kerogen"* (Ed. Bull. Centres Rech. Explor.-Prod. Elf-Aquitaine) 5, 637-650 (1981).
19. Pullen, J.R., in *"Coal Science"*, 2, (Eds. M.L. Gorbaty, J.W. Larsen and I. Wender), Academic Press, New York, 173-228 (1983).
20. Neavel, R.C., in *"Coal Science"*, 1, (Eds. M.L. Gorbaty, J.W. Larsen and I. Wender), Academic Press, New York, 1-19 (1982).

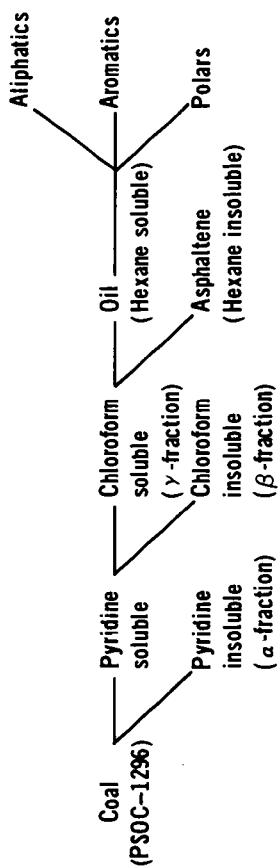


Figure 1. Solvent Extraction and Fractionation Scheme

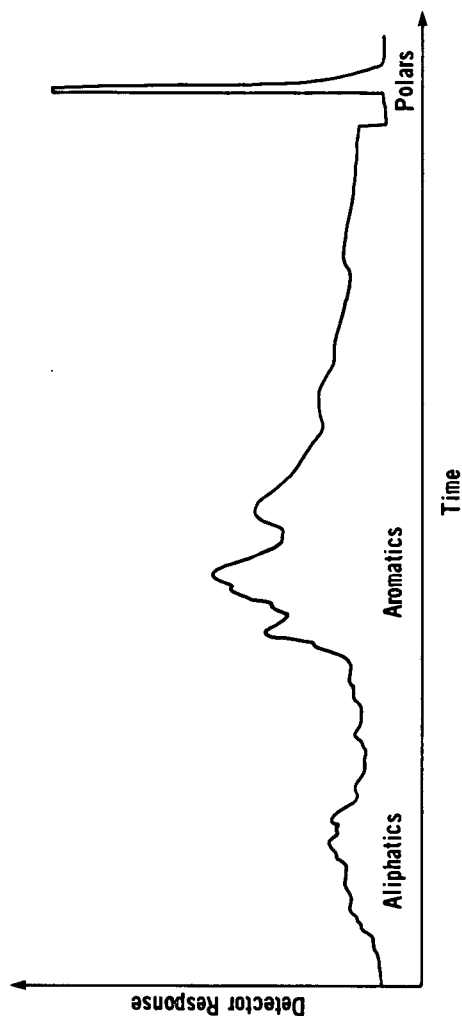


Figure 2. Absorbance Response of HPLC Fractions

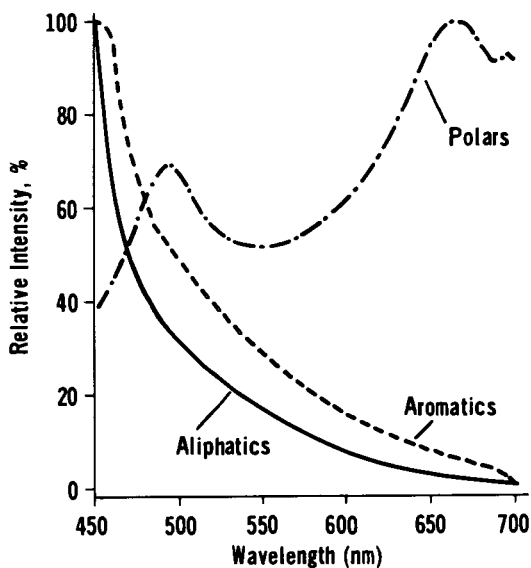


Figure 3. Fluorescence Spectra of HPLC Fractions

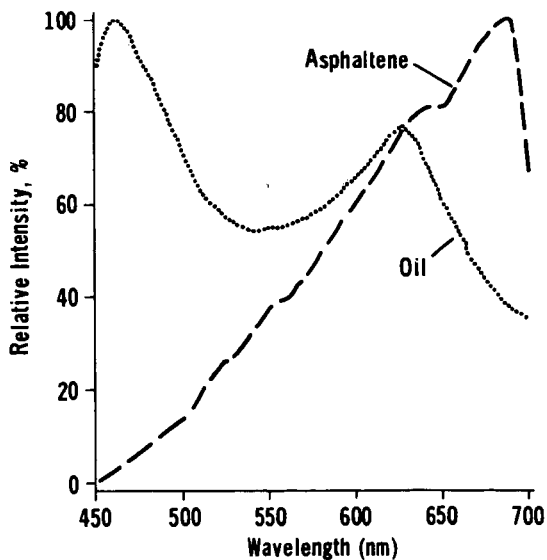


Figure 4. Fluorescence Spectra of Oil and Asphaltene

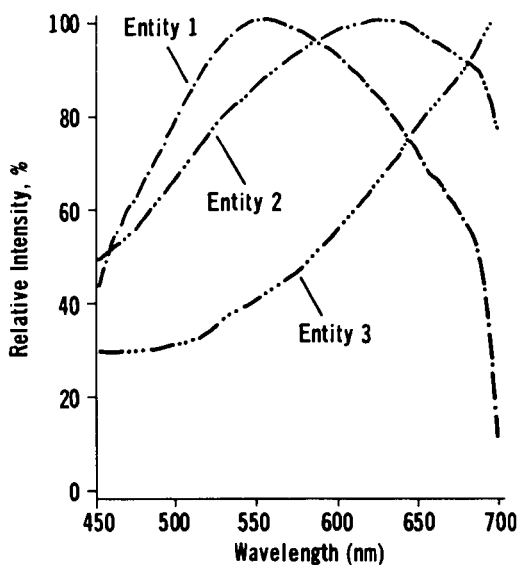


Figure 5. Fluorescence Spectra of Three Entities in γ -fraction

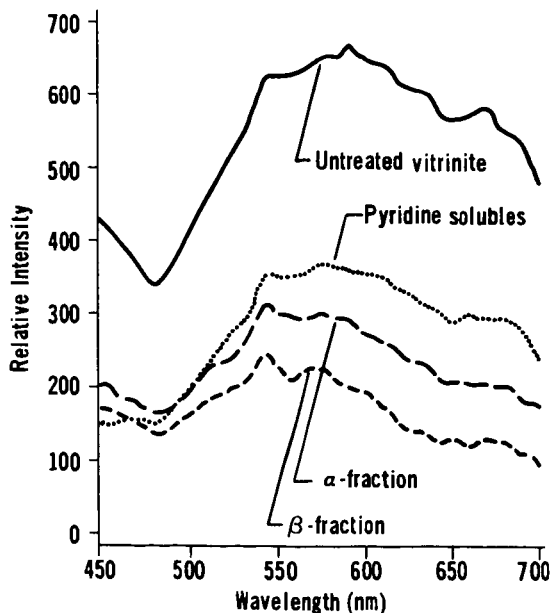


Figure 6. Fluorescence Spectra of Untreated Vitrinite, Pyridine Solubles, α -fraction and β -fraction

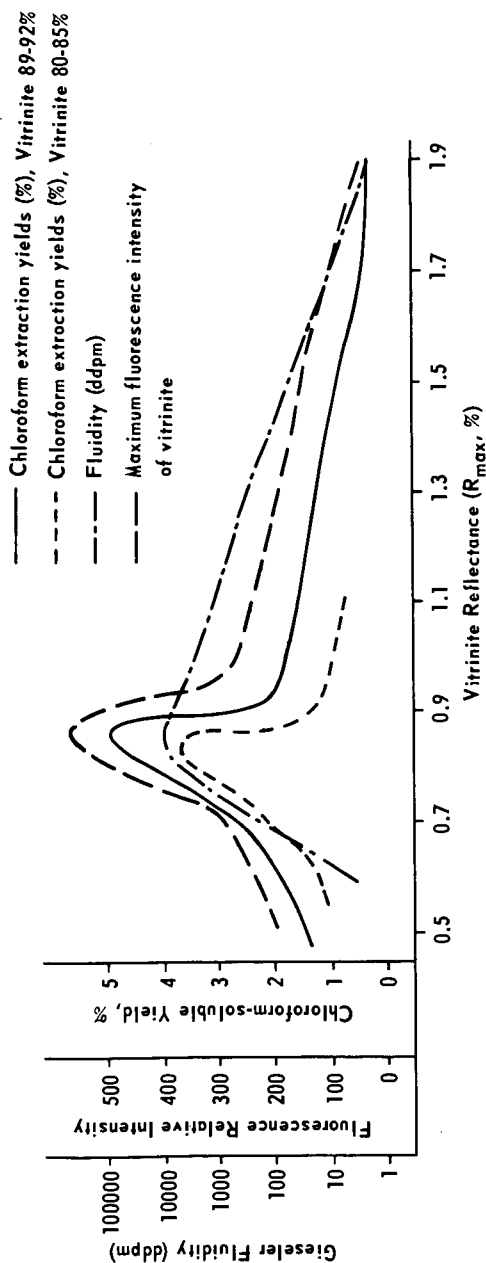


Figure 7. Relations among Fluorescence Intensity, Chloroform Extraction Yields and Fluidity for Coals of Different Rank

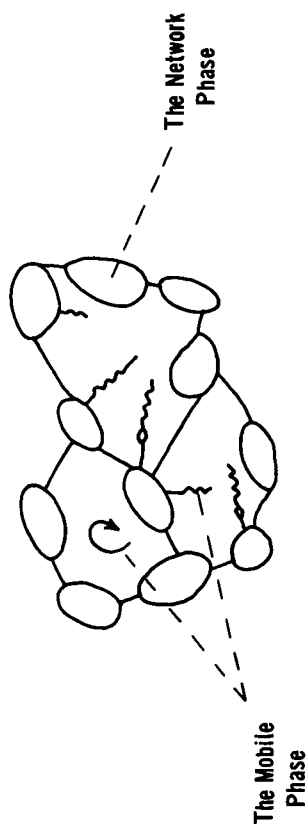


Figure 8. Two-phase Model of Vitrinite Structure (Modified after Giver and Derbyshire (6) and Neavel (20))

A Study of Catalytic Coal Liquefaction in the Absence of Solvent

F. J. Derbyshire, A. Davis, R. Lin, P. G. Stansberry,
and M-T. Terrer

Fuel Science Program
The Pennsylvania State University
University Park, PA 16802, USA

Abstract

In attempting to gain insight into the reactions involved in coal liquefaction and their relationship to coal structure, an approach has been adopted in which coals are reacted only with hydrogen gas in the presence of an impregnated molybdenum catalyst. The products from reaction at 400°C and lower have been characterized in terms of the yields of light gases and chloroform-soluble extracts. The composition of the latter has been examined by a number of analytical techniques. The extent of conversion has been measured as a function of time and temperature. Unlike liquefaction in a solvent medium, conversion increases progressively with reaction time. Consistent with other research, the molybdenum should be present in the sulfided form for high activity. Following reaction, unextracted coal samples were examined by reflected fluorescent light microscopy. The vitrinite fluorescence was found to correlate with the yield of chloroform-soluble extract and, essentially, to originate from these materials. This microscopic technique provided a direct visual observation of the chemical changes taking place within the coal structure.

Introduction

Early propositions concerning the structure of coal¹⁻² have formed the basis for the development of a concept in which coal is considered as a three-dimensional macromolecular network containing lower molecular weight species (the so-called mobile phase) accommodated in open, closed or partially closed pores.³⁻⁴ We have initiated research to investigate this concept and have adopted an approach used by other workers in coal liquefaction studies. To avoid complications in data interpretation only dry coal, hydrogen and catalyst were changed to the reactor.⁵

In the present research, coal samples have been impregnated with molybdenum salts and reacted in tubing bombs at temperatures up to 400°C, the objective being to attempt to convert the macromolecular structure into a soluble form while minimizing condensation and cracking reactions.

Experimental

Catalytic Hydrogenation

Samples of a high-vitrinite hvAb coal from the Lower Kittanning seam were obtained undried as lumps 12 mm top size from the Penn State Coal Sample Bank (PSOC-1266). Properties of the coal are shown in Table 1. The coal was crushed in a glove box under oxygen-free nitrogen to 0.8 mm top size and a number of approximately 20 g representative splits were sealed in vials without drying.

The procedure for catalyst impregnation was to mix a sample of coal with the quantity of ammonium heptamolybdate, $(\text{NH}_4)_6\text{Mo}_7\text{O}_{24} \cdot 4\text{H}_2\text{O}$ (supplied by courtesy of the Climax Molybdenum Co.) necessary to give the desired molybdenum loading, and sufficient deionized water to form a thick slurry. The mixture was stirred for 30 min at room temperature and the excess water was then removed in a vacuum desiccator overnight.

For some experiments, the ammonium molybdate solution was first converted to one of ammonium tetrathiomolybdate by bubbling through H_2S at room temperature. Impregnation with this salt should lead directly to the formation of MoS_2 which is considered to be the active form of the catalyst.

Hydrogenations were carried out in tubing bomb reactors. The gaseous products were analyzed by gas chromatography to determine the yields of CO , CO_2 , and C_1-C_4 hydrocarbons. The nongaseous reaction products were separated by Soxhlet extraction into chloroform-soluble and chloroform-insoluble fractions. The procedure has been described in detail elsewhere.

Fluorescence Microscopy

Samples of hydrogenated unextracted coals, the chloroform-soluble extracts and chloroform-insoluble residues were examined using spectral fluorescence photometry. Details of the sample preparation and the experimental arrangement have been described.

Results and Discussion

Product Yields

The yields of gaseous and chloroform-soluble products from dry catalytic hydrogenation at different temperatures are summarized in Table 2. The yield of chloroform-soluble extract from the unreacted coal was 2.0% dmmf. The mass balances were obtained from the differences between the combined yield of gas and liquids, calculated from the weight of insoluble residue, and the sum of the gas and extract yields determined experimentally. In considering the insoluble residue it was assumed that the molybdate salt had been converted to MoO_3 , although some of the molybdenum probably exists as MoS_2 . The potential error in conversion arising from this assumption is less than 1%. As the extract yield increases so does the mass balance deficit, suggesting that, at high extract yields, proportionately more low-boiling liquids are produced by reaction and lost during product work-up.

In all cases the gas yields were low, the maximum total being 2.38% dmmf coal. Carbon dioxide was detected in all reactions and its yield increased with reaction temperature. Methane was only found in detectable quantities at 400°C; higher hydrocarbons were not detected. Above about 350°C, under the conditions investigated, there was a sharp increase in extract yield, which was accompanied by a change in coal particle morphology; the particles lost their original shape and tended to form sticky agglomerates.

The extracts were characterized by elemental analysis, high resolution mass spectrometry, 1H n.m.r. and Fourier Transform Infrared Spectroscopy. Reaction in the presence of catalyst produced a higher concentration of mono-aromatic phenols than would otherwise be produced, suggesting that one of the catalyst functions involves ether cleavage. In general, however, no major compositional changes were observed as the yield increased from 2.0 to over 30% of dmmf coal. This is not to state that the products are similar at all levels of conversion or that important changes are not occurring. As more of the coal is converted to soluble form, compositional differences in successive conversion increments will be difficult to detect because of the weighting effect of the material which has already been converted to soluble form.

The extract yields obtained using the ammonium heptamolybdate salt are substantially lower than those reported in earlier work.¹⁰ One of the more likely reasons for this behavior is that only a fraction of Mo is converted to MoS_2 by reaction with sulfur in the coal. To ensure complete sulfiding of the metal, ammonium tetrathiomolybdate was employed as the catalyst precursor. The product

yields obtained from dry hydrogenation at 400°C with 1% Mo loading are summarized in Table 3 for reaction at different times.

A comparison of the results obtained after 60 min at 400°C, Tables 2 and 3, shows the much greater effectiveness of introducing Mo as ammonium tetrathiomolybdate; the extract yield was increased by about 70% while the Mo loading was reduced from 5 to 1%. In other experiments it has been found that the addition of a small quantity of CS₂ to coal impregnated with ammonium heptamolybdate was equally as effective as loading with the thio-salt.

It can be seen from Table 3 that a high proportion of coal can be converted to soluble form, with low attendant gas make, by reaction with an active dispersed catalyst under conditions of much lower severity than normally used in liquefaction systems. Conversion increases progressively with time, unlike solvent liquefaction which is usually characterized by two regimes; an initial rapid conversion of part of the coal followed by a much slower conversion rate. The mechanism of liquefaction by dry catalytic hydrogenation is not at all clear although presumably the liberated liquids play an integral role in the conversion of the remaining coal.

Fluorescence Microscopy

As the temperature of catalytic hydrogenation was raised, there was an increase in the maximum fluorescence intensity (I_{\max}) of the vitrinite in the unextracted coals. This intensity change closely parallels the increase in extract yield, Figure 1. The close correspondence between I_{\max} and the yield of chloroform-solubles suggests that the increase in fluorescence is directly related to the liberation of extractable liquids, which presumably occurs through breakdown of the macromolecular structure of the coal. After removal of the chloroform-solubles, the residue exhibited only a low level of fluorescence.

The fluorescence spectra for the hydrogenated vitrinites, normalized to a peak intensity of 100%, show a red shift in the wavelength at peak intensity, λ_{\max} , for the runs between 350-400°C, as shown in Figure 2. The shift may correspond to an increase in the concentration of condensed aromatics in the extractable liquids.

The fluorescence spectra of the hexane-soluble (oil) and hexane-insoluble (asphaltene) fractions of the extract obtained at 400°C were found to be quite different. The peak fluorescence intensity of the oil fraction occurred at about 550 nm whereas that for the asphaltene fraction was greater than 700 nm. These differences suggest that the red-shift observed in λ_{\max} for the spectra of the whole extracts on going from 350-450°C may be due to an increase in asphaltene concentration.

Summary and Conclusions

Dry catalytic hydrogenation of coal, using an impregnated Mo catalyst, has been found to considerably increase the yield of chloroform-soluble extract at temperatures of 400°C and less. For high activity the Mo should be present in sulfide form. Examination of the hydrogenated coals by fluorescence microscopy has shown that the intensity of vitrinite fluorescence increases in a parallel manner with extract yield. In the context of the mobile phase-network concept of coal structure, it is considered that, at high yields, a considerable proportion of the chloroform-solubles is derived from the breakdown of the macromolecular structure. The enhanced fluorescence would correspond to the liberation of smaller molecular fragments from a highly cross-linked network.

Acknowledgements

Three of the authors, Derbyshire, Stansberry and Terror, wish to acknowledge the support of the U.S. Department of Energy for their support of part of this research (Grant No. DE-FE22-83PC60811).

References

1. van Krevelen, D. W., Fuel, 1976, 44, 229
2. Brown, H. R. and Waters, P. L., Fuel, 1966, 45, 17 and 41.
3. Given, P. H., "The Organic Geochemistry of Coal," in Coal Science, Volume 3 (editors, M. L. Gorbaty, J. W. Larsen and I. Wender), Academic Press, 1984.
4. Green, T., Kovac, J., Brenner, D., and Larsen, J. W., in "Coal Structure" (Ed. R. A. Meyers), Academic Press, New York, 1982, pp. 199-282.
5. Hawk, C. O. and Hitshue, R. W., U.S. Bureau of Mines Bulletin 622, 1965.
6. Naumann, A. W., Behan, A. S., and Thorsteinson, E. M., Proceedings of the Fourth International Conference on the Chemistry and Uses of Molybdenum, Golden, CO, 1982, pp. 313-318.
7. Given, P. H. and Derbyshire, F. J., Report to the U.S. Department of Energy, Rept. No. DOE-PC-60811-3,4,5, 1984.
8. A. Davis, Derbyshire, F. J., Finseth, D. H., Lin, R., Stansberry, P., and Terror, M.-T., submitted to Fuel.
9. Anderson, R. R. and Bockrath, B. C., Fuel, 1984, 63, 329.
10. Given, P. H., Cronauer, D. C., Spackman, W., Lovell, H. L., Davis, A., and Biswas, B., Fuel, 1975, 54, 34.

TABLE 1
COAL PROPERTIES

	<u>PSOC-1266</u>
Seam	L. Kittanning
County	Mahoning
State	Ohio
Province	Eastern
ASTM rank class	hvAb
Moisture content % wt (a.r.)	3.4
Mineral matter % wt dry coal	6.1
<u>Elemental Composition % dmmf</u>	
C	83.2
H	5.0
O**	8.6
N	2.1
S	1.3
<u>Sulfur Forms % Dry Coal</u>	
Organic	0.51
Sulfate	0.02
Pyritic	0.87
<u>Maceral Group Analysis % Vol.</u>	
Vitrinite	91
Liptinite	3
Inertinite	6

* Determined by low-temperature ashing

** By difference

TABLE 2

PRODUCT YIELDS FROM DRY CATALYTIC HYDROGENATION
(5% Mo as ammonium heptamolybdate, 1 h, 7 MPa
cold H₂ pressure)

Reaction Temperature (°C)	Gas ¹		Yields (% wt dmmf coal)		Mass Balance %
			CHCl ₃ -soluble ¹ extract	Gas+Extract ²	
250	CO _x	0.39	1.5	1.8	100.1
	C ₁ -C ₄	--			
300	CO _x	0.52	2.3	5.3	97.5
	C ₁ -C ₄	--			
350	CO _x	0.52	8.6	13.0	96.1
	C ₁ -C ₄	--			
400	CO _x	2.03	31.6	46.5	87.4
	C ₁ -C ₄	0.35			

¹Determined directly

²Calculated from CHCl₃-insoluble residue

TABLE 3

PRODUCT YIELDS FROM DRY CATALYTIC HYDROGENATION
(1% Mo as ammonium tetrathiomolybdate,
400°C, 7 MPa cold H₂ pressure)

Reaction Time (min)	Gas ¹		Yields (% wt dmmf coal)		Mass Balance %
			CHCl ₃ -soluble ¹ extract	Gas+Extract ²	
5	CO _x	0.11	7.3	4.8	102.6
	C ₁ -C ₄	0.02			
15	CO _x	0.31	23.4	24.0	99.6
	C ₁ -C ₄	0.72			
30	CO _x	0.81	35.4	35.8	98.8
	C ₁ -C ₄	0.78			
60	CO _x	0.32	53.9	60.3	94.7
	C ₁ -C ₄	0.80			

¹Determined directly

²Calculated from CHCl₃-insoluble residue

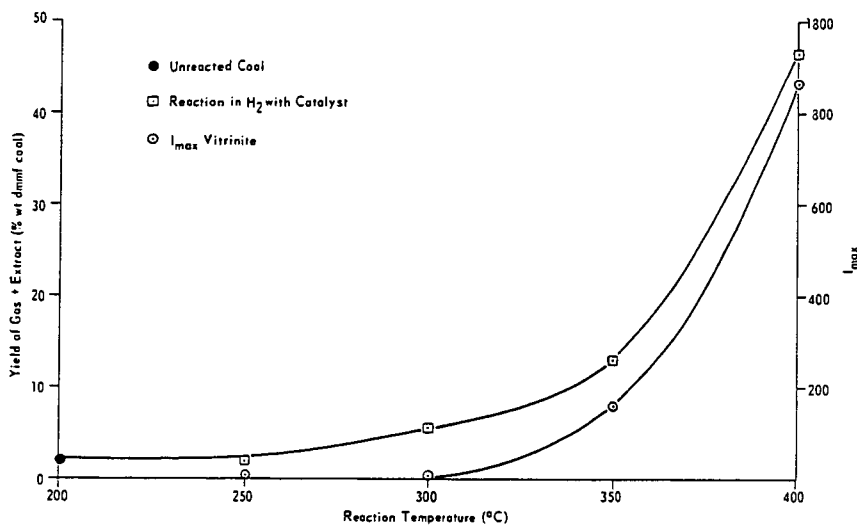


Figure 1. Correspondence between yield of chloroform-soluble extract and maximum fluorescence intensity of vitrinite.

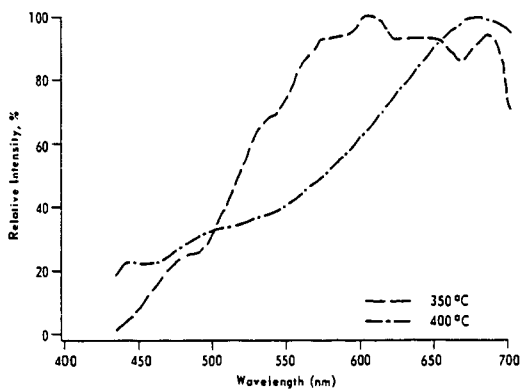


Figure 2. Fluorescence spectra of unextracted coals after dry catalytic hydrogenation.

DEHYDROGENATION OF ITSL COAL, COAL EXTRACT, AND PROCESS SOLVENT

R. P. Skowronski, L. A. Heredy, L. R. McCoy, J. J. Ratto,* and M. B. Neuworth**

Rockwell International, Rocketdyne Division, 6633 Canoga Avenue,
Canoga Park, CA 91304

*Rockwell International, Science Center, 1049 Camino Dos Rios,
Thousand Oaks, CA 91360

**Mitre Corporation, 1820 Dolley Madison Blvd., McLean, Virginia 22102.

INTRODUCTION

Catalytic dehydrogenation is an important method for determining the hydroaromatic contents of coals, coal extracts, and process solvents. Past investigations by others have focused on the dehydrogenation of coal.(1-4) Most of that work was conducted with phenanthridine because it is a relatively good solvent for coal and, at its boiling point, catalytic dehydrogenation usually proceeds at a rapid rate. However, a literature survey carried out by Neuworth has shown that secondary reactions such as those involving oxygenated structures had a significant impact on dehydrogenation results at elevated temperatures.(5) Consequently, in the present work, we have attempted to identify other, lower-boiling solvents suitable for dehydrogenation in order to minimize secondary reactions.

The objective of the work described in this preprint was to develop a refined dehydrogenation method and apply it to investigate the hydroaromatic contents of the coal, coal extract, and process solvent used in the Integrated Two-Stage Liquefaction (ITSL) process. Determination of the hydroaromatic contents of these materials is important in order to achieve an understanding of the structure of these materials and obtain an insight into the chemistry of the process. Furthermore, catalytic dehydrogenation is one of the best ways to determine the donor quality of a process solvent.

EXPERIMENTAL

The desired amount of substrate, depending on its estimated hydrogen content (e.g., about 0.25 g for tetralin), is weighed into a 40-ml flask. Next, 7.50 g of the selected solvent, 0.55 g of catalyst (5 wt. % Pd on CaCO_3), and a pyrex-encased Alnico stirrer are introduced into the flask. The dehydrogenation system is then assembled as described in detail in Reference 6. This system was designed to provide for automatic data recording. Such capability is particularly useful in experiments which require overnight operation. Connections from the gas collection burette are made of glass to minimize diffusion losses of hydrogen. Gas sampling is provided for by a gas collection port.

Key to the unattended operation of this equipment is the mercury pressure switch. As gas is evolved by dehydrogenation of the sample, the small increase in pressure actuates the switch. When this occurs, the circuitry in the motor/switch interface box turns on the motor for a 10-s interval. The motor is connected to a threaded rod carrying the leveling tube. Rotation of the rod repositions the bulb to balance the pressure increase. The top of the rod is attached to a 10-turn potentiometer through a reducer (48:1) which reduces the number of turns required to achieve leveling to the 10-turn capability of the potentiometer. Fifteen volts are imposed across the potentiometer by a precision power supply located in the motor/switch interface box. By connecting the potentiometer wiper and the neutral lead to the recorder, the output voltage can be employed to define the position of the leveling bulb. Consequently, it provides a continuous recording of the gas volume within the gas collection tube.

Elemental analysis to determine C, H, N, S, and O content was performed using a Perkin-Elmer Model 240C elemental analyzer. Number-average molecular weights of the distillate fractions were determined using vapor-phase osmometry (VPO). The molecular weight determinations as well as the elemental analyses were conducted by Galbraith Laboratories, Inc.

Proton nuclear magnetic resonance (^1H NMR) spectra were obtained with a JEOL FX-60-Q Fourier transform NMR spectrometer using an observation frequency of 59.79 MHz. The spectra were recorded with an internal deuterium lock system. The NMR samples and reference were contained in 10-mm tubes, with a probe temperature of 30°C. Chloroform- d was the solvent used. A 45° pulse, which corresponds to 14 μs , was used during multiple-scan accumulation. The pulse repetition time was 6.0 s. The ^1H spectra are referenced to tetramethylsilane (TMS) at 0.0 ppm chemical shift (δ).

The ^{13}C NMR spectra were recorded using ^1H -decoupling with an internal deuterium lock system utilizing 10-mm sample tubes. A 45° pulse was used during multiple scan accumulation corresponding to 6 μs . The pulse repetition time was 2.0 s. The samples were dissolved in chloroform- d ; the spectra were referenced to the center peak of the solvent at 77.0 ppm and tetramethylsilane at 0.0 ppm.

RESULTS AND DISCUSSION

The initial experiments were conducted with model compounds. Tetralin (1,2,3,4-tetrahydronaphthalene), 1,2,3,4,5,6,7,8-octahydrophenanthrene, and 9,10-dihydroanthracene were used as substrates. Durene, 2-methylnaphthalene, and quinoline were tested as solvents. Quinoline was found to give the fastest rate of dehydrogenation and was used in most subsequent experiments.⁽⁶⁾

The middle distillation fraction (750-850°F) of the ITSL process solvent (Illinois No. 6 coal, 8-in. PDU BTMS Run 108, 80/20 blend, June 17, 1983) was selected as the next material for investigation by dehydrogenation. It was chosen because prior characterization by proton NMR had shown that it contained a substantial percentage of hydroaromatic compounds. Approximately 3 g of this material was dehydrogenated using 1.1 g of Pd catalyst in 15 g of quinoline. The gas evolution rate was approximately 0.15 ml/min during the first day, and the experiment was allowed to continue until the rate decreased to about 20% of that observed initially. After 5 days, the experiment was terminated on this basis. A total of 270 ml of gas was obtained. Based on the elemental analysis of this solvent fraction and the quantity used, it was calculated that 11% of the total hydrogen in the sample was collected.

Elemental analysis of the dehydrogenated process solvent showed an 11% loss of hydrogen, which is consistent with the 11% loss that was calculated based on the volume of gas collected and the sample amount. The number-average molecular weight determined by VPO for the original and dehydrogenated process solvent were 263 and 259, respectively. This result indicates that, as expected, the dehydrogenation procedure had no significant effect on the number-average molecular weight.

The proton NMR spectra of the original distillation fraction of the process solvent and of the dehydrogenated material are shown in Figures 1 and 2, respectively. An increase in the aromatic portion of the sample and a decrease in the aliphatic portion as a result of the dehydrogenation procedure are evident. This qualitative result is confirmed by Table 1 which presents the results of the integration of the spectra over characteristic proton regions.

Changes in the carbon distribution of the process solvent fraction as a result of dehydrogenation were determined by analyses of the carbon-13 NMR spectra. The data are shown in Table 2. These data give additional support to the observation of an increase in aromatic protons at the expense of the aliphatic protons by indicating an increase in the aromatic carbon at the expense of the aliphatic carbon.

A more detailed evaluation of the spectra was made to obtain additional information with regard to the main reactions that take place during catalytic dehydrogenation. It was determined that, although the intensity of the well-defined β -aliphatic absorption at 1.86 ppm was strongly reduced (indicating the dehydrogenation of tetralin-like structures), mostly α -aliphatic protons were eliminated during dehydrogenation. The most probable structures of this type which can participate in the dehydrogenation reaction are 9,10-dihydrophenanthrene and 4,5-dihdropyrene. The chemical shift of the $-\text{CH}_2-\text{CH}_2-$ group of 9,10-dihydrophenanthrene is 2.86 ppm. The chemical shift of this group in 4,5-dihdropyrene is not available.

The data indicate that a typical reaction which takes place in this system on catalytic dehydrogenation is the loss of hydrogen from 4,5-dihdropyrene-type structures with the ultimate formation of pyrene or chrysene derivatives or some other similar, more highly condensed aromatic compounds. To distinguish between smaller (1-3 rings) and larger (4+ rings) condensed aromatic systems, the aromatic absorption area was divided into two sections at the chemical shift value of 7.85 ppm, which corresponds to a minimum between two absorption peaks at about 7.7 ppm and 8.0 ppm. This division applies to most condensed aromatic hydrocarbons. (Anthracene is one exception; it has about equal absorptions in both regions.) The relative absorption intensities in these sections of the spectra of the untreated and the dehydrogenated process solvent fractions are shown in Table 3. As a result of the dehydrogenation, a considerable shift toward larger condensed aromatic structures has taken place.

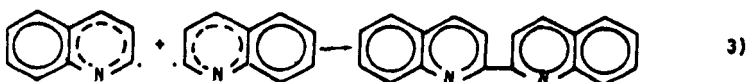
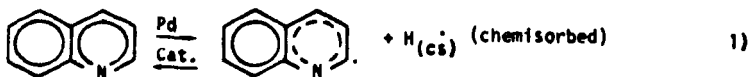
It was hypothesized that if a coal is first partially dehydrogenated and then subjected to depolymerization, this reaction sequence may make it possible to distinguish between cyclic and acyclic CH_2 -bridges in the coal. Cyclic bridge structures would be rendered inert to depolymerization because of aromatization in the dehydrogenation reaction. Therefore, the benzene-soluble fraction from the depolymerization of a dehydrogenated coal would contain fewer CH_2 -bridges than the same product of the direct depolymerization of coal. A coal dehydrogenation/-depolymerization experiment was therefore conducted, and the products were separated by solvent fractionation.⁽⁶⁾

Depolymerization of the dehydrogenated coal yielded 10% more benzene-soluble product containing 36% more CH_2 -bridges than the depolymerization of the untreated coal. Since catalytic dehydrogenation would have converted at least a fraction of the cyclic CH_2 -bridges to nonreactive aromatic structures, the increased amount of CH_2 -bridges identified in the benzene-soluble fraction indicate that they originate from acyclic bridge structures in the coal. It is possible that a few more reactive acyclic CH_2 -bridges have formed by the catalytic dehydrogenation of hydroaromatic rings linked to acyclic CH_2 -bridges in the coal. Assuming that each acyclic CH_2 -bridge is linked to aromatic/hydroaromatic ring structures corresponding to a total formula weight of 450, these acyclic CH_2 -bridges form the linkage in about 10 wt. % of the organic coal material.

Several control experiments were conducted with quinoline and catalyst (i.e., without a substrate) in parallel with the experiments described above.⁽⁶⁾ The main conclusions from these experiments are: (1) under these conditions evolution of H_2 occurs; (2) such H_2 evolution is believed to be due to the dimerization

of quinoline on the basis of GC-MS data; (3) the rate of dimerization of quinoline depends on the H_2 concentration of the atmosphere above the reactant; (4) consequently, the dimerization rate is greatly reduced when the inert gas atmosphere is replaced with H_2 ; (5) the dimer formation is not reversible under the conditions of the dehydrogenation reaction, the dimer will slowly accumulate in the system; (6) quinoline can be catalytically hydrogenated to form THQ in this reactor system at a temperature below the boiling point of quinoline; and (7) the presence of the process solvent suppresses hydrogen release by the quinoline. Conclusion (7) is supported by the fact that the quantity of gas evolved during the dehydrogenation of the process solvent fraction agreed well with the differences in the hydrogen contents of the original and dehydrogenated materials. The presence of hydrogen from the substrate in the system markedly reduces the hydrogen contribution from the quinoline dimerization.

A tentative reaction schematic of the quinoline dimerization reaction can be written as follows:



Reactions 1) and 2) are reversible. Therefore, increased H_2 partial pressure reduces the rate of formation of the quinolinyl radical, and thus, also the rate of formation of the dimer. Reaction 3) is not reversible. Therefore, the dimer will slowly accumulate in the solution, with the rate of dimer formation depending on the hydrogen pressure.

ACKNOWLEDGMENT

This research was supported by the U.S. Department of Energy under Contract DE-AC22-83PC60020.

REFERENCES

1. Raymond, R., Wender, I., and Reggel, L., *Science* **137**, 631 (1962)
2. Reggel, L., Wender, I., and Raymond, R., *Fuel* **43**, 229 (1964)
3. Reggel, L., Wender, I., and Raymond, R., *Fuel* **47**, 373 (1968)
4. Reggel, L., Wender, I., and Raymond, R., *Fuel* **49**, 281 (1970)
5. Neuworth, M. B., MITRE Report WP-83W00409 to the U.S. Department of Energy under Contract Number DE-AC01-ET13800 (September 1983)
6. Heredy, L. A., McCoy, L. R., Skowronski, R. P., and Ratto, J. J., Final Report on the Chemistry of the Extractive Phase of Coal Liquefaction to the U.S. Department of Energy under Contract Number N45569 (January 1985)

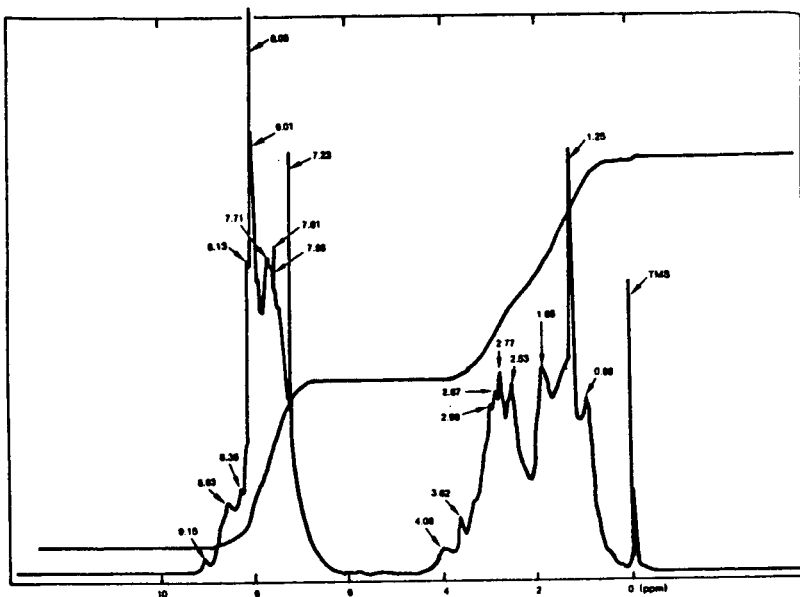


Figure 1. Proton NMR Spectrum of 750 to 850°F Fraction of Process Solvent

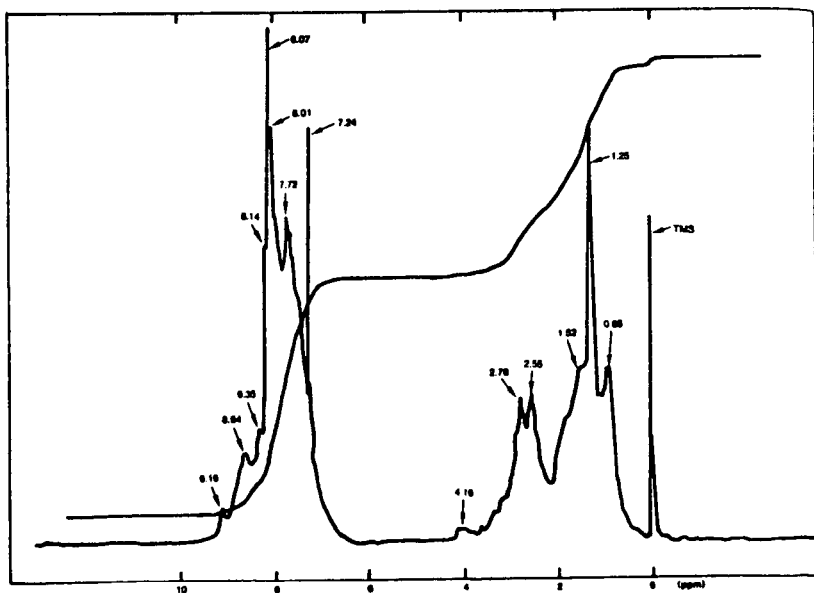


Figure 2. Proton NMR Spectrum of Dehydrogenated 750 to 850°F Fraction of Process Solvent

TABLE 1
PROTON-TYPE DISTRIBUTIONS OF ORIGINAL AND
DEHYDROGENATED PROCESS SOLVENT FRACTION*

Structural Region	Original Solvent (%)	Dehydrogenated Solvent (%)
Aromatic 6.0 to 10.0 ppm	44	52
α -Aliphatic 2.0 to 4.5 ppm	25	17
β -Aliphatic 1.0 to 2.0 ppm	29	28
γ -Aliphatic 0.0 to 1.0 ppm	2	3

*750 to 850°F

TABLE 2
CARBON DISTRIBUTION IN THE PROCESS
SOLVENT FRACTION* BEFORE AND AFTER
DEHYDROGENATION

Carbon Distribution	Original Fraction (%)	Dehydro- genated (%)
C _{Al} (0-68 ppm)	28	18
C _{Ar} (108-200 ppm)	72	82
C _{HA} (22-31 ppm)	15	9

*750-850°F

TABLE 3
AROMATIC PROTON-TYPE DISTRIBUTION OF
ORIGINAL AND DEHYDROGENATED PROCESS
SOLVENT FRACTION

Structural Region	Original Solvent (%)	Dehydro- genated Solvent (%)
Aromatic (1-3 rings, 6.9-7.85 ppm)	55	43
Aromatic (4+ rings, 7.85-9.2 ppm)	45	57

COAL CONVERSION IN CO/WATER:
THE ROLES OF PYROLYSIS AND PHENOLICS IN CONVERSION

David S. Ross and Georgina P. Hum

Fuel Program
SRI International
Menlo Park, CA 94025, USA

Thomas K. Green

Department of Chemistry
Western Kentucky University
Bowling Green, KY 42101

Introduction

The relationship of coal liquefaction behavior to coal structure has been a subject of study for several years, particularly with respect to loss of coal oxygen (1). Traditionally, the liquefaction behavior of a coal has been defined in terms of its product solubility in a particular solvent such as pyridine, benzene, or tetrahydrofuran. However, an inherent complication in trying to relate reactivity to liquefaction, defined in terms of product solubility, is that a variety of factors contribute to the product's overall solubility in a given solvent

The chemical nature of the product, i.e., the sum of its aromaticity, heteroatom content, and functional group distribution, will determine its solubility to a large degree. The molecular weight distribution of the product will also play an important role. The complex interactions evolving from the various possible combinations of these specific factors thus rule out the development of any reasonably simple correlation between structure and reactivity. And it follows that product solubility is not necessarily a good relative measure of a coal's reactivity in a given conversion medium, particularly among a set of coals of substantially different chemical constitution.

This work is dealt with here in work with the separate CO/water and N₂/water treatments of several coals from the Eastern Province of the U.S. The research focuses on a development of some insight into effects of oxygen functionality on conversion, with particular focus on phenolic functionality.

Background and Approach

Two requirements for a study aimed at developing a correlation between coal structure and reactivity are (i) a diagnostic for conversion that is free from problems associated with solubility, and (ii) a means of separating the reductive conversion chemistry from the parallel pyrolytic chemistry also in effect.

Most common liquefaction media employ an H-donor component such as tetralin, which transfers hydrogen to the coal. In such a medium the coal is reduced and degraded to yield a more soluble, lower molecular weight product. In principle, the more hydrogen added to the coal, the greater the overall solubility of the products. However, given the complexities of solubility just noted, the quantity of hydrogen transferred to the coal would seem to be a better measure of its reactivity, or its propensity toward reduction.

Yet even with this approach there are complicating factors. Conversion, of course, always accompanies thermal treatment of coal in H-donor media. Accordingly there is no way to separate or distinguish products that are a result of pyrolytic processes, and independent of conversion. Additionally, conversions in such media yield products contaminated by the solvent through chemical incorporation.

Conversions conducted in a carbon monoxide/water system circumvent both of these problems. First, the medium is totally inorganic and provides an organic product derived solely from the coal. Second, N_2 can be used in place of CO to provide a product that has not been reduced, but has been otherwise subjected to the same time-temperature conditions as the product obtained using CO. This product can be considered as a "blank run" and can provide a basis for comparison. Finally, and perhaps most significantly, carbon monoxide/water and tetralin share some mechanistic features; thus insights gained from studies using CO/H₂O can be confidently applied to conversion in tetralin (2).

The results of several published studies show that conversions in CO/H₂O generally decrease with increasing carbon content of the starting coal. Appell et al., using synthesis gas (H₂ and CO) and water, found that a lignite gave higher conversion than a bituminous coal (3). Ouchi and Takemura, using CO/H₂O and a cobalt-molybdenum catalyst, found that conversion decreased with increasing carbon content for a series of coals ranging from 50% to 90% carbon (4). Oelert and Siekmann found that conversion increased with increasing O/C ratio of the starting material (5). These results, taken together, suggest that oxygen functionalities strongly influence the conversion behavior of the coal. These past studies have dealt with materials of widely different origin and geologic age, however, and any structure-reactivity relationship derived from such studies can provide only limited mechanistic insight. In the work reported here we have confined our effort to a series of Eastern Province coals to minimize this factor.

Experimental

The elemental analyses of the coals are shown in Table 1. The coals were ground and sieved under dry N_2 until all coal passed a 100-mesh sieve. The coals were then dried under vacuum at 105°C overnight before use. All reactions were performed in a 300-mL Magne-Drive-stirred Hastelloy C autoclave. The autoclave was loaded with 5 g of dry coal and 30 g of H₂O that was previously adjusted to a pH of 13.0 with solid KOH. The system was sealed, purged with N_2 , purged again with either N_2 or CO, and then filled with either N_2 or CO (500 psig).

Table 1
ELEMENTAL ANALYSIS (Wt%) OF EASTERN PROVINCE COALS (dmmf)^a

PSOC No.	Seam	C	H	N	S	O ^b	O _{OH} ^c	Mineral Matter
278	Ohio No. 9	81.5	6.0	1.1	5.4	6.0	4.7	18.0
306	Ohio No. 12	82.4	6.1	1.8	2.6	7.1	3.4	34.1
307	Ohio No. 12A	83.1	5.9	1.7	3.6	5.7	3.9	25.6
1099	Pittsburgh	86.8	5.7	1.4	2.2	3.9	2.8	12.8
268	Lyons	88.0	5.3	1.4	1.6	3.7	2.5	6.2

^aOur determinations.

^bBy difference.

^cDetermined by Given and coworkers by O-acetylation (8).

The coal was converted by heating the autoclave to 400°C (± 5°C) for 20 min. Maximum pressures attained ranged from 3500 to 4000 psig. The heat-up and cool-down times were each about one hour.

Quantitative analyses of the product gases CO, CO₂, and H₂ were made by gas chromatography using known standards. The aqueous phase was pipetted from the

autoclave, and suspended material was filtered if necessary. The nonvolatile coal products were quantitatively removed from the autoclave with tetrahydrofuran (THF) and transferred to a round-bottom flask. The THF was removed by rotary evaporation. 400 mL of toluene was added, and the mixture was refluxed for 2 h with a Dean-Stark trap.

Azeotropic distillation removed any water. After cooling, the mixture was filtered to separate the toluene soluble material (TS) from the toluene-insoluble material (TI). The toluene was removed from the filtrate by rotary evaporation. Both the TS and TI fractions were dried overnight at 80°C and weighed. Carbon, hydrogen, and nitrogen analysis of the products were made using a Control Equipment 241 microanalyzer.

Results

In earlier work we described our use of CO/water conversion for bituminous coals and discussed how the conversions to toluene-soluble products were dependent on the initial pH of the aqueous medium (6). We have found that, at least for Illinois No. 6 coal, about 50% of the starting oxygen in the coal is lost under conversion conditions (7). This O is loosely bound and is lost rapidly whether CO or N₂ is used. We concluded that under conversion conditions there is a rapidly produced pyrolytic product, which is then the true precursor to subsequently formed upgraded products.

The CO/water conversion parallels the water-gas-shift reaction (WGSR).



An intermediate in the WGSR, most likely formate, is principally responsible for conversion, rather than the H₂ derived from the shift reaction.

In the work discussed here, both the toluene-solubilities and the H/C of the products from runs in both N₂/H₂O and CO/H₂O were measured and compared for each coal. The results are interpreted in terms of the phenolic contents of the starting coals.

Toluene-Soluble Products. All coals were converted by heating to 400°C for 20 min in either CO/H₂O or N₂/H₂O at a starting pH of 13.0. The conversions to toluene-soluble material (TS) in both N₂/H₂O and CO/H₂O were measured for each coal. The results are shown in Table 2. Conversion to %TS is defined on a dry, mineral-matter-free basis and is calculated as

$$\% \text{TS} = (\text{wt TS} / \text{wt dmmf coal}) \times 100 \quad 2)$$

The N₂-runs yielding results due to only pyrolytic chemistry, surprisingly show for some of the coals substantial liberation of TS material. The difference in conversions in the two media yields the net conversion due to reduction alone:

$$\% \text{TS}(\text{net}) = \% \text{TS}(\text{CO}/\text{H}_2\text{O}) - \% \text{TS}(\text{N}_2/\text{H}_2\text{O}) \quad 3)$$

The conversions do not take into account production of light hydrocarbon gases. The major hydrocarbon gases were always methane and ethane; however, they accounted for less than 2% of the total amount of carbon charged to the reactor in both CO/H₂O and N₂/H₂O runs, as determined by gas chromatography.

Carbon and Hydrogen Analyses of TS and TI Products. Carbon recoveries based on the C-content of the starting coal ranged from 70% to 94% for runs in N₂/H₂O and from 89% to 98% for runs in CO/H₂O. Thus, recoveries were consistently better in CO/H₂O runs.

Table 2
TOLUENE SOLUBILITIES AND H/C RATIOS OF PRODUCTS

PSOC No.	x_{TS}		$x_{TS, net}$	H/C_{TS}		H/C_{TL}		$H/C_{Composite}$		$\Delta H/100\text{ C}$
	N_2/H_2O	CO/H_2O		N_2/H_2O	CO/H_2O	N_2/H_2O	CO/H_2O	N_2/H_2O	CO/H_2O	
278	21	85	58 ^a	1.14	1.09	0.76	0.79	0.84	1.06	21
	--	72		--	1.09	--	0.81	--	1.04	
306	16	38	22	1.18	1.03	0.70	0.85	0.78	0.92	14
307	10	44	34	1.10	1.04	0.69	0.84	0.75	0.94	19
1099	10	44	34	1.10	1.02	0.70	0.71	0.74	0.86	12
268	10	35	26 ^b	1.03	0.98	0.64	0.68	0.68	0.79	11
	8	--		1.07	--					

^aUsing the average of the CO/H_2O values.

^bUsing the average of the N_2/H_2O values.

The H/C ratios of the products are listed in Table 2. For the N_2/H_2O runs, there is a net loss of hydrogen relative to carbon, whereas in CO/H_2O runs there is a net gain. Based on our view that the true precursor of the conversion products is the initially formed product from pyrolysis, we can calculate the net gain in hydrogen per 100 carbon atoms by the composite values for the TS and TI fractions.

$$\Delta H/100C = [H/C_{comp}(CO/H_2O) - H/C_{comp}(N_2/H_2O)] \times 100 \quad 4)$$

Discussion

The yields of TS in the runs with N_2 /water shown in Table 2 are unexpected, particularly in view of some of the pyrolytic hydrogen losses. The N_2 -result with PSOC 278 yielding a product with 21% toluene solubility is striking, as is the high H/C ratio of the TS fraction. The very high TS value for the CO /water runs is therefore in part due to the large component resulting from pyrolysis. This result demonstrates the important role pyrolysis can play in conversion and the need to separate pyrolysis and reduction in liquefaction studies.

For PSOC 278 the loss of starting hydrogen in the N_2 -runs is minimal, suggesting a possible reciprocal relationship between pyrolytic H-loss and pyrolytic conversion. The results for PSOC 306, however, rule against any direct link between the two, since there is a significant 16% TS fraction from N_2 /water, while the H/C ratio decreases by about 11%.

The phenolic contents of a number of coals including those studied here have been established by Given and coworkers (8). Figure 1 plots the %TS solubilities (right-hand ordinate) for the CO /water conversions of the Eastern Province coals as a function of these values. The figure shows a rough correlation between the two components. However, the trend of increasing TS values with increasing O_{OH} is set by the extreme solubility value of around 80% for PSOC 278. If that result is excluded, there appears to be no real correlation over an O_{OH} spread of almost a factor of 2.

One problem with this attempted correlation is the narrow range of TS values for most of the coals. The complication introduced through considering product solubility as the diagnostic is clearly apparent here. Another part of the problem is the use of the full solubility, and ignoring the fact that there are significant levels of pyrolytic formation of TS fractions for some of the coals.

A better view of the conversion due solely to reduction can be derived from considering the $H/100C$ values from in Table 2. These data are also presented in Figure 1, and in this case a very good linear relationship is obtained. For the Eastern Province coals, the line fits the equation

$$\Delta H/100C = 4.8 O_{OH}/100C + 0.5 \quad 5)$$

with a correlation coefficient of 0.97. The excellent fit confirms the need to avoid solubility as the diagnostic for conversion, and to correct liquefaction data for pyrolytic reactions. Thus the H/C ratio of the original coal is not a proper characteristic for comparison.

The fact that the extended line passes near the origin suggests that a mechanistic correlation exists between the hydrogen uptake by the coal, and the phenolic content. Phenol functions thus seem to play a direct role in the specific reduction chemistry. The slope of the line dictates that 5 hydrogens are added to the coal structure for each phenolic group, and at present we have no scheme to explain that value. We have noted that the phenolic content stays reasonably constant with conversion and that unaccounted or loosely bound oxygen represented the major source of lost oxygen (7). It therefore seems that, although phenol functions in the coal may be the key to the introduction of hydrogen into coal

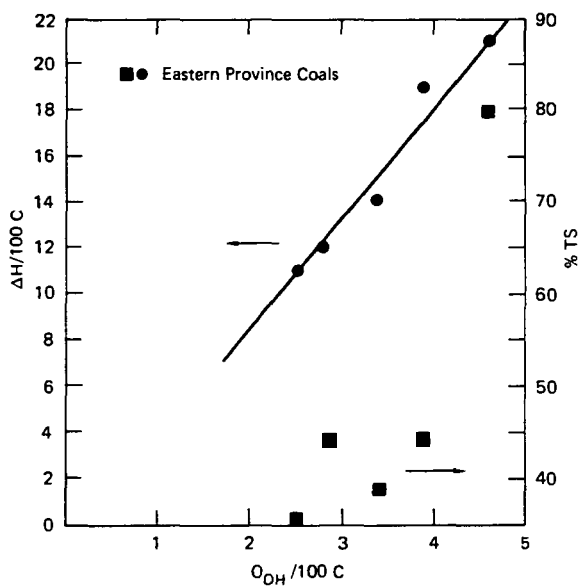
during CO/water conversion, they are not directly removed by the conversion chemistry.

Acknowledgment

We acknowledge the generous support of this work by the U.S. Department of Energy.

References

1. (a) A. J. Szladow and P. H. Given, Amer. Chem. Soc. Div. of Fuel Chemistry Preprints, 23 (4), 161-168 (1978).
(b) J. S. Youtcheff and P. H. Given, Fuel, 61, 980-987 (1982).
(c) J. S. Youtcheff and P. H. Given, Amer. Chem. Soc. Div. of Fuel Chemistry Preprints, 29 (5), 1-8 (1984).
(d) D. D. Whitehurst in Organic Chemistry of Coal, J. W. Larsen, Ed., pp. 1-35, ACS Symposium Series 71 (American Chemical Society, Washington, D.C., 1978).
2. D. S. Ross in Coal Science, Vol. 3, pp. 301-337, M. Gorbaty, J. Larsen, and I. Wender, Eds., (Academic Press, New York, 1984).
3. H. R. Appell, R. D. Miller, E. G. Illig, E. G. Moroni and F. W. Steffgen, "Coal Liquefaction in Synthesis Gas," U.S. Department of Energy Representative PETC/TR-79, Technology Information Center, U.S. Department of Energy, Washington, D.C.
4. K. Ouchi and Y. Takemura, Fuel 62, 1133-1137 (1983).
5. H. Oelert and R. Siekmann, Fuel 55, 39-42 (1976).
6. D. S. Ross, J. E. Blessing, Q. C. Nguyen, and G. P. Hum, Fuel, 63, 1206-1210 (1984).
7. D. S. Ross, D. F. McMillan, S. J. Chang, G. P. Hum, T. K. Green, and R. Malhotra, "Exploratory Study of Coal Conversion Chemistry," Final Report, Contract No. DE-AC22-81PC40785, December 1984.
8. Z. Abdel-Baset, P. H. Given, and R. F. Yazab, Fuel 57, 95-99 (1978).



JA-3304-74

FIGURE 1 PLOT OF HYDROGEN UPTAKE AND $\% \text{ TS}$
VERSUS PHENOLIC OXYGEN

The circles refer to $\Delta H/100\text{ C}$; the squares refer to $\% \text{ TS}$.

EXPERIMENTS AND MODELING OF COAL DEPOLYMERIZATION

Peter R. Solomon, and Kevin R. Squire

Advanced Fuel Research, Inc., 87 Church Street, East Hartford, CT 06108

Direct liquefaction of coal is accomplished by the depolymerization of the coal molecule with stabilization of the polymer fragments by hydrogen from coal and the liquefaction solvent. For bituminous coals containing between 80 and 88% carbon, the initial liquefaction reactions produce high molecular weight soluble products and efficiently consume the donatable hydrogens. Up to 80% yields can be produced in short contact time liquefaction (1,2). On the other hand, the production of soluble products from lignites is hindered by crosslinking, resulting in inefficient use of the internal hydrogen and low yields. A correlation between short contact time yields and the crosslink density was discussed by Whitehurst et al (1). As the average crosslink density goes up with decreasing rank, liquefaction yields go down. The crosslink density was determined from solvent swelling ratios (discussed by Larsen and coworkers (3,4)).

While there appears to be a higher starting crosslink density in lignites and low rank coals (1-5), many new crosslinks are introduced by reactions starting above 300°C. Suuberg, Lee and Larsen (6) compared pyridine swelling ratios for pyrolysis chars of a lignite and a bituminous coal heated at approximately 1000°C/sec. The results show that lignites crosslink at temperatures (~650 K) far below those where bituminous coals crosslink (800 K). While the tar evolution from bituminous coals is nearly complete before crosslinking begins, crosslinking seems to precede the tar and gas evolution in the case of lignites. In liquefaction, these retrogressive crosslinking reactions reduce the coal's solubility, add thermally stable bonds to the coal structure and consume hydrogen to produce water. Liquefaction of low rank coals could be improved by reducing or eliminating these retrogressive reactions, but little data are available on the mechanisms and relative rates of the crosslinking and bond breaking reactions.

This paper considers the processes of depolymerization and crosslinking under pyrolysis conditions in the absence of a liquefaction solvent. The same depolymerization and crosslinking chemistry which operates in short-contact time liquefaction also controls the yields and molecular weight distributions of the soluble products (tars and liquids) from pyrolyses. In our experimental studies we are determining distributions of depolymerization fragments for coals, lignites, and model polymers (7-11). We consider the factors which control crosslinking such as rank and functional group composition and alteration of the crosslinking reactions by chemical modification of the coal or by variations of the reaction conditions. The results are being used to develop a Monte Carlo devolatilization model including the combined effects of depolymerization, crosslinking and vaporization processes (12).

EFFECT OF CROSSLINKING ON MOLECULAR WEIGHT DISTRIBUTION OF PYROLYSIS PRODUCTS

Field Ionization Mass Spectroscopy (FIMS) has been used to provide the data on the molecular weight distribution of pyrolysis products. In Fig. 3, FIMS spectra for four coals are presented. The detailed shapes of these spectra were discussed in a previous publication (9). These spectra were collected at Stanford Research Institute by direct pyrolysis at 3°C/min into the inlet of the mass spectrometer (13). Since field ionization produces very few fragment peaks, these spectra can roughly be interpreted as the molecular weight distributions of tars. They include single aromatic ring clusters ("monomers") as well as larger coal fragments containing several ring clusters ("oligomers"). It can be seen that the lignite and subbituminous coals have tars with much lower average molecular weights than the spectra for the Illinois #6 and Kentucky #9 bituminous coals. Figure 2 shows a similar dependence with maceral type. The high hydrogen content, fluid macerals produce high molecular weight tars, while the more hydrogen poor macerals produce

lower molecular weight tars. Experiments with coals and model polymers suggest that high molecular weights distributions are characteristic of melting materials and, are often accompanied by high liquid yields because of efficient use of the materials donatable hydrogens. Low molecular weight distributions for tars are characteristic of crosslinked or thermosetting materials with low liquid yields. For low molecular weight tars, more bonds must break and more hydrogen is required to stabilize each gram of product. As discussed in Refs. 7-12 the shape of the molecular weight distribution of pyrolysis decomposition fragments is controlled by the decomposition reactions and by the volatility of the fragments. In the absence of crosslinking, random bond breaking and stabilization by hydrogen abstractions reduce the average molecular weight of the fragments until they are small enough to volatilize. The predicted molecular weight distribution is flat up to the vaporization cutoff. Crosslinking produces two effects, the first is to increase the average molecular weight of fragments, moving many of them above the vaporization limit. The second is to create a network which limits the transport of large fragments out of the reacting coal particle (this network also limits the penetration of solvent and the mobility of coal hydrogen-donor molecules). Both effects lead to the drop off in molecular weight distribution observed for materials which are initially crosslinked or undergo crosslinking during pyrolysis.

MODIFICATION OF THE CROSSLINKING REACTIONS

Modifications of the crosslinking reactions were accomplished in two ways. Pyrolysis experiments were performed (11) on modified coals supplied by Ron Liotta of the Exxon Corporation. In these coals, the hydroxyl and carboxylic acid groups were modified by methylation. Methylation of low rank coals makes their behavior in pyrolysis look like that of easily liquified, fluid, high rank coals. Figure 3 compares the FIMS spectra for a methylated and unmodified coal. The methylated coal produces the high molecular weight distributions, high yields, and fluid properties in agreement with the hypothesis of reduced crosslinking. In a related experiment, very high yields were obtained for a Wyodak subbituminous coal, by Padrick (14), when a strong hydrogen bonding solvent was used. In both experiments the hydroxyl and carboxyl groups which make up the hydrogen bonding network in the coal are tied up (either by methylation or by hydrogen bonds to the solvent) rather than undergoing crosslinking.

The second way in which crosslinking reactions were modified was through control of the reaction conditions. Recent experiments in a heated tube reactor (HTR) at heating rates of 20,000°C/sec (11, 15-17) suggest that in very rapid pyrolyses of lignites the detrimental effects of crosslinking reactions are minimized. In these experiments, the yields of tars are much higher than in low heating rate pyrolyses, the chars have melted and swelled, and the molecular weight distributions of the tars are comparable to those obtained for bituminous coals.

Figure 4 compares scanning electron micrographs of lignite chars produced at 800°C with heating rates of 600°C/sec and 20,000°C/sec. The 600°C/sec char shows little evidence of fluidity while the 20,000°C/sec HTR char shows fluidity, bubbling, and swelling.

Figure 5 shows the variation of the molecular weight distribution with high heating rates. Figures 5a and 5b are spectra of tars collected in a heated grid reactor at heating rates of 3 and 600°C/sec, respectively. Figure 5c is a FIMS spectrum of a tar collected in the HTR at a heating rate of 20,000°C/sec. The effect of higher heating rates is to produce tars from lignites which have higher average molecular weights, like the FIMS spectra from higher rank coals (see Figs. 1d and 2c) or methylated coal (Fig. 3b).

FT-IR spectra in Fig. 6 show the tars at high heating rates apparently have not lost their oxygen functionalities as do tars at low heating rates. At low heating rates, these oxygen functional groups are lost in crosslinking reactions accompanied by the evolution of CO, CO₂, and H₂O.

Swelling experiments on chars produced in very rapid pyrolysis confirm that crosslinking reactions in a lignite have been shifted in temperature and no longer precede depolymerization. In Fig. 7 pyridine swelling ratios are compared to tar and liquid (tar plus extract) yields. It can be seen that both crosslinking and tar formation reactions are occurring at about the same rates. These results differ from those of Suuberg et al. obtained at lower heating rates (6). However, for experiments at low heating rates in our laboratory, the swelling ratio went to zero at 300°C (well before any depolymerization can occur), in agreement with the results of Ref. 6. Thus, the sequence of crosslinking followed by tar formation observed for lower heating rates is replaced with simultaneous crosslinking and tar formation at very high heating rates.

POLYMER MODELS FOR COAL STRUCTURE

Model polymers have been used in our laboratory to study the depolymerization and crosslinking reactions believed to occur in coal (7-10,12). Several of the structures studied are illustrated in Fig. 8. For softening coals (no crosslinking), the ethylene-bridged polymers, #1, #3 and #4 were used. The use of this type of polymer allowed examinations of the combined pyrolysis and evaporation processes in a well-characterized material. The tar formation from the polymer has a number of similarities with bituminous coal. Thermal decomposition yields tar consisting of oligomers which, like coal, are similar in composition (except for molecular weight) to their parent polymer. As the original polymer molecular weight is too high for evaporation, tar formation must involve bond breaking. The weak bonds in the polymer system are between the two aliphatic bridge carbons. These ethylene bridges are expected to have bond energies similar to the bonds controlling tar formation in coals. The hydrogens in the ethylene bridges also supply donatable hydrogens for free radical stabilization. Finally, like bituminous coal, these polymers melt prior to tar formation. The vapor pressures for the pure hydrocarbon molecules from the polymers are, however, expected to be higher than for the same size molecules in coals.

A comparison of kinetic rate constants for several of the polymers, some model compounds and coal is presented in Fig. 9. The results show that the bond breaking rate for polymer #1 is similar to that for bibenzyl (18,19), but somewhat lower than that recently measured for coal pyrolysis (10,15,16). The bond breaking rates for the ethylene bridged methoxy-benzene polymer, #2, and an ethylene bridged anthracene polymer, #3, were slightly higher than the formation rate for coal tar. The molecular weight distribution for the naphthalene polymer in Fig. 10a extends to higher masses than for melting coals (as expected due to the higher vapor pressure), but shows similar trends.

The rates of decomposition of ethylene bridged pure hydrocarbon polymers are in reasonable agreement with those for low rank coals, but the molecular weight distributions are quite different. However, the product molecular weight distributions in Fig. 10c for polymer #2, which crosslinks, does show the sharp drop in molecular weight exhibited by low rank coals (Fig. 1a). It is interesting to note that this polymer showed a molecular weight distribution (Fig. 10b) characteristic of a non-crosslinking material (e.g. Fig. 10a) at a lower temperature. The shape changed at higher temperatures, presumably as the crosslinking reactions started.

DEPOLYMERIZATION THEORY OF VAPORIZATION AND CROSSLINKING

The initial reactions occurring during coal liquefaction are thought to involve homolytic cleavage of weak bonds between aromatic rings in coals followed by stabilization of the free radicals by donatable hydrogens from the coal or liquefaction solvent and transport of the products away from the reaction zone (or coal particle) (1,2,20,21). The radicals can also decompose, rearrange, and condense with other radicals or molecules (7,8, 12, 22-24). These secondary reactions lead to the evolution of light gases and to the formation of crosslinks. The processes of

depolymerization, gas evolutions, and crosslinking are thought to be in competition with each other (7,8,12,25). The relative importance of each one is determined by reaction conditions and the availability of donatable hydrogens. These reactions have been studied extensively and modeled for a series of polymers representative of coal structure by Solomon and King (7) and Squire and Solomon (8,12,24). These theories combine random cleavage of weak bonds (similar to the concept used by Gavalas et al. (26) with transport of depolymerization fragments by vaporization and diffusion (like Unger and Suuberg (25) to predict product yields and composition.

The Depolymerization Equation for Ethylene Bridged Polymers - The weak bonds in the depolymerization-vaporization-crosslinking (DVC) theory are the ethylene bridges which homolytically cleave as a first order process with rate constant k_D (see Fig. 9) to form two methyl groups. The radicals which are formed during homolysis of these $-CH_2CH_2-$ bonds are capped by abstracting two hydrogens from a second ethylene bridge. The overall stoichiometry for the depolymerization reaction in the DVC model is, therefore, two ethylene bridges react to form two methyl groups and an olefinic ($-CH=CH-$) bridge.

The Crosslinking Equation - The crosslinking reaction is modeled as a bond formation between the crosslink sites on any two monomers. Crosslinks between separate sites on the same polymer are allowed. The hydrogens which are freed during this bond formation are modeled as the evolution of H_2 gas. The exact nature of the crosslinking sites in coals is unknown. They could be associated with phenols or carboxylic acid groups or could simply be sites where ring condensations occur. We have found that an important property of crosslink sites is that the probability of having a crosslink site in the molecule goes up with the number of monomers in the molecule. Long polymer chains containing many monomers are more likely to crosslink than are short polymer chains. This behavior leads to tar molecular weight distributions which are characteristic of crosslinking polymers. For the simulations presented in this paper for polymer #4 we have assumed that the crosslinking reaction is first order in the concentration of crosslink sites. The rate constant, shown in Fig. 9 was chosen to make the crosslinking reaction faster than depolymerization at 300°C but slower at 900°C for the benzene polymer #4.

The Vaporization Equations - The vaporization part of the DVC model is treated in the same manner as in the Solomon and King model (7). The rate of vaporization depends on molecular weight, temperature and pressure.

Monte Carlo Simulation Techniques - In solving the DVC model, it is necessary to keep track of the structure of each polymer molecule as bonds break and crosslinks form. This has been accomplished through use of Monte Carlo solution technique. This technique follows a representative sample of polymer molecules through probable pyrolysis reactions. The application of the technique to depolymerization and vaporization of polymers has recently been described (12). In this work we have added crosslinking reactions to the model. The model allows a detailed description of the reaction chemistry involving large numbers of oligomers. For the ethylene bridged polymer, the model keeps track of the concentrations of ethylene and olefinic bridges, methyl groups, crosslink sites, crosslinking bridges, and evolved H_2 gas. The molecular weights of each polymer chain are also continuously monitored in order to determine their volatilities. Examples of these Monte Carlo solutions to the DVC model for the benzene polymer, #4, are presented in Figs. 11 and 12 for a polymer of chainlength 30. The figures show the total number of molecules in each oligomer group, including smaller and larger masses due to the pressure or absence of methyl groups or hydrogen.

The Effects of Crosslink Site Densities - In Fig. 11 the probability of each monomer containing a crosslink site was varied from 67 to 0%. The heating rate was held constant. The respective char yields decrease from 55 to 0%. In addition, the average molecular weights of the tars increase from 286 to 389 amu. These increased averages for molecular weights are accompanied by higher concentrations of the larger

polymer fragments. This occurs because the probability of a monomer containing a crosslink site is assumed to be equal for every monomer. Long polymer chains contain more crosslink sites and are, therefore, more likely to be lost in crosslinking reactions. The net effect of crosslinking is a preferential decrease in the concentrations of high molecular weight polymer chains and a shift in the tar (those polymer chains which succeed in volatilizing) towards lower average molecular weights. The prediction for 67% crosslinking, Fig. 11a shows the trends of the crosslinked polymer (Fig. 10c) and the low rank coals (Figs. 1a and 3a). The prediction with 0% crosslinks (Fig. 11c) show the trends of the hydrocarbon polymer (Fig. 10a), the high rank coals (Fig. 1d), the methylated coal, Fig. 3b and the high heating rate case (Fig. 5c).

The Effects of Heating Rates - In Fig. 12 the effects of heating rates on tar molecular weight distributions are simulated. The simulations of Figs. 12a-c were carried out for an ethylene bridged benzene polymer in which 67% of the monomers contained crosslink sites. As heating rates are increased from 3 K/min to 20,000 K/s char yields are decreased from 56 to 13% and the fall off in molecular weight occurs at higher values. When pyrolyses are carried out under high heating rate conditions, all of the processes leading to tar formation take place at higher temperatures. These higher temperatures change the relative speeds of the depolymerization, vaporization, and crosslinking processes. As shown in Fig. 9, at high temperatures, depolymerizations are faster than the crosslinking reactions. The net result is that depolymerizations at very high heating rates rapidly reduce the molecular weight of the polymer molecules, making them volatile enough to escape as tar, before the crosslinking reactions can trap them into the char. Char yields are decreased and more dimers, trimers, and tetramers volatilize as tar. In Fig. 12d a tar molecular weight distribution is presented for this polymer when it contains no crosslink sites but is still heated at 20,000 K/s. It can be seen that the shapes and average tar molecular weights of the simulated mass spectra for 20,000 K/s tars are nearly the same with (Fig. 12c) or without (Fig. 12d) crosslink sites. Apparently, at these very high heating rates the effects of the crosslinking reactions are minimized.

These simulations provide an explanation for the changes with heating rates observed in the FIMS spectra of lignite tars, Fig. 5. At low heating rates, Fig. 5a, the FIMS spectrum shows the rapid fall-off with increasing molecular weight which is characteristic of a crosslinking polymer. As heating rates are increased, crosslinking becomes less important and more dimers, trimers, etc. can volatilize. At the very high heating rate, Fig. 5c, the effects of the crosslinking reactions are minimized and the FIMS spectrum of a lignite looks very much like that of a bituminous coal.

CONCLUSIONS

1. In pyrolysis (as in liquefaction) low rank coals undergo crosslinking reactions which reduce the char's fluidity and lead to low yields of low molecular weight soluble products with inefficient use of the coal's internal donatable hydrogen.
2. These reactions can be reduced by methylation or with high heating rates where the coals become fluid and produce higher yields of high molecular weight products.
3. Crosslinking behavior was observed in an ethylene linked benzene polymer containing methoxyl groups. Similar polymers without methoxyl groups do not show the crosslinking behavior.
4. The results have been successfully simulated using a Monte Carlo model for the combined depolymerization, crosslinking and vaporization process.

ACKNOWLEDGEMENT

The support of the Morgantown Energy Technology Center of the United States Department of Energy and the Gas Research Institute is gratefully acknowledged for the work on coal and polymers, respectively. The authors wish to thank Ron Liotta of the Exxon Corporation for supplying the methylated coals.

REFERENCES

1. Whitehurst, D.D., Mitchell, T.O., and Farcasiu, M., "Coal Liquefaction, The Chemistry and Technology of Thermal Processes", Academic Press, NY (1980).
2. Whitehurst, D.D., in "Coal Liquefaction Fundamentals", Ed. D.D. Whitehurst, ACS Symposium Series, 139, 133, (1980).
3. Green, T.K., Kovac, J., and Larsen, J.W., Fuel, 63, 935, (1984).
4. Green, T.K., Kovac, J., and Larsen, J.W., in "Coal Structure", R.A. Meyers, Ed., Academic Press, NY (1982).
5. Lucht, L.M. and Peppas, N.A., ACS Div. of Fuel Chem. Preprints, 29, #1, 213 (1984).
6. Suuberg, E.M., Lee, D., and Larsen, J.W., "Temperature Dependence of Crosslinking Processes in Pyrolyzing Coals", submitted to Fuel (1985).
7. Solomon, P.R. and King, H.H., Fuel, 63, 1302, (1984).
8. Squire, K.R., Solomon, P.R., and DiTaranto, M.B., "Synthesis and Study of Polymer Models Representative of Coal Structure", Annual Reports for GRI Contract No. 5081-260-0582, (1983 and 1984).
9. Solomon, P.R., Squire, K.R., and Carangelo, R.M., ACS Div. of Fuel Chem. Preprints, 29, #1, 19 (1984).
10. Solomon, P.R. and Hamblen, D.G., "Measurements and Theory of Coal Pyrolysis", DOE Topical Report No. DOE/FE/05122-1668, (1984).
11. Solomon, P.R., Hamblen, D.G., and Best, P.E., "Coal Gasification Reactions with On-Line In-Situ FT-IR Analysis", DOE Quarterly Reports for Contract No. DE-AC21-81FE05122, (1981-1985).
12. Squire, K.R., Solomon, P.R., DiTaranto, M.B., and Carangelo, R.M., ACS Div. of Fuel Chem. Preprints, 30, #1, 385, (1985).
13. St. John, G.A., Buttrill, S.E., Jr., and Anbar, M., in "Organic Chemistry of Coal", Ed. J. Larsen, ACS Symposium Series 71, 223, (1978).
14. Padrick, T.D. and Lockwood, S.J., ACS Div. of Fuel Chem. Preprints, 29, #1, 153 (1984).
15. Solomon, P.R., Serio, M.A., Carangelo, R.M., and Markham, J.R., ACS Div. of Fuel Chem. Preprints, 30, #1, 266 (1985).
16. Solomon, P.R., Serio, M.A., Carangelo, R.M. and Markham, J.R., "Very Rapid Coal Pyrolysis", submitted to Fuel.
17. Solomon, P.R., Hamblen, D.G., Carangelo, R.M., Markham, J.R. and DiTaranto, M.B., ACS Div. of Fuel Chem. Preprints, 29, 2, 83, (1984).
18. Sato, Y., Fuel, 58, 318, (1979).
19. Miller, R.E. and Stein, S.E., J. Phys. Chem., 85, 580, (1981).
20. Wiser, W., Fuel, 47, 475, (1968).
21. Neavel, R.C., in Coal Science, Vol. 1, Eds. M.L. Gorbaty, J.W. Larsen, and I. Wender, New York, (1982), p. 1.
22. Stein, S.E., ACS Symposium Series 169, 208, (1981).
23. Stein, S.W., "Free Radicals in Coal Conversion" to appear in "Coal Conversion Chemistry", Ed. R. Schlosberg, (1983).
24. Squire, K.R., Carangelo, R.M., DiTaranto, M.B., and Solomon, P.R., "Tar Evolution from Coal and Model Polymers II: The Effects of Aromatic Ring Sizes and Donatable Hydrogens", submitted to Fuel for publication (1984).
25. Unger, P.E. and Suuberg, E.M., 18th Symposium (Int) on Combustion, The Combustion Institute, Pittsburgh, PA, 1203 (1981).
26. Gavalas, G.R., Cheong, P.H., and Jain, R., Ind. Eng. Chem. Fundam., 20, 113 and 122, (1981).

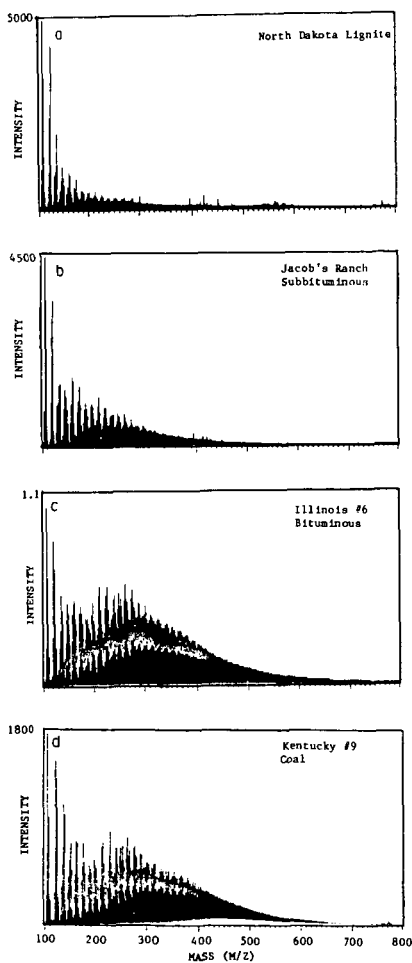


Figure 1. FIMS Spectra of a Lignite and 3 Coals.

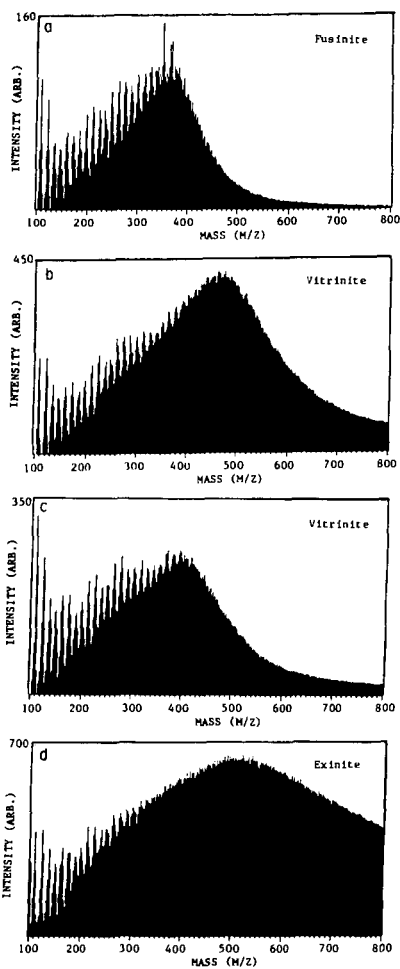


Figure 2. FIMS Spectra for Pure Coal Macerals.

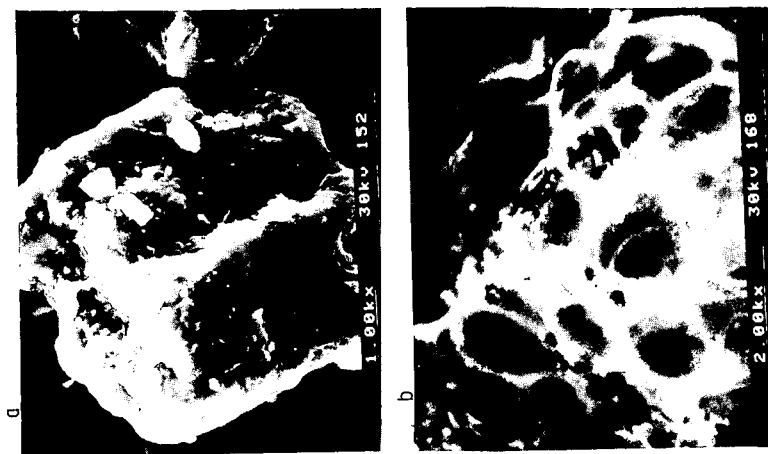


Figure 4. Scanning Electron Micrographs of North Dakota Lignite Chars. a) 600°C/sec Heating Rate, and b) 20,000°C/sec Heating Rate.

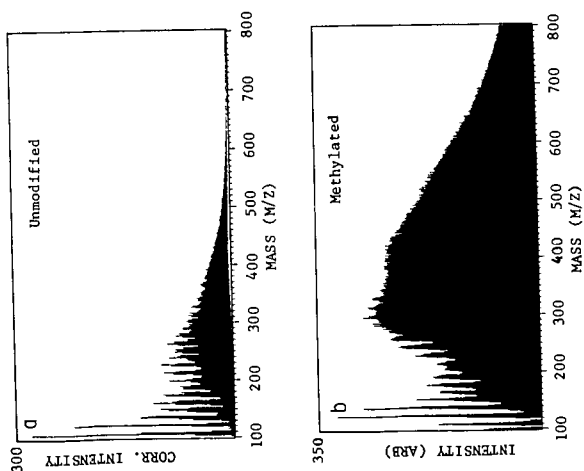


Figure 3. Comparison of FIMS Spectra for Raw and Perdeutero-Methylated Big Brown Texas Lignite.

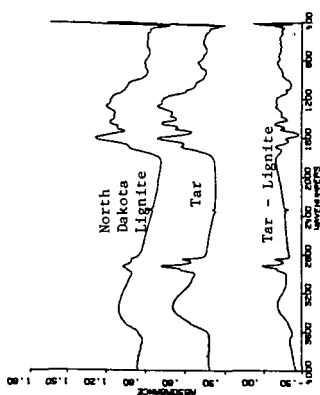


Figure 6. Comparison of FT-IR Spectra of a Lignite and its Pyrolysis Tar. Heating Rate = 20,000°C/sec.

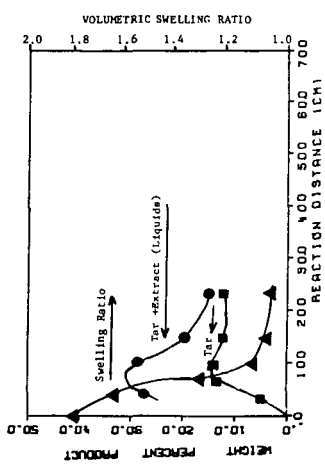


Figure 7. Comparison of Volumetric Swelling Ratios, Tar and Liquid Yields for North Dakota Lignite Heated in the HTR at 800°C.

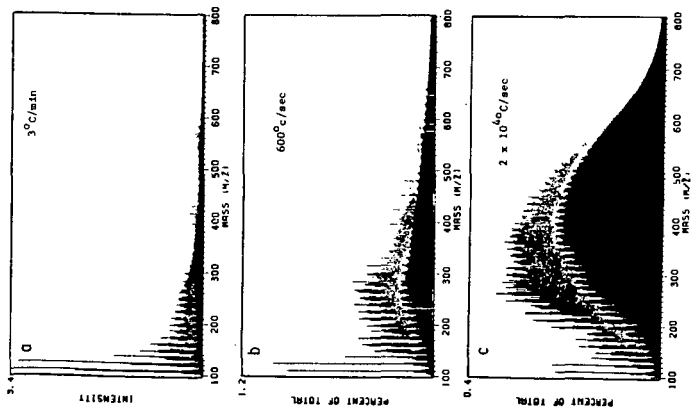


Figure 5. Comparison of Tar Molecular Weights for a Lignite at Three Different Heating Rates.

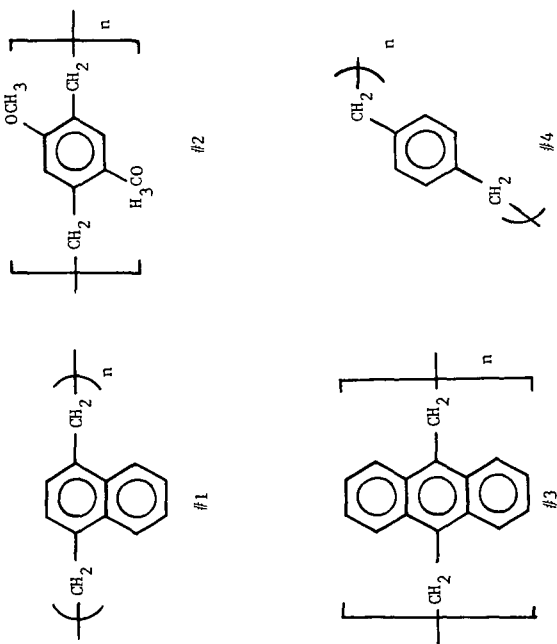


Figure 8. Model Polymers Already Synthesized or Collected.

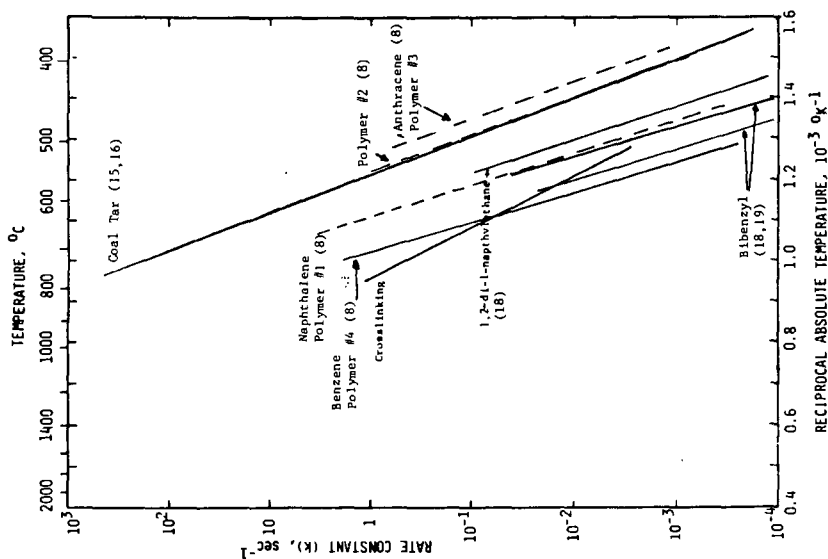
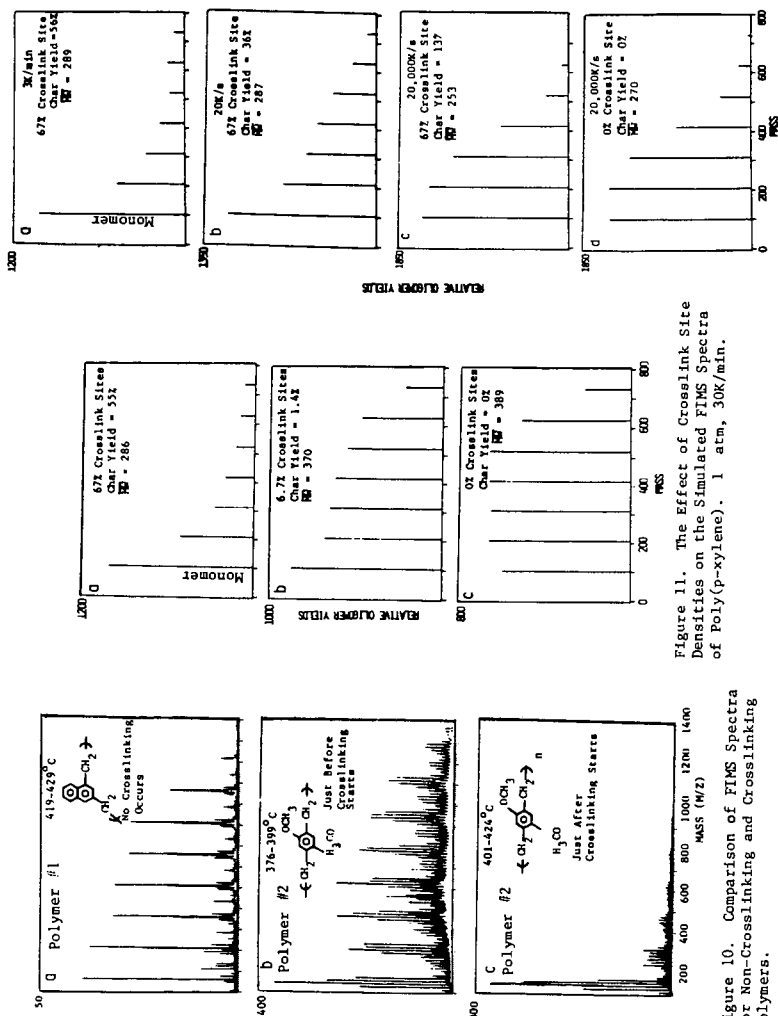


Figure 9. Comparison of Kinetic Rates for Tar Evolution from Polymers, Coal and Model Compounds.



DISSOLUTION OF SULFUR COMPOUNDS IN COAL AND COAL-DERIVED PYRITE WITH PERCHLORIC ACID

Chris W. McGowan* and Richard Markuszewski
Ames Laboratory, Iowa State University, Ames, Iowa 50011.

ABSTRACT

Knowledge of the ease by which various sulfur forms contained in coal can be removed during treatment under oxidizing conditions can be used as a guideline for controlling process conditions during desulfurization. To investigate these properties, perchloric acid was chosen as the oxidizing agent because its potential can be varied by changing its concentration. The stepwise oxidation of an Illinois #6 coal and a coal-derived pyrite was effected by carrying out the reactions in a modified Bethge apparatus to control the boiling point and thus the concentration and oxidizing power of perchloric acid. Sulfur was determined as sulfate in the reaction mixture. Volatile sulfur gases were trapped in an aqueous hydrogen peroxide scrubber and determined as sulfate. Sulfatic sulfur and the other forms of sulfur in coal were clearly delineated. Some delineation was made between pyritic sulfur and organic sulfur. However, the anticipated delineation between various organic sulfur forms was not observed. Total sulfur was recovered from the reaction of coal with boiling concentrated perchloric acid at 203°C. The oxidation of large samples of pyrite (>0.1 g) produced a yellow precipitate identified as ferric hydroxide sulfate.

INTRODUCTION

Of the various methods proposed for the desulfurization of coal, several have involved the use of oxidizing conditions. By knowing the ease with which the various sulfur species in coal can be removed, the oxidation conditions used during a process could be optimized for maximum sulfur removal and recovered heat content. The ease of removal of sulfur species in coal can be measured by using perchloric acid as an oxidizing agent. This paper discusses the reaction of perchloric acid with sulfur in coal and in a coal-derived pyrite and the relationship of the sulfur products produced in these reactions.

It was hoped that by varying the boiling point of perchloric acid, and thus its concentration, some delineation among the various forms of sulfur in coal could be made. Perchloric acid was chosen as an oxidizing agent because the apparent reduction potential of perchloric acid can be varied by changing its concentration as a function of boiling temperature. In this manner, stepwise oxidation of the sulfur species could be performed by varying the reduction potential of the oxidizing agent. Smith (1) has demonstrated that the apparent reduction potential of perchloric acid rises slowly as the boiling point and concentration increase. McGowan and Diehl (2,3) have used this property of perchloric acid to oxidize the kerogen of Green River oil shale.

*Present address: Department of Chemistry, Tennessee Technological University, Cookeville, Tennessee 38505

Total sulfur in coal has been determined previously using perchloric acid in combination with other acids. Smith and Deem (4) used a combination of nitric acid and perchloric acid to oxidize the coal and then determined sulfate in the resulting solution. They reported that the sulfur results were low, possibly due to inefficient precipitation of barium sulfate from perchloric acid solution. In light of the present study and studies by Kahane (5) and Bethge (6), the low results were probably due to loss of a volatile sulfur compound. Spielholtz and Diehl (7) oxidized coal with a mixture of perchloric acid and periodic acid. In that study, sulfur gases were trapped in 3% H_2O_2 , which was then added to the perchloric acid solution, boiled to fumes of perchloric acid, and the total sulfur was determined as sulfate. The total sulfur values were consistent with those determined by ASTM procedures. However, there was a foaming problem with some coals. Those coals that foamed generally caused an explosion with boiling concentrated (70-72%) perchloric acid, but explosions were avoided if a starting concentration of ~68% perchloric acid was used. Being aware to this danger, special precautions were taken during the course of the present work. Markuszewski et al. (8,9) have determined total sulfur in coal using a mixture of nitric, phosphoric, and perchloric acids for the dissolution and determining sulfate in the resulting solution by nephelometry. As shown in the present work, addition of phosphoric acid inhibits the formation of volatile sulfur gases.

The present investigation consisted of four series of experiments. The first was the oxidation of an as-received Illinois #6 coal, the second was the oxidation of a finely ground sample of the same Illinois #6 coal, the third was the oxidation of 1.0-g samples of coal-derived pyrite, and the fourth was the oxidation of 0.06-g samples of the coal-derived pyrite. To follow the course of the oxidation, the amount of solid remaining after the reaction, the amount of sulfate sulfur in the aqueous phase, and the amount of sulfur collected from the vapor phase during the reaction were monitored.

EXPERIMENTAL

The Illinois #6 (IL 6) coal used in this study came from the Captain Mine, Percy, Illinois, and is described further in the Ames Laboratory Coal Library report (10). Perchloric acid oxidations of the coal were performed on as-received and on ground samples. Grinding was performed to make the sample more homogeneous. The coal-derived pyrite (CP 1) was separated from an Iowa coal during cleaning (Chuang et al., 1980). The sample was ground to -16 mesh, with at least 75% being -100 mesh. Acids used were commercial reagent grade. All perchloric acid oxidations were done with a modified Bethge apparatus, described by McGowan and Diehl (2), in a hood and behind an explosion shield.

Several different samples were oxidized with perchloric acid of varying concentration and boiling point. In the tables, the sample designations IL 6 and CP 1 are followed by the boiling point of the perchloric acid used to oxidize a particular sample. A lower case letter following the boiling point indicates that more than one

reaction was run at that boiling point employing different experimental conditions.

For the oxidation experiments, perchloric acid was added to the Bethge apparatus, and the boiling point adjusted to the desired temperature. By varying the initial amount of perchloric acid added, a final volume of approximately 50 mL was obtained. After cooling, 5 or 10 mL of phosphoric acid was added for some of the pyrite oxidations. A weighed sample of the coal or pyrite was placed in the Bethge apparatus, and a gas absorption bottle containing 100 mL of 15% H_2O_2 was added to the top of the Bethge apparatus (this absorption bottle was not used on the as-received coal samples). Using nitrogen as a purge gas, the reaction vessel was heated and the stable reaction temperature was noted. The reaction was allowed to proceed for 1.5 hours, and then the heat was removed. For the ground coal samples foaming was a problem. To overcome this foaming problem, the heat was removed when foaming began and reapplied when foaming ceased. Eventually, foaming ceased completely, and the reaction mixture was allowed to reach the boiling point. The system was purged for 30 minutes with nitrogen. The solution in the absorption bottle, designated with an end letter "G", was boiled to insure oxidation of the sulfur to sulfate and to reduce the volume to 25 mL. The samples were then diluted to 50 mL and the sulfate was determined by ion chromatography. After cooling, the reaction mixture was filtered. The solid phase, designated with an end letter "S", was dried at 60° in a vacuum oven and weighed. The percentage undissolved material was calculated. The aqueous phase, designated with an end letter "P", was diluted to 250 mL and analyzed for sulfate by nephelometry.

The solid samples were analyzed for sulfur by the Analytical Services of Ames Laboratory. IL 6 was analyzed by the ASTM procedure. CP 1 was analyzed for total sulfur using a Fisher Total Sulfur Analyzer. It was assumed that all of the sulfur existed as pyritic sulfur in the pyrite sample. The results of these analyses appear in Table 1.

In the aqueous phase of each reaction, sulfate was determined by precipitation with barium and the turbidity of the resultant barium sulfate suspension was measured spectrophotometrically. Since some of the aqueous phases contained a solid material, the solutions were allowed to sit at least overnight, and the sample used for the analysis was pipetted from the supernatant liquid. Since most of the solutions were also colored, the absorbance of the sample without added barium was measured and subtracted from the absorbance of the test solutions.

RESULTS AND DISCUSSION

The sulfate results from the aqueous phases of the as-received coal and the ground coal samples appear in Table 2 and Table 3, respectively. At temperatures of 150° and below, the sulfate content in the aqueous phase is constant and in the range of sulfatic sulfur reported by the ASTM procedure. This is native sulfate in the coal which may have undergone some oxidation since the ASTM assay. Above 150°, the sulfate

content begins to increase rapidly up to 165°, reaching a point which is somewhat below the assay for sulfatic plus pyritic sulfur. The increase then slows with increased temperature to a value somewhat less than the total sulfur assay.

Note that the results for the ground sample appear to have more "noise" than the as-received sample at temperatures of about 170° and especially at 203°. This was probably due to the foaming of samples about 170° and the lowering of the temperature until foaming ceased. Hence, these reactions spent more time at lower temperatures, where the production of sulfur gases was favored. The as-received samples did not have a foaming problem. There were some high results for two of the reactions with as-received coals. These results were most likely due to a sampling problem with the as-received coal, i.e., a large particle of pyrite was observed in some of the 1-g samples which would give an unrepresentative high sulfur value for that sample. Thus, the as-received coal posed a sampling problem which was alleviated by grinding the sample. However, the ground coal had a problem with foaming.

For the ground coal reactions and for one as-received coal reaction, the gases produced during the reaction were bubbled through a solution containing 15% H_2O_2 . Based on the sulfate determined using ion chromatography, the production of sulfur gases was low at low temperatures, increased as the temperature increased, and then decreased as the temperature increased above 170°C. This indicated that sulfur gases were produced at low temperatures when the oxidizing ability of perchloric acid was low. As the oxidizing ability of perchloric acid increased, the production of sulfate was favored. The low results at 170° and 203°C appeared to be due to an unidentified systematic error introduced on the same day of analysis. The high result at 203° was apparently due to the large amount of time this particular sample spent at lower temperatures to overcome the foaming problem described earlier for the ground coals. There are several sulfur compounds that could be produced in these reactions. Bethge (6) proposed that hydrogen sulfide, sulfur dioxide, and carbonyl sulfide were likely gases produced. Since some sulfur gases are produced at 130°C where perchloric acid has very little oxidizing ability, some native sulfide may have been converted to hydrogen sulfide. The data for the total sulfur recovered (the sum of the sulfate in the aqueous solution and the trapped sulfur gases) indicated that approximately 95% of the total sulfur was recovered at 180° and 100% was recovered at 190° and above.

In order to ascertain the effect of perchloric acid on FeS_2 , several samples of a coal-derived pyrite were dissolved. In the first series, 1-g samples of pyrite were used so that a large amount of sulfate would be produced making the determination of sulfate in a large excess of perchloric acid easier. The results appear in Table 4. At temperatures below 164°, the reactions proceeded as expected. However, above 164° a yellow precipitate formed. The amount of precipitate produced increased as the boiling point of perchloric acid increased, with the maximum amount produced at 203°. When 2 reactions were run on 0.1-g samples at 203°, the yellow precipitate formed again, but the

relative amount was significantly smaller. The precipitate was filtered, vacuum dried at 60°, and analyzed by a scanning electron microprobe (SEM) to reveal the presence of iron and sulfur as the major components of the solid. Since SEM can detect all elements above neon, oxygen was not eliminated as a component, but chlorine was eliminated. X-ray diffraction analysis proved the solid to be ferric hydroxide sulfate, $\text{Fe}(\text{OH})(\text{SO}_4)$. Analysis of the solid produced at 194° gave a result of 17.6% total sulfur (theoretical is 18.99% sulfur). Recognizing the presence of silica and residual coal impurities, this result was remarkably close. There are many ferric hydroxy sulfates known which vary mostly by hydration but also by the ratio of iron, hydroxide and sulfate; all of these compounds are yellow and precipitate from acid solution (12). Sulfate was also determined in the aqueous phases using nephelometry; however, no correlations could be made.

Since no yellow precipitate was formed during the coal oxidations, it was decided to oxidize CP 1 samples that would correspond in size to the amount of pyrite known to be in the coal sample, i.e., 0.06-g. Several reactions were run, some with the addition of phosphoric acid in an attempt to drive the dissolution of pyrite by forming an iron-phosphate complex. Phosphoric acid has been used with perchloric acid to speed the dissolution of iron ores (13).

The results of these reactions appear in Table 5. Microscopic observation of the solid material from each reaction showed that no yellow precipitate formed during these reactions. The percentage of undissolved material was determined for each reaction except those at 203°C; the undissolved material for 203° reactions was quite small and existed as small white crystals, probably quartz. In general, the addition of phosphoric acid does not increase the dissolution of pyrite at low temperatures (150-160°C). In fact, phosphoric acid appears to inhibit dissolution at these temperatures. Even though over 90 percent of the sample was dissolved by perchloric acid at 155-160°, the remaining solid still contained a small amount of pyrite. However, no pyrite was observed at 170° or at 203°. Sulfate was determined in the aqueous phase using nephelometry and in the peroxide trap using ion chromatography. With no phosphoric acid present, total sulfur recovered approached 100% for boiling points of 160° and above (total sulfur in the sample was assayed at 42.77%). The presence of phosphoric acid at 160° produced a much lower sulfur recovery, but the presence of phosphoric acid at 203° produced a sulfur recovery identical to that for perchloric acid alone at 203°, both approaching 100%. The presence of phosphoric acid at 203° did inhibit the formation of sulfur gases. Only 0.1% sulfur was recovered in the peroxide trap, while 39.9% sulfur was recovered as sulfate in the aqueous phase.

CONCLUSIONS

Sulfatic sulfur in coal can be removed by perchloric acid that has no oxidizing ability other than the hydrogen ion. Any hot acid should remove sulfate. Sulfatic sulfur in coal can be determined by using perchloric acid with a boiling point below 150°, and measuring the sulfate in the reaction mixture. Boiling perchloric acid at 160°, approximately 1.5 volts (14), is required to remove 100% of the pyrite.

However, at this temperature, some oxidation of the organic material will also occur. About 80% of the pyrite can be removed at 150°, approximately 1.3 volts, without significant oxidation of the organic material. A boiling point of 180°, approximately 1.7-1.8 volts, is necessary to remove the organic sulfur. However, at this temperature the organic material has been oxidized to the point dissolution. Total sulfur in coal can be determined with boiling concentrated perchloric acid. Two forms of sulfur are produced as reaction products: sulfur which is retained in solution as sulfate and a sulfur-containing gas which can be removed in a peroxide trap. Both forms of sulfur need to be measured for the determination of total sulfur. Since phosphoric acid inhibits the formation of sulfur gases at 203°, it may be possible to determine total sulfur without measuring the sulfur trapped by the peroxide solution.

The oxidation of pyrite can produce a precipitate of ferric hydroxide sulfate if the concentration of iron and sulfate are high enough. A 0.06-g sample of pyrite does not form a precipitate; a 0.1-g sample will form a small amount, and a 1.0-g sample will form a large amount of precipitate. The oxidation of a 1.0-g sample of coal which contains approximately 0.06-g of pyrite does not form any observable precipitate. It is possible that a small amount of sulfate may be tied up with iron in the reaction mixtures of the coal and 0.06-g pyrite samples. This may account for the fact that the results for sulfur recovery never quite approach the theoretical (even though they are within 5% of the theoretical).

Clear delineation has been made between sulfatic sulfur and the other forms of sulfur. Some delineation has been made between pyritic sulfur and organic sulfur. The anticipated delineation among the various forms of organic sulfur was not achieved.

LITERATURE CITED

1. Smith, G. F., "The Dualistic and Versatile Reaction Properties of Perchloric Acid," Analyst, 80, 16, 1955.
2. McGowan, C. W. and Diehl, H., "The Oxidation of Green River Oil Shale with Perchloric Acid. Part I - The Reaction of Green River Oil Shale with Perchloric Acid of Varying Concentration and Boiling Point," in print Fuel Proc. Tech.
3. McGowan, C. W. and Diehl, H., "The Oxidation of Green River Oil Shale with Perchloric Acid. Part II - The Analysis of Oxidation Products," in print Fuel Proc. Tech.
4. Smith, G. F. and Deem, A. G., "Determination of Sulfur in Coal by Perchloric Acid Method," Ind. Eng. Chem., Anal. Ed., 4, 227, 1932.
5. Kahane, E., "Determination of Sulfur in Rubber," Caoutchouc et Gutta-Percha, 24, 13549, 1927.
6. Bethge, P. O., "Apparatus for the Wet Ashing of Organic Matter," Anal. Chim. Acta., 10, 317, 1954.

7. Spielholtz, G. I. and Diehl, M., "Wet Ashing of Coal with Perchloric Acid Mixed with Periodic Acid for the Determination of Sulphur and Certain Other Constituents," Talanta, 13, 1002, 1966.
8. Markuszewski, R., Wheeler, B. C., Johnson, R. S., and Hach, C. C., "Rapid Dissolution of Coal for Analysis for Sulfur, Iron, and Other Elements," Am. Chem. Soc. Div. Fuel Chem. Preprints 28(4), 292ff (1983).
9. Kilpatrick, P. and Markuszewski, R., "Rapid Determination of Sulfur and Iron in Coal," presented at the Iowa Academy of Science Meeting, Iowa City, IA, April 27-28, 1984.
10. Biggs, D. L., et al., "Status Report of the Collection and Preparation of Coal Samples for the Ames Laboratory Coal Library," presented at the Coal Sample Bank Workshop, Atlanta, GA, March 27-28, 1981.
11. Chuang, K. C., Chen, M.-C., Greer, R. T., Markuszewski, R., and Wheelock, T. D., "Pyrite Desulfurization by Wet Oxidation in Alkaline Solutions," Chem. Eng. Commun. 12(1-3), 137-159 (1981).
12. Posnjak, E. and Merwin, H. E., "The System, $\text{Fe}_2\text{O}_3\text{-SO}_3\text{-H}_2\text{O}$," J. Am. Chem. Soc., 44, 1965, 1922.
13. Diehl, H., Quantitative Analysis, Oakland Street Science Press, Ames, Iowa, 2nd edition, 1974, 232.
14. Smith, G. F., "The Wet Chemical Oxidation of Organic Compositions Employing Perchloric Acid With-or-Without Added $\text{HNO}_3\text{-H}_2\text{IO}_6\text{-H}_2\text{SO}_4$," The G. Frederick Smith Chemical Co., Inc., Columbus, Ohio, 1965.

ACKNOWLEDGEMENT

Ames Laboratory is operated for the U. S. Department of Energy by Iowa State University under Contract No. W-7405-Eng-82. This work was supported by the Assistant Secretary for Fossil Energy, Division of Coal Utilization, through the Pittsburgh Energy Technology Center.

Table 1. Sulfur Assays for Coal and Pyrite Samples (in %)

Sample	Sulfatic Sulfur	Pyritic Sulfur	Organic Sulfur	Total
IL 6	0.26	2.41	2.17	4.85
CP 1	----	42.77 ^a	----	42.77

^a Assumed that all sulfur was pyritic.

Table 2. Oxidation of As-Received Illinois #6 Coal with Perchloric Acid

Sample	Sample Weight (g)	Boiling Point (°C)	Reaction Temperature (°C)	Reaction Time (hr)	Undissolved Material (%)	Sulfur Aqueous As SO_4^{2-} (%)
IL6-130	0.9751	134	126	1.5	91.34	0.39
IL6-140	1.0213	144	135	1.5	93.77	0.46
IL6-151	0.9991	155	146	1.5	99.43	1.26
IL6-160	0.9960	164	157-61	1.5	88.91	2.44
IL6-169	0.9513	173	166	1.5	52.93	6.68
IL6-170	1.0269	174	166-7	1.5	59.09	3.21
IL6-179	1.0048	183	174-1	1.5	17.96	3.56
IL6-180	0.9718	184	175-1	1.5	12.44	4.71
IL6-190	1.0408	194	183	1.5	8.50	3.98
IL6-200a	0.1431	203	202	0.5	7.41	4.30
IL6-200b	0.0408	203	202	1.0	7.89	4.54

Table 3. Results of the Oxidation of the Ground Coal with Perchloric Acid

Sample	Sample Weight (g)	Boiling Point (°C)	Reaction Temp. (°C)	Reaction Time (hr)	Undissolved Material (%)	Sulfur Aqueous As SO_4^{2-} (%)	Sulfur As Gas (%)	Total Sulfur (%)
IL6-130b	0.9897	130	124-5	1.5	93.63	0.39	0.17	0.56
IL6-140b	1.0023	140	131	1.5	91.38	0.41	0.66	1.07
IL6-150b	1.0146	150	140-38	1.5	90.62	0.49	1.44	1.93
IL6-160b	0.9996	160	152	1.5	81.18	1.87	1.78	3.65
IL6-170b	0.9904	170	162-3	1.5	31.50	2.65	0.03 ^a	2.68
IL6-171b	0.9936	171	162-3	1.5	34.95	2.78	0.31 ^b	3.09
IL6-180c	1.0181	180	174	1.5	14.24	3.06	1.37	4.43
IL6-190b	0.9945	190	178-7	1.5	9.03	4.07	1.03	5.10
IL6-203a	0.9974	203	196-9	1.3	6.94	3.01	1.59	4.60
IL6-203b ^c	1.0190	203	201	1.5	7.19	3.43	0.10 ^a	3.53

^a These two samples were run on the same day. All samples run on the ion chromatograph that day appeared to be low.

^b This sample went dry during processing and H_2SO_4 was lost.

^c This sample used the coarse, as-received coal.

Table 4. Results of the Oxidation of 1-g Pyrite Samples with Perchloric Acid

Sample	Sample Weight (g)	Boiling Point (°C)	Reaction Temp. (°C)	Reaction Time (hr)	Undissolved Material (%)	Sulfur Aqueous As SO_4^{2-} (%)
CP1-140	1.0042	144	139	1.5	47.92	4.13
CP1-150	1.0063	154	149	1.5	11.54	13.6
CP1-160	1.0027	164	156-8	1.5	11.60	13.2
CP1-170	1.0185	174	164-6	1.5	19.75 ^a	12.3
CP1-180	0.9922	184	175-8	1.5	57.11 ^a	6.4
CP1-190	1.0089	194	186-8	1.5	101.5 ^a	---
CP1-200a	0.9794	203	202	1.5	83.29 ^a	---
CP1-200b	1.0177	203	202	0.33	78.01 ^a	---
CP1-200c	0.1010	203	203	0.67	3.47 ^a	---

^a A yellow precipitate was produced during the reaction.

Table 5. Results of the Oxidation of 0.06-g Samples of Pyrite

Sample	Sample Weight (g)	H_3PO_4 Added to HClO_4	Boiling Point (°C)	Reaction Temp. (°C)	Reaction Time (hr)	Undissolved Material (%)	Sulfur Aqueous (%)	Sulfur As Gas (%)	Total Sulfur (%)
CP1-150b	0.0577	0	154	152-3	1.5	3.12	21.7	----	----
CP1-150c	0.0658	5 ^a	150	145	1.5	22.49 ^c	6.4	28.6	35.3
CP1-156a	0.0613	5 ^b	156	144-52 ^d	1.5	15.2	9.3	----	----
CP1-160b	0.0604	0	164	157-64 ^d	1.5	2.98	27.3	----	----
CP1-160c	0.0609	10 ^b	160	152	1.5	20.0	12.0	20.7	32.9
CP1-160d	0.0614	0	160	149	1.5	7.3	17.3	22.8	40.1
CP1-170b	0.0574	0	170	161-66	1.5	1.4	19.5	22.5	42.0
CP1-203b	0.0622	0	203	203	1.0	---	35.9	3.9	39.8
CP1-203c	0.0566	5 ^a	203	200	1.5	---	39.9	0.1	40.0

^a Added after boiling point adjustment.

^b Added before boiling point adjustment.

^c Oven temperature reached 170° during drying process causing oxidation.

^d Condensate escape during reaction.

INFLUENCE OF REDUCING GAS IN THE COPROCESSING OF COAL AND BITUMEN

S. Coulombe, P. Rahimi, S. Fouda, M. Ikura and H. Sawatzky

Canada Centre for Mineral and Energy Technology, Department of Energy,
Mines and Resources, 555 Booth Street, Ottawa, Ontario K1A 0G1

INTRODUCTION

Coproprocessing of bitumen/heavy oils with coals can offer a viable route for production of synthetic crudes. Under certain conditions these low grade materials can have mutual beneficial synergistic effects during hydroprocessing. Also, additional synthetic crudes become available from coal during the upgrading of bitumen/heavy oils. There is an added advantage over the conventional coal liquefaction process in that no solvent recycling is required. A comparison is made between synthesis gas and hydrogen as reducing gases for the coprocessing of an Alberta subbituminous C coal and Cold Lake vacuum bottoms. Product yields and qualities are compared at two levels of processing severity.

EXPERIMENTAL

The feed was a mixture of Cold Lake vacuum bottoms containing 83.2% pitch (+525°C material) and subbituminous C coal from Alberta (1). This slurry was processed under two different reducing feed gases: pure hydrogen and synthesis gas (30 mol % carbon monoxide in hydrogen). The liquid products were obtained at 60% and 70% pitch conversion. Pitch is defined as the material boiling above 525°C and pitch conversion is a measure of the difference in pitch concentration before and after coprocessing (1).

The products were distilled to obtain a naphtha fraction (<205°C), a distillate fraction (205°C-525°C) and a residue. This residue was further characterized by solubility in order to quantitate the residual oil (pentane-soluble), the asphaltenes (pentane-insoluble, toluene-soluble) and the preasphaltenes (toluene-insoluble, tetrahydrofuran-soluble).

The distillate portion (205°C-525°C) was combined with the residual oil (pentane-soluble residues) and hydrocarbon-type separation was performed using a modified API procedure developed by Sawatzky et al. (2). A column was packed with silica-alumina adsorbents. The solvents and the sequence of elution of the different fractions are shown in Table 1.

The polyaromatic fraction from hydrocarbon-type separation was separated by HPLC on a bonded amino column in order to quantitate the triaromatics, the tetraaromatics and molecules having five or more aromatic rings (3,4).

Fractions from hydrocarbon-type separation and polyaromatic subfractions from HPLC were characterized by gas chromatography equipped with a Dexsil 300 packed column and FID detector. Molecular weights of all aromatic fractions and concentrations of HPLC subfractions were determined from these runs according to a method published elsewhere (4).

RESULTS AND DISCUSSION

The primary characterization of the products is shown in Table 2. As expected, higher processing severity leads to lighter products. Gas and distillate yields are significantly higher for the high conversion products whereas residue levels were definitely lower.

Table 2 shows that the use of hydrogen results in less residue and leads to a higher coal conversion at both levels of severity. Also, the naphtha yield is significantly higher when using hydrogen especially under lower pitch conversion. Conversely, distillates over 200°C are favored by the synthesis gas especially at higher pitch conversion. This may indicate that when using hydrogen larger molecules are cracked into smaller units to a greater extent. However, most of these results are not indicative of a definite trend for designating the best reducing gas but they indicate that synthesis gas does not have an adverse effect on the quality of the products. Nevertheless, the use of synthesis gas resulted in less hydrogen equivalent consumption particularly at lower severity. This is also a positive aspect of the use of synthesis gas.

Besides product slate, quality of the products is obviously an important factor. Hydrocarbon-type separations were thus performed on each of the four samples in order to assess the quality of some of the products. Only distillates over 200°C combined with the residual oil were used in this chromatographic separation. Table 3 shows that the distribution of the recovered samples is similar for the two reducing gases. Gas chromatographic runs of the various fractions showed very similar chromatograms for the same concentration. Since the chromatograms were very similar, the calculated average molecular weights were also practically the same for all aromatic fractions. In some of the chromatograms, we noticed the presence of unresolved peaks having a high retention time. However, the concentration of these compounds was not high enough to affect the average molecular weights or the molecular weight distribution.

The most important feature about the hydrocarbon-type separation is that recoveries of material from the column were much higher for the synthesis gas. This would indicate that synthesis gas induces a higher conversion of very polar/basic molecules at both conversion levels. Compounds that can be strongly retained on such a system are highly polar and basic material or very heavy molecules similar to asphaltenes. In order to explain the differences between the material recoveries noted in Table 3, elemental analysis was performed on the samples that were separated on the hydrocarbon-type columns (Table 4). Unfortunately, the differences in heteroatomic levels cannot be significantly related to the column holdback. Sulphur levels seem to indicate that pure hydrogen is slightly better for eliminating sulphur compounds. Nitrogen levels are the same within experimental error and oxygen levels do not designate a particular gas. Although the elemental analysis results do not explain the differences in recovery between the two reducing gases, these recoveries strongly indicate that there is a significant difference between the two products. The higher recoveries using synthesis gas cannot be explained at

this point but they are reproducible indicating that the use of pure hydrogen produces a strong adsorption of very polar or heavy material on the column. This might be an indication that pure hydrogen and synthesis gas would react with the slurry feed in different ways thus leaving molecules of different polarity and basicity in the products. For example, it is known that carbon monoxide interacts directly with oxygen functionality in low-rank coals. A similar behaviour could be expected in subbituminous coals. In any case, the strongly retained compounds can be assumed to be undesirable material in view of production of synthetic fuels therefore the use of synthesis gas has advantages. Since the composition of the recovered material is not significantly different for the two reducing gases, we can at least conclude that the use of synthesis gas would not be deleterious. Moreover, in cases where carbon monoxide is cheaper than hydrogen, synthesis gas would be an advantageous alternative.

CONCLUSIONS

This study shows how the use of synthesis gas in coprocessing of coal and bitumen could be advantageous over hydrogen. Although most results indicate that pure hydrogen and synthesis gas have similar hydrocarbon yields, synthesis gas seems to be advantageous for the cracking/hydrogenation of very polar undesirable molecules that could be present in the valuable products. Compared with hydrogen it also enhances the formation of distillates. Finally, synthesis gas shows a significantly lower hydrogen equivalent consumption especially under moderate operating severity.

REFERENCES

1. Kelly, J.F., Fouda, S.A., Rahimi, P.M. and Ikura, M., CANMET Coprocessing: A Status Report, Proceedings CANMET Coal Conversion Contractors' Review Meeting, Calgary, Alberta, November 1984.
2. Sawatzky, H., George, A.E., Smiley, G.T. and Montgomery, D.S., Fuel, 55, 16 (1976).
3. Chmielowiec, J., Beshai, J.E. and George, A.E., Fuel, 59, 838 (1980).
4. Coulombe, S. and Sawatzky, H., in Polycyclic Aromatic Hydrocarbons: Mechanisms, Methods and Metabolism, edited by M. Cooke and A.J. Dennis, Battelle Press, p. 281, 1985.

Table 1 - Hydrocarbon-type separation procedure

Solvent	Quantity	Fraction
Pentane	250 mL	Saturates
5% toluene/pentane	300 mL	Monoaromatics
15% toluene/pentane	300 mL	Diaromatics
Toluene	100 mL	Polyaromatics
Methanol/toluene (50/50)	100 mL	Polars
Methanol	100 mL	Polars

Note: The column is flushed with pentane at the end of the sequence to ensure complete elution of the methanol.

Table 2 - Composition of products from coprocessing

	Severity			
	60% pitch conversion		70% pitch conversion	
Reducing gas	H ₂	H ₂ /CO	H ₂	H ₂ /CO
H ₂ equivalent consumption (%)	3.32	2.0	3.15	2.90
Coal conversion (%)	74.0	73.7	83.8	78.5
Fractionation:				
C ₁ -C ₄ yield (%)	5.3	5.0	6.6	7.2
Naphtha (%)	16.3	9.7	15.2	13.1
Distillate +205°C (%) *	45.1	46.5	49.7	54.2
Residual oil (%)	15.0	16.2	11.2	11.8
Asphaltenes (%)	6.3	9.3	5.7	5.8
Preasphaltenes (%)	3.8	3.4	1.6	2.1
Residue (%) **	32.5	37.1	23.4	26.3

* In hydrocarbon-type separation, the distillates are combined with the residual oil.

** The residue includes residual oil, asphaltenes and preasphaltenes and tetrahydrofuran insolubles (unreacted coal).

Table 3 - Hydrocarbon-type separation of coprocessing products
(distillates 205-525°C + residual oil)

Fractions	60% pitch conversion		70% pitch conversion	
	H ₂	H ₂ /CO	H ₂	H ₂ /CO
Saturates (%)	30.4	35.0	38.8	36.7
Monoaromatics (%)	11.1	10.4	9.7	12.3
Diaromatics (%)	12.9	13.8	10.9	10.9
Polyaromatics (%) *	12.0	13.6	15.4	15.3
Triaromatics (%)	5.0	6.2		
Tetraaromatics (%)	4.0	4.7		
Higher aromatics (%)	3.0	2.7		
Polars (MeOH/Tol) (%)	18.6	20.4	11.9	19.0
Polars (MeOH) (%)	1.9	1.8	1.6	2.9
Recovery **	86.9(3)	95.0(2)	88.3(2)	97.1(2)

* Polyaromatics = triaromatics + tetraaromatics + higher aromatics.

** The number in parenthesis indicates the number of replicates.

Table 4 - Elemental analysis of products (distillates 205-525°C
+ residual oil, wt %)

	60% pitch conversion		70% pitch conversion	
	H ₂	H ₂ /CO	H ₂	H ₂ /CO
Carbon	84.60	84.93	84.90	84.35
Hydrogen	10.43	10.56	10.40	10.43
Sulphur	2.02	2.32	2.07	2.46
Nitrogen	0.60	0.55	0.68	0.64
Oxygen (by difference)	2.35	1.64	1.95	2.12

**THE EFFECT OF CARRIER GAS ON THE ENTRAINED BED
PYROLYSIS OF WESTERN KENTUCKY No. 9 COAL.**

by

Shi-Jin Shen, Uriel M. Oke (*) and Alberto I. LaCava.

Department of Chemical Engineering
The City College of the City University
of New York
New York, NY 10031

(*) Cities Service Oil and Gas Corporation
Tulsa, Oklahoma

INTRODUCTION

Flash pyrolysis in different gases has been studied as an alternative process for the simultaneous gasification and liquefaction of coal. Experimental studies on flash hydrolysis, steam pyrolysis, and inert gas pyrolysis of various types of coal have been reported in the literature (1-26). Investigations on the effect of steam and hydrogen on the pyrolysis of hydrocarbons, coal and vacuum residue (24, 27) indicate that both steam and hydrogen influence the yield. Szuba and Michalik (24) have shown that the total production of liquids from pyrolysis is higher in the presence of steam than in an inert atmosphere, but is still lower than the liquid production from hydrolysis. These studies have examined in detail, the effect of the process variables (temperature, pressure, solids contact time, gas phase residence time, etc.) on the total yield of products and on the selectivity of the reaction.

However, there is a lack of liquid product characterization. Simple analytical techniques such as gas chromatography and elemental analysis do not provide enough information on their nature. This is due to the chemical complexity of these liquids and the large number of individual components.

Adequate characterization of the liquid obtained is important in the evaluation of a coal liquefaction process. In the industrial operation of upgrading coal liquids, three factors must be considered. The first is the known instability of these liquids upon heating in the presence of oxygen, i.e. their tendency to polymerize. The second is that the removal of heteroatoms calls for expensive upgrading in a catalytic reaction that consumes hydrogen heavily. The last consideration is that the liquid has to be reformed to a desired molecular size and carbon to hydrogen ratio. The liquefaction products need characterization to provide information on which and how much of this processing is required.

Hydrocarbon liquid production by coal pyrolysis in an inert gas is not attractive as an industrial process. It yields low conversions, produces unstable liquids, and has low selectivity towards desirable products. As a result, more emphasis is placed on hydrolysis and steam pyrolysis. These two processes involve different chemical reactions. Present interest in flash steam pyrolysis stems from the economical advantage of using steam in place of expensive hydrogen, and from that steam has higher selectivity than inert gas towards the production of desirable liquids (10). A knowledge of the differences between hydrogen and steam pyrolysis

products and reaction mechanisms is useful when considering both processes as potential routes to liquid and gaseous fuels. The goal of this research project was to find a meaningful way of characterizing the products and to apply this characterization to steam and hydrogen pyrolysis liquids.

To achieve these objectives, coal was treated under identical reaction pressure and temperature in three reaction environments: hydrogen, a steam/helium mixture, and pure helium. A comparison was then made on the effect of the reaction environment on the gas and liquid yields. The characterization technique was used then, to establish the structure of the major fractions of components in the liquids produced by hydrogen and steam/helium pyrolysis. The analogies and differences between different parts of the liquids, their dependence upon the reaction environment and the chemical reactions that explains the differences which are discussed in this paper.

THE CHARACTERIZATION TECHNIQUE

Previous experience with the characterization of pyrolysis derived liquids in our laboratory has shown the limitations of conventional analytical techniques (10). For example, the gas-chromatographic separation of the liquids failed to elute a significant part of the liquid. Most of the material remained in the column.

The characterization of groups in coal derived liquids has been used widely. The information obtained by hydrogen and carbon NMR and FTIR has been very useful in elucidating the functional structure of the liquid. Functional characterization of the liquid, however, is not enough to characterize the physical and chemical properties of the liquid. It is also necessary to establish to what kind of molecule the functional group is attached, its molecular size and other groups in the molecule. Also, it is essential to know how functional groups, molecular sizes and other properties (such as aromaticity) are distributed in the liquid.

With a simple liquid mixture, the obvious answer would be to separate all components and identify them. With coal pyrolysis liquids, with hundreds of individual components, this is not a practical solution. Even if such a laborious task is accomplished, the components should be lumped in families with some common properties, to make any practical use of the results of the separation.

Sequential Elution Solvent Chromatography (SESC) (28, 29) is a technique that was developed for the separation of coal liquefaction products in several fractions. Each fraction has some common features, such as characteristic functional groups, polarity or basicity. SESC offered for our application a balance point between detail in the separation and low number of fractions separated. Although SESC was not applied to the characterization of coal pyrolysis liquids before this work, the theory of the method was applicable to coal pyrolysis products and the probabilities of success were high.

In preliminary work with the technique, we found that no fraction did elute with pyridine as a solvent. We did eliminate pyridine from the sequence. Since the method is not the original SESC of Farcasiu (28), it will be called modified-SESC or M-SESC in this paper.

Following the separation, each fraction was further characterized by Steric Exclusion HPLC (molecular size distribution), Boiling Point Distribution (GC method), ^1H -NMR (aromatic and aliphatic ^1H , ^1H containing functional groups), Elemental Analysis and density.

The information obtained is useful as a more detailed and accurate model of the coal liquid obtained by pyrolysis. The information can be used to discuss the characteristics of the reaction paths during pyrolysis in different gas environments, as shown in this paper.

EXPERIMENTAL

The coal used was Western Kentucky No. 9 (from the Pyro Mine, Kentucky). The composition of the coal is given in Table I.

The pyrolysis system was operated in 6.9 MPA with pure hydrogen, pure helium, or a mixture of 7.6 mole percent of steam in helium. Coal was fed at a rate of 1 kg/hr into the reactor which was 7.9 cm in diameter and 100 cm in length. All the tests were conducted at 740 °C in a 30 cm long hot zone. The superficial velocity of the gases fed into the reactor varied from 5 to 8 cm/s. For the hydrogen and steam/helium runs, the free falling coal particles were maintained in the hot reactor zone for one second. Full details of this apparatus are given elsewhere(4).

The liquids from the steam/helium and hydrogen runs were then characterized. Note that the helium run was included solely to assess the effect of reaction environment on the total yield and thus was not further analyzed. An account of the experimental details of the M-SESC fractionation and the characterization of each fraction has been given by Shen (32).

RESULTS

A comparison of the products from coal pyrolysis in hydrogen, the steam/ helium mixture, and pure helium is presented in Figure 1. The overall yield from steam pyrolysis is higher than the yield from inert gas (helium) pyrolysis under the same operating conditions. The data for the three processes reveal that hydrolysis produces the largest amount of coal-derived products. The liquid products from the hydrogen and the steam/helium runs were further analyzed and the results are presented below.

Table II gives the elemental composition of the liquid products. Figure 2 shows the results of the Modified SESC (M-SESC) fractionation of the coal liquids. Figures 4 and 5 give the results of the elemental analyses of the Modified SESC fractions from both of the coal-derived liquids.

The boiling point distribution analysis of the M-SESC fractions for both liquids shows a boiling range of 50 to 400 °C for Fraction I, and of 300 to 550 °C for Fractions II and III. Fractions IV and higher did not elute from the GC column.

From the experimental molecular size distribution curves, the number average molecular weights were calculated with the formulas given by Schanne and Haemel (30). The average molecular weights of the M-SESC fractions are given in Figure 3.

Figures 6 and 7 summarize the information obtained from H¹NMR spectroscopy of the samples and fractions analyzed. The proton spectra are used primarily for the determination of the percentages of aromatic and aliphatic hydrogen contained in each sample.

DISCUSSION

The structure of the M⁺SESC fractions, as obtained in the present research, is summarized in table 3. The table reports the common features of each fraction for both liquids. Behind the similarities between corresponding fractions, however, there are also significant differences between the two coal liquids. These differences reflect chemical reactions that occur under the influence of different gas environments.

Figure 8 shows a list of the chemical reactions that can play a role in coal pyrolysis in hydrogen, steam and inert gas. The differences between the properties of the liquids obtained in different gases can be attributed to these chemical reactions. In the following discussion, an attempt is made to explain our experimental results with the reactions of figure 8.

Analysis of Results

Figure 1

Steam Pyrolysis produces higher CO_x yields than the other pyrolysis processes, due to reaction (15) (carbon steam gasification). In He and H₂, CO_x is probably produced from the decomposition of carboxylic and carbonyl groups. The production of light hydrocarbon gases is enhanced in H₂ due to reactions (4) (capping of alkyl radicals), (8) (thermal dealkylation) and (11) (thermal hydrogasification). Pyrolysis in He or Steam can yield light hydrocarbon gases only from (1) (cracking) and (4) (hydrogen abstraction from another molecule). The yield of BTX is enhanced in the presence of hydrogen through reactions (5) and (7) (capping of single ring aromatic radicals), (9) (thermal hydrocracking of several-ring molecules), (8) (thermal dealkylation of alkylbenzenes) and reactions (12), (13) and (14) (side chain heteroatom removal). The yield of liquids (heavier than BTX) in hydrogen is higher than in inert gas through reactions (5) and (7) (several-ring aromatic free radical capping) which competes with reaction (6) (recombination to form char). However, the yield is less than in steam, since hydrogen participates in reactions that break down large molecules, such as (8) (thermal dealkylation) (9) (thermal hydrocracking) and (10) (thermal hydrogenation, facilitates hydrocracking). In steam, the yield of liquids is higher than in inert gas. A tentative explanation is that reaction (15) may open the coal matrix, liberating fragments. Another possibility is the participation of steam in the breakdown of the virgin coal (reactions (1), (2) and (3)), through a heterolytic mechanism. The total conversion of coal by pyrolysis in hydrogen gives the highest yield, through reactions (5) and (7) which compete with reaction (6) (recombination to form char). The total conversion in steam pyrolysis is higher than in He due to reaction (15) (char gasification) and to an enhancement of the liquid yield, previously discussed.

Figure 2

Fractions 1 and 2 in hydrogen pyrolysis are increased from fractions 3, 4 and 5 through reactions (9) (thermal hydrocracking) and (12), (13) and (14) (heteroatoms removal). Fraction 6 in hydrogen pyrolysis (very basic heteroatoms) could be increased from coal through reactions (5) and (7) or from fraction 5 through the elimination of acid groups, reaction (14). The fraction is not converted easily, since the basic heterocyclics have to be first hydrogenated through reaction (10) and the ring opened by hydrogenolysis (reaction similar to (9)) before reactions (12), (13) and (14) could proceed. Fraction 9 in both liquids (material not eluted from the M+SESC column) is probably a degradation product (coke), insoluble.

Figure 3

Fractions 1, 2, 3, 4, 5 and 6 of the hydrogen pyrolysis liquids have higher molecular weight than the corresponding steam pyrolysis liquids. Smaller molecules in these fractions can be converted to BTX and gas through reactions (9) (thermal hydrocracking) and (11) (thermal hydrogasification). The larger molecules in these fractions may be more difficult to break, hence increasing the average molecular weight of the fraction.

Figure 4

The nitrogen content of the hydrogen pyrolysis liquids fractions 1 and 2 is virtually zero, lower than in the steam pyrolysis liquids. This is due to its elimination from the fractions by hydrogen through reaction (13). In other fractions, nitrogen appears in the heterocyclic form, basic, and is more difficult to eliminate, as discussed before. The hydrogen content is comparable in the fractions of both liquids, although higher in hydrogen pyrolysis fraction 1, the most abundant. There is an upward trend in both liquids: higher fractions contain more hydrogen.

Figure 5

The carbon content in the fractions of both liquids is comparable. The downwards trend is required to accommodate the higher heteroatoms content of the higher fractions. Oxygen + sulphur in both liquids follow an upwards trend, in agreement with the SESC fractionation theory. Fractions 1 and 2, the most abundant, show less heteroatoms in hydrogen pyrolysis, confirming the influence of reactions (12) and (14). Other fractions (heterocyclics) do not show the same effect, due to the difficulty associated with breaking ring heteroatoms.

Figure 6

The fractions in both liquids follow an upwards trend, higher fractions have a higher hydrogen to carbon ratio. There are differences between the two liquids, but they do not follow a clear trend.

Figure 7

Fractions 3, 4 and 5 from hydrogen pyrolysis show the effect of extensive hydrogenation through reaction (10) (ring hydrogenation). However, the hydrogen to carbon ratios do not reflect a large difference (see Figure 6). The explanation is that although reaction (10) adds hydrogen to the aromatic structure, net hydrogen is also lost from the molecule through reaction (8). Hydrogen pyrolysis liquids are more hydroaromatic, but with less side chains. The stripped side chains partially explain the formation of high methane yields during hydrogen pyrolysis.

CONCLUSIONS

The M=SESC technique used here, and accompanied by further characterization of each one of the fractions, is demonstrated as a powerful tool that allows a deep insight into coal pyrolysis liquids structure and composition.

Basic differences in the structure and composition of coal liquids, revealed through M=SESC and fraction characterization techniques has been explained in this work through the thermal reactions where hydrogen participates.

The characterization technique, and the discussion offered here, presents an extra dimension in the understanding of coal pyrolysis liquids and the reactions that form them and the reactions where they participate.

REFERENCES

1. Chen, W., A. I. LaCava and R. A. Graff, FUEL, 1983, 62, 56.
2. Cypress, R. and S. Furfari, FUEL, 1982, 61, 447.
3. Eklund, H. and W. Wanzl, Proc. "Int. Kohlenwiss Tag., 1981, 701.
4. Fling, W. A., A. F. Gulbrandsen, J. A. Hanshar, U. M. Oko, and R. Matyas, "Flash Hydropyrolysis of Western Kentucky No. 9 Bituminous Coal with Catalysts," Annual Report, DE-Ac22-79ET14943, 1979
5. Franklin, H., W. Peters, and J. Howard, FUEL, 1982, 61, 1213.
6. Furfari, S., "Hydropyrolysis of Coal," Report ICTLS/TR20, IEA Coal Research, London, October 1982.
7. Furfari, S. and R. Cypress, FUEL, 1982, 61, 453.
8. Fynes, G., W. R. Ladner, and J. Newman, Proc. "Int. Kohlenwiss Tag. 1981, 681.
9. Gavalas, G. R., "Coal Pyrolysis," Elsevier Sci. Publ. Co., 1982.
10. Graff, R. A., A. I. LaCava, and Yerushalmi, "Improved Techniques for Gasifying Coal," Final Report, DOE/FE-2340-F, January 1982.
11. Hauge, R. H., L. Fredin, J. Chu, and J. L. Margrave, ACS Symposium, 1983, 28, 1, 35.

12. Howard, J. B. "Fundamentals of Coal Pyrolysis and Hydropyrolysis" in "Chemistry of Coal Utilization. Second Supplementary Volume," John Wiley, New York, 1981.
13. Juntgen, H. and K. H. Van Heek, FUEL PROCESSING TECH., 1979, 2, 261.
14. Mackie, J. C. and K. R. Doolan, Proc. -Int. Kohlenwiss Tag. 1981, 714.
15. McCown, M. S. and D. P. Harrison, FUEL, 1982, 61, 1149.
16. Niksa, S., W. Russel, and D. Saville, FUEL, 1982, 61, 1207.
17. Scaroni, A., P. Walker, Jr., and K. Essenhight, FUEL, 1981, 60, 71.
18. Schaub, G., W. Peters, and J. Howard, Proc. -Int. Kohlenwiss Tag., 1981, 229.
19. Solomon, P., R. Hobbs, D. Hamblen, W. Chen, A. I. LaCava, and R. A. Graff, FUEL, 1981, 60, 342.
20. Solomon, P., D. Hamblen, and R. Carangelo, "Coal and Coal Products Analytical Characterization Techniques," E. L. Fuller, Ed., ACS Symposium Series, 1982, 205, 77.
21. Stangeby, P. and P. Sears, FUEL, 1981, 60, 131.
22. Suzuki, T., M. Mishima, M. Itoh, Y. Watanabe, and Y. Takegami, NENRYOKYOKAISHI, 1982, 61, 397.
23. Suzuki, T., M. Itoh, Y. Takegami, and Y. Watanabe, FUEL, 1982, 61, 403.
24. Szuba, J. and R. Michalik, FUEL, 1982, 81, 1201.
25. Tyler, R. and H. N. Schafer, FUEL, 1980, 59, 487.
26. Wilson, M., H. Rottendorf, P. Collin, A. Vassallo, and P. Barron, FUEL, 1982, 61, 321.
27. Graff, R., Letter Report 29 to C. Karr (DOE), Contract NO. DE-AC21-80 Mc15875.
28. Farcasiu, M., FUEL, 1977, 56, 9.
29. Whitehurst, D. D., M. Farcasiu, and T. Mitchell, "The Nature and Origin of Asphaltenes in Processed Coals," Annual Report, EPRI AF-252, February 1976.
30. Schanne, L. and M. Haemel, FUEL, 1980, 60, 556.
31. Juntgen, H., FUEL, 1984, 63, 731.
32. Shen, Shi-Jin, "Liquid Characterization by Coal Pyrolysis in Different Gases", Ph.D. Thesis, The City University of New York, New York, 1984.

TABLE 1

COMPOSITION OF WESTERN KENTUCKY No. 9 COAL

(Weight Percent)	
Carbon	74.17
Hydrogen	5.12
Nitrogen	1.19
Sulfur	2.64
Oxygen (by difference)	-
Ash (MF)	7.31
Volatiles Matter	9.57
	35.30

TABLE 2

AVERAGE PROPERTIES OF COAL LIQUIDS
(before M-SECC Fractionation)

	Flash	Steam/Me
	Hydrogenation	Pyrolysis
Carbon	87.01	81.61
Hydrogen	5.60	4.60
Nitrogen	1.37	1.37
Oxygen + Sulfur	5.89	11.42
Hydrogen/Carbon ratio	0.77	0.67
Number Avg. Molecular Size	172.00	203.00
* Aromatic Hydrogen (by NMR)	83.30	89.50

TABLE 3

STRUCTURE OF THE MODIFIED SESC FRACTIONS

FRACTION	STRUCTURE	BOILING RANGE	DENSITY	AVE. MOL. SIZE
I	Aromatics, low heteroatoms	50 - 400 C	1.11	190
II	Aromatics, alkyl-aromatics, low heteroatoms	300 - 500 C	1.18	190
III	Polar aromatics, with non-basic heteroatoms	300 - 600 C	0.996	250 - 400
IV	Alkyl-polar aromatics phenol and methoxy groups	*	n.a.	250 - 400
V	Basic heterocyclics and phenol groups	*	n.a.	300 - 400
VI	Basic heterocyclics alkyl and phenol groups	*	0.987	250
VII	Polyphenols, non-condensed aromatics high heteroatoms	*	n.a.	300 - 420
VIII	Polyphenol, alkyl chains	*	1.194	350 - 450

*Did not elute from G.C. in boiling point simulating analysis

FIGURE 1
Product Distribution from Hydrogen
and Steam/He Pyrolysis

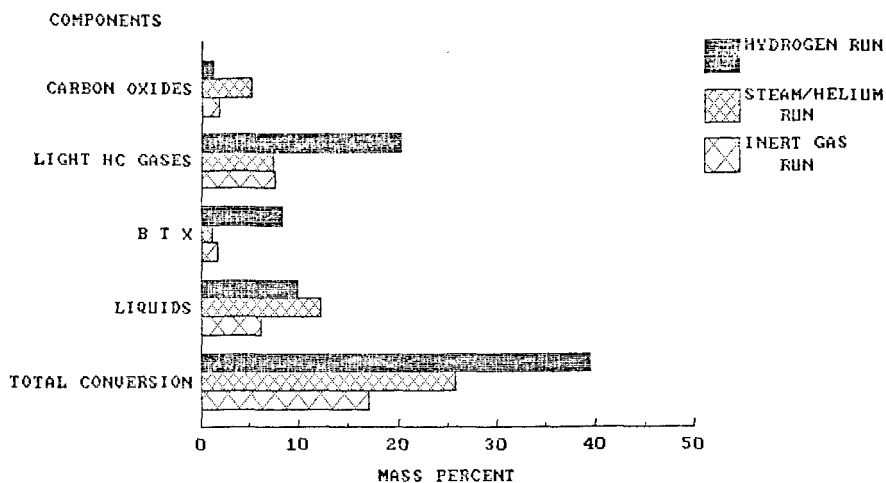
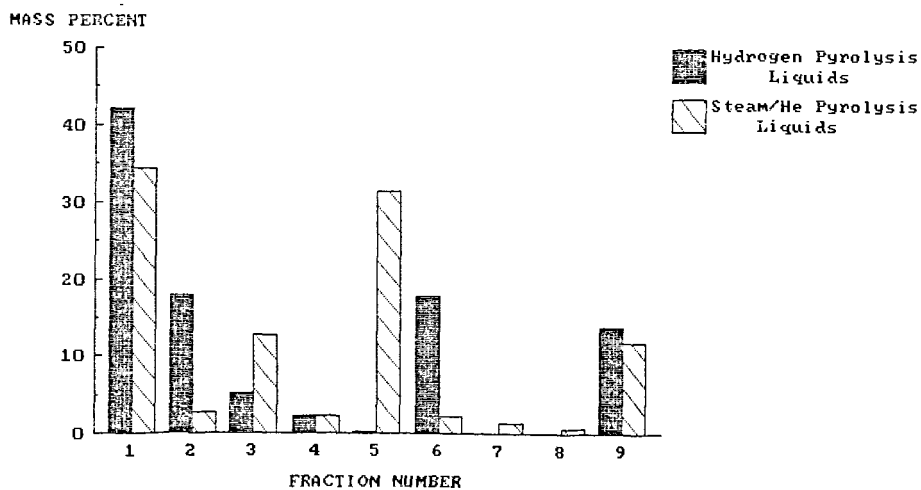


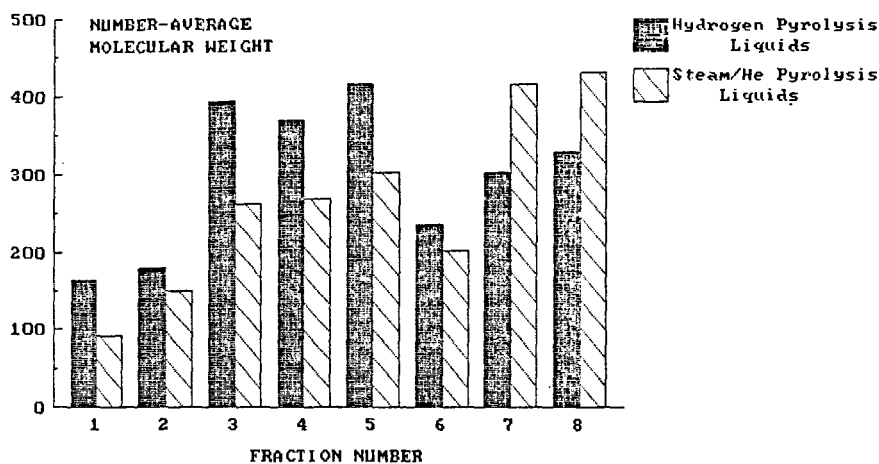
FIGURE 2 : M-SESC MASS DISTRIBUTION
OF FRACTIONS



Fraction 9 is the mass not eluted.

FIGURE 3 : AVERAGE MOLECULAR SIZES
OF M-SESC FRACTIONS.

MOLECULAR WEIGHT



Obtained by Steric Exclusion HPLC

FIGURE 4
HYDROGEN AND NITROGEN CONTENT
OF M-SESC FRACTIONS

MASS PERCENT

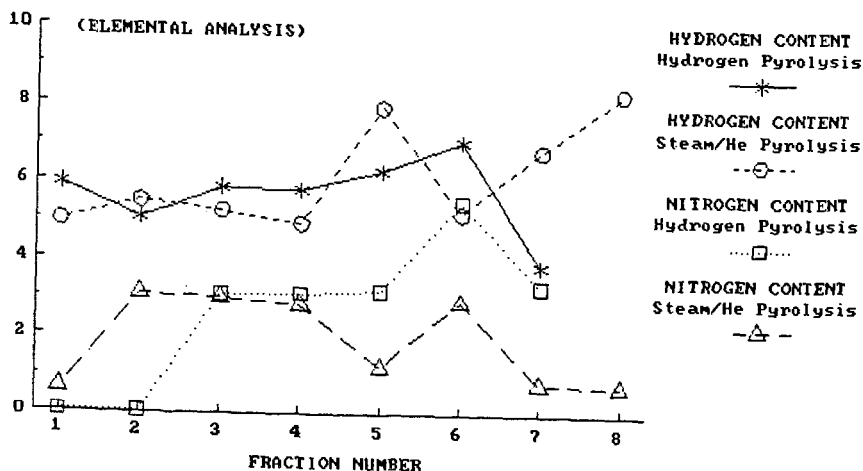


FIGURE 5
CARBON AND OXYGEN+SULFUR CONTENT
OF M-SESC FRACTIONS

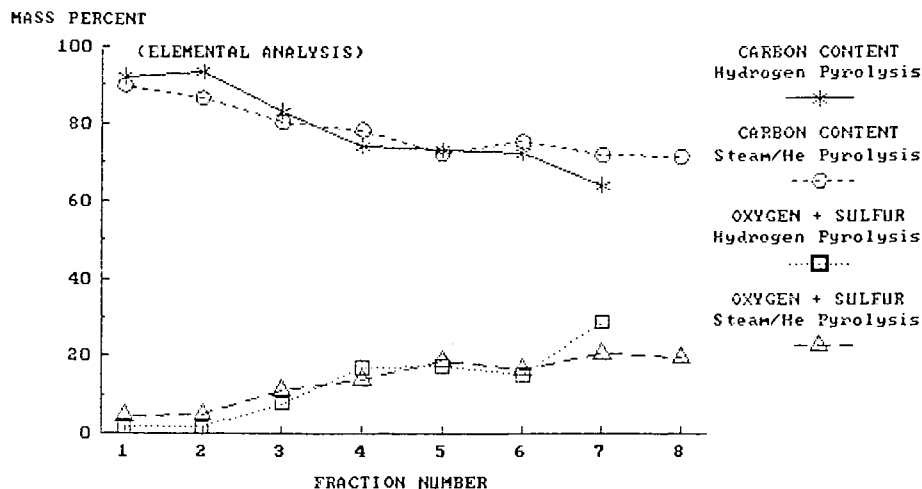


FIGURE 6
HYDROGEN TO CARBON RATIOS
OF M-SESC FRACTIONS

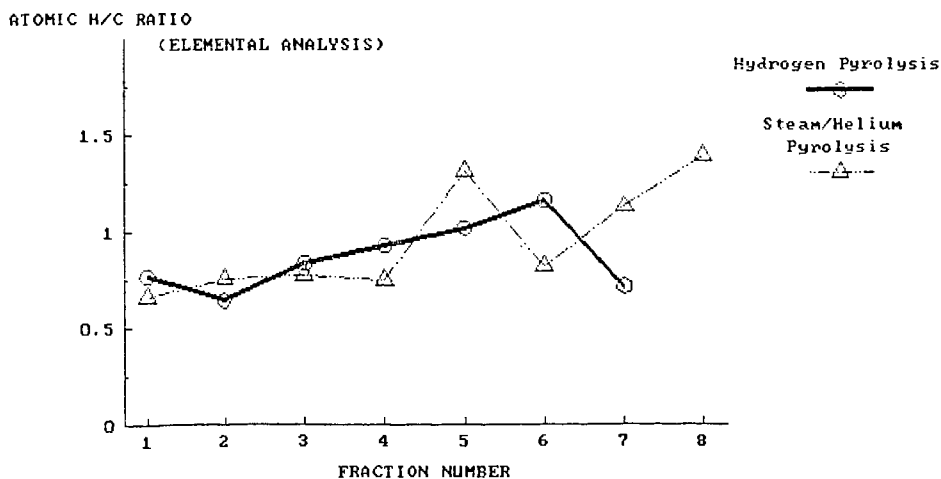


Figure 8 CHEMICAL REACTIONS IN STEAM AND HYDROGEN PYROLYSIS

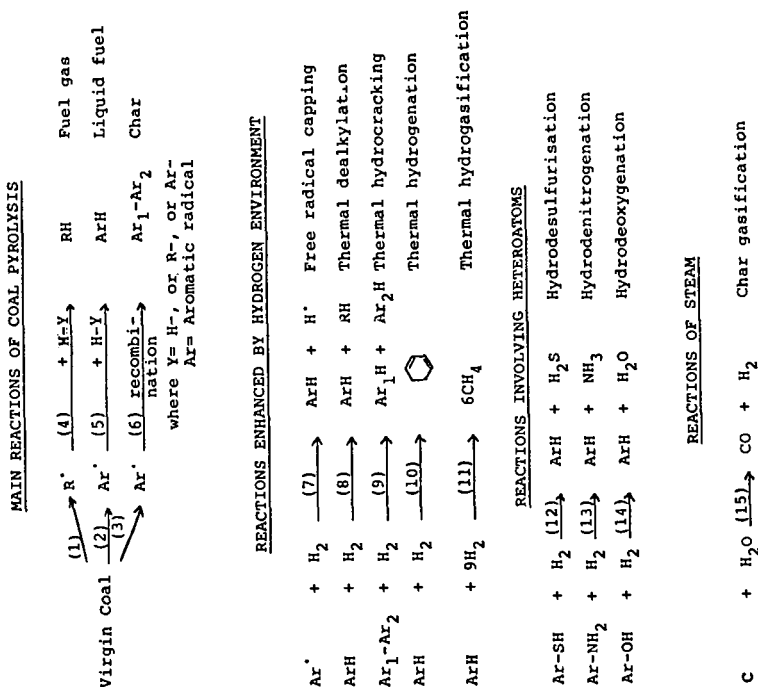
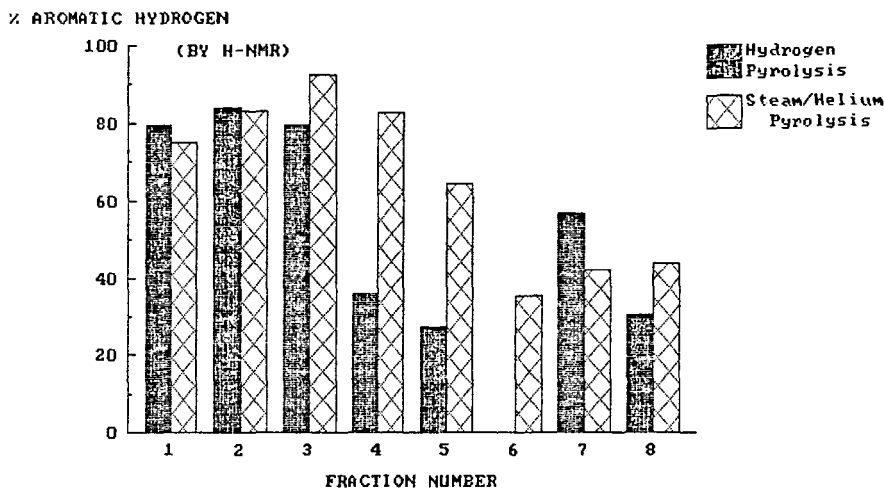


FIGURE 7
AROMATICITY OF M-SESC FRACTIONS



CO-OXIDATIVE DEPOLYMERIZATION OF COAL

Rita K. Hessley, William G. Lloyd and Renae D. Rosencrans

Department of Chemistry
Western Kentucky University
Bowling Green, Kentucky 42101

Introduction

Recently a number of industry-sponsored coal conversion projects have suffered set-backs in the acquisition of government financial support that have all but dismantled the synfuels industry in the United States. Although the requirement for reduced sulfur emissions can be identified as one of the problems currently holding back the development of direct coal liquefaction processes, it is the prohibitively high cost associated with liquefaction technology which has been the stumbling block for private corporate investors and governmental agencies.

In undertaking this project, we proposed to explore the possibility that a useful feedstock could be prepared from coal using a totally different approach to the basic problem involved in fracturing the complex and highly crosslinked coal matrix. Rather than relying on thermal bond cleavage and hydrogen transfer under high pressure, we believed that a mild, limited oxidation process could achieve the desired depolymerization of coal. Under special conditions involving a solvent capable of undergoing free radical oxidative chain reactions, C-C bond cleavage in the coal might be achieved. Oxidation of coal, even mild oxidation, is generally undesirable. Progressive oxidation results in destructive degradation - lost heating value and swelling properties, and even ignition (1,2). A number of studies of controlled oxidation of coal have been made (3-6). From these studies, it was apparent that even controlled oxidation is not satisfactory for the liquefaction of coal.

It is important, however, that coal oxidation is believed to be a free radical process (7-16). From polymer chemistry it is well known that a chain reaction, similar to those proposed for coal conversion reactions at high temperatures, occur readily between two reactive substrates under oxidizing conditions, and at temperatures well below 400-450°C (the temperature range used commonly to achieve coal thermolysis). Figure 1 illustrates the system we proposed (17). R_1H and R_2H represent two hydrocarbon substrates--in our case a solvent and coal. Free radical initiation to produce R_1^{\bullet} is a relatively low energy process. The reaction with pure oxygen or air to form R_1OO^{\bullet} has an activation energy of ~ 0 . Abstraction of hydrogen can involve labile carbon-hydrogen bonds in either R_1H or R_2H , and the cycles shown in the figure can be repeated a number of times. The products of this co-oxidative free radical chain reaction are hydroperoxides. Cumene (isopropyl benzene) is a hydrocarbon which is known to undergo the kind of oxidation reaction described in Figure 1. We have chosen it as our principle solvent. Using an initiator, and in some cases a small quantity of a transition metal ion, cumene hydroperoxide can be produced at 80°-100°C (18). In dilute acid at a temperature as low as 60°C, the decomposition of cumene hydroperoxide results in C-C bond scission. Thus, we proposed that analogous scission could be induced in the coal matrix subsequent to the oxidative formation of the coal hydroperoxide, R_2OOH . We predicted that the C-H bond energy of tertiary ($-CH-$) and secondary ($-CH_2-$) bridging sites in coal is comparable to that of the C-H bond in cumene.

Experimental

Co-oxidation. Three coals were selected for this study. All were western Kentucky hvB or hvC bituminous coals obtained from the coal bank at Western Kentucky University. The elemental analysis for each coal is given in Table I. The coals

were not dried before use. Determination of the optimum conditions for co-oxidation involved a number of variables: solvent, temperature, pressure, and reaction time were identified as the four principle variables. These were varied within limits selected as a useful range for ultimate commercial application. Temperatures were tested in the range 30-185°C; gas pressures were varied from 1-7 atmospheres (0.1-0.7 MPa); reaction times were 0.5-24 hours. Solvents tested are listed in Table II.

Typically, 10 g coal (-60 mesh), 100 ml solvent, and 1.0 g of initiator were used. For reactions at atmospheric pressure, air or oxygen was passed continuously into the reaction slurry at a rate sufficient to maintain a moderately turbulent system. At elevated temperatures (above the normal b.p. of the solvent) or pressures, the reactants were charged to a 300 ml stainless steel Parr reactor (equipped with mechanical stirring and temperature control) which was sealed and pressurized with oxygen as desired. The free radical initiators which were used in each temperature range were azobisisobutyronitrile (65-88°C), ditertiary butyl peroxide (117-143°C), tert-butyl hydroperoxide (121-147°C) and cumene hydroperoxide (154-194°C)(19).

After each reaction, the slurry was cooled and filtered to recover the coal. The coal was washed with acetone and was dried for a minimum of 16 hours at 150°C in an evacuated drying oven.

Determination of Hydroperoxides

For reactions using cumene, gas chromatographic analysis of the reaction filtrate was used to detect the extent of oxidation of the solvent. The titrimetric method described by Lundberg (20) was used to detect hydroperoxides in the coal after co-oxidation. For this test, 2 g sodium iodide and 25 ml acetic acid were purged 5 minutes with nitrogen. The dried, co-oxidized coal was slurried in the solution for a minimum of 25 minutes and the nitrogen purge was continued. The solution was decanted and immediately titrated potentiometrically with sodium thiosulfate. A blank was run as well as a test using a 1% solution of commercial cumene hydroperoxide.

Oxygen Uptake Analysis

Elemental analysis of co-oxidized coal was carried out. This data is included in Table I. Infrared analysis was carried out on selected samples of co-oxidized coal. A 1% by weight KBr sample was prepared. A Nicolet 10-MX FT-IR was used to obtain the spectra.

Hydroperoxide Decomposition

The decomposition, via C-C bond scission, of hydroperoxides is critical to the success of this process. Although hydroperoxides are generally thermally unstable and can be decomposed by heat, several methods were tested using co-oxidized coal. These are shown in Table III.

Determination of Depolymerization

Soxhlet extraction in refluxing N,N-dimethylformamide (DMF) was used to determine whether co-oxidation had increased the extractability of the coal. Duplicate samples (~5g) were weighed into pre-dried and pre-weighed cellulose extraction thimbles. Extraction with DMF was carried out for 24 hours. The DMF was replaced by methanol which was used to rinse the coal for a minimum of 6 hours. The thimbles and residue were dried in vacuo at 150°C. The weight loss was used to calculate the weight percent extracted. Extraction values reported here are relative to the extractability of the raw coal.

Table I

Analyses of Coals before and after Co-oxidation (Selected Trials)

Coal (Trial)	M**	VM	Ash	C	H	N	S	O**
9100	7.09	40.6	8.36	74.08	5.11	1.50	3.59	7.34
(1-40 ^a)	1.67	37.01	7.68	73.72	5.05	1.68	2.93	8.94
9036	5.33	46.8	6.44	76.48	5.37	1.60	3.29	6.79
(253 ^b)	0.87	36.59	5.71	75.38	5.09	2.08	2.71	9.03
7827	2.84	35.88	9.49	74.49	5.22	1.53	3.33	5.94
(66 ^c)	2.01	36.64	9.28	75.20	5.24	1.50	3.10	5.68
(A-1 ^d)	0.45	37.06	9.32	73.59	5.00	1.58	3.19	7.32
(A-2 ^e)	1.08	35.86	9.51	73.10	4.98	1.56	3.01	7.84

** Moisture, as determined; Oxygen by difference; other values on dry basis

^a 2 hr., 1 atm., 90°C, 10:1 (v/w) Cumene:Coal

^b 15 hr., 1 atm., 115°C, 10:1 (v/w) Cumene:Coal + 0.1M Co(ac)₂ and 0.1 M HBr

^c 0.5 hr., 20 psig. O₂, 165°C, 15:1 (v/w) Cumene:Coal

^d 3 hr., 1 atm., 90°C, 15:1 (v/w) Cumene:Coal

^e 2 hr., 20 psig. O₂, 115°C, 2:1 (v/w) Cumene:Coal, + 0.1M Co(ac)₂ and 0.1M HBr

Table II

Solvent Screening^a

Solvent	Change in Extractibility, % ^b
Cumene	+ 7
Benzonitrile	-18
o-dichlorobenzene	-16
Diphenylmethane	- 4
Fluorene	0 ^c , -2 ^d , -10 ^e
Tetralin	+ 1
Diphenylether	- 2

^a Oxidation: 2 hr., 100°C, 1 atm., 10:1 (v/w) Cumene:Coal

^b 24 hour Soxhlet extraction, 6 hr. MeOH rinse, 150°C vac. dry;

% = Wt. sample - Wt. resid./Wt. sample x 100. Value shown is relative to the extraction of unoxidized coal.

^c 20% (w/v) in Cumene

^d 20% (w/v) in o-dichlorobenzene

^e 20% (w/v) in benzonitrile

Results

Table II through Table VI summarize the results of approximately 200 reaction trials. Each piece of data was determined by multiple trials. Table II shows that cumene was the most effective solvent tested. Benzonitrile, o-dichlorobenzene and diphenylether were tested because of their relatively higher boiling point. They were not expected to participate in co-oxidation.

Table IV shows the effect of temperature and the effect of pressure above atmospheric (1 atm - 0.101 MPa - 14.696 psig). No enhanced solubility is indicated by the data at a temperature above 100°C or above atmospheric pressure of air (or oxygen).

Table III

Effect of Post-Treatment on Extraction of Co-oxidized Coal^a

<u>Treatment</u>	<u>Change in Extractability, %^b</u>
Thermolysis at 260°C 10 min.	-18 to +5
Sat'd aq. KI in HOAc/CHCl ₃ 25°C	
2 - 15 hrs.	-2 to 0
60°C	
2% H ₂ SO ₄ in acetone; 60°C, 2 hr.	+4
N ₂ H ₄ neat or 10% in O-Cl ₂ Benzene 25°C	
2 - 24 hrs.	+4
60°C	

^aOxidation: 2 hr. at 100°C, 1 atm. O₂, 10:1 (v/w) Cumene:Coal^b24 hour Soxhlet extraction, 6 hr. MeOH rinse, 150°C vac dry;

% = Wt. sample-Wt. resid./Wt. sample x 100. Value shown is relative to the extraction of unoxidized coal.

Table V summarizes the results of trials using various combinations of mixed solvents tested. Dimethylformamide drastically inhibited the oxidation of cumene itself, and has been reported to undergo free radical addition reactions (21). Of the other solvent systems, acetic acid in dioxane showed the most promise. Overall, however, there was little evidence that this type of reaction medium could overcome the barrier being consistently encountered.

The data in Table VI show that the extractability of the coal has been enhanced by the co-oxidation reactions which were carried out in the presence of aqueous or alcoholic base in addition to cumene. Subsequent trials showed, however, that the action of the alkaline medium alone, even in a nitrogen atmosphere, also led to an observed increase in the solubility of the treated coal.

Table IV

Effect of Temperature, Pressure, and Time on Co-oxidation of Coal^a

<u>Trial</u>	<u>Temp. °C</u>	<u>O₂ Press. atm</u>	<u>time. hrs.</u>	<u>% Extracted^b</u>
22	100	1	2	-2
23	130	1	2	0
41	130	6.8	1	+8
65	168	2.7	0.5	-6
69	185	1.7	1.0	-7
71	130	3.4	0.5	-6
72	85	1	0.5	-7
73	31	2.9	0.5	-4
75	69	2.6	0.5	-5
113	85	1	6.5	+1
78	160	1	0.75	-8

^a1:10 w/v coal:cumene and appropriate initiator.^bRelative to extractability of raw coal into DMF.

Table V

Effect of using Mixed Solvents on the Extraction of Co-oxidized Coal

Solvent System Change in Extractability, %
 --- 85°C, 1 atm., 20:1 (v/w) Solvent: Coal ---

25% DMF in Cumene
 2.25 hr. -10
 22 hr. + 7
 26 hr. + 2

11% DMF in Cumene
 21 hr. - 3
 27 hr. + 5

--- 75°C, 2.25 hr., 1 atm., 20:1 (v/w) Solvent:Coal ---

Dioxane - 6
 4:1 (v/v) Dioxane:4-picoline -12
 15:4:1 (v/v) Dioxane:Picoline:CS₂ -18
 4:1 (v/v) Dioxane:ethylenediamine -14
 4:1 (v/v) Dioxane:acetic acid - 2

^a24 hour Soxhlet extraction, 6 hr. MeOH rinse, 150°C
 vac. dry; % = Wt. sample-Wt. resid./Wt. sample x 100.
 Value shown is relative to the extraction of unoxidized
 coal.

Table VI

Effect of Base on the Co-oxidation of Coal^a

Trial	Base ^b	Temp, °C	O ₂ Press, atm	Time, hrs	% Ext ^d ^c
45	pH 10 Na ₂ CO ₃	100	1	1.5	+13
46	pH 10 Na ₂ CO ₃	100	1	3	+ 4
52	pH 10 Buffer	100	1	1	+18
81	pH 10 Buffer	160	1.5	0.75	-10
84	pH 10 Buffer	160	1	0.75	- 9
91	10% KOH in t-butyl alcohol	130	1.5	0.75	- 9
94	10% KOH in t-butyl alcohol	85	1	3	+ 6
95	10% KOH in t-butyl alcohol	85	1	1	+10
85	pH 10 Buffered	100	1	1	- 6
96	10% KOH in t-butyl alcohol ^d	85	1	1	+13
121	10% KOH in t-butyl alcohol ^d	85	1	1	+17
107	10% KOH in t-butyl alcohol ^e	85	1	1	+ 7

^a1:10 w/v coal:cumene, appropriate initiator.

^b2:1 base:solvent.

^cRelative to extractability of raw coal into DMF.

^dNo cumene present.

^eNo cumene or O₂ present. (N₂)

Table III shows that no appreciable quantity of hydroperoxide was detected in co-oxidized coal or solvent, and also shows that thermolysis of co-oxidized coal at 260°C did not exhibit a positive effect on the subsequent extraction of the coal.

Infrared analysis of several samples of co-oxidized coal showed absorbance at about 1670 cm^{-1} which is characteristic of carbonyl signals. This was not observed in IR spectra of unoxidized coal.

Discussion

Co-oxidation. In a two hour period, cumene alone, is oxidized approximately 50%. In the presence of coal, the oxidation of cumene is reduced by one half. Along with the data showing oxygen uptake by the coal (Table I), this indicates that coal oxidation is occurring under these relatively mild conditions. Extraction values, however, were not enhanced, and post-oxidative treatment designed specifically to promote C-C bond cleavage associated with hydroperoxide decomposition were depressingly unsuccessful. Use of swelling solvents, or temperatures and pressures considered 'elevated' in this regard were not effective. Not only is it likely that DMF added to the coal matrix (21), temperatures at or above the boiling point of solvents certainly diminish oxygen solubility, and high pressure may have actually promoted further oxidative crosslinking (4,7). Failure to detect hydroperoxides in the co-oxidized coal does not prove their absence. Penetration by iodide into the pore system may in fact have been minimal. Similarly acid-catalyzed decomposition of hydroperoxides using 2% H_2SO_4 in acetone (18) at 60°C for 1 hour may have been ineffective for the same reason.

It is known that phenolic species are present in coal (22), and phenol is an oxidation product of cumene. Effective inhibition of the free radical reaction may have occurred in the absence of any reagent to neutralize phenolics. The enhanced extraction observed when co-oxidation was carried out in a cumene/KOH (aqueous or isopropyl alcohol) slurry lends support to this notion. However, base alone in the absence of an oxidant is also known to solubilize coal, perhaps by ether or ester hydrolysis (23-25). If keto groups are being formed, as the preliminary IR suggest, some enhanced extraction can be accounted for after alkaline hydrolysis. It is not clear, however, that carbonyl formation should occur in preference to hydroperoxide formation.

Conclusions

At this stage, co-oxidation does not seem to be an effective means of achieving bond cleavage in coal. Three critical features of the process have not been thoroughly investigated, however, and are the object of our on-going research. First, only high rank coals were tested. It is likely that subbituminous or lignitic coals will be more susceptible to co-oxidation and hydroperoxide formation.

Hydroperoxide formation in coal is a relatively facile process. Thermal decomposition of hydroperoxides is also believed to occur at temperature as low as 70°C (26). If this is so, co-oxidation at lower temperatures (~70°C) may be necessary to prevent spontaneous decomposition of hydroperoxides. More important in this regard, is the fact that in this investigation, the co-oxidized coal was always dried at 150°C, and thermolysis was attempted at 250-260°C. Cleavage of hydroperoxides in an inert atmosphere at these temperatures may have indeed cleaved hydroperoxides, but also may have generated free radical species which combined to form more crosslinks in the coal. Not only may thermolysis be achieved at much lower temperatures, the presence of a suitable 'donor' medium, such as cumene or hydrogen, may result in effective depolymerization.

21. G. P. Gardini, F. Minisci and G. Pollo, *Tet. Let.*, No. 1, 59, 1971.
22. W. G. Lloyd, *Chemtech*, 2, 182 (1972); F. R. Mayo, J. G. Huntington and N. A. Kirshen in "Organic Chemistry of Coal," J. W. Larsen, Ed., American Chemical Society, Washington, D. C., 1978, p. 126.
23. D. S. Ross and J. E. Blessing in Coal Liquefaction Fundamentals," D. D. Whitehurst, T. O. Mitchell and M. Faracasius, Eds., Academic Press, New York, 1980, p. 306.
24. J. G. Speight, *op. cit.*, p. 235.
25. R. M. Davidson in "Coal Science," Vol. 1, M. L. Corbaty, J. W. Larsen, and I. Wender, Eds., Academic Press, New York, 1982, p. 95.
26. R. E. Jones and D. T. A. Townend, *J. S. C. I.*, 68, 197 (1949).

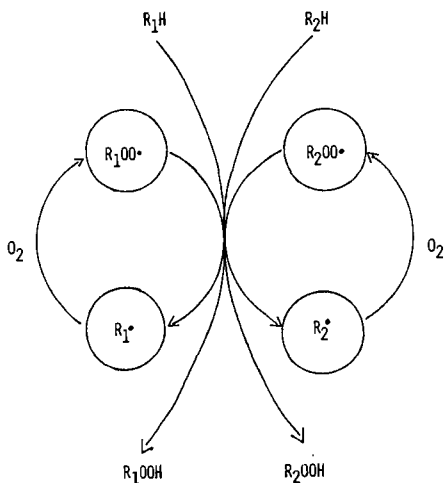


FIGURE 1. AUTOXIDATION OF MIXED SUBSTRATES (17).

Acknowledgement

This work was supported by the Electric Power Research Institute, Palo Alto, CA under Contract No. RP 2383-2.

References

1. D. J. Schlyer and A. P. Wolf in "New Approaches in Coal Chemistry," B. D. Blaustein, B. C. Bockrath and S. Friedman, Eds., American Chemical Society, Washington, D. C., 1981, p. 93.
2. J. G. Speight, "The Chemistry and Technology of Coal," Marcel Dekker, New York, 1983, pp. 215-221.
3. J. Solash, R. N. Hazlett, J. C. Bennett, P. A. Climenson, and J. R. Levine, Fuel, **59**, 667 (1980).
4. J. G. Huntington, F. R. Mayo and N. A. Kirshen, Fuel, **58**, 24 (1979).
5. F. R. Mayo and N. A. Kirshen, Fuel, **58**, 698 (1979).
6. R. Hayatsu, R. E. Winans, R. G. Scott, L. P. Moore, and M. H. Studier in "Organic Chemistry of Coal," J. W. Larsen, Ed., American Chemical Society, Washington, D. C., 1978, p. 108.
7. D. C. Cronauer, R. G. Ruberto, R. S. Silver, R. G. Jenkins, I.M.K. Ismail, and D. Schlyer, Fuel, **62**, 1116 (1983).
8. W. H. Wiser in "Scientific Problems of Coal Utilization," Technical Information Center, U.S.D.O.E. Symposium Series 46, CONF 770509, 1978, pp. 219-236.
9. R. C. Neavel, Fuel, **55**, 237 (1976).
10. R. Tschamler, E. deRutter in "Chemistry of Coal Utilization," Supp. vol., H. H. Lowry, Ed., John Wiley and Sons, Inc., New York, 1963, pp. 78-85.
11. L. Petrakis, D. W. Grandy, and G. L. Jones, Chemtech, **14**, 52 (1984).
12. L. Petrakis and D. W. Grandy, Fuel, **59**, 227 (1980).
13. L. Petrakis, D. W. Grandy, and G. L. Jones, Fuel, **62**, 665 (1983).
14. M. Poutsma and C. Dyer, J. Org. Chem., **47**, 4903 (1982).
15. K. E. Gilbert and J. J. Gajewski, J. Org. Chem., **47**, 4899 (1982).
16. K. E. Gilbert, J. Org. Chem., **49**, 6 (1984).
17. "Methods in Free Radical Chemistry," Vol. 4, Earl S. Huyser, ed., Marcel Dekker, New York, 1973, p. 26.
18. K. Weissermiel and H. J. Arpe, "Industrial Organic Chemistry," Verlag Chemie, Weinheim, Germany, 1978, pp. 309-310.
19. E. S. Huyser, Ed., "Methods in Free Radical Chemistry," Vol. 4, Marcel Dekker, New York, 1973, pp. 15, 26.
20. "Autoxidation and Autoxidants," Vol. 1, W. O. Lundberg, ed., Interscience Publs., New York, 1961, pp. 370-373.

DONOR SOLVENT CHEMISTRY IN LIGNITE LIQUEFACTION

by

J. Y. Low

PHILLIPS PETROLEUM COMPANY
PHILLIPS RESEARCH & DEVELOPMENT CENTER
BARTLESVILLE, OK 74004

INTRODUCTION

Coal liquefaction by donor solvent processes (DSP) has been studied over the years by many people throughout the world.⁽¹⁻⁶⁾ However, lignite liquefaction by DSP was less intensively studied. We were interested in determining how the properties of donor solvents related to lignite liquefaction, particularly with lignites and under low pressure liquefaction conditions.

Our approach was to synthesize a series of donor solvents with different properties by catalytically hydrotreating anthracene oil under various conditions. These solvents were tested for lignite liquefaction under a standard set of conditions. The liquefaction conditions we used were similar to those used by the National Coal Board in their Liquid Solvent Extraction (LSE) process.^(7,8) The criteria used for determining the effectiveness of the donor solvents were lignite conversion and filtrate to filter cake ratio. We have tried to correlate these two criteria with the properties of the donor solvent. These properties include total hydrogen content, aromatic content, donatable hydrogen, and molecular weight of the solvent.

We also have studied the effects of other reaction parameters, such as solvent to lignite ratio and the difference between the nominal and real solvent to lignite ratio.

EXPERIMENTAL

A. Chemicals

Anthracene oil was purchased from Crowley Chemical Co. The pure grade tetralin was commercially available from Fischer Scientific. The two lignites used in these experiments were from the Gulf Coast, and their properties are given in Table 1.

B. Apparatus

The reactors used for the solvent/coal ratio studies are better known as "Tubing Bomb" reactors. They were made of 316 stainless steel tubing (3/4" OD, 0.63" ID, 5" long). Both ends were closed with Swagelok caps. A tee was welded at the center of the reactor to accommodate the gas charge port, valve, and pressure transducer. The design is shown in Figure 1. The reactor volume is roughly 23 ml (and has a maximum working pressure of 4400 psig at 538°C).

The reactor used for the solvent quality studies was a 1-liter Magnedrive autoclave from Autoclave Engineers, Inc.

The hydrotreating unit for preparing anthracene oil donor solvents is a continuous feed unit. It has a 300 cc trickle bed reactor. The reactor is filled first with 100 cc of inerts (ceramic beads), then 100 cc 1/16" extrudates Ni-Mo/Al₂O₃ catalyst from United Catalysts, and finally the remaining 100 cc with inerts again. The arrangement is shown in Figure 2.

C. Experimental Procedure

Experiments for solvent quality studies were carried out with a 1-liter autoclave. For the solvent to lignite ratio studies, the tubing bomb reactors were used.

For a typical solvent quality study experiment, 300 g of hydrotreated anthracene oil and 200 g of lignite A (dried, 40 mesh-) were placed in the reactor. The reactor was pressure tested for leaks at 1000 psig with nitrogen. The nitrogen gas was released to atmospheric pressure before starting the heating.

While stirring at 1000 rpm, the reactor was heated slowly (about 90 minutes) to 400°C and was kept at this temperature for one hour. The maximum pressure for these runs was about 600-800 psig. After reaction, the reactor was cooled quickly with cold water (the reactor is equipped with an internal cooling coil). The reaction mixture (liquid and solid) was transferred and filtered through a 15 cm diameter Whitman #4 paper filter. The filter funnel was heated with steam during filtration. The filtration was stopped when there was no obvious liquid left in the filter funnel. The filter cake was then mixed with 300 ml of quinoline. The mixture was stirred for 30 minutes and then filtered as above, except no steam was used. The filter cake was washed with 100 ml of quinoline and then it (the quinoline insolubles) was dried overnight in a vacuum oven at 110°C. The quinoline conversion was calculated as shown below:

$$\text{Quinoline Conversion \%} = 100\% - \% \text{ quinoline insoluble (ash free)}$$

The quinoline conversion includes the gas yield.

For the solvent ratio studies, 2 grams of dried 40 mesh-lignite B was placed in the tubing bomb along with the appropriate amount of tetralin (2, 4, 6, or 8 grams). For the reactor loading studies, the solvent to lignite ratio was constant at 2, but the total amount of the mixture varied (5.5, 6.6, 8.8, and 12.1 grams).

For each test, the experiment was duplicated. The results reported are averaged values. For a typical run with tubing bomb reactors, 4 reactors were secured on a rack which was then lowered into the preheated (410°C) fluidized sand bath. After shaking the reactor at 180 rpm for one hour, the reactors were lifted from the sand bath and quickly quenched with cold water. The reactors were then depressurized. The gas mixture was not analyzed. The reaction mixture (liquid and solid) was diluted with 50 ml of cyclohexane and stirred for 30 minutes. The mixture was then filtered with a medium

fritted glass funnel. The filter cake was washed with 20 ml of cyclohexane and then was dried overnight in a vacuum oven at 110°C. The cyclohexane insoluble filter cake was used to calculate the cyclohexane conversion, as was done for the quinoline conversion.

For tetrahydrofuran (THF) conversions, the cyclohexane insoluble was further mixed with 50 ml of tetrahydrofuran, stirred, filtered, washed, and dried in the same manner as described above. The THF conversions were calculated similarly. Again, all these conversions (quinoline, cyclohexane, and THF) include the gas yields.

The donatable and aromatic hydrogens were measured by proton NMR.

RESULTS AND DISCUSSION

A total of 15 donor solvents were synthesized by catalytic hydrotreating of anthracene oil at various conditions. Their properties are listed in Table 2. These solvents were tested as lignite liquefaction solvents under low pressure with no added molecular hydrogen during liquefaction. The reaction pressure varied from 600-800 psig because of the difference in vapor pressure of the solvents at reaction temperature. The unhydrotreated (raw) anthracene oil was also used for comparison purposes. We analyzed our results in relation to the individual properties of the solvent, such as total hydrogen content, aromatic hydrogen content, donatable hydrogen, and average molecular weight. In reality, probably each of the above properties contributes to a different degree in each solvent. This may explain some of the scatter in the data. The results and discussions will be grouped under the solvent properties mentioned above. We will also discuss the difference between the real and nominal solvent to lignite ratio effect in lignite liquefaction.

A. Effect of Total Hydrogen Content

We tried to correlate the total hydrogen content of the sixteen solvents (15 prepared from hydrotreating anthracene oil and one from the raw anthracene oil) with the lignite liquefaction conversions (quinoline conversions). The results are shown in Figure 3. The lowest conversion (71%) is associated with lowest total hydrogen content of 6.5%. As the total hydrogen is increased slightly to 7.22%, the conversion improves significantly from 71 to 89%. With further increases in total hydrogen content, the conversion only increases slightly and levels off at about 98%, when the total hydrogen content is about 8-9%. When the total hydrogen is again increased further to the neighborhood of 10%, the conversions decrease to the low 90's. The optimum total hydrogen seems to be in the area of 8 to 9%.

B. Effect of Aromatic Hydrogen

The lignite liquefaction conversion (quinoline) is plotted versus the aromatic hydrogen content (Figure 4). The effect of aromatic hydrogen on lignite liquefaction conversion is very similar to that of total hydrogen content. The low conversions are found on the two extreme ends of the aromatic hydrogen content scale. For example, the low conversions of 71 and 91% are found with the highest

aromatic hydrogen content of 4.6% and the lowest aromatic content of 1.85%, respectively. The maximum conversion is located in the middle of the aromatic hydrogen content scale (about 3%). In other words, a good process solvent shouldn't be either too saturated or too aromatic.

C. Effect of Donatable Hydrogen

The general definition of donatable hydrogen is that hydrogen of any molecule that can be donated to the coal molecules or radicals during liquefaction reactions. We have tried to find quantitatively how much of this type of hydrogen in the solvent is necessary for high conversion. We tried to determine the value of potentially donatable hydrogen (hydrogen α to the aromatic ring) by proton NMR. The values are expressed in terms of absolute weight percent of the hydrogen in the solvent that are potentially donatable. These reported values may not be the same amount of actual donatable hydrogen that is required or consumed during liquefaction reactions. The donatable hydrogen from our solvents ranges from 1.43 to 2.76 wt %. These values are plotted against their corresponding conversion values (Figure 5). The raw anthracene oil has a very small amount of donatable hydrogen (1.43 wt %) and, as expected, gives a correspondingly low conversion value of 71%. Overall, the conversion values seem to increase with the increase in the amount of donatable hydrogen. There is no maximum point found in this curve as was found with the other two (total and aromatic hydrogen curves, Figures 3 and 4). In other words, over the range studied there is no limit; the more, the better.

D. Effect of Total Hydrogen on Filtrate Yield

A liquefaction process may include filtration as a solid/liquid separation step. We were interested to see if the solvent properties that enhance high conversion also enhance high yield of filtrate. It is possible that a good donor solvent may not be a good solvent for dissolving liquefied lignite products. High yield of filtrate may be just as important as high quinoline or cyclohexane conversions, because in a commercial process the use of an extraction solvent, such as quinoline, would be prohibitively expensive.

The reaction mixture, after having cooled to ambient temperature, was filtered. The weight ratio of the filtrate to the filter cake is plotted against the total hydrogen content of the solvent (Figure 6). This plot produces a curve which is similar to that of conversion vs total hydrogen. The maximum occurs at 8 to 9% of total hydrogen content. The maximum quinoline conversions also occur in this region. This suggests that the best donor solvent produces the highest conversion and also produces the highest filtrate to filter cake weight ratio, or the highest liquid product yield.

E. Effect of Molecular Weight

The average molecular weight of the 16 solvents studied ranges from 160 to 260. The conversion data are somewhat scattered (Table 2). However, the solvents that have high conversions (97%+) seem to have a higher molecular weight (200+). On the other hand, the

solvents with low conversion seem to associate with lower molecular weights. The reason for this will be explained in our solvent to lignite ratio studies.

F. Effect of Solvent to Lignite Ratio

For the study of solvent to coal ratio effect, we used THF and cyclohexane conversions. For example, THF conversion is the yield of gases and THF soluble lignite products. The results are illustrated in Figures 7 and 8. The data suggest that there is a difference between nominal and real solvent to lignite ratio. The nominal ratio is defined as the weight of the solvent divided by the weight of lignite charged to the reactor. The real ratio is defined as the calculated weight of the solvent in the liquid state at reaction temperature divided by the weight of the lignite charged into the reactor. The real ratio is considerably smaller than the nominal ratio because a considerable amount of the solvent is vaporized at reaction temperature of 410°C.

The conversion results (cyclohexane) are plotted against the nominal weight ratio (open triangle) and real weight ratio (filled squares). The difference is that the conversion won't start leveling off until after 3/1 for the nominal and 1.5/1 for the real ratio. Thus, for the higher molecular weight solvent, less starting solvent is needed for the equivalent conversion.

The experiment with nominal solvent to lignite ratio of 2/1 was repeated with 1000 psig of hydrogen in one run and nitrogen in the other. The conversion (cyclohexane) is increased from 33% (nominal ratio) to 62%, and there is no difference in conversion found between the run with hydrogen and nitrogen. This suggests that the difference in conversion is due to the pressure effect. That is, the presence of the high pressure of hydrogen or nitrogen suppresses the vaporization of the solvent. Thus, it is the liquid solvent that is important for promoting high conversion.

The fact that the solvent has to be in a liquid state for optimum conversion is again demonstrated in another set of experiments. In this series of experiments, the solvent to lignite ratio is held constant at 2. The percent of the reactor volume being filled with the solvent and lignite mixture varied from 25, 30, 40, and 55 volume %. The conversions, both cyclohexane and THF, are plotted against the volume % of reactor filled with slurry as shown in Figure 8. The conversion results show that the conversion increases dramatically with the increase in the reactor volume usage of 30 to 40%. From 40 to 50% only a slight increase is found. This means the difference between nominal and real solvent (tetralin) to lignite ratio is small once the reactor is more than 40% full.

To sum up, from our solvent property studies, the ideal solvent should not be too aromatic or too saturated. The presence of an aromatic group and saturated group in the same solvent molecule (such as hydroaromatics) is necessary to provide a source of donatable hydrogen. For our particular solvent system (derived from anthracene oil), the optimum solvent should have about 3% aromatic hydrogen, a total hydrogen content of 8 to 9%, some donatable hydrogen (2.5%), and

a high boiling range. From our solvent ratio studies, a solvent in a liquid phase is important for promoting high liquefaction conversion, and the solvent to lignite ratio should be in the neighborhood of 2 for high conversion.

CONCLUSIONS

The results from solvent property correlation studies suggest that the optimum lignite liquefaction solvent should have the following characteristics:

1. Some aromatic groups (3% aromatic hydrogen content),
2. Total hydrogen content of 8-9%,
3. Some donatable hydrogen (2.5%),
4. And a high boiling point range (preferably 500-1000°F).

The results from solvent to lignite ratio studies have suggested that only the solvent in the liquid phase is important for promoting high conversion in these high temperature reactions. The optimum solvent to lignite ratio is in the neighborhood of 2. These requirements for high liquefaction conversion are probably more demanding for our system than any other processes because all the required hydrogen for stabilizing the lignite liquefaction products come from the starting solvent. We don't add molecular hydrogen to our system; thus, hydrogen shuttling through the solvent system is insignificant.

References

1. Curran, G. P., Struck, R. T., and Gorin, E., Am. Chem. Soc. Div. Petrol. Chem. Preprints 10 (2) C-130-148, (1966).
2. Whitehurst, D. D., Mitchell, T. O., and Farcasiu, M., "Coal Liquefaction", Academic Press, New York, 1980, p. 274.
3. Masato, Aiura, Fuel 63, 1138 (1984).
4. Neavel, R. C., Fuel 55, 237 (1976).
5. Ruberts, R. G., Cronaur, D. C., Jewell, D. M. and Shesadri, K. S., Fuel 56, 25 (1977).
6. Maa, P. S., Trachte, K. L., and Williams, R. D., 1981, Annual Meeting of the Am. Chem. Soc., Aug., New York, NY.
7. Kimber, G. M., 13th Biennial Conference on Carbon, August 1977, Irvine, California.
8. Clark, J. W. and Rantell, T. D., Fuel 59, 35 (1980).

Table 1
Lignite Characteristics

	<u>Gulf Coast Lignite</u>	
	<u>A</u>	<u>B</u>
Moisture (%) Ash Received	31.69	22.4
Proximate, %, Dry Basis		
Ash	15.77	11.5
Volatiles	54.69	45.
Fixed Carbon	29.54	44.
Ultimate, %, Dry Basis		
Carbon	59.21	64.3
Hydrogen	5.53	4.5
Nitrogen	0.55	1.2
Sulfur	2.91	1.2
Ash	15.77	11.5
Oxygen	16.03	17.4
H/C	1.12	0.84
Btu/lb, Dry Basis (calc.)	10988	10964

Table 2
Donor Solvent Characteristics

<u>Solvent</u> <u>No.</u>	<u>Solvent Characteristics¹</u>				<u>Conversions (%)²</u>
	<u>H_t(%)</u>	<u>H_a(%)</u>	<u>H_d(%)</u>	<u>Mwt</u>	
1*	6.5	4.6	1.43	173	71
2	7.22	4.08	1.92	174	89
3	10.26	1.85	2.05	157	91
4	7.13	2.85	2.35	157	92
5	9.84	2.36	2.46	169	92
6	9.9	2.28	2.38	166	93
7	7.84	2.63	2.43	181	94
8	9.99	2.20	2.20	164	94
9	9.95	2.19	2.49	168	95
10	9.9	2.19	2.39	166	95
11	8.19	2.67	2.46	169	96
12	10.08	2.12	2.32	166	96
13	9.05	2.79	2.43	196	97
14	8.35	2.72	2.34	252	98
15	8.11	3.08	2.43	204	98
16	8.93	2.98	2.76	260	98

¹H_t, total hydrogen content; H_a, aromatic hydrogen; H_d, donatable hydrogen determined by proton NMR.

²Conversion is the sum of gas yield and quinoline soluble, on maf basis.

*Raw anthracene oil.

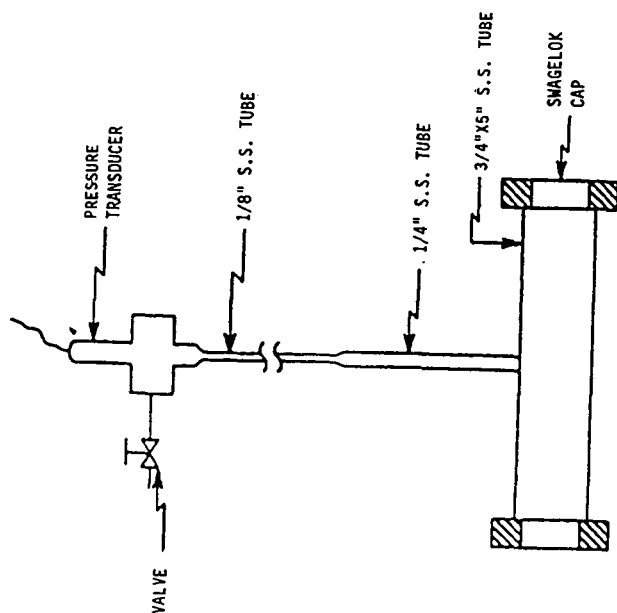


FIGURE 1
TUBING BOMB REACTOR

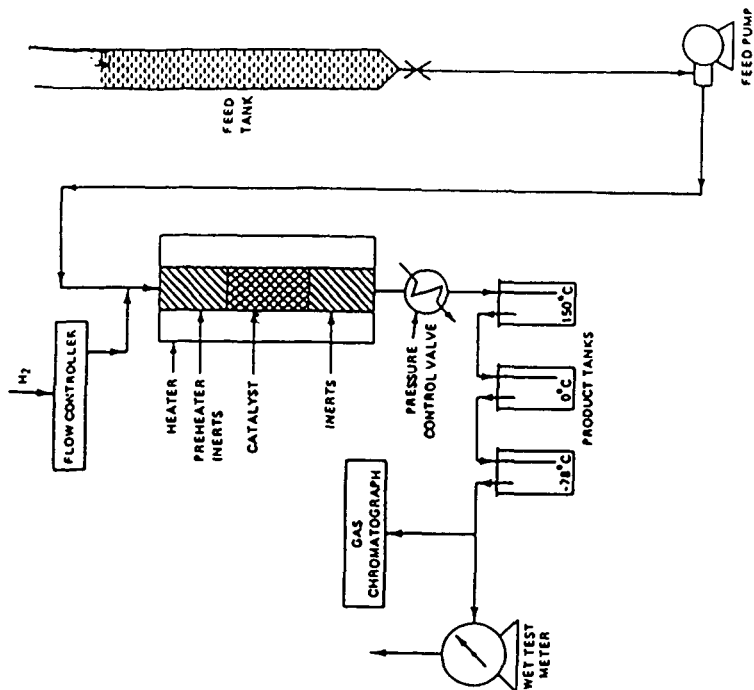


Figure 2
SUPERCritical AL HYDROTREATING SYSTEM

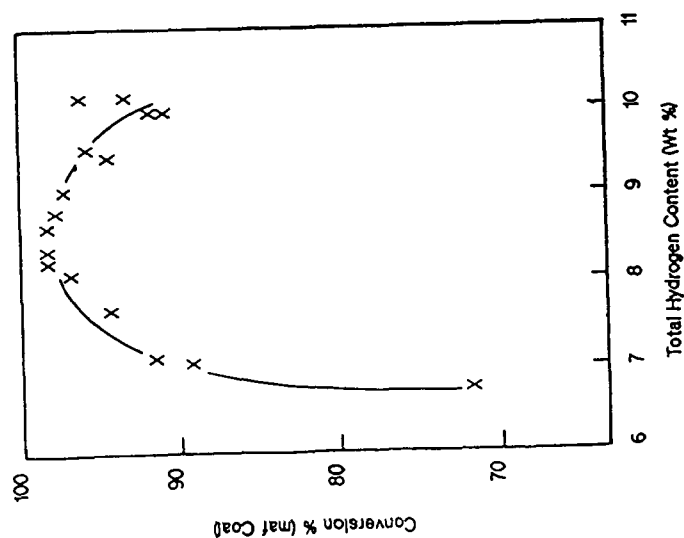


FIGURE 3. EFFECT OF TOTAL HYDROGEN ON CONVERSION

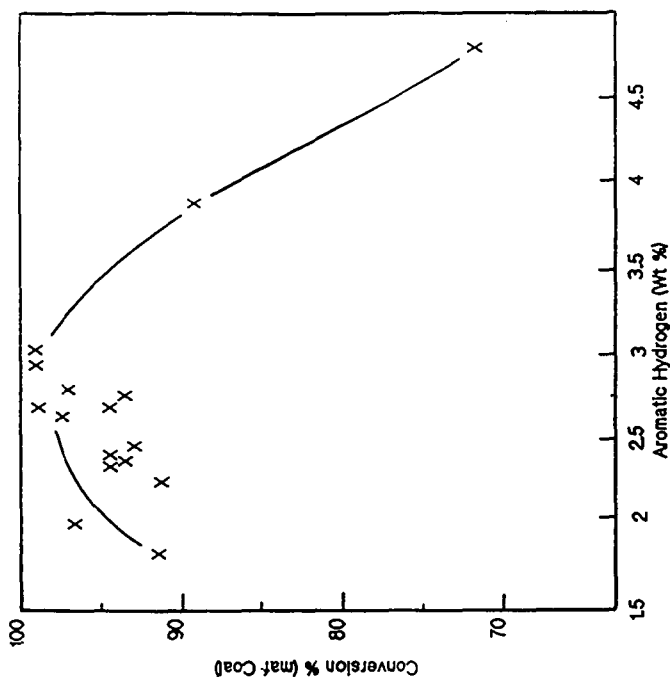


FIGURE 4. EFFECT OF AROMATIC HYDROGEN ON CONVERSION

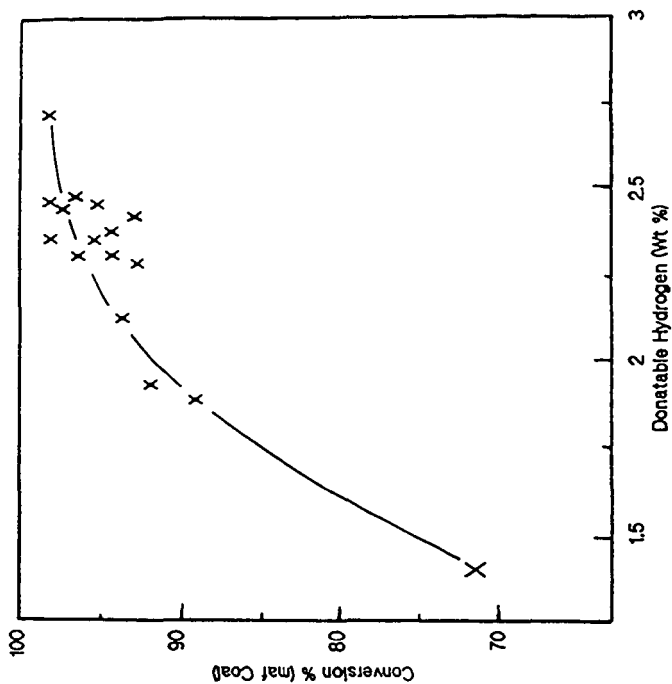


FIGURE 5. EFFECT OF DONATABLE HYDROGEN ON CONVERSION

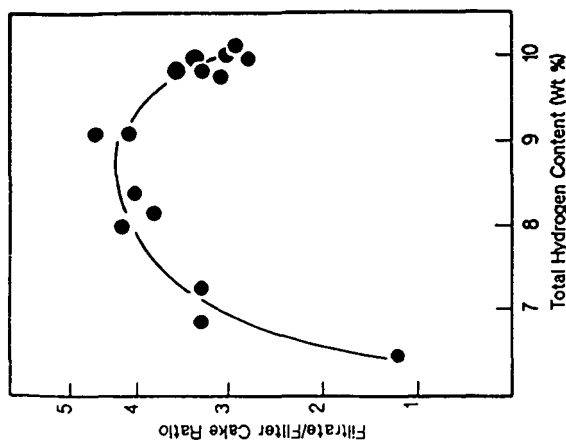


FIGURE 6. EFFECT OF TOTAL HYDROGEN ON FILTRATE YIELD

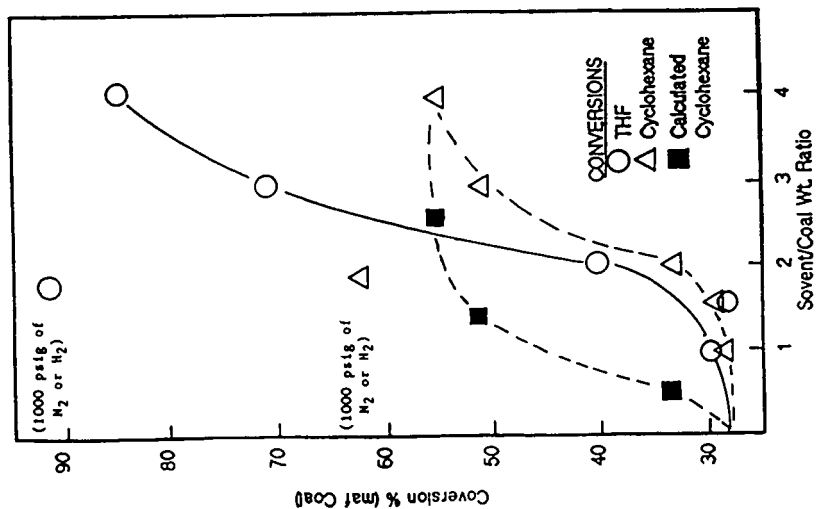


FIGURE 7. SOLVENT TO COAL RATIO EFFECT
(2 g Ugnite B, Tetralin, 410 C, 1 hour)

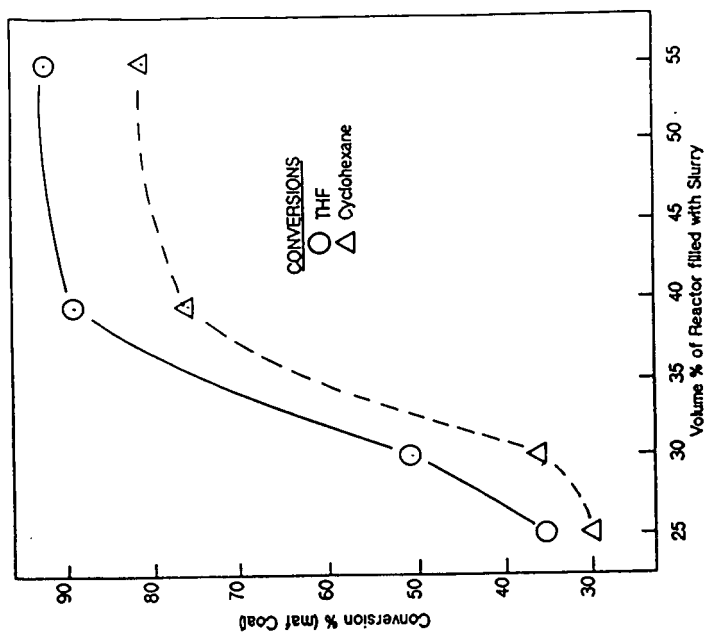


FIGURE 8. REACTOR LOADING EFFECT
(Ugnite B, 410 C, S/C = 2, 1 hour)

COAL LIQUEFACTION IN AMINE SYSTEMS

F. Kazimi, W.Y. Chen, J.K. Chen, R.R. Whitney and B. Zimny

Gulf South Research Institute, P. O. Box 26518, New Orleans, LA 70186

I. INTRODUCTION

In developing a third generation coal liquefaction technology, reaction severity, a critical cost factor, must be minimized to make the process economically competitive with petroleum refining. Accordingly there is an incentive for the development of lower severity processes which could significantly reduce conversion costs.

The novelty of the process we are developing arises from both the liquefaction solvent selection and the design of liquefaction conditions. Low molecular weight nitrogen compounds were selected for liquefaction solvents in accordance with recent attention on the high dissolution power of nitrogen heterocycles in coal liquefaction. An excellent review of the role of these nucleophilic solvents was reported by Atherton and Kulik at the AIChE Annual Meeting in 1982. In a separate approach, supercritical fluid technology was also applied to coal liquefaction to enhance solubility of coal-derived products, minimize mass transfer limitation and, therefore, reduce process severity (Williams, 1981). The low molecular weight solvents chosen for use in the present study allowed liquefaction to be performed at supercritical solvent conditions while maintaining operating temperatures well below the most commonly used liquefaction temperature (400°C). These design criteria were applied to achieve high conversion at mild conditions.

In our first year of the study, complete dissolution of two low rank coals in amine was achieved at temperatures below 300°C (Chen and Kazimi, 1984). This level of conversion in a single stage operation at such mild conditions is strikingly higher than any other reported organic dissolution of coal at equivalent temperatures. In this paper, we report our continuing efforts to develop a coal liquefaction process using amines. The effects of processing variables, solvent property and coal rank on coal conversion have been examined. Further, the product quality, solvent removal from products and chemical recovery of the solvent are discussed.

II. EXPERIMENTAL

A. Liquefaction

Three different systems were used for liquefaction of the coal samples. The slow heating tubing bomb system was described in an earlier paper (Chen and Kazimi, 1984). The Parr bomb, used for chemical conversion of incorporated solvent, is described in the next section. A second tubing bomb system which provides rapid heating, and therefore isothermal kinetic study, is shown in Figure 1. Approximately 1 g of coal sample was placed in the upper end of the vertical part of the 3/8 in. O.D. stainless steel tube. The sample was held in place by a plug of loosely packed glass wool. Glass wool was also placed in the side unions of the reactor and held in place by 200 mesh stainless steel screen on either side of the union (Fig. 1). The reactor was pressure tested with helium gas for possible leaks and then evacuated for ten min. A heating tape was tightly wrapped around the entire horizontal section of the reactor. Three thermocouples were placed at three different locations to monitor the temperature uniformity of the reactor. Convective heat loss was minimized by wrapping an insulating tape on top of the heating tape. A second heating tape was then wrapped on the top vertical section of the reactor with a thermocouple monitoring the temperature.

The amount of solvent added to give a desired solvent density in the pre-evacuated reactor was measured by a buret connected to the solvent charge line. Solvent density was calculated from the measured volume of the reactor and the density of the solvent at room temperature. After charging the horizontal section

of the reactor with solvent the lower heating tape was turned on. The temperature was allowed to reach approximately 10°C above the desired value. The charge cylinder was evacuated and pressurized with helium gas to a pressure of 1100 psig. The solenoid valve was then pulsed for 1-1.5 s, thus pushing the coal sample into the heated solvent. The temperature controller was then lowered to give the desired steady state reaction temperature, which was usually reached in 1 to 2 min. At the same time, the upper heating tape was turned on to provide the same temperature to the vertical tube.

At a predetermined time heating was stopped, the insulation removed and the system allowed to cool to room temperature (temperature dropped 100°C in 5 min). Solvent and product were discharged into a flask at approximately -10°C. The reactor was then washed with pyridine until the effluent ran clear. To insure that no soluble product remained on any reactor surfaces, the reactor was washed again using the liquefaction solvent. In some cases the pyridine wash was left out. The system was then purged with helium for 10 min and evacuated for five min. The 3/8 in. reactor was disengaged from the system and weighed. The tube was stored in a desiccator containing CaSO_4 or P_2O_5 absorbent.

Weight loss data were obtained from the direct measurement of the residue removed from the reactor. Liquid products were centrifuged, filtered and then rotary evaporated. The distillate and evaporation residue were saved for further analysis.

B. Chemical Conversion of Incorporated Solvent

To provide a large amount of product for the study of chemical conversion of incorporated solvent, a one liter stirred Parr reactor vessel was used. The reactor was loaded with 47.6 g coal, then pressure tested with helium for possible leaks and evacuated. The amine (250 ml) was added by a buret. The Parr vessel was placed in a preheated heating jacket at 290°C for 5 hrs. The liquefaction solution was filtered and the filter cake washed with pyridine until the filtrate was clear. The filtrate was rotary evaporated and the two fractions (distillate and evaporation residue) were saved for further analysis. The distillate was recycled to the filtration unit as the washing solvent, then back to the rotary evaporator. Evaporation and filtration were performed in a closed loop to prevent solvent contact with air. (Amine was found to react with CO_2 , forming undesired products. This was also the reason pyridine was used as washing solvent.) Dried residue in the filtration funnel was weighed to obtain weight loss data. Weight loss data from the tubing bomb and Parr bomb reactors were consistent.

Chemical conversion of incorporated solvent was studied using a 0.75 in. o.d., 9.75 in. long 316 stainless steel batch reactor sealed by two caps. The reactor was loaded with a known amount of the tarry coal-derived product and the stripping solvent in a helium-filled glove box. For steam stripping experiments, 20.38 g of aqueous H_2SO_4 solution at pH 0.39 was added into the reactor with 1.64 g of the tarry liquefaction product. Solution volume was determined to maintain reactor pressure below 1500 psi at reaction temperature. The weight of the tarry sample was chosen so that the final pH value would be 3.0, assuming complete neutralization of incorporated amine by the acid. In methanol and ethanol stripping runs, solution volume was calculated to achieve supercritical conditions. By keeping the ratio of moles of solvent to sample weight the same in all runs, sample sizes used in methanol and ethanol runs were 0.64 g and 0.59 g, respectively. The reactor was placed in a preheated furnace at 271°C for 2.5 hrs, then cooled to room temperature. The extract and residue were separated by filtration. Steam run filtrate was further extracted three times using 6 ml toluene. The water fraction was titrated with NaOH solution to pH 11.03. A precipitate formed. After filtering, the water fraction was again extracted 3 times using 6 ml toluene. Filtrates from methanol and ethanol runs were rotary evaporated to flash off the stripping solvent until a constant condensate weight was obtained.

included PSOC1351, Ill. #6 seam, high volatile C bituminous; PSOC1405P, Upper Wyodak Seam, subbituminous B; and PSOC1406P, Kinnema Creek Seam, lignite. These minus 20 mesh samples were shipped in one pound cans filled with argon, then transferred into small vials under dry helium and stored in a helium-filled desiccator. A summary of the proximate and ultimate analyses for each coal is shown in Table 1.

It is assumed that water is completely removed by the solvent during liquefaction, i.e.,

$$\text{conversion to solvent extract} = \frac{\text{as received weight loss} - \text{moisture content}}{1 - \text{moisture content} - \text{ash content}} \\ (\text{daf, i.e., dry and ash free})$$

Since the primary interest is the conversion of organics in the coal to extracts, daf basis will be used in the subsequent discussion unless otherwise mentioned.

III. RESULTS AND DISCUSSION

A. Effect of Solvent Property

Dissolution of coal was found to be strongly dependent on the choice of the nitrogen containing solvent. Seven solvents with an assigned solvent property number were examined. The correlation of conversion and the assigned property number is illustrated in Figure 2. It is evident that as the number increases conversion also increases.

B. Effect of Temperature

Temperature is the most important processing variable in these studies. For example, in one of the selected amines the conversion of North Dakota lignite to solubles increased continuously from 60 percent at 220°C to 100 percent at 275°C (Figure 3). When compared with some other liquefaction solvents, such as recycle distillate cuts (Bockrath and Illig, 1984), 1,2,3,4-tetrahydroquinoline (Atherton and Kulik, 1982) and indole and indoline (Padrick et al. 1984), the amines chosen by us show an equal or higher conversion at considerably lower temperatures. This implies that reaction severity can be greatly reduced using the solvents we selected. Results of a comparative study of liquefaction in amine with vacuum pyrolysis and tetralin hydrolification, included in Figure 3, also suggest that the same or higher conversion can be obtained under very mild conditions using the solvents we selected. Figure 3 also shows that a sharp increase in reactivity took place between 230 and 250°C. This observation is consistent with the study of reaction time effect at different temperatures (Section III.F).

C. Effect of the Coal Rank

Figure 3 includes the liquefaction results of subbituminous and bituminous coals. While a complete dissolution of lignite (North Dakota coal) and subbituminous (Wyodak coal) was achieved at temperatures lower than 300°C, dissolution of the bituminous coal (Illinois #6 coal) was lower than the low rank coals. However, this was still much higher than dissolution in commonly used solvents. These results support speculation that interactions between oxygen functionals in the coal and the nitrogen solvent may be the governing factor in liquefaction at mild conditions (Atherton, 1984).

D. Effect of Solvent Density and Solvent-to-Coal Ratio

Solvent density was varied from 0.2 g/ml to 0.6 g/ml. Conversion to soluble materials appeared to be independent of the system density. In addition, solvent to coal ratio (s/c) did not appear to effect conversion when s/c was above 1/1 (w/w). Some of the North Dakota lignite conversion data shown in Figure 3 were obtained at a different density, but were found to fit the curve drawn for temperature effect at a constant density. It should be mentioned that solvent density changed from subcritical to supercritical within this density range. Therefore, since conversion is not dependent on density it could be implied that conversion is limited by chemical reactions.

E. Effect of Hydrogen

Figure 3 also shows data from liquefaction experiments with amine and hydrogen mixture. In the presence of hydrogen the same level of conversion can be achieved

while reducing the reaction temperature by 10°C.

F. Effect of Reaction Time

Since the process under study appeared to be governed by chemical reaction, the reactor system was modified to provide rapid heating and minimize non-isothermal effects (Fig. 1). These conditions facilitated the kinetic interpretation of experimental data. The conversion data were taken at three different temperatures, and at least three different reaction times for each temperature were studied.

Figure 4 shows data obtained at 230, 250 and 275°C at reaction times between 30 and 120 minutes. Conversion increased continuously with increasing time for all three temperatures. At 275°C complete dissolution of coal was observed in 90 min, while at lower temperatures the conversion is substantially lower. Conversion greater than (daf) 100% was observed. This phenomena may be due to dissolution of some ash (mineral matter) from the coal.

G. Process Chemistry

Figure 5 is a flow chart of one liquefaction experiment showing the subsequent product handling. Careful monitoring of stoichiometric balance was essential since mass balance is the first step in understanding chemical reactions and pathways. The chart also contains a number of analyses performed on selected samples.

1. Mass Balance

Reaction gases were collected from a tubing bomb liquefaction run and analyzed on a GC using 1/4 in. S.S. Chromosorb 102 column and an 1/8 in. S.S. molecular sieve column. Fig. 5 shows the analysis of a gas sample. From the identification of all the major gaseous products, it was determined that less than 1% of the carbon present in the coal was converted to these gases. Total gases produced were approximately 0.2% of the daf coal weight used for liquefaction. CO₂ was notably absent in the gas stream, having possibly reacted with the amine to form other compounds. The presence of NH₃ and butane in the gas product also indicated that the amine was hydrogenated and cleaved during liquefaction.

After collecting the gas sample the liquefaction residue was washed with fresh solvent. The resulting solution was centrifuged, filtered and rotary evaporated to obtain two distinct fractions. Selected solid samples were chosen for characterization. The residues produced in centrifugation and filtration steps were 1.68% and 2.2% of the as received coal, respectively. From energy dispersive X-ray analysis, the centrifuge residue contained high concentrations of calcium and silicon, as well as measurable amounts of Al, S, Fe, Cu, Mg and Ni.

2. Product Characterization

Following fractionation a set of characterization techniques, summarized in Fig. 5, were used to explore the governing chemistry. Two distinct fractions were obtained after rotary evaporation. One was black tarry material (solid products) and the other clear liquid (distillate). The solid sample's weight was 2.5 times that of the original daf coal, which indicates extensive solvent incorporation during liquefaction.

The pure solvent and the distillate fraction from evaporation were analyzed by GC (Fig. 6). The major liquefaction product in the distillate appears to be



The structure of the concentrated (through distillation) compound was established by GC/MS, IR, and ¹H NMR. Its presence suggests that amine attacks carbonyl groups in coal and may be a hydrogen source in liquefaction. This compound may be a key in evaluating solvent recovery processes. Solvent impurity peaks a and b have repeatedly been shown to have same retention time, Figure 6.

The tarry residue after evaporation was stored in a vacuum desiccator for 40 days at which time the solid, now fairly dry, reached a constant weight 1.39 times the original daf coal. The detailed desorption study is described later in this paper. After desorption the condensed tarry compound was characterized by sequential Soxhlet extraction, vapor pressure osmometry, elemental analysis, GC/MS, ^1H NMR, ^{13}C NMR and TGA. The results, discussed below, can also be compared with the previously reported analysis of tarry sample before 40 days storage (Chen and Kazimi, 1984).

In sequential Soxhlet extractions, the procedure developed by Mima, *et al.* (1976) was employed. The conversion of this solid product to oils, asphaltenes and preasphaltenes were 31.9%, 55.0% and 9.61%, respectively. Only 3.5% was pyridine insoluble. The average molecular weight of the tarry products, using vapor pressure osmometry, was about 610. Pyridine was used as solvent in the analysis.

Elemental analysis was performed on selected samples. These analyses showed that most oxygen and sulfur in lignite converts to liquid products in the distillate after rotary evaporation of the whole dissolved product (Fig. 5). This strengthens the theory that cleavage of oxygen functionals is critical in the early stage of coal liquefaction, and that nucleophilic solvents are very efficient in accomplishing this reaction.

Solvent incorporation can also be deduced from the nitrogen content of the solid product. As mentioned earlier, the solid product reached a constant weight 1.39 times that of the original daf coal after 40 days *in vacuo*. Assuming the weight gain, 0.39 g per 1 g of daf coal, was due to incorporated solvent in its original molecular form, then the nitrogen content of the solid product would be 6.39%. Direct elemental analysis showed 5.68% nitrogen content. The difference between the two numbers indicates that solvent condensation took place during liquefaction. In fact, a significant amount of NH_3 was present in the product gases.

In the ^1H NMR spectrum of the solid sample dissolved in dimethylsulfoxide, Figure 7, it is interesting to note that no clear aromatic hydrogen peaks appear around δ 7 or conjugated double bonds between δ 4.5 to 8. Similar results were also obtained when the sample was dissolved in D_5 -pyridine and CDCl_3 . This observation led us to perform a ^{13}C NMR analysis. A sharp peak around 120 ppm indicates the existence of aromatic carbon. The absence of aromatic hydrogen could imply that carbons at the outskirts of fused aromatic clusters were substituted during coal liquefaction in amine.

The thermogravimetric curve of the tarry product is shown in Figure 8. The sample was derived from the Parr reactor rather than the tubing bomb, differing mainly in the use of pyridine wash after liquefaction (see Experimental Section). The thermogravimetric analysis was performed in nitrogen with $20^\circ\text{C}/\text{min}$. heating rate. The thermogram indicates that the sample lost 50% of its weight below 300°C and all organics had been volatilized below 800°C .

H. Solvent Incorporation and Recovery

Evaporation of the pyridine washed and liquefaction amine washed samples produced a tarry product which had a weight 1.65 and 2.5 times the original daf coal weight, respectively. To measure the solvent recovery three different tests were conducted.

1. Washing with a Second Solvent

To measure the incorporated solvent, an amine other than the liquefaction solvent was used to wash the reactor. The combined liquefaction and washing solution was analyzed by GC. The analysis indicated that 0.59 g of the liquefaction solvent was consumed per 1 g daf coal. Generally 2.0 g of amine was used with 1.0 g of coal in liquefaction.

2. Physical Desorption

After rotary evaporation, the tarry product (2.5 times the daf coal weight) was stored in vacuo for desorption studies. From elemental analysis of this sample, the evaporated fraction was found to be rich in nitrogen-containing compounds. The desorption process follows the Langmuir equation (the rate of desorption is proportional to the amount of absorbed material):

$$Y = 1.001e^{-0.65t} + 0.166e^{-0.065t} + 1.390$$

where Y = sample weight/daf coal wt
t = time in days.

Y approached an asymptotic value, 1.390, which implied that 0.39 g solvent per 1 g daf coal was incorporated into the coal product. The presence of two exponential terms indicates that the solvent removal is a two step process. One may be the evaporation of a light or loosely held fraction (e.g., Van der Waal force-bonded) from a tarry matrix, while the other step may require the removal of a fraction which is heavier or more tightly bound.

3. Chemical Conversion of Incorporated Solvent

Coal liquefaction was reported to involve the cleavage of oxygen cross-links such as esters (van Bodegom, et al., 1984); therefore, it was speculated that solvent amine was incorporated into products as amide. Aqueous acid, ethanol, and methanol were employed to remove nitrogen containing species from coal derived products. Using this approach, amides might be converted into amines and carboxylic acids through nucleophilic substitution by water and alcohols. North Dakota lignite was used in this study because it has a very high oxygen content (24%, daf).

Figure 9 illustrates the sample handling flow chart and major analyses for the products derived from methanol stripping, which dissolved 52.4% of the tarry products. The solid residue was characterized by sequential Soxhlet extractions, vapor pressure osmometry (V.P.O.) and elemental analysis. Conversion of this solid product to hexane, benzene and pyridine solubles was 10.8, 8.6 and 55.7%, respectively, while 24.8% was pyridine insoluble. V.P.O. was used for determination of molecular weight, with pyridine as the solvent. The measured average molecular weight was 1951. The liquid phase after stripping was filtered and then evaporated under vacuum at 40°C. The resulting tarry fraction (0.55 g) was also characterized by sequential Soxhlet extractions, V.P.O. and elemental analysis. More than 92% of this tarry fraction was hexane soluble and it was completely dissolved in pyridine.

Material balance indicated that 63% of the nitrogen in the tarry liquefaction product was converted to extracts and 13% to the distillate fraction. Analyses of the distillate fraction by GC/MS and interpretation of the spectra are currently being performed. In ethanol stripping, similar results were obtained.

Figure 10 illustrates the sample flow chart in steam treatment. Only 15% of coal liquefaction products dissolved in steam, and based on the elemental analysis more than 39% nitrogen was removed from the coal liquefaction products. From V.P.O. analysis, the average molecular weight of steam treated products was 648, which is slightly higher than the tarry product before stripping. In sequential Soxhlet extractions, the conversion of hexane, benzene and pyridine was 41.7, 15.1 and 34.2%, respectively. Toluene extraction fractions and precipitation solids are currently under analysis.

The total solid products recovered after stripping with methanol, ethanol and steam were 92, 85 and 96%, respectively. In the calculation of alcohol stripping data, solids left in the stripping unit and evaporator were taken into consideration. It is worth mentioning that total asphaltene fraction decreased during stripping. From the Soxhlet extraction data of all three stripping products, it is clear that asphaltene converted to preasphaltene and pyridine-insolubles. Only a small fraction of asphaltene converted to oil in alcohol strippings. All

stripping products showed higher oxygen content, indicating that water and alcohol were involved in the reaction. We intend to perform IR analysis so that the specific pathway of oxygen functionals can be elucidated.

IV. CONCLUSIONS

Systematic study of coal liquefaction with amine continues to demonstrate the promise of the process under development. The following table compares some of our experimental results with those of a typical tetrahydroquinoline extraction (Atherton and Kulik, 1982)

	Amine (GSRI)	THQ
Temperature, °C	275	400
Pressure, psi	<500	1100
Gas Product, wt%	<1%	~10%
Conversion to Solubles (daf)	100%	95%
Product Undistillable at 500°C	~30%*	~80%†
Molecular weight of tarry product	610	--

*See Figure 8.

†Undissolved coal is included as undistillable.

We are particularly encouraged by the fact that the majority of the tarry product is distillable at 500°C. This suggests that the incorporated solvent is likely to be removed by distillation. Further development of the process requires a better understanding of process chemistry to determine 1) the governing chemical interactions between amines and coal and 2) the type of solvent recovered by physical separation or chemical conversion so that it can be recycled.

ACKNOWLEDGEMENTS

Valuable discussions with Dr. Lloyd Lorenzi, Jr., the project manager at the Department of Energy, are gratefully acknowledged. The authors would also like to thank Dr. David Baker (University of Alabama), Earl Pratz and John Troost for their NMR, TGA and GC analyses. This work was supported by the U.S. Department of Energy under contract DE-AC22-83PC60046.

REFERENCES

- Atherton, L.F., Coal Liquefaction Research Status Report, EPRI Journal, Jan/Feb, 1984, pp. 37-39.
- Atherton, L.F. and C.J. Kulik, "Advanced Coal Liquefaction," Paper presented to the 1982 AIChE Annual Meeting, Los Angeles, CA, November, 1982.
- Bockrath, B.C. and E.G. Illiq, "Coal Liquefaction and Hydrogen Utilization at Low Temperatures," Preprint of ACS Div. of Fuel Chemistry, 29 (5), 76 (1984).
- Chen, W.Y. and F. Kazimi, "Coal Liquefaction with Supercritical Ammonia and Amines," Presented at AIChE Annual Meeting in San Francisco, Nov. 25-30, 1984.
- Mima, M.J., H. Schultz and W.E. McKinstry, "Method for the Determination of Benzene Insolubles, Asphaltenes and Oils in Coal Derived Liquids," PERC-RI-7616 (1976).
- Padrick, T.D. and S.J. Lockwood, "Liquefaction of Wyodak Coal in Indoline," Preprint of ACS Div. of Fuel Chem., 29 (5), 92 (1984).
- van Bodegom, B., J.A.B. van Veen, G.M.M. van Kessel, M.W.A. Sinnige-Nijssen and H.C.M. Stuijver, "Action of Solvents on Coal at Low Temperature 1. Low-rank Coals," Fuel, 63 (3), 346 (1984).
- Williams, D.F., "Extraction with Supercritical Gases," Chem. Eng. Sci., 36 (11), 1769 (1981).

1. The identities of the solvent are not disclosed in this paper because the patent application is pending. We plan to disclose this information at the ACS meeting.

Table 1. Properties of Coals Used in the Liquefaction Study

Sample	PSOC-1351	PSOC-1405P	PSOC-1406P
Rank	HVCB	SUBB	Lignite
Province	Interior	N. Gr. Plains	N. Gr. Plains
State	Illinois	Wyoming	N. Dakota
Moisture	8.08	18.82	29.64
Ash	10.56	7.15	8.23
Volatile matter	37.08	38.23	21.32
Fixed carbon	44.28	34.80	30.80
C, daf, %	76.26	74.44	67.72
H, daf, %	4.85	5.46	4.97
N, daf, %	1.32	1.34	1.40
S, daf, %	5.31	2.03	1.33
O, (% by diff.)	12.26	16.73	24.58
H/C (atomic)	0.76	0.88	0.88

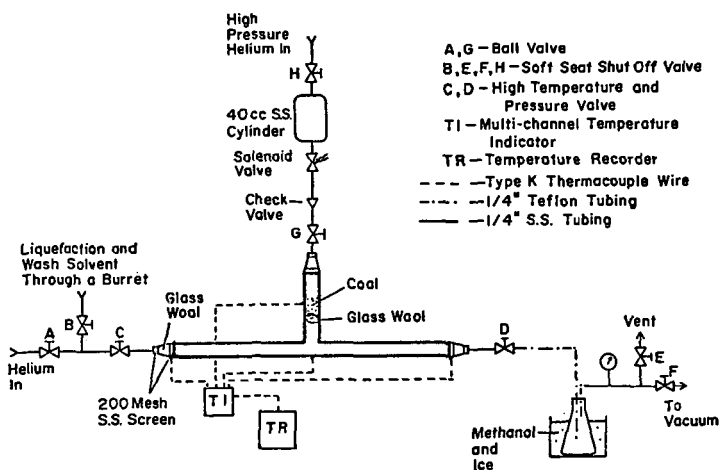


Figure 1. Experimental Arrangement

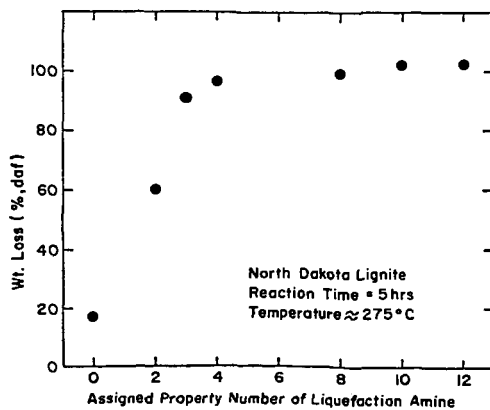


Figure 2. Property Number Effect

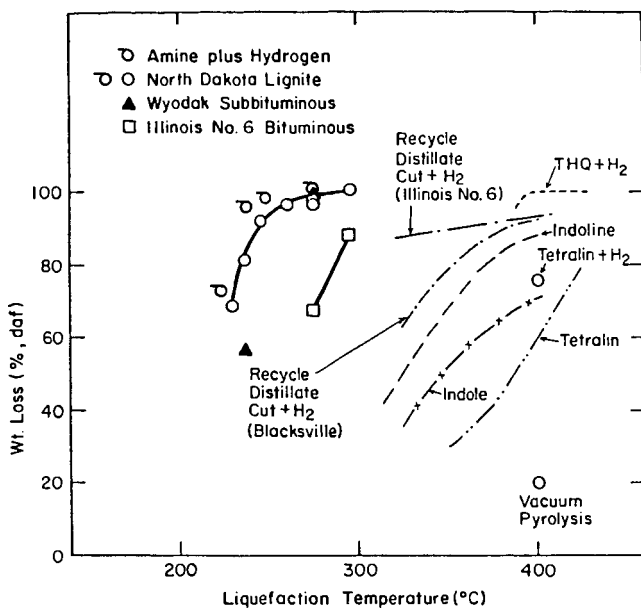


Figure 3. Effect of Temperature, Coal Rank and Hydrogen on Liquefaction Conversion. Symbols Represent GSRI Data, Broken Lines Represent Other Literature Data

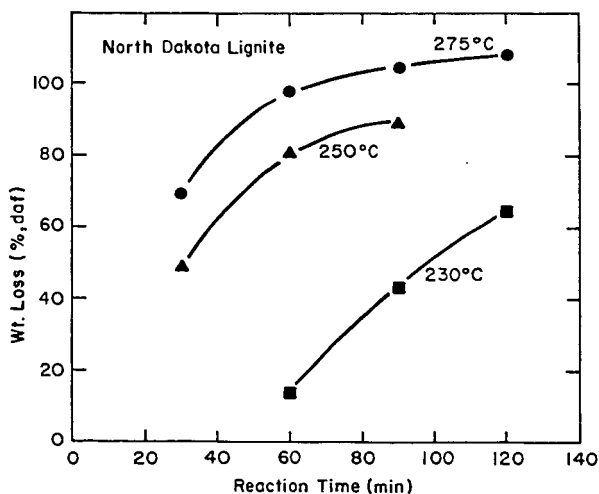


Figure 4. Reaction Time Effect

2.0 g North Dakota Lignite (as received)
2.0 g (2.7 ml) amine in 12.2 ml Reactor

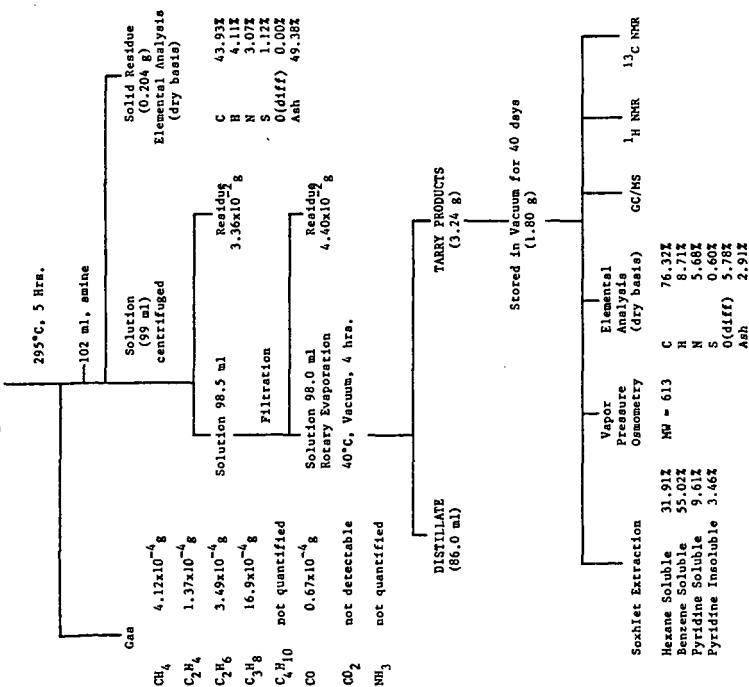


Figure 5. Liquefaction Flow Chart

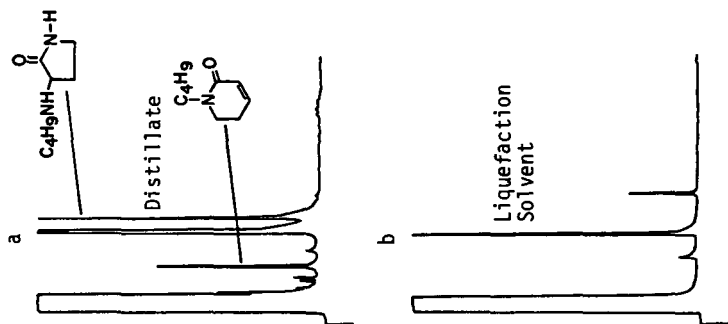


Figure 6. Chromatograms of Solvent and Distillate Fraction

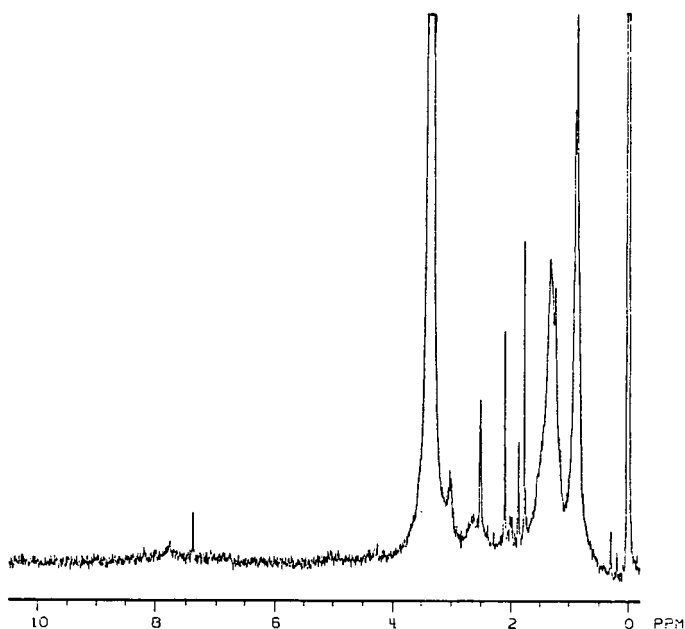


Figure 7. ^1H NMR Spectrum of Solid Products in Dimethylsulfoxide (Nicolet N-200)

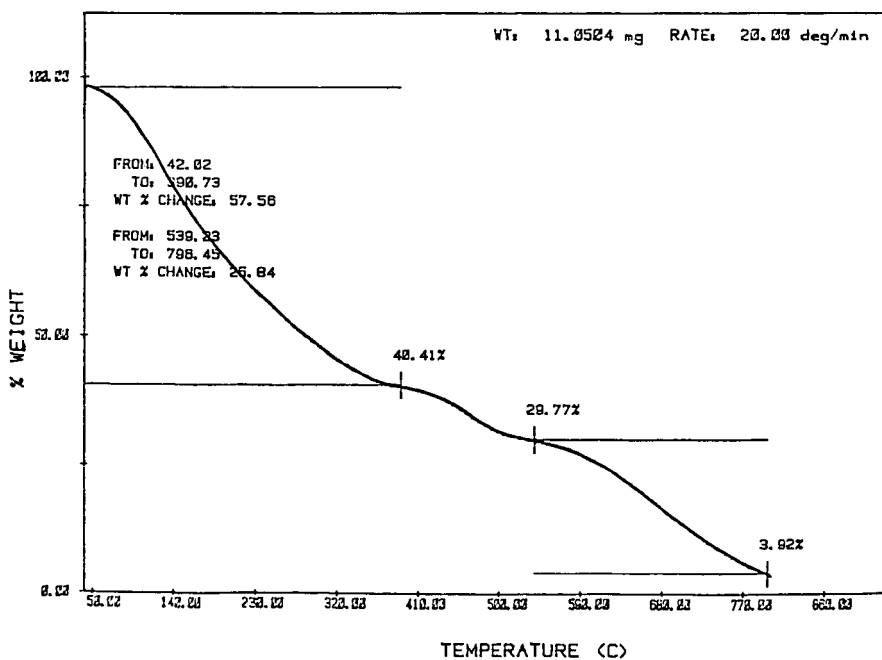


Figure 8. Thermogram of Solid Products

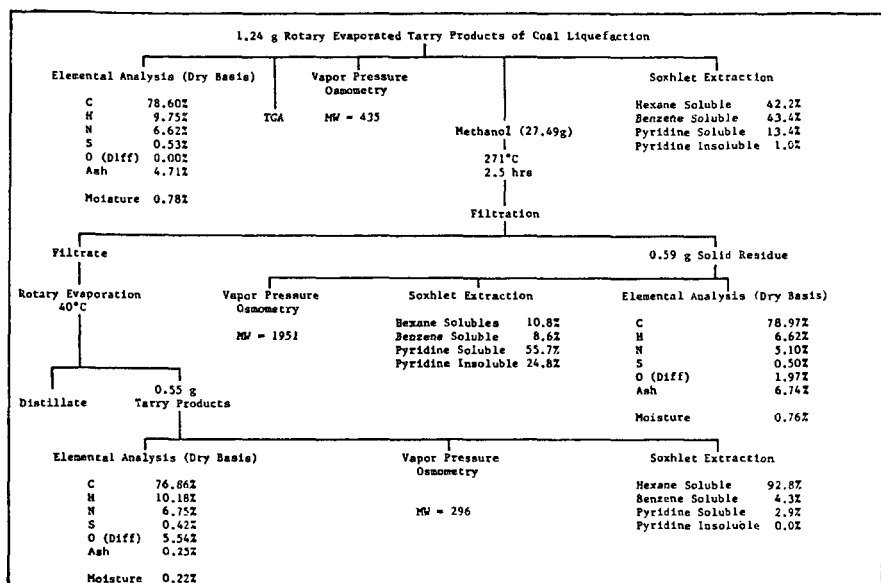


Fig. 9. Methanol Stripping and Related Products Characterization

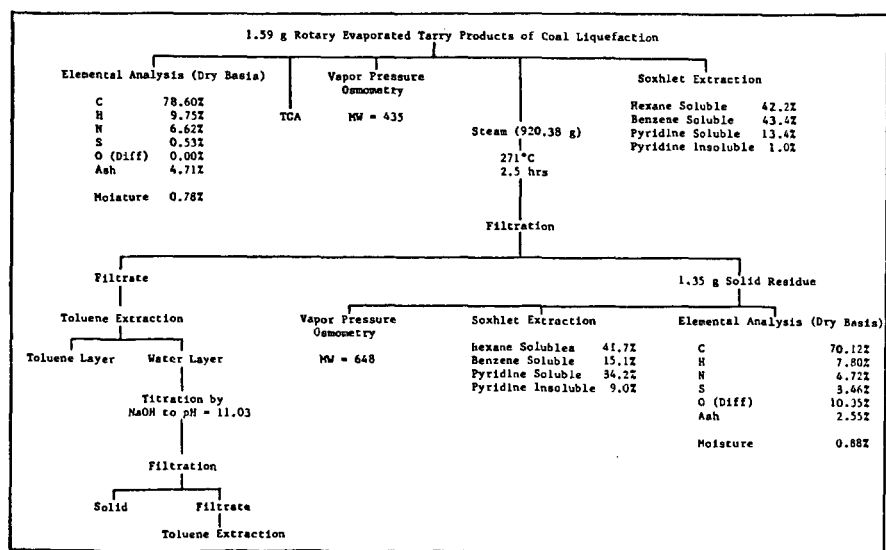


Fig. 10. Steam Stripping and Related Products Characterization